UNIVERSIDAD CARLOS III DE MADRID

TESIS DOCTORAL

Four essays on commodity markets:
Asset allocation, pricing, and risk management

Autor:

Carlos González Pedraz

Directores:

Juan Ignacio Peña Sánchez de Rivera
Manuel Moreno Fuentes

Departamento de Economía de la Empresa

Getafe, July 2014

Four essays on commodity markets:
Asset allocation, pricing, and risk management

Carlos González-Pedraz

Universidad Carlos III □
□ Getafe, Madrid

For my parents

Contents

List of Figures

List of Tables

Preface

My interest in derivatives and risk management has its origins in the graduate classes taught by Manuel Moreno and Juan Ignacio Peña at Universidad Complutense and Universidad Carlos III de Madrid. Some time after that, this thesis started to take shape during the course of a dinner and different conversations that took place in Castellón during the productive dead times of the Spanish Finance Forum. By then, we had already envisioned an analysis of commodity markets from a financial perspective, taking into account their stylized characteristics, as an interesting area of research.

Since the mid-2000s, many investors have entered into commodity markets; investment banks, hedge funds, and other portfolio managers increasingly view commodities as an alternative asset class. Furthermore, commodity futures indexes, exchange traded funds, and different forms of commodity derivatives have become mainstream. The large variability of commodity prices also has increased economic and political interest in these markets.

For that reason, a better understanding of the behavior of commodity prices from a multivariate and univariate perspective, especially when extreme events occur, is of paramount importance for accurate asset valuation, risk management, and portfolio decisions. This thesis tries to contribute in this respect.

Our study is divided into two parts. The first part (Chapter 2 and Chapter 3) analyzes the multivariate distribution of commodity returns and its impact on portfolio selection and tail risk measures. Chapter 2 solves the portfolio selection problem of an investor with three-moment preferences when commodity futures are part of the investment opportunity set, providing a conditional copula model for the joint distribution of returns that allows for time-varying moments and state-dependent tail behavior. Chapter 3 approximates the exposure of physical and financial players to energy price risk using linear combinations of energy futures; it also analyzes the tail

behavior of energy price risk using a dynamic multivariate model, in which the vector of innovations is generated by different generalized hyperbolic distributions.

The second part (Chapter 4 and Chapter 5) considers the valuation of real assets and commodity derivatives in the presence of non-Gaussian shocks in a continuous time framework. Specifically, Chapter 4 employs a jump diffusion model for the price differentials and proposes a valuation tool for the connection between two electricity markets. Chapter 5 proposes a reduced-form model for the data generating process of commodity prices together with a more flexible change of measure, capable of changing the mean-reversion rate of Gaussian and jump processes under the risk-adjusted probability measure.

Some parts of this thesis have been presented in different seminars, workshops, and conferences. Chapter 2 was presented at the 2011 INFINITI Conference on International Finance (Trinity College, Dublin), the 2011 Conference of the Multinational Finance Society (LUISS, Rome), the 2012 International Conference of the Financial Engineering and Banking Society (ESCP, London), the 2012 International Finance and Banking Society Conference (Valencia), the 2012 Meetings of the European Financial Management Association (University of Barcelona), and Universidad Autónoma de Madrid. A previous version of Chapter 3 was presented at the 2010 AEEE Conference on Energy Economics (University of Vigo). Chapter 4 was presented at the 2010 Finance Forum (CEU, Elche), the 2011 AEEE Conference on Energy Economics (University of Barcelona), University of Duisburg-Essen, and Birkbeck-University of London. Previous drafts of Chapter 5 were presented at the 2009 Conference on Energy Finance (Universities of Oslo and Agder), the 2010 Industrial-Academic Forum on Commodities, Energy Markets, and Emissions Trading (Fields Institute, Toronto), and the 2011 Energy and Finance (Erasmus School of Economics).

Acknowledgements

I am very grateful to my advisors, Juan Ignacio Peña and Manuel Moreno, for giving me the opportunity to return to the academic world and helping me navigate throughout all the stages of this project. This thesis has benefited enormously from their wisdom, help, and patience.

I am also deeply indebted to Álvaro Cartea for inviting me to spend a semester in the Department of Mathematics of University College London (UCL); I have learned a lot from him. He has been a great role model, assuming the function of a third advisor.

During all these years, I had the chance to meet great academics and

practitioners who have served as an inspiration. I thank Pablo Villaplana for his generous advice since the first stages of this thesis and for offering me a Research Fellowship in the Spanish Energy Commission. Fred Espen Benth is a great coauthor and invited me to the Centre of Mathematics for Applications at University of Oslo to work in the early versions of Chapter 5.

I also thank the faculty, staff, and graduate students of the QF doctoral program, the Department of Business Administration of Carlos III University, and the Department of Mathematics of UCL, for creating great and positive environments to conduct research. Specially, I want to mention Juan José Camio, Alfonso Novales, Cristina Mazón, Jesús Ruiz, Jeon Beop Yong, Isabel Figuerola-Ferreti, Ricardo Correia, José Penalva, Pedro Serrano, Sergio Mayordomo, Dennis Tuerk, and Carlo Marinelli.

Very special thanks must go to my friends and family; I owe them so much. To Marisa and Álvaro, for their understanding and encouragement; to Andrés, Marcos, Pedro, and Sergio, for our long, and sometimes fruitful, discussions about science, politics, and life. Thanks very much to Judith and Pepe for their confidence and counsel, and for always finding the right words to say. Last but not least, to Marta, for bearing with me the ups and downs of this period and being so patient. Without her help this thesis would not have been possible.

My greatest debt is to my parents, Alejandra and Ubaldo. This thesis is dedicated to them: for their unconditional support during all these years, for being always there, and for being exemplars of hard work and love.

C.G.P.
East London, 2013.

1
Introduction

SOME HISTORICAL STUDIES offers examples of commodity futures trading in India at about 2000 B.C., as well as the origins of modern organized markets in Europe and Japan in the 17th and 18th centuries. Primitive futures contracts written on rice were traded in Osaka in the mid-18th century (Duffie, 1989). In their modern version, commodity futures contracts were first traded in the middle of 19th century in the corn and wheat markets of Chicago. Despite these long traditions, commodities are a lesser known asset class compared with other, more traditional assets such as bonds and stocks, and they have been relatively ignored by the investment community until recently.

Since the beginning of the 2000s though, commodities have become increasingly popular for many traditional investors, as part of their long-term diversification strategies. Prior to the financial meltdown of 2008-2009, financial analysts recommended long-only investments in commodities as an alternative asset class, to decrease expected portfolio risk, increase expected portfolio returns, and hedge macroeconomic risk (Goldman Sachs, 2004). During that period, commodity prices and volatility increased significantly, as we can see in Figure 1.1. In addition to futures and options contracts, other financial products that allowed investors to gain exposure to commodities –such as commodity index funds, over-the-counter (OTC) swap agreements, and exchange traded funds– were also widely popularized. According to some estimates, index investment in commodities increased from around $15 billion at the end of 2003 to more than $200 billion in 2008, just prior to the financial crisis. The notional amounts outstanding in OTC markets and the open interest of futures contracts (see Exhibits 1 and 2 of Figure 1.2, respectively) experienced rapid growth in the last decade. Furthermore, players other than traditional producers and retailers

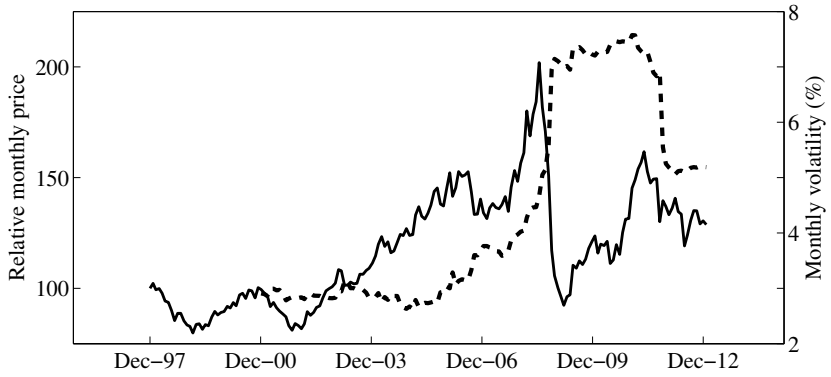

Figure 1.1. Relative price and moving volatility of the CRB index
This figure plots (solid line) the monthly relative price of the Commodities Bureau Research (CRB) Index from 1998 to the end of 2012, together with the moving monthly volatility (dotted line) of the CRB Index calculated using the previous 36 observations. Source: Reuters.

started to trade physical assets. For example, some investment banks owned power plants and pipelines and purchased other commodity assets to use as hedging tools (Carmona and Ludkovski, 2006).

The recent volatility of commodity prices and the rise in commodity investing also renewed academic interest in the behavior of commodity markets. In this opening chapter, we describe commodity markets, paying special attention to energy commodities. We also introduce the salient features of the univariate and multivariate behavior of commodity price dynamics, along with some of the models and estimation methodologies employed in this thesis.

1.1 Commodity markets

In a financial context, the term "commodity" refers to a relatively homogeneous consumption good (Geman, 2005). Commodities differ from stocks and bonds, in that they do not generate a stream of future cash flows. Grains, livestock, energy, metals, foodstuffs, and textiles are traditional examples of commodity classes. Weather, carbon dioxide emission allowances, and computing resources are examples of new commodity markets.

There is considerable diversity among commodities. Most are storable at some cost, but some, such as electricity are impossible or very costly to store.

Exhibit 1: Notional amounts in OTC derivatives

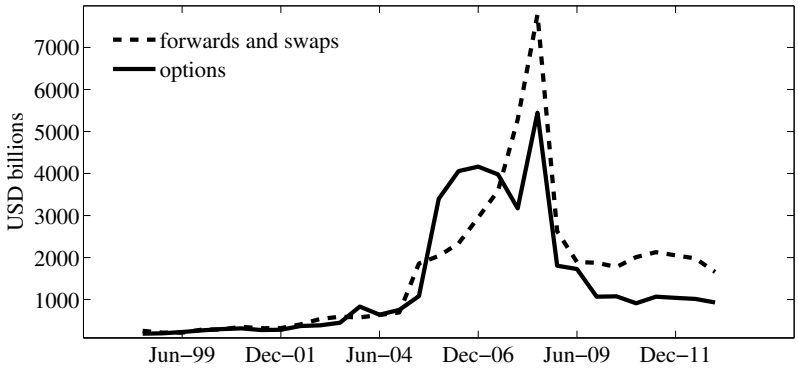

Exhibit 2: Open interest in gold and oil

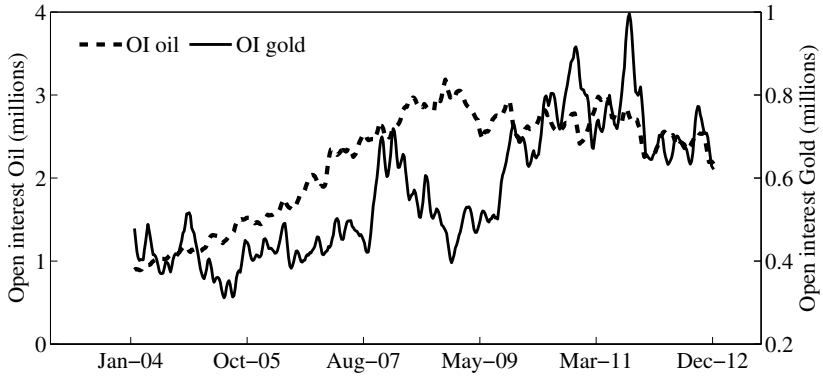

Figure 1.2. Notional amounts and open interest
Exhibit 1 plots the notional amounts (in billions of USD) outstanding at the end of each semester from 1998 to 2012 of OTC derivatives (forwards and swaps, and options) traded globally. Exhibit 2 plots the total open interest in oil and gold futures contracts traded on the New York Mercantile Exchange (NYMEX) and the Commodity Exchange Inc. (COMEX), respectively. Sources: Bank of International Settlements and U.S. Commodity Futures Trading Commission.

Supply and demand patterns also establish differences among commodities. Some commodities exhibit substantial seasonality in demand (e.g., natural gas, electricity) but are produced continuously, whereas other commodities are produced periodically (e.g., grains). Thus, storability, demand, and supply characteristics determine the different behavior of commodity prices and present a challenge to modelers (Pirrong, 2012).

Buyers and sellers can trade commodities in spot markets, where delivery is immediate or following a very small lag; or they can trade them using forward agreements with a given future delivery date, either in organized futures exchanges or OTC markets. Commodity forward contracts allow firms to obtain insurance for the future value of their outputs or inputs, whereas investors in these contracts receive compensation for bearing the risk of short-term commodity price fluctuations (Gorton and Rouwenhorst, 2006).

There are many active and liquid commodity futures markets, including crude oil, heating oil, natural gas, gold, silver, copper, and aluminum futures traded in the New York Mercantile Exchange (NYMEX); corn, soybean, and wheat futures traded in the Chicago Board of Trade (CBOT); non-ferrous metals in the London Metal Exchange (LME); and oil, natural gas, electricity, freight, and agriculturals in the Intercontinental Exchange (ICE) in London. Other commodity exchanges in emerging markets have gained importance in recent years, especially the Dalian Commodity Exchange and the Shanghai Futures Exchange for agriculturals and non-precious metals trading.

1.2 Energy spot and futures markets

The market for energy is huge. The world's population consumes about 15,000 gigawatts of power (1 gigawatt is the capacity of the largest coal-fired power station). That means a business of $6 trillion a year, one-tenth of the world's economic output (The Economist, 2008). Energy markets have been liberalized in the the recent years and are still developing. The crude oil market is the most liquid and global commodity market. Other important energy markets are power, natural gas, and coal. Natural gas is used for heating purposes and as an input for power generation. In Western Europe and the United States, coal is mainly used for power generation.

Since the end of last century, there has been a continuous process of liberalization and deregulation of energy markets. These developments have resulted in the separation of services into generation, transmission, distribution, and retail, with the goal of creating more competition and

liquidity. They also have created new market risk exposures, which must be managed at every interface of the formerly integrated chain. The players in this growing risk management market consist of two major categories: physical and financial players. The first are engaged in the energy markets due to their physical exposure, such as utilities and oil and gas producers. Most actively engage in hedging and trading activities, both physically and financially. The second group comprises by investment banks, hedge funds, and trading houses, which act as risk managers and intermediaries or trade in their own accounts. As mentioned previously, some financial players introduce physical assets into their operations, but most of them remain focused only on financial aspects.

Energy markets exhibit some special features that differentiate them from other commodity markets. Natural gas or power markets have a great variety of traded contracts, including forwards with multiple maturities and different delivery periods and short-term contracts, such as weekly, day-ahead, and real-time prices. Electricity cannot be stored, and natural gas storage is costly and inflexible. Therefore, there is no clear price convergence among the different contracts. Location is also very important in these markets, because each gas or power hub has a different price every day and hour.

When modeling the evolution of gas and power prices, we also must consider the presence of extreme price spikes, seasonality, and mean reversion. Furthermore, energy markets are closely intertwined by substitution, complementary, and production relationships that complicate the modeling of the dependence among these commodities (Casassus, Liu, and Tang, 2013).

Chapters 3, 4, and 5 considers European and U.S. energy markets in their empirical applications. More specifically, Chapter 3 analyzes portfolios of U.S. energy futures composed of crude oil, natural gas, coal, and electricity; Chapter 4 studies the spread between five European power markets; and Chapter 5 uses U.K. natural gas and electricity spot and futures data.

Some commodity derivatives and physical assets that are operated in these markets have complex payoffs. Asian, spread, and swing options are examples of exotic options that provide a hedge against price and volume risks. Such options also appear in the real option approach to the valuation of physical assets and contracts, such as power plants, interconnections, or gas storage. Chapter 4 considers an application of real options to the valuation of interconnectors between different European electricity markets.

1.3 Multivariate behavior of commodity returns

Recently, some studies have focused in the multivariate behavior of commodities and their diversification benefits when they are included in a traditional portfolio. With a mean-variance framework, Erb and Harvey (2006) and Gorton and Rouwenhorst (2006) study the performance of an equally weighted portfolio of commodity futures using data series that end in 2004-2005. They find that their portfolio was zero or negatively correlated with stocks and bonds and, in some cases, had statistically significant returns, close to those of equity. Their analysis thus showed that the commodity futures distribution exhibited positive skewness, whereas stocks revealed negative skewness. Both distributions were fat tailed with respect to the normal distribution, but equities exhibited more downside risk than commodities. Kat and Oomen (2007a,b) also study the individual and multivariate return properties of some groups of commodities, paying special attention to correlation and tail-dependence from the investor's point of view. They find that no evidence of abnormal tail behavior in the relationship among commodity futures, bonds and equity returns. However, since 2004, the flow of index investment into commodity markets could have increased the integration with stock and bond markets, as well as the price co-movements between different commodities (Tang and Xiong, 2012). Furthermore, Büyükşahin, Haigh, and Robe (2010) identify substantial variations over time in the potential diversification benefits that commodities could bring to equity investors, especially during periods of financial market stress.

Since correlation seems to vary with the business cycle, commodities do not diversify risk equally at all times. Thus, a purely passive investment in commodities may not be optimal, and it seems reasonable to extend the portfolio selection to a conditional and non-linear framework. In Chapter 2, we propose a conditional, non-Gaussian model for the joint distribution of commodity futures returns and analyze its effect on portfolio selection.

1.4 Pricing and estimation methodologies

Because of the special characteristics of commodities, pure unconditional Gaussian models are not the most suitable framework to describe the multivariate and univariate behavior of these assets. Consequently, traditional approaches to deal with commodity market risk and price commodity derivatives have to be reconsidered. Furthermore, in this context of nonnormality, nonlinear econometric techniques would be required to estimate realistic

commodity pricing models. Some of the most promising distributions for modeling heavy-tailed and asymmetric returns are those belonging to the generalized hyperbolic (GH) class (McNeil, Frey, and Embrechts, 2005). The GH distributions exhibit some attractive properties: They are closed under affine transformations, can display different tail behavior, and can be both symmetric and skewed. Chapter 3 develops a multivariate model for energy returns based on GH distributions.

When the joint distribution of returns is nonelliptical, the linear correlation is no longer sufficient to describe the dependence structure, and nonlinear dependence functions can be more informative (see Patton, 2004). Copula theory allows us to obtain the dependence function, or copula, of a n-dimensional joint distribution, and use it to model the dependence between n arbitrary univariate densities. For example, using a skewed t copula, we can distinguish between the tails of the marginal distributions and the presence of dependence in the tails, as well as between asymmetry in the distribution of individual returns and asymmetry in their dependence structure. This approach is employed in Chapter 2.

From a continuous time perspective, we also consider the presence of heavy tails and skewness in the dynamics of commodity prices. A no-arbitrage spot price model, especially for energy commodities, should capture: large price spikes or jumps, strong mean reversion of large deviations, and the presence of a seasonal component. For that purpose, and following the no-arbitrage models of Schwartz and Smith (2000) and Casassus and Collin-Dufresne (2005), we can add mean-reverting jump-diffusion factors to the space of state variables. The presence of jumps in the dynamics of prices prevents us from estimating the model parameters using techniques based on Gaussian hypothesis. Other approaches such as non-parametric jump filters (see Chapter 4) or Markov chain Monte Carlo (MCMC) methods (see Chapter 5) have to be employed.

Because of the presence of discontinuous processes, establishing a link between the data generating measure and the risk-neutral measure is more difficult than in traditional pure Gaussian cases. A natural way to price derivative contracts consists of employing Fourier transforms and the characteristic function of the process for the spot price (Chapter 4).

Furthermore, when analyzing the behavior of commodity forward contracts, some questions arise. For example, how are the data generating and risk-adjusted measures related? Spot price dynamics are much easier to model than dynamics under the risk-adjusted measure, because the former are observed, whereas the latter can only be inferred from the price dynamics of instruments written on the spot commodity, such as forward

contracts. Defining new changes of measure, we can model the possibility that participants in energy markets price contracts under the risk-adjusted measure by varying how long deviations from the seasonal component last. In this context, Chapter 5 tries to establish a new link between the data generating measure and the risk-adjusted measure in commodity pricing.

1.5 Organization of the thesis

The remainder of this thesis is organized as follows. Chapter 2 investigates the portfolio selection problem of an investor with three-moment preferences, taking positions in commodity futures. To model the asset returns, we propose a conditional asymmetric t copula with skewed and fat-tailed marginal distributions, such that we can capture the impact on optimal portfolios of time-varying moments, state-dependent correlations, and tail and asymmetric dependence. In the empirical application with oil, gold, and equity data from 1990 to 2010, the portfolios corresponding to conditional t copulas achieve better performance than those based on more conventional strategies. The specification of higher moments in the marginal distributions and the type of tail dependence in the copula also have significant implications for the out-of-sample portfolio performance.

Chapter 3 analyzes the tail behavior of energy price risk using a multivariate approach, in which exposure to energy markets is given by a portfolio of oil, gas, coal, and electricity. To accommodate various dependence and tail decay patterns, this study models energy returns using different generalized hyperbolic conditional distributions and the time-varying conditional mean and covariance. Employing daily energy futures data from August 2005 to March 2012, we recursively estimate the models and evaluate tail risk measures for the portfolio's profit-and-loss distribution for long and short positions at various horizons and confidence levels. Both in-sample and out-of-sample analysis applied to different energy portfolios show the importance of heavy tails and positive asymmetry in the distribution of energy risk factors. We find that models with exponential tail decay yield inferior tail estimates for short positions compared with models with polynomial tail decay, especially for the far tail of utility portfolios.

In Chapter 4, we focus on the value of interconnecting electricity markets. An interconnector is an asset that gives the owner the option to transmit electricity between two locations. In financial terms, the value of an interconnector is the same as a strip of real options written on the spread between power prices in two markets. We model the spread based on a seasonal

trend, a mean-reverting Gaussian process, together with a mean-reverting jump process, and express the value of these real options in closed-form. The valuation tool is applied to five pairs of European neighboring markets to value a hypothetical one-year lease of the interconnector, using different assumptions about the seasonal component of the spread and different liquidity caps to proxy for the depth of the interconnected power markets. We derive no-arbitrage lower bounds for the value of the interconnector in terms of electricity futures contracts and find that, depending on the depth of the market, the jumps in the spread can account for between 1% and 40% of the total value of the interconnector. The two markets where an interconnector would be most (least) valuable are Germany and the Netherlands (France and Germany). Finally, we provide rules of thumb to interpret the differences in the interconnector values.

In Chapter 5, we analyze risk premia in commodity markets. We propose a new change of measure that allows changes in the speed of mean-reversion under the risk-adjusted probability. The stylized facts of the behavior of commodity spot prices have been extensively studied. The main two features, as we mentioned already, are the presence of a deterministic trend and the mean reversion of deviations from this trend. But what are the stylized facts under the risk-neutral measure? We set out to answer this question by analyzing how risk-averse investors adjust the statistical measure of price dynamics when pricing risky securities written on commodities. We model the market price of risk so that market participants bearing spot commodity risk are compensated for jump-arrival risk, jump-size risk, and speed of mean reversion risk of both diffusion and jumps. Our approach can also be viewed as a special case of stochastic discount factors that not only affect the mean of the process but also its variance through the persistence of shocks to the economy. We consider an arithmetic model that includes positive and negative jumps in the prices of commodities. When pricing under the risk-adjusted measure, agents change the time it takes to return to the seasonal trend, alter the mean of the process, and change the intensity of the jumps and their average size.

I

Portfolio and risk management: A multivariate approach

2

Portfolio selection with commodities under conditional copulas and skew preferences

FINANCIAL INVESTORS MAINLY take positions in commodity futures contracts as a natural way to gain exposure to commodity risk without owning the physical asset. Erb and Harvey (2006) and Gorton and Rouwenhorst (2006) find that historically, commodity futures exhibited little co-movements, zero or even negative correlations with stock returns, and Sharpe ratios fairly close to those of equities. Therefore, according to traditional portfolio theory, commodities should increase diversification when included in equity portfolios and may help enhance the portfolio's risk-return profile. Possibly boosted by the potential for such diversification benefits, investments in commodity futures indexes and related instruments grew quickly after the early 2000s[1] (see Büyükşahin and Robe (2010), Etula (2013), Hong and Yogo (2012), and Tang and Xiong (2012) for some analysis about this recent boom).

Despite the growing interest in commodities as investment vehicles, few studies have analyzed the optimal portfolio allocation taking into account the stylized features of commodity futures. A standard mean-variance framework might not be appropriate for portfolios that contain commodity futures due to their returns' specific distributional characteristics, such as the presence of serial correlation, heavy tails, and skewness (Daskalaki and

[1]Investments in commodity index funds increased from around $50 billion, at the end of 2004 to a peak of $200 billion in 2008; after a drop during the recession, they increased again to a second peak of around $300 billion at the end of the third quarter of 2010. See Irwin and Sanders (2011).

Skiadopoulos (2011); Gorton and Rouwenhorst (2006); Kat and Oomen (2007b); Börger, Cartea, Kiesel, and Schindlmayr (2009)). Instead, we propose a more flexible model to be used in the portfolio selection problem of an equity investor when cash-collateralized commodity futures are part of the investment opportunity set. Our approach combines a three-moment preferences specification with time-varying multivariate density models that describe the statistical properties of commodities and equity returns, as well as their interactions.

With respect to the investor's preferences, we consider an allocation problem in which the investor's objective function is determined by the mean, variance, and skewness of portfolio returns (similarly to Guidolin and Timmermann (2008); Harvey, Liechty, Liechty, and Müller (2010); and Jondeau and Rockinger (2012)). With fairly general assumptions, investors show a preference for positive skewness in return distributions and aversion to downside risk (negative skewness). That is, in our proposed three-moment preferences specification, the investor is eager to decrease the chance of large negative deviations, which could reduce the final value of the portfolio. Expanding the standard mean-variance set-up by including the third moment of the portfolio returns has been investigated for traditional assets, such as stocks.[2] As far as we know, however, this approach has not yet been analyzed for a portfolio choice problem with commodities, for which skewness seems likely to play a role due to the specific features of commodity assets. For instance, the possibility of shortages in supply may produce jumps in prices, leading to skewness in the returns of futures contracts.

Regarding the multivariate density model, we offer a flexible approach to specify the joint distribution of returns using conditional copula models. Copula functions help disentangle the particular characteristics of the univariate distributions of equity and commodity returns from their dependence structure. We combine conditional copula theory, as presented in Patton (2006a,b), with the implicit copula functions of multivariate normal mixtures defined by Demarta and McNeil (2005) and Embrechts, Lindskog, and McNeil (2003). As our most general model, we propose a conditional skewed t copula with generalized Student's t marginal distributions. Although the skewed t copula has very interesting properties, it has not been

[2]Some early works on how skewness affects portfolio selection include Samuelson (1970) and Kraus and Litzenberger (1976). Harvey and Siddique (2000) build on these ideas to provide an empirical test of the effect of co-skewness on asset prices. Barberis and Huang (2008) and Mitton and Vorkink (2007) also suggest, from different perspectives, that the skewness of individual assets may also influence investors' portfolio decisions.

previously used in this context. This copula model allows for asymmetric and tail dependence in a multivariate framework, and includes symmetric and linear dependence as special cases. Furthermore, the conditional set-up enable us to capture time-varying investment opportunities through time-varying moments and changes in the dependence parameters. These copula models are particularly easy to sample from, and therefore, we opt for solving numerically the optimization problem using Monte Carlo simulations.

We apply our theoretical approach to weekly data of crude oil and gold futures and the S&P 500 equity index, for the period from June 1990 to September 2010, reserving the observations from September 2006 to September 2010 for an out-of-sample performance evaluation. We examine four primary issues:

(1) Is there asymmetric and tail dependence among commodities and equity returns?
(2) Are there discrepancies in the optimal portfolio allocations between our conditional copula approach and other more traditional benchmarks, such as the equally weighted or Gaussian strategies?
(3) Do these discrepancies translate into economically relevant performance differences among methods?
(4) Is there a single key factor explaining these discrepancies?

First, our preliminary statistics and in-sample and out-of-sample results show evidence in favor of heavy tails and skewness in the univariate behavior and extreme and asymmetric dependence among oil, gold, and equity. Second, we also uncover substantial discrepancies between portfolio optimal weights of conditional t copulas and the portfolio weights provided by more conventional alternatives, especially for more aggressive investors and when there are no restrictions on short selling positions in equity. Third, in most cases, the discrepancies in portfolio weights translate into economically more profitable investment ratios and better relative performance measures with respect to the alternative procedures. Depending on the investor's preferences specification, the gains of considering the conditional copula model with tail and asymmetric dependence instead of the equally weighted portfolio represent up to 86 basis points per year for the period 2006-2010. When variance and loss aversion increase, portfolio strategies based on more flexible copulas are less likely to produce large performance differences. Fourth, no single factor offers a sufficient explanation of these differences. Rather, we find various explanatory elements, including, the specification of the univariate processes, in terms of conditional volatility, skewness, and fat tails; and the presence of tail and asymmetric dependence.

The remainder of this chapter is organized as follows: Section 2.1 formulates the investor's objective function and the portfolio choice problem. In Section 2.2, we describe the multivariate conditional copula model, the estimation methodology, and the numerical implementation. Section 2.3 presents the empirical application: the data description and preliminary statistics, the in-sample estimations, and the out-of-sample portfolio allocation results. We conclude in Section 2.4.

2.1 Portfolio choice with commodity futures and skewness

In this section, we present the portfolio selection problem of an investor with mean-variance-skewness preferences that takes positions in commodity futures and other risky spot contracts, such as stocks.

No money changes hands when futures are sold or bought; just a margin is posted to settle gains and losses. Without any upfront payment, it is not clear how to define the rate of return (Dusak (1973)). Following the common approach in the literature to analyze commodity futures as an asset class (Gorton and Rouwenhorst (2006); Hong and Yogo (2012)), we assume that long and short positions are fully collateralized. That is, the initial margin deposit corresponds with the overall notional value of the futures contract and indicates the initial capital investment related to that position (long or short). In this way, we control for the leverage involved in futures positions, and we can make fair comparisons with spot contracts.[3] Therefore, taking collateral in futures contracts into account would affect the computation of their rates of return and the budget constraint of the investor's problem, as we will see.

Formally, our portfolio choice problem can be formulated in terms of an investor who maximizes expected utility at period $t+1$ by building at time t a portfolio that includes two group of assets: a group with n commodity futures contracts, and another group with $N-n$ spot contracts, such as stocks. Taking the collateral into account, the gross return of a position in the commodity futures contract i at time $t+1$ is given by

$$(1+R_{i,t+1}) = \frac{S_{i,t+1}}{S_{i,t}}(1+R^f_{t+1}), \quad i = N-n+1,\ldots,N, \tag{2.1}$$

where $S_{i,t}$ and $S_{i,t+h}$ are the futures settlement prices at times t and $t+1$, respectively, and $(1+R^f_{t+1})$ is the gross return on cash over the period, or

[3]This assumption can also be relaxed, and smaller fractions of the nominal value can be considered in the problem set-up.

the interest earned on the initial margin deposit (Hong and Yogo (2012)). For this set of N investment opportunities, the wealth at time $t+1$ equals the gross return of the portfolio over the period, $1 + R_{t+1}(\boldsymbol{\omega}_t)$, defined as

$$1 + R_{t+1}(\boldsymbol{\omega}_t) = 1 + \sum_{j=1}^{N} \omega_t^j (\exp(r_{j,t+1}) - 1)\,, \tag{2.2}$$

where $\boldsymbol{\omega}_t = (\omega_t^1, \ldots, \omega_t^{N-n}, \omega_t^{N-n+1}, \ldots, \omega_t^N)'$ is the vector of portfolio weights (for spot and futures contracts), chosen at time t, and $r_{j,t+1} = \log(1 + R_{j,t+1})$ is the continuously compounded return of asset j over the period.

As is well known, returns on financial assets generally deviate from the Gaussian distribution, displaying heavy tails and skewness. This departure from normality is even greater in the case of commodities, magnified by the well-documented presence of positive and negative spikes in the data-generating process of commodity returns (see for example Cartea and Figueroa (2005) and Casassus and Collin-Dufresne (2005), among others). The fundamentals underlying commodity price formation are key determinants of these statistical properties. Accordingly, the presence of jumps can be explained by the convex relation between commodity prices and the balance among supply, inventories, and demand (see Routledge, Seppi, and Spatt (2000)). Thus, adding commodity assets to traditional portfolios will constitute a significant source of skewness for the portfolio's returns, increasing the importance of considering the third moment in the portfolio selection problem.

For that reason, in our approach, the investor's objective consists of choosing a wealth allocation $\boldsymbol{\omega}_t = (\omega_t^1, \ldots, \omega_t^N)$ that maximizes the expected portfolio return penalized for the variance and negative skewness of the portfolio returns. That is, for each time t, the optimal weights are given by

$$\boldsymbol{\omega}_t^* = \underset{\boldsymbol{\omega}_t \in \mathcal{D}}{\arg\max} \left(\mathbb{E}_t[R_{t+1}(\boldsymbol{\omega}_t)] - \varphi_{\mathrm{V}} \operatorname{Var}_t[R_{t+1}(\boldsymbol{\omega}_t)] + \varphi_{\mathrm{S}} \operatorname{Skew}_t[R_{t+1}(\boldsymbol{\omega}_t)] \right), \tag{2.3}$$

where $\mathbb{E}_t(\cdot)$, $\operatorname{Var}_t(\cdot)$, and $\operatorname{Skew}_t(\cdot)$ are the first three moments of the portfolio returns conditioned on the information set $\mathcal{F}_t$ available at time t. The parameters $\varphi_{\mathrm{V}} \geqslant 0$ and $\varphi_{\mathrm{S}} \geqslant 0$ determine the impact of variance (traditional risk aversion) and skewness (loss aversion) on the investor's utility. By adding aversion to negative skewness, we acknowledge the possibility that an investor might accept a lower expected return if there is a chance of high positive skewness, such as in the form of a large probability of positive jumps.

As in Harvey, Liechty, Liechty, and Müller (2010), the parameters φ_{V} and φ_{S} in the objective function of equation (2.3) can take arbitrary values to

describe particular investor's preferences. Alternatively, following Guidolin and Timmermann (2008) and Jondeau and Rockinger (2012), among others, the three-moment preferences assumption could be interpreted as the expected value of the third order Taylor series expansion of a power utility function with coefficient of risk aversion $\mathcal{A}$. That is,

$$\begin{aligned}\mathbb{E}[U(1+R_{t+1}(\boldsymbol{\omega}_t))] \approx \mathbb{E}(R_{t+1}(\boldsymbol{\omega}_t)) - \frac{\mathcal{A}}{2}\,\mathbb{E}(R_{t+1}(\boldsymbol{\omega}_t)^2) \\ + \frac{\mathcal{A}(\mathcal{A}+1)}{6}\,\mathbb{E}(R_{t+1}(\boldsymbol{\omega}_t)^3).\end{aligned} \tag{2.4}$$

where $U(W) = \frac{W^{1-\mathcal{A}}}{1-\mathcal{A}}$ for $\mathcal{A} > 1$ and $U(W) = \log(W)$ for $\mathcal{A} = 1$. In this case, the impact of variance and skewness in the investor's decision rule would be a function of the coefficient of risk aversion $\mathcal{A}$ ($\varphi_{\mathrm{V}} = \frac{\mathcal{A}}{2}$ and $\varphi_{\mathrm{S}} = \frac{\mathcal{A}(\mathcal{A}+1)}{6}$).

Finally, in equation (2.3), the domain $\mathcal{D} \subset \mathbb{R}^N$ represents the budget constraint defined by

$$\mathcal{D} = \Big\{(\omega_t^1, \ldots, \omega_t^N) : \sum_{j=1}^{N-n} \omega_t^j + \sum_{i=N-n+1}^{N} \left|\omega_t^i\right| = 1\Big\}. \tag{2.5}$$

Because both long and short positions in commodity futures contracts require the same initial collateral, we have to take the absolute value of the futures weights $(\omega_t^{N-n+1}, \ldots, \omega_t^N)$, such that short positions in futures contracts cannot be used to increase holdings of other assets. Furthermore, if the investor is short-sales constrained, the weights of spot contracts must satisfy that $(\omega_t^1, \ldots, \omega_t^{N-n}) \in [0,1]^{N-n}$.

Once we have the set-up of the investor's problem, we need to define density forecasts of the returns joint distribution in order to compute the optimal portfolio weights. In the next section, we describe our multivariate density model.

2.2 Multivariate conditional copula with asymmetry

We employ multivariate conditional copulas to obtain a flexible model for the multivariate distribution of assets' log-returns $\boldsymbol{r}_{t+1} = (r_{1,t+1}, \ldots, r_{d,t+1})$, where $d \leqslant N$ is the number of risky assets. Every d-variate distribution consists of d marginal distribution functions or *margins* that describe each univariate behavior, as well as a joint dependence function that defines the relations among individual processes. Unlike traditional multivariate distributions, such as the Gaussian and Student's t distributions, copula

models support the construction of multivariate distributions with arbitrary univariate processes and dependence.

Formally, a d-variate copula is a d-dimensional distribution function on the unit interval $[0,1]^d$, that is, a joint distribution with d uniform marginal distributions. Consider a multivariate conditional distribution $F_t(r_{1,t+1}, \ldots, r_{d,t+1})$ formed by d univariate conditional distributions $F_{i,t}(r_{i,t+1})$, where the subscript t denotes that joint and marginal distributions are conditioned on the information set $\mathcal{F}_t$ available at time t. Following Patton (2006b), there must exist a function C_t that maps the domain $[0,1]^d$ toward the interval $[0,1]$, called the *conditional copula*, such that

$$F_t(r_{1,t+1}, \ldots, r_{d,t+1}) = C_t\left(F_{1,t}(r_{1,t+1}), \ldots, F_{d,t}(r_{d,t+1})\right) . \tag{2.6}$$

This expression constitutes a d-dimensional extension of Sklar's (1959) theorem for conditional copulas.[4]

Using the expression in equation (2.6), any copula C_t can be employed to define a joint distribution $F_t(\boldsymbol{r}_{t+1})$ with the arbitrary marginal distributions $F_{1,t}, \ldots, F_{d,t}$. Thus, using a bottom-up approach, we model the marginal distributions of asset returns, followed by the conditional copula function that describes their dependence structure.

2.2.1 Modeling univariate processes

We first specify the univariate distribution functions of the asset returns $\boldsymbol{r}_{t+1}$. Our multivariate copula model supports the use of various marginal distributions. Thus we can attend to the particular characteristics of each asset return, which is an useful feature when different types of assets appear in the portfolio, such as commodities and stocks. We present a marginal distribution model that captures individual skewness and heavy tails, as well as time-varying moments. We build on the autoregressive conditional density models of Hansen (1994), Harvey and Siddique (1999), and Jondeau and Rockinger (2003), and we propose a generalized Student's t distribution with possibly time-varying parameters. Thus, the univariate process for each

[4]This generalization of Sklar's theorem is a direct application of the concept of a conditional copula (Patton (2006b), Theorem 1) to a multivariate case (Nelsen (2006), Theorem 2.10.9), and requires simply that conditioning variables be the same for all marginal distributions and the copula. If margins are continuous, this copula is unique.

asset returns $r_{i,t+1}$ $(i = 1, \ldots, d)$ can be expressed as follows:

$$r_{i,t+1} = \mu_{i,t+1} + \sqrt{\sigma^2_{i,t+1}}\, z_{i,t+1}\,, \tag{2.7}$$

$$\mu_{i,t+1} \equiv \mathbb{E}_t\left(r_{i,t+1}\right) = \mu_{0,i} + \boldsymbol{\beta}_i' \boldsymbol{X}_t + \sum_{j=1}^{p} \Phi_{i,j} r_{i,t+1-j}\,, \tag{2.8}$$

$$\begin{aligned}\sigma^2_{i,t+1} &\equiv \mathrm{Var}_t\left(r_{i,t+1}\right) \\ &= \alpha_{0,i} + \alpha^+_{1,i}\,\sigma^2_{i,t} z^2_{i,t}\,\mathbb{1}_{\{z_{i,t}\geqslant 0\}} + \alpha^-_{1,i}\,\sigma^2_{i,t} z^2_{i,t}\,\mathbb{1}_{\{z_{i,t}<0\}} + \alpha_{2,i}\,\sigma^2_{i,t}\,,\end{aligned} \tag{2.9}$$

$$z_{i,t+1} \sim g_{i,t}(z_{i,t+1}\,;\, \nu_{i,t+1}\,, \lambda_{i,t+1})\,, \tag{2.10}$$

where $\mu_{i,t+1}$ and $\sigma^2_{i,t+1}$ are the mean and variance conditioned on $\mathcal{F}_t$ for the i-th asset returns, and $z_{i,t+1}$ is the corresponding residual.

The conditional mean, defined in equation (2.8), is a linear function of p lagged returns, $r_{i,t+1-j}$ $(j = 1, \ldots, p)$, and m further explanatory variables $\boldsymbol{X}_t$, with the coefficients $\Phi_{i,j}$ and $\boldsymbol{\beta}_i$, respectively, and the drift parameter $\mu_{0,i}$. This specification can capture the possible presence of autocorrelation and predictability in asset returns. As the exogenous regressors $\boldsymbol{X}_t$, we consider explanatory variables employed in previous literature (Hong and Yogo (2012)) to predict variation in stocks and commodity futures returns, including the short rate, default spread, momentum, basis, and growth in open interest (see Appendix A.2 for a detailed definition of the explanatory variables).

As we describe in equation (2.9), we employ an asymmetric or leveraged GARCH dynamic for the conditional variance. This specification is designed to account for volatility clustering and leverage effects, such as possible asymmetric responses to positive and negative shocks that have occurred in the previous period (Campbell and Hentschel (1992)).[5] equation (2.10) then denotes that the univariate innovations $z_{i,t+1}$ are drawn from a generalized Student's t distribution, $g_{i,t}$, which can capture heavy tails and individual skewness through the degrees of freedom ν_i and asymmetry parameter λ_i (Hansen (1994)).[6]

Finally, our specification of the marginal distributions addresses the

[5]To guarantee positive and stationary volatility, the parameters of the variance dynamics in equation (2.9) must satisfy the following constraints: $\alpha_{0,i} > 0$; $\alpha^+_{1,i}, \alpha^-_{1,i}, \alpha_{2,i} \geqslant 0$; and $\alpha_{2,i} + (\alpha^+_{1,i} + \alpha^-_{1,i})/2 < 1$.

[6]The technical details of this univariate distribution can also be found in Jondeau and Rockinger (2003). We summarize them briefly in Appendix A.1.

possibility of time-varying higher moments as follows:

$$\nu_{i,t+1} = \Lambda_{(2,\infty)}\Big(\delta_{0,i} + \delta^{+}_{1,i}\, z_{i,t}\, \mathbb{1}_{\{z_{i,t}\geqslant 0\}} + \delta^{-}_{1,i}\, z_{i,t}\, \mathbb{1}_{\{z_{i,t}<0\}} + \delta_{2,i}\Lambda^{-1}_{(2,\infty)}(\nu_{i,t})\Big)\,, \tag{2.11}$$

$$\lambda_{i,t+1} = \Lambda_{(-1,1)}\Big(\zeta_{0,i} + \zeta^{+}_{1,i}\, z_{i,t}\, \mathbb{1}_{\{z_{i,t}\geqslant 0\}} + \zeta^{-}_{1,i}\, z_{i,t}\, \mathbb{1}_{\{z_{i,t}<0\}} + \zeta_{2,i}\Lambda^{-1}_{(-1,1)}(\lambda_{i,t})\Big)\,, \tag{2.12}$$

where $\delta_{0,i}, \delta^{+}_{1,i}, \delta^{-}_{1,i}, \delta_{2,i}, \zeta_{0,i}, \zeta^{+}_{1,i}, \zeta^{-}_{1,i}$ and $\zeta_{2,i}$ are constant parameters, and $y \equiv \Lambda_{(l,u)}(x) = (u + l\mathrm{e}^{x})/(1+\mathrm{e}^{x})$ denotes the modified logistic map designed to keep the transformed variable y in the domain (l,u) for all $x \in \mathbb{R}$. Thus, shape parameters $\nu_{i,t+1}$ and $\lambda_{i,t+1}$ may depend on their lagged values and react differently to positive and negative shocks. This general specification also includes some well-known univariate distributions as particular cases. For instance, if the asymmetry parameter goes to 0, we obtain the symmetric Student's t distribution; as degrees of freedom tend to infinity, we would converge to a Gaussian distribution.

2.2.2 Modeling copula functions

In this section, we present the copula functions that determine the dependence structure of our model. Following Sklar's theorem in equation (2.6), the copula function acts like a joint distribution of the probability transformed vector $(F_{1,t}(r_{1,t+1}), \ldots, F_{d,t}(r_{d,t+1})'$, where $F_{i,t}(r_{i,t+1})$ are the marginal distribution functions of asset returns $r_{i,t+1}$, as described in equations (2.7)-(2.10). In particular, we employ three multivariate copula functions: two well-known elliptical copulas, the Gaussian and the t copula (Embrechts, Lindskog, and McNeil (2003)), and an asymmetric multivariate dependence, the so-called skewed t copula (Demarta and McNeil (2005)). They are all implicit dependence functions of various multivariate normal mixtures. More specifically, they are the parametric copula functions contained in the multivariate Gaussian, Student's t, and generalized hyperbolic skewed t distributions, respectively.

Through a direct application of Sklar's theorem, we can obtain these implicit copulas by evaluating a given multivariate distribution (e.g., generalized hyperbolic skewed t) at the quantile functions of its corresponding marginal distributions. For instance, the skewed t copula is given by:

$$C^{\mathrm{SK}}(\, u_1, \ldots, u_d \,;\boldsymbol{P}, \nu, \boldsymbol{\gamma}\,) = H(\, H_1^{-1}(u_1\,;\nu,\gamma_1), \ldots, H_d^{-1}(u_d\,;\nu,\gamma_d)\,;\boldsymbol{P},\nu,\boldsymbol{\gamma}\,)\,, \tag{2.13}$$

where $H(\cdot\,; \boldsymbol{P}, \nu, \boldsymbol{\gamma})$ is the generalized hyperbolic skewed t distribution with $d \times d$ correlation matrix $\boldsymbol{P}$, degrees of freedom ν, and d-dimensional asymmetry parameter vector $\boldsymbol{\gamma} = (\gamma_1, \ldots, \gamma_d)$. The $H_i(\cdot\,; \nu, \gamma_i)$ are the d univariate skewed t distributions, the H_i^{-1} are the corresponding quantile functions, and $(u_1, \ldots, u_d)'$ is the probability-transformed vector. Similarly, we can extract the Gaussian and t copulas, $C^{\mathrm{G}}(u_1, \ldots u_d\,; \boldsymbol{P})$ and $C^{\mathrm{T}}(u_1, \ldots u_d\,; \boldsymbol{P}, \nu)$, from their respective multivariate distributions.

In Appendix A.3, we derive explicitly the density functions of these three copulas. For illustrative purposes, in Figure 2.1, we present the contour plots and probability density functions of these copulas for a two-dimensional case. Although the examples in Figure 2.1 are for a bivariate case, a useful property of all three copulas considered is that they can be employed directly to specify the dependence structure of an arbitrary number of risky assets.

As Figure 2.1 reveals, using these three copulas, we can model three different types of dependence. The Gaussian copula, $C^{\mathrm{G}}(\cdot\,; \boldsymbol{P})$, defines linear, symmetric dependence, completely determined by the correlation matrix $\boldsymbol{P}$. Thus it is unable to capture tail dependence or asymmetries. The t copula, $C^{\mathrm{T}}(\cdot\,; \boldsymbol{P}, \nu)$, is also elliptically symmetric but allows for tail dependence through the degrees-of-freedom parameter, ν. The plots in Figure 2.1 show that the t copula assigns more probability to the extremes than does the Gaussian copula. The greater the degrees of freedom, the smaller the level of tail dependence, converging in the limit $\nu \to \infty$ to the Gaussian copula. Finally, the skewed t copula, $C^{\mathrm{SK}}(\cdot\,; \boldsymbol{P}, \nu, \boldsymbol{\gamma})$, can capture extreme and asymmetric dependence of the asset returns. Through the d-dimensional vector of asymmetry parameters $\boldsymbol{\gamma}$, the skewed t copula can assign more weight to one tail than the other. For example, in Figure 2.1, all elements of the asymmetry vector are negative, and therefore, the density contour is clustered in the negative-negative quadrant. Eventually, if $\boldsymbol{\gamma} \to \mathbf{0}$, asymmetric dependence goes to 0, and we recover the symmetric t copula.

Once we have defined the functional forms of the three implicit copulas, we can build the multivariate distribution model for our vector of asset returns. This multivariate distribution forms from the marginal distributions of the previous section and one of the implicit copulas we described previously. In addition, following pioneering works by Patton (2006a,b), we can parametrize time variation in the conditional copula function of our multivariate model. For that purpose, and in the spirit of Engle's (2002) dynamic conditional correlation model, we extend the notion to other types of dependence beyond the Gaussian one and allow that the dependence matrix $\boldsymbol{P}_t$ of our conditional copula may evolve over time, according to some GARCH-type process. In the most general case, the vector of return innovations,

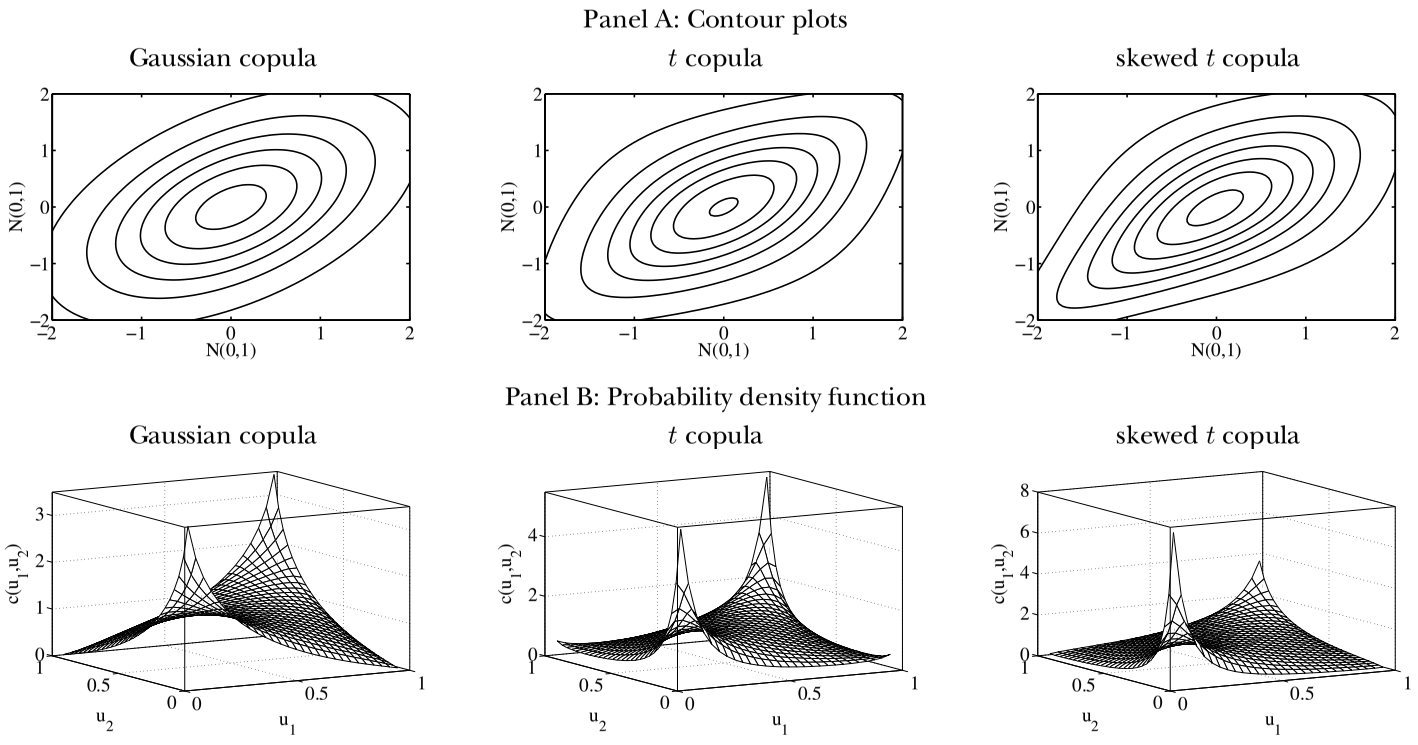

Figure 2.1. Copula functions

Panel A shows the contour plots of the distribution for three copulas: Gaussian, t, and skewed t. To compare just the copula function, all of them are evaluated using standard normal marginal distributions, N(0,1). Panel B shows a bivariate representation of the probability density function $c(u_1, u_2)$ for the three copulas. The next parameters have been employed: $\rho = 0.5$ for the Gaussian copula, $\nu = 5$ and $\rho = 0.5$ for the t copula, and $\nu = 5$, $\boldsymbol{\gamma} = (-0.5, -0.5)'$, and $\rho = 0.5$ for the skewed t copula.

$\boldsymbol{z}_{t+1} = (z_{1,t+1}, \ldots, z_{d,t+1})'$, follows the distribution specification:

$$\begin{aligned}\boldsymbol{z}_{t+1} \;\sim\; C_t^{\mathrm{SK}}\big(\, & g_{1,t}(z_{1,t+1}\,;\nu_{1,t+1},\lambda_{1,t+1}),\;\ldots,\\ & g_{d,t}(z_{d,t+1}\,;\nu_{d,t+1},\lambda_{d,t+1})\,;\,\boldsymbol{P}_{t+1},\nu,\boldsymbol{\gamma}\,\big)\,,\end{aligned} \tag{2.14}$$

where the $g_{i,t}(z_{i,t+1}\,;\nu_{i,t+1},\lambda_{i,t+1})$ are the conditional univariate distributions in equation (2.10), and the evolution equation for $\boldsymbol{P}_{t+1}$ is given by:

$$\boldsymbol{P}_{t+1} = \Lambda_{(-1,1)}\Big(\,\omega_0\,\boldsymbol{P}_{\mathrm{c}} + \omega_1\,\frac{1}{M}\sum_{m=1}^{M}\boldsymbol{x}_{t+1-m}\,\boldsymbol{x}'_{t+1-m} + \omega_2\,\boldsymbol{P}_t\,\Big). \tag{2.15}$$

In this case, $\boldsymbol{x}_t$ is the vector of transformed variables, $(H^{-1}(u_{1,t};\nu,\gamma_1),\ldots,$ $H^{-1}(u_{d,t};\nu,\gamma_d)\,)'$; $\boldsymbol{P}_{\mathrm{c}}$ is the constant correlation matrix; ω_0,ω_1 and ω_2 are constant parameters; and M is the number of lags we consider. The modified logistic function $\Lambda_{(-1,1)}(\cdot)$ ensures that the elements of $\boldsymbol{P}_{t+1}$ remain in the domain $(-1,1)$.

2.2.3 Model estimation and portfolio optimization

Our model structure, formed by the marginal distributions and the copula, allows for a two-step estimation procedure, similar to the conditional setups of Jondeau and Rockinger (2006) and Patton (2006a). In the first step, we obtain the maximum likelihood (ML) estimates of the individual processes; then, we determine the parameter estimates of the copula function.[7] From this ML approach, we can compute the asymptotic and robust standard errors for the estimates.

Formally, this procedure can be expressed as follows: Let $\bar{\boldsymbol{r}}_T = \{\boldsymbol{r}_1,$ $\ldots, \boldsymbol{r}_T\}$ be the sample of returns of length T, where $\boldsymbol{r}_t = (r_{1,t},\ldots,r_{d,t})$ for $i = 1,\ldots,T$. We want to find the set of parameter estimates $\widehat{\boldsymbol{\theta}}$ that maximizes the log-likelihood function $\mathcal{L}$, that is,

$$\widehat{\boldsymbol{\theta}} \equiv \arg\max_{\boldsymbol{\theta}\in\boldsymbol{\Theta}}\,\mathcal{L}(\boldsymbol{\theta}\,;\bar{\boldsymbol{r}}_T) = \arg\max_{\boldsymbol{\theta}\in\boldsymbol{\Theta}}\sum_{t=1}^{T}\log f_t(\boldsymbol{r}_{t+1};\boldsymbol{\theta})\,, \tag{2.16}$$

where $f_t(\boldsymbol{r}_{t+1};\boldsymbol{\theta})$ is the probability density function of the multivariate model conditioned by the information set $\mathcal{F}_t$ and parameterized by $\boldsymbol{\theta}\in\boldsymbol{\Theta}$.

[7] This procedure is also known as the inference functions for margins method. A similar two-stage approach is used to estimate some multivariate GARCH models, such as the constant (CCC) and dynamic (DCC) conditional correlation models (see Engle and Sheppard (2001)).

From the assumptions of Sklar's theorem in equation (2.6), we can decompose the log-likelihood function $\mathcal{L}$ in equation (2.16) into two parts, the margins and the copula (see the details in Appendix A.4):

$$\begin{aligned}\mathcal{L}(\boldsymbol{\theta}_M, \boldsymbol{\theta}_C\,; \bar{\boldsymbol{r}}_T) &= \sum_{i=1}^{d} \mathcal{L}_i(\boldsymbol{\theta}_{i,M}; \bar{\boldsymbol{r}}_T) + \mathcal{L}_C(\boldsymbol{\theta}_C; \boldsymbol{\theta}_M, \bar{\boldsymbol{r}}_T) \\ &= \sum_{i=1}^{d}\sum_{t=1}^{T} \log f_{i,t}(r_{i,t+1}\,\boldsymbol{\theta}_{i,M}) \\ &\quad + \sum_{t=1}^{T} \log c_t(u_{1,t+1}, \ldots, u_{d,t+1}\,; \boldsymbol{\theta}_C). \end{aligned} \tag{2.17}$$

where $\mathcal{L}_i$ and $\mathcal{L}_C$ are the log-likelihood functions for the i-th marginal process and the copula, $\boldsymbol{\theta}_M$ denotes the set of parameters corresponding to the d marginal distributions, $(\boldsymbol{\theta}_{1,M}, \ldots, \boldsymbol{\theta}_{d,M})'$, and $\boldsymbol{\theta}_C$ denotes the parameters of the copula function. The $u_{i,t+1}$ are the marginal distributions, $F_{i,t}(r_{i,t+1}\,; \boldsymbol{\theta}_{i,M})$, with corresponding marginal density functions $f_{i,t}(r_{i,t+1}; \boldsymbol{\theta}_{i,M})$; and $c_t(\cdot\,; \boldsymbol{\theta}_C)$ is the copula density function.

Once we have estimated the model density function, we use this information to obtain the optimal portfolio. For our parametric density models, the integrals defining the portfolio return moments involved in the investor's optimization problem of equation (2.3) do not have a closed-form solution. Using Monte Carlo simulations to estimate the value of these integrals, we can solve numerically the optimization problem. In this respect, an advantage of our implicit copulas is that it is easy to sample from them, as long as we are able to sample from the normal mixture distribution from which they are extracted. The following procedure outlines the implementation of the model estimation and the portfolio optimization:

1. Following equation (2.17), estimate sequentially the d marginal distributions models and the copula function:[8]

$$\widehat{\boldsymbol{\theta}}_{i,M} = \arg\max\, \mathcal{L}_i(\boldsymbol{\theta}_{i,M}; \bar{\boldsymbol{r}}_T)\,, \text{ for } i = 1, \ldots, d\,, \text{ and}$$
$$\widehat{\boldsymbol{\theta}}_C = \arg\max\, \mathcal{L}_C(\boldsymbol{\theta}_C; \widehat{\boldsymbol{\theta}}_M, \bar{\boldsymbol{r}}_T)\,.$$

   Some remarks should be considered though. First, the quality of the copula estimation depends strongly on the goodness of fit of the parametric functions we use for the marginal distribution models. Second,

[8] Patton (2006a) shows that one-step maximum likelihood estimators and two-stage estimators are equally asymptotically efficient.

t copulas require the estimation of shape parameters ν and $\boldsymbol{\gamma}$, apart from the correlation matrix $\boldsymbol{P}$; in these cases, because the objective function often falls in local maximums, convergence difficulties may arise when maximizing the log-likelihood function $\mathcal{L}_C$ directly. To overcome this problem, we perform the estimation of the t copulas using an iterative procedure: An inner function computes $\boldsymbol{P}$ maximizing the likelihood given the values of the shape parameters; then, this function is maximized with respect to the shape parameters.[9]

2. Use the parameter estimates $\widehat{\boldsymbol{\theta}} = (\widehat{\boldsymbol{\theta}}_M, \widehat{\boldsymbol{\theta}}_C)'$ and the dynamics of the return vector $\boldsymbol{r}_{t+1}$, defined in equations (2.7)-(2.10) and (2.14), to obtain the forecast density for the next period; then, generate Q=10,000 independent draws $\{\boldsymbol{r}_t^q\}_{q=1}^Q$ sampling from that density:

   (i) Generate Q random vectors $\{\boldsymbol{u}_{t+1}^q\}_{q=1}^Q$ from the implicit copulas. For example, for the skewed t copula: $\boldsymbol{u}_{t+1}^q = (H_1(x_1^q; \widehat{\nu}, \widehat{\gamma}_1), \ldots, H_d(x_d^q; \widehat{\nu}, \widehat{\gamma}_d))$, where the $(x_1^q, \ldots, x_d^q)$ are random vectors from the multivariate distribution $H(\mathbf{0}, \widehat{\boldsymbol{P}}, \widehat{\nu}, \widehat{\boldsymbol{\gamma}})$ generated using equation (A.8).[10] Similarly, we can sample from the Gaussian and t copulas.

   (ii) Use the inverse functions of the conditional marginal distributions to obtain Q draws of the innovations $\{\boldsymbol{z}_t^q\}_{q=1}^Q$, where $\boldsymbol{z}_{t+1}^q = (g_{1,t}^{-1}(u_{1,t+1}^q; \widehat{\nu}_1, \widehat{\lambda}_1), \ldots, g_{d,t}^{-1}(u_{d,t+1}^q; \widehat{\nu}_d, \widehat{\lambda}_d))$; then employ the forecast conditional mean and variance to generate $\{\boldsymbol{r}_t^q\}_{q=1}^Q$.

3. To obtain the optimal portfolio weights $\boldsymbol{\omega}_t^*$, maximize the investor's objective function in equation (2.3) subject to the non-linear budget constraint of equation (2.5) using the generated simulations to estimate the moments of the portfolio return.

[9]Furthermore, we employ a global optimization approach, consisting of simulated annealing (Goffe, Ferrier, and Rogers (1994)), to check the validity of the local optimization results.

[10]Note that, for the estimation and simulation of the skewed t copula, to improve the feasibility of the computations related to the cumulative density and inverse functions of the univariate generalized hyperbolic skewed t distribution, H_i and H_i^{-1}, we approximate its density function h_i using cubic splines.

2.3 Empirical application

In this section, we first present the data and their main univariate and multivariate statistical properties. Then, we estimate the conditional copula models and analyze their in-sample fitting performance. Finally, we solve the portfolio problem for the copula models numerically and obtain the optimal weights, investment ratios, and relative performance measures over the out-of-sample period.

2.3.1 Data and preliminary analysis

Our empirical application relies on three risky assets: two commodity futures, oil and gold, and the S&P 500 equity index. The oil futures correspond to West Texas Intermediate (WTI) crude oil from the New York Mercantile Exchange (NYMEX). The gold futures correspond to the gold bar, with a minimum of 0.995 fineness, from the New York Commodities Exchange (COMEX). These futures are two of the most actively traded commodity contracts in the world, and they do not have tight restrictions on the size of daily price movements.[11] In both cases, we employ the most liquid futures contracts, measured by daily trading volume, of all maturities available. The risk-free rate is computed from the three-month U.S. Treasury bills provided by the Federal Reserve System. All data are in U.S. dollars and came from Thomson-Reuters Datastream. The sample period considered ranges from June 20, 1990 to September 8, 2010, for a total of 1056 weekly observations. We divided the sample in two subperiods, such that the period from June 20, 1990 to June 20, 2006 (836 observations) supported the in-sample estimation analyses of the models, and the remaining 220 observations from June 20, 2006 to September 8, 2010 were reserved for the out-of-sample portfolio performance exercise.

Univariate analysis

We first analyze the univariate behavior of the three asset returns. In the online Appendix, we report the summary statistics for the weekly returns of the gold and oil futures and the equity index for the sample periods, as well

[11] At the end of 2011, gold and crude oil futures represented 30% of the Dow Jones-UBS Commodity Index and 38% of the S&P-Goldman Sachs Commodity Index.

Table 2.1. Descriptive statistics for oil, gold, and equity weekly returns

This table reports sample statistics of the weekly returns for the crude oil futures (NYMEX), gold futures (COMEX), and equity index (SP500). The full sample period ranges from June 1990 to September 2010, and includes 1056 observations. The in-sample period runs from June 1990 to June 2006 (836 observations) and the out-of-sample period from June 2006 to September 2010 (220 observations). *Mean, Std. Dev., Min., Max., and VaR 5%* are expressed in weekly percentages. *Sharpe* is the ratio of mean returns over the standard deviation. *JB* and *KS* refer to the Jarque-Bera and Kolmogorov-Smirnov normality test statistics, respectively. *LB(10)* and *LM(10)* are the Ljung-Box and the Lagrange-Multiplier test statistics, both conducted using 10 lags, to test for the presence of autocorrelation in returns and squared returns, respectively. The *p-values* are reported in parentheses.

	Full sample: 1990–2010			In-sample: 1990–2006			Out-of-sample: 2006-2010		
Assets	oil	gold	equity	oil	gold	equity	oil	gold	equity
Mean	0.136	0.120	0.104	0.163	0.061	0.147	0.033	0.343	-0.059
	(0.341)	(0.082)	(0.145)	(0.285)	(0.353)	(0.045)	(0.929)	(0.114)	(0.766)
Std. Dev.	4.634	2.236	2.326	4.401	1.896	2.129	5.441	3.210	2.958
Min.	-36.53	-13.21	-16.45	-36.53	-11.04	-9.04	-16.63	-13.21	-16.45
Max.	23.98	12.88	10.18	14.55	12.88	10.18	23.98	10.92	9.639
Sharpe	0.029	0.054	0.045	0.037	0.032	0.069	0.006	0.107	-0.020
VaR 5%	6.892	3.294	3.744	6.494	2.737	3.483	7.717	4.753	4.931
Skewness	-0.598	0.007	-0.552	-0.929	0.102	-0.134	0.114	-0.205	-1.024
	(0.000)	(0.927)	(0.000)	(0.000)	(0.229)	(0.115)	(0.489)	(0.215)	(0.000)
Kurtosis	8.259	7.343	7.238	9.860	8.258	5.000	4.914	4.536	8.012
	(0.000)	(0.000)	(0.000)	(0.000)	(0.000)	(0.000)	(0.000)	(0.000)	(0.000)
JB	1280	829.8	843.9	1759	964.3	141.9	34.06	23.18	268.7
	(0.000)	(0.000)	(0.000)	(0.000)	(0.000)	(0.000)	(0.000)	(0.002)	(0.000)
KS	0.446	0.467	0.469	0.450	0.473	0.470	0.442	0.459	0.467
	(0.000)	(0.000)	(0.000)	(0.000)	(0.000)	(0.000)	(0.000)	(0.000)	(0.000)
LB(10)	27.93	25.97	29.98	14.27	29.12	24.05	35.99	17.08	22.55
	(0.002)	(0.004)	(0.001)	(0.161)	(0.001)	(0.007)	(0.000)	(0.073)	(0.013)
LM(10)	90.38	189.6	138.7	54.76	72.11	84.29	39.40	64.06	31.52
	(0.000)	(0.000)	(0.000)	(0.000)	(0.000)	(0.000)	(0.000)	(0.000)	(0.000)

as, plots of the relative price moves of each asset over the full-sample period. Here, we summarize the main findings.

Table 2.1 reports summary statistics for the weekly returns of the gold and oil futures and the equity index for the sample periods. With Exhibit 1 of Figure 2.2, we display the relative price moves of each asset over the full-sample period.

We observe substantial changes in the sample moments of returns over time. The mean returns are all positive, except for equity during the out-of-sample period (Jun. 2006 – Sep. 2010). Returns volatilities per week for oil, gold, and equity increased from 4.4%, 1.9%, and 2.1% in the in-sample period to 5.4%, 3.2%, and 3.0% during the out-of-sample period. Looking at the ratio of the mean over the volatility (Sharpe's ratio), we find that for the in-sample observations, equity (0.07) performs better than oil (0.04) and gold (0.03). This pattern changed during the 2006-2010 period, during which ratios of oil (0.01) and equity (-0.02) were below their historical average, whereas gold's ratio (0.11) moved significantly above its historical average. According to the Ljung-Box (LB) and Lagrange multiplier (LM) statistics, reported in Table 2.1, there is evidence of serial correlation in the returns and squared returns for all time series (except for oil returns over the in-sample period).

Assets returns are non-normal, skewed, and heavy tailed. According to the Jarque-Bera (JB) and Kolmogorov-Smirnov (KS) tests, normality in the returns' unconditional distribution is strongly rejected for all samples. Skewness and kurtosis of returns differs across assets and sample periods. From the in-sample to the out-of-sample period, the equity returns' skewness grew much more negative, while gold returns changed from positive to negative skewness, and oil returns from negative to positive. During 2006-2010, the oil and gold returns' kurtosis decreased with respect to the previous period, but equity returns' kurtosis strongly increased, as expected.

Multivariate analysis

It is also important to describe the interactions observed in the sample among the oil, gold, and equity index returns. In Table 2.2, we report some multivariate statistics and preliminary tests for the three-dimensional vector of asset returns. We first focus on the characteristics of the linear dependence; then we turn to analyzing non linear features observed in the vector of returns. Technical details of the multivariate statistics and tests for the three-dimensional vector of asset returns are reported in Appendix A.5.

Exhibit 1: Relative price movements

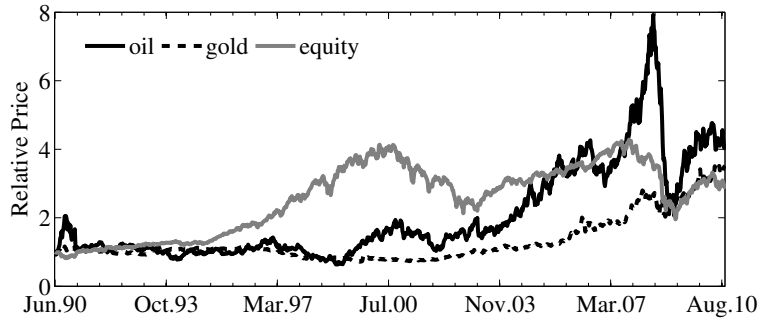

Exhibit 2: qq-plot to test ellipticity

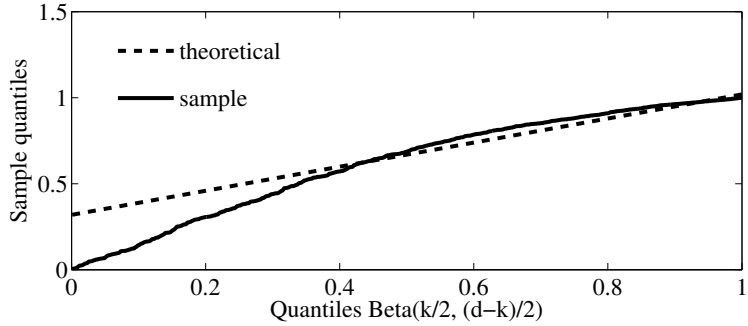

Exhibit 3: qq-plot to test multivariate normality

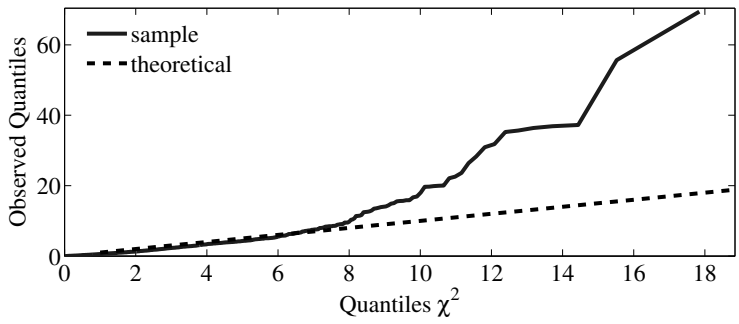

Figure 2.2. Descriptive statistics: relative price performace and qq-plots
Exhibit 1 plots the relative price movement of each asset to compare their performance over the full-sample period. Exhibit 2 compares the qq-plot of sample against the beta distribution, where $d = 3$ is the dimension of the vector of returns, and k is chosen to be roughly equal to $d - k$ (see McNeil, Frey, and Embrechts (2005)). The empirical observations are denoted by the solid line; the theoretical quantiles are represented by the dashed line. Exhibit 3 shows the qq-plot associated with Mardia's (1970) test of multivariate normality.

Table 2.2. Descriptive multivariate statistics for oil, gold, and equity weekly returns

This table reports the descriptive multivariate statistics of crude oil, gold, and equity index weekly returns. The full sample period ranges from June 1990 to September 2010 and includes 1056 observations. The in-sample period runs from June 1990 to June 2006, and the out-of-sample period from June 2006 to September 2010. Panel A shows the sample correlation for each period. In Panel B, we present the results of the Engle and Sheppard (2001) test for constant correlation. The *p-values* reported in parentheses indicate the probability of constant correlation. In Panel C, we report the results of the Mardia (1970) test of joint normality, which is based on the multivariate measures of skewness and kurtosis, denoted by s_3 and k_3. In Panel C, we also present the Kolmogorov-Smirnov (*KS*) statitics associated with the test of ellipticity (see McNeil, Frey, and Embrechts (2005)). In Panel D, we present the estimates of the upper and lower tail dependence parameters, τ^U and τ^D, of the symmetrized Joe-Clayton (SJC) copula (Patton (2006b)) for each pair of asset returns: oil-gold (o-g), oil-equity (o-e), and gold-equity (g-e).

	Full sample: 1990-2010			In-sample: 1990-2006			Out-of-sample: 2006-2010		
Panel A: Unconditional correlation									
i	oil	gold	equity	oil	gold	equity	oil	gold	equity
$\rho_{i,\text{oil}}$	1.000	0.268	0.080	1.000	0.205	-0.061	1.000	0.394	0.393
		(0.000)	(0.009)		(0.000)	(0.079)		(0.000)	(0.000)
$\rho_{i,\text{gold}}$		1.000	0.012		1.000	-0.079		1.000	0.165
			(0.698)			(0.022)			(0.014)
Panel B: Test of dynamic correlation									
s lags	5	10	20	5	10	20	5	10	20
stat.	28.64	41.79	45.19	15.12	28.22	32.85	16.09	24.84	42.49
(*p-val.*)	(0.000)	(0.000)	(0.002)	(0.019)	(0.003)	(0.048)	(0.013)	(0.001)	(0.004)
Panel C: Mardia's test and test of ellipticity									
	s_3	k_3	*KS*	s_3	k_3	*KS*	s_3	k_3	*KS*
coeff.	1.318	33.73		1.436	31.62		2.166	26.63	
stat.	232.0	55.57	0.174	199.7	43.86	0.168	79.41	15.75	0.216
(*p-val.*)	(0.000)	(0.000)	(0.000)	(0.000)	(0.000)	(0.000)	(0.000)	(0.000)	(0.000)
Panel D: Tail dependence estimates of SJC copula for each pair of returns									
	o-g	o-e	g-e	o-g	o-e	g-e	o-g	o-e	g-e
τ^U	0.042	0.000	0.000	0.030	0.000	0.000	0.044	0.073	0.041
(*p-val.*)	(0.157)	(0.282)	(1.000)	(0.267)	(0.808)	(0.704)	(0.773)	(0.368)	(0.684)
τ^L	0.167	0.061	0.001	0.080	0.000	0.000	0.380	0.321	0.102
(*p-val.*)	(0.000)	(0.031)	(0.093)	(0.031)	(0.902)	(0.767)	(0.000)	(0.000)	(0.214)

Panel A of Table 2.2 reports unconditional correlation coefficients. We find a large increase in linear dependence for the 2006-2010 period with respect to historical values. The sample correlation between oil and gold returns rises from 0.21 to 0.39. Furthermore, equity index returns, which were negatively correlated with oil (-0.06) and gold (-0.08) in 1990-2006, became positively correlated with both of these commodity returns over the 2006-2010 period, with coefficients equal to 0.39 and 0.17, respectively. These findings suggest that dependence between commodities and equity is no longer constant and evolves with time. To check this assumption, we carry out Engle and Sheppard's (2001) test for constant correlation. The probabilities of constant correlation (test p-values) reported in Panel B of Table 2.2) are less than 0.05 in all cases; therefore, we reject the hypothesis of constant dependence.

Panel C of Table 2.2 reports the tri-variate measures of skewness and kurtosis proposed by Mardia (1970) to test multivariate normality. The corresponding statistics suggest that the hypothesis of multivariate normality should be rejected for the three sample periods considered. In addition, following McNeil, Frey, and Embrechts (2005), we test whether the standardized vector of returns is consistent with a spherical distribution. The corresponding KS test statistics reject the ellipticity hypothesis for all samples. Visually, their associated quantile-quantile plots, in Exhibits 2 and 3 of Figure 2.2), reveal that multivariate normality and elliptical symmetry are strongly rejected for our sample.

Finally, to check for the presence of asymmetric dependence between asset returns in our sample, we analyzed the exceedance correlation and tail dependence. For each pair of asset returns, Figure 2.3 plots the exceedance correlation function proposed in Ang and Chen (2002) and Longin and Solnik (2001), which depicts the correlation between returns above or below a given quantile. In the case of symmetric dependence, the correlation for both extremes should be similar and equal to zero for Gaussian dependence. According to these plots, any assumptions of normality or symmetry seem unrealistic for our sample. Oil and gold do not display the same level of diversification for bear and bull markets, and correlation between oil and equity is highly positive for large negative returns but smaller for large positive returns. The correlation between gold and equity is close to 0 for large negative returns and significantly positive for very large positive returns. Although oil and gold are very positively correlated for large negative returns, are not or even are negatively correlated for large positive returns. Büyükşahin, Haigh, and Robe (2010) also find patterns of extreme and asymmetric dependence between commodity indexes and equity.

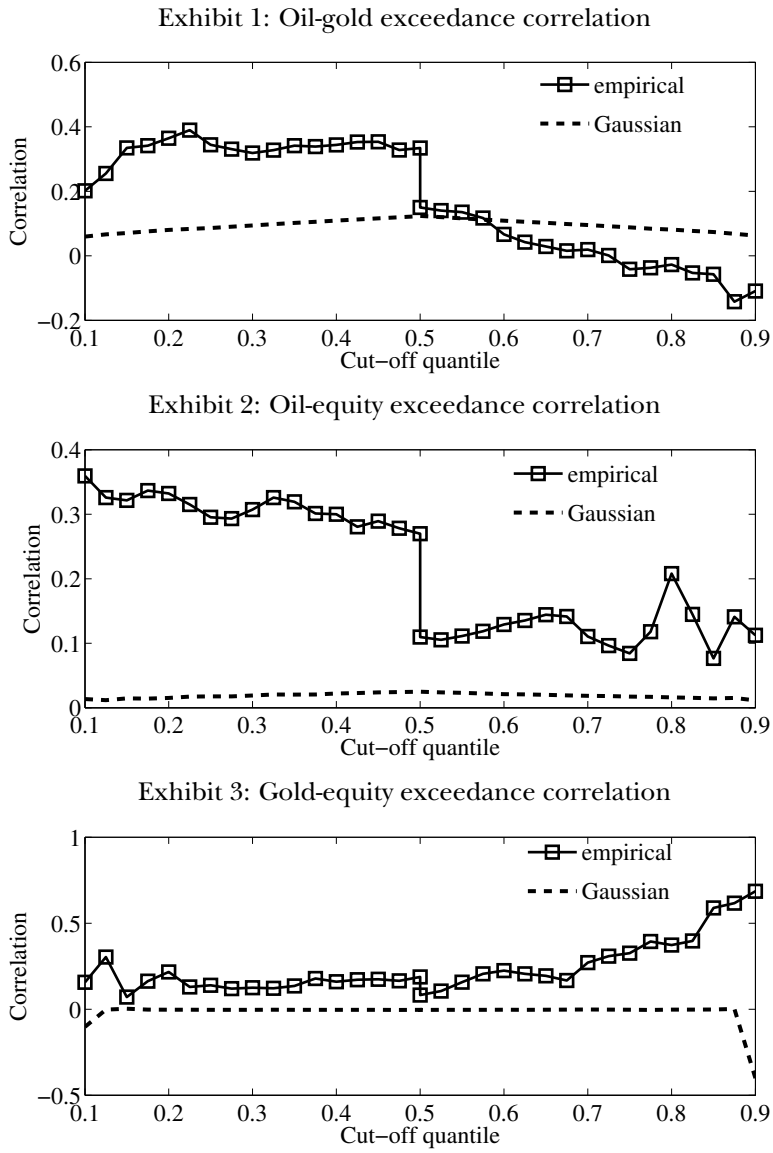

Figure 2.3. Descriptive statistics: exceedance correlations
Exhibits 1, 2, and 3 present the exceedance correlations for each pair of returns (see Longin and Solnik (2001) and Ang and Chen (2002)). The line with squares represent the actual exceedence correlation, whereas the dotted line represents the theoretical correlation between simulated normal return exceedances, assuming a Gaussian return distribution with parameters equal to the sample means and covariance matrix of the weekly returns (see Table 2.1). The x-axis shows the cutoff quantile, and the y-axis presents the correlation between the two returns, given that both exceed that particular quantile.

Furthermore, when we estimate the tail dependence of each pair of returns in our sample, we also observe an asymmetric pattern. For illustrative purposes, Panel D of Table 2.2 reports the fitted upper and lower tail dependence parameters, τ^U and τ^D, corresponding to the symmetrized Joe-Clayton (SJC) copula, defined by Patton (2006b). We observe that tail dependence increases over the 2006-2010 period, and lower tail dependence estimates are generally larger than the upper ones, especially in the last sample period.

In summary, both univariate and multivariate analyses suggest that the assumptions of normality and symmetry for the individual processes and dependence functions are very restrictive and probably should be rejected. A flexible model that captures all the features analyzed in the data thus is required. In the next section, we estimate the conditional copula model proposed in Section 2.2 for our vector of oil, gold, and equity returns. Subsequently, we investigate whether capturing these features (e.g., non-normality of the individual processes, time-varying moments, asymmetric dependence) using the more flexible model leads to economically better portfolio decisions.

2.3.2 Estimation of the conditional copula model

In this section, we estimate the conditional copula model using the multi-stage maximum likelihood procedure explained in Section 2.2.3. We first present the in-sample estimation and goodness-of-fit test results for the marginal distribution models. In a second stage, we analyze the results for the copula model.

In-sample results for the marginal distributions

Table 2.3 presents maximum likelihood estimates of the parameters of the marginal distributions for oil, gold, and equity index returns. We compute robust standard errors of these estimates and report their corresponding p-values in parentheses. These estimates correspond to the generalized t marginal distribution function with time-varying moments, described in equations (2.7)-(2.12) of Section 2.2.1.

In the mean equation, we find that the basis (for oil returns) and momentum and risk-free rate (for gold returns) are significant explanatory factors. The results for the variance equation further show that volatility is strongly persistent for all returns. For equity, only negative returns have an

Table 2.3. In-sample results for the marginal distribution models

This table reports the maximum likelihood parameter estimates of the marginal distribution model for oil, gold, and equity-index returns with generalized Student's t distribution and time-varying moments. Parameters of the mean, variance, degrees of freedom, and asymmetry are defined in equations (2.7), (2.9), (2.11), and (2.12), respectively. The results corresponds to the estimation period from June 1990 to June 2006 (836 observations). The *p-values* of the estimates appear in parentheses and are computed using the robust standard errors. The *logL* is the log-likelihood of the marginal distribution model. η_{c}, λ_{c}, and $logL_{\mathrm{c}}$ are the degrees of freedom, asymmetry parameter, and log-likelihood of the constant version of the model.

	oil		gold		equity	
	coeff.	(*p-val.*)	*coeff.*	(*p-val.*)	*coeff.*	(*p-val.*)
mean equation						
μ (/100)	0.140	(0.316)	0.474	(0.037)	0.130	(0.037)
$basis_{t-1}$	-0.031	(0.216)				
$momentum_{t-1}$			-0.175	(0.153)		
r^f_{t-1}			-0.111	(0.013)		
r_{t-1}					-0.108	(0.002)
r_{t-2}			-0.041	(0.213)		
r_{t-3}	0.050	(0.110)				
variance equation						
α_0 (/1000)	0.025	(0.175)	0.013	(0.012)	0.016	(0.022)
α_1^+	0.085	(0.001)	0.183	(0.001)	0.000	(0.956)
α_1^-	0.060	(0.030)	0.029	(0.189)	0.145	(0.000)
α_2	0.920	(0.000)	0.870	(0.000)	0.890	(0.000)
degrees-of-freedom equation						
δ_0	0.100	(0.000)	0.025	(0.042)	-0.200	(0.054)
δ_1^+	-0.732	(0.576)	-3.633	(0.000)	21.138	(0.049)
δ_1^-	5.514	(0.007)	-3.257	(0.002)	-2.489	(0.383)
δ_2	0.998	(0.000)	1.009	(0.000)	0.966	(0.000)
asymmetry parameter equation						
ζ_0 (/10)	0.085	(0.177)	0.088	(0.111)	-0.250	(0.099)
ζ_1^+	-0.357	(0.313)	-0.903	(0.041)	-0.374	(0.798)
ζ_1^-	0.218	(0.702)	0.592	(0.222)	-2.553	(0.034)
ζ_2	0.998	(0.000)	1.001	(0.000)	0.981	(0.000)
logL	1,515.4		2,262.7		2,149.6	
η_{c}	11.24	(0.002)	4.792	(0.000)	12.25	(0.009)
λ_{c}	-0.093	(0.070)	0.018	(0.577)	-0.230	(0.000)
$logL_{\mathrm{c}}$	1,503.2		2,253.0		2,140.5	

effect on subsequent variance. This result is consistent with the leverage effect studied by Campbell and Hentschel (1992), among others. Yet for both commodities, especially gold, we observe an *inverse* leverage effect; that is, positive shocks have a stronger effect on variance than do negative ones of the same size.

Regarding the dynamics of the degrees-of-freedom and asymmetry parameters, we find that both higher moments are rather persistent for all asset returns over the in-sample period. Large moves in oil returns, especially negative ones, diminish the posterior degrees of freedom ($\delta_1^- = 5.51\,(0.01)$, $\delta_1^+ = -0.73\,(0.58)$, with p-values in parentheses), increasing the likelihood of posterior large shocks. For equity returns, large moves, especially positive ones, increase the subsequent degrees of freedom ($\delta_1^- = -2.49\,(0.38)$, $\delta_1^+ = 21.14\,(0.05)$), so large returns are less likely. For gold returns, extreme events are generally more likely to cluster in periods of large positive moves: Positive shocks are followed by a decrease in posterior degrees of freedom ($\delta_1^+ = -3.63\,(0.00)$), whereas negative shocks generally are followed by an increase ($\delta_1^- = -3.26\,(0.00)$).

In general, lagged values of the asymmetry parameter are more significant for subsequent parameter values than is the effect of the previous returns shock. Over our study's in-sample period, only positive shocks in gold returns ($\zeta_1^+ = -0.90\,(0.04)$) and negative shocks in equity returns ($\zeta_1^- = -2.55\,(0.03)$) seem to have effects of opposite signs on the posterior asymmetry parameters. Therefore, for the three assets returns, we find significant time variation in the moments of the univariate processes. As a benchmark, Table 2.3 also reports the degrees-of-freedom and asymmetry parameters, η_c and λ_c, of the conditional distribution with constant shape parameters. We find that for the in-sample period, the left tail of the conditional distribution of oil and equity returns is fatter than the right tail, with parameters η_c and λ_c equal to 11.24 and -0.09 for oil returns, and 12.25 and -0.23 for equity returns. In contrast, gold returns have positive (though not significant) asymmetry parameter (λ_c=0.02) and heavier tails than oil and equity returns (η_c =4.79).

A reliable estimation of copula models requires an appropriate specification of the univariate density functions (see Patton (2006a,b) and Jondeau and Rockinger (2006)). Therefore, to avoid misspecified copula models, we conduct the in-sample goodness-of-fit test suggested by Diebold, Gunther, and Tay (1998) for our estimated marginal distribution models. If the marginal model is correctly specified, the probability integral transform should be i.i.d. Uniform(0,1). According to the the LM statistics in Panel A of Table 2.4, we must reject serial dependence in the first four moments

Table 2.4. DGT and LR tests of the marginal distribution models

In Panel A, we report the statistics and p-values of the Diebold, Gunther, and Tay (1998) (DGT) test for the marginal distribution model for oil, gold, and equity-index returns with generalized Student's t distribution and time-varying moments. The DGT test consists of two stages: (1) Lagrange multiplier statistics (LM) over 20 lags for the first four moments of the residuals to test for serial correlation, and (2) a goodness-of-fit test for the adequacy of the distribution model (see also Figure 2.4). In Panel B, we provide the likelihood ratio test statistics (LR) with respect to different restrictive versions of the marginal distribution model. All the restrictive models have the same conditional mean and variance dynamics, which are described in the chapter, but we consider four conditional distributions: (i) the generalized Student's t distribution with constant degree-of-freedom and asymmetry parameters, the Student's t distribution with (ii) time-varying and (iii) constant degrees of freedom, and (iv) the univariate Gaussian distribution. The *dof* are the number of constraints under the null condition. All the tests results corresponds to the in-sample period from June 1990 to June 2006 (836 observations).

Panel A: DGT test for the generalized Student's t

		oil		gold		index	
		stat.	(*p-val.*)	*stat.*	(*p-val.*)	*stat.*	(*p-val.*)
(1)	1st moment LM(20)	25.39	(0.187)	21.02	(0.396)	21.57	(0.364)
	2nd moment LM(20)	23.96	(0.244)	21.49	(0.369)	18.72	(0.54)
	3rd moment LM(20)	18.45	(0.558)	21.74	(0.355)	12.97	(0.879)
	4th moment LM(20)	24.45	(0.223)	17.66	(0.610)	17.00	(0.653)
(2)	Goodness-of-fit test	7.66	(0.990)	11.30	(0.913)	7.80	(0.989)

Panel B: Loglikelihood ratio tests (LR)

		oil		gold		index	
	dof	*LR stat.*	(*p-val.*)	*LR stat.*	(*p-val.*)	*LR stat.*	(*p-val.*)
(i) generalized t const. par.	6	24.50	(0.000)	19.48	(0.003)	18.16	(0.006)
(ii) t time-varying df.	4	9.794	(0.044)	12.13	(0.016)	31.23	(0.000)
(iii) t constant df.	7	27.71	(0.000)	19.64	(0.006)	38.57	(0.000)
(iv) Gaussian	8	47.00	(0.000)	92.89	(0.000)	52.38	(0.000)

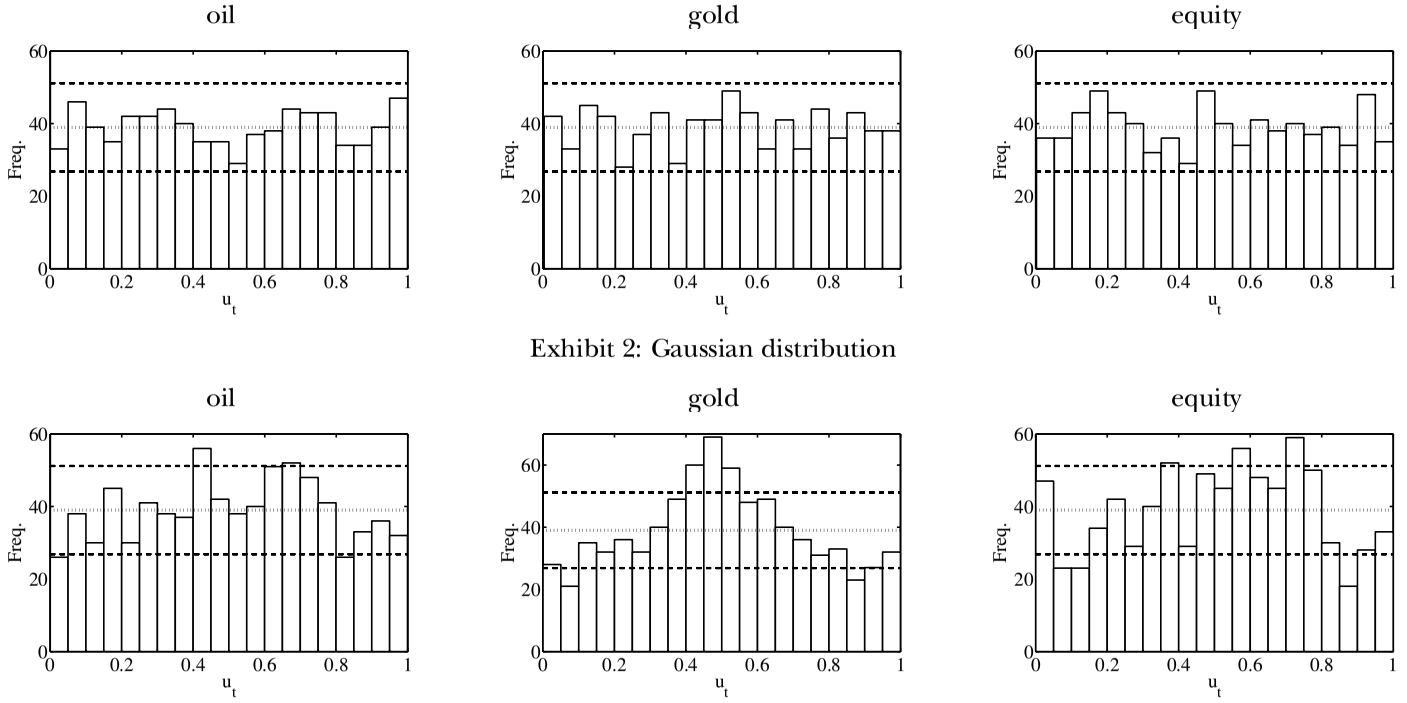

Figure 2.4. Goodness-of-fit test

In this figure, we plot the goodness-of-fit test for the estimates of the density of $u_{i,t}$, $i = 1, 2, 3$ and $t = 1, ..., T$ (Diebold, Gunther, and Tay (1998)) for two marginal distribution models for oil, gold, and equity-index weekly returns: one with a generalized Student's t distribution and time-varying moments (Exhibit 1), and the other with a Gaussian distribution (Exhibit 2). Dotted line and horizontal dashed lines represent the mean and 95% confidence interval, respectively.

of the probability integral transform (all p-values > 0.15). In addition, the KS statistics suggest that the shape of the conditional distribution model is correctly specified for the three returns (p-values > 0.90). Visually, the goodness-of-fit plots in Figure 2.4 also supports these results. Furthermore, the asymmetric marginal model performs substantially better than the Gaussian and symmetric models, even for constant higher moments.

Finally, using likelihood ratio (LR) tests, we compare our more general skewed t marginal model against different constrained alternative models. In Panel B of Table 2.4, we report the LR test statistics for the next four alternative marginal models: the generalized t distribution with constant parameters, the standard Student's t distribution with time-varying and constant degrees of freedom, and the standard Gaussian distribution. In all cases, we reject the restricted specification in favor of a more general model, at least at a 5% significance level (p-values < 0.05).

In-sample results for the copulas

In this second stage, we estimate the dependence function that links the three marginal distribution models. We analyze the three time-varying or conditional copula functions described in Section 2.2.2 : the Gaussian, t, and skewed t copulas. Table 2.5 presents the in-sample ML estimates of the three conditional copula models, estimated on the transformed residuals of the generalized t univariate model. This table also reports the estimates p-values, computed from the asymptotic covariance matrix, and the likelihood values at the optimum for the conditional and unconditional copulas.[12]

According to the ML estimates, for all copula models, the dependence coefficient between oil and gold returns, $\rho_{\text{oil, gold}}$, is positive, whereas the dependence coefficient between gold and equity index returns, $\rho_{\text{gold, equity}}$, is negative, and that between oil and equity, $\rho_{\text{oil, equity}}$, is insignificantly different from 0. Therefore, the estimated dependence coefficients are consistent with the observed unconditional correlations reported in Table 2.2.

Estimates of the degrees of freedom ν are strongly significant for symmetric and skewed t copulas, indicating the presence of a significant level of dependence in the extremes. Regarding the estimation of the skewed t copula, we find that all elements of the asymmetry parameters vector

[12]In this empirical application, the conditional dependence follows the dynamics in equation (2.15) for $M = 4$, which are the number of lags consistent with the autoregressive lags considered in the univariate models.

Table 2.5. In-sample results and LR tests for the copula models

This table presents the maximum likelihood parameter estimates of the copula models under different assumptions of the conditional joint dependence. The results corresponds to the period from June 1990 to June 2006 (836 observations). In each case, the copula is defined by the next set of parameters: the correlation matrix ($\{\rho_{i,j}\}$), the degrees of freedom (ν), the asymmetry vector (γ), and the parameters of the dynamics (ω_0, ω_1, and ω_2) (see equation (2.15)). For each parameter estimate, we report in parentheses the *p*-values computed from the asymptotic covariance matrix. The conditional copula likelihood at the optimum is denoted by CL, whereas CL_{uncond} reports the likelihood at the optimum of the corresponding unconditional version of the copula. We also report the likelihood ratio test statistics (LR) for different restrictive specifications of the copula models.The LR(vs. Uncond.) corresponds to the LR test with respect to the corresponding unconditional version of the copula model. In LR(vs. Symmetric), we test with respect to the conditional t copula. In LR(vs. Gaussian) the restrictive model is the conditional Gaussian copula. With LR(vs. Uncond. Symmetric) and LR(vs. Uncond. Gaussian), we test the conditional copulas with respect to the unconditional t and Gaussian copulas. Finally, with LR(Uncond. vs. Symmetric) and LR(Uncond. vs. Gaussian), we test the unconditional versions of the copulas with respect to the unconditional t and Gaussian copulas.

	Conditional copulas					
	Gaussian		t copula		Skewed t	
	coeff.	(*p-val.*)	*coeff.*	(*p-val.*)	*coeff.*	(*p-val.*)
$\rho_{\text{oil,gold}}$	0.159	(0.000)	0.157	(0.000)	0.161	(0.000)
$\rho_{\text{oil,equity}}$	-0.020	(0.556)	-0.016	(0.653)	-0.013	(0.653)
$\rho_{\text{gold,equity}}$	-0.064	(0.064)	-0.058	(0.108)	-0.057	(0.108)
ν			18.998	(0.025)	19.050	(0.031)
γ_{oil}					-0.268	(0.027)
γ_{gold}					-0.018	(0.934)
γ_{equity}					-0.141	(0.139)
ω_0	0.136	(0.223)	0.128	(0.192)	0.127	(0.265)
ω_1	0.079	(0.055)	0.069	(0.054)	0.060	(0.082)
ω_2	1.647	(0.000)	1.666	(0.000)	1.676	(0.000)
CL	18.680		20.828		23.136	
CL_{uncond}	12.453		15.222		18.134	
LR(vs. Uncond.)	12.454	(0.006)	11.212	(0.011)	10.004	(0.019)
LR(vs. Gaussian)			4.296	(0.038)	8.913	(0.063)
LR(vs. Symmetric)					4.617	(0.202)
LR(vs. Uncond. Gaussian)			16.750	(0.002)	21.367	(0.003)
LR(vs. Uncond. Symmetric)					15.829	(0.015)
LR(Uncond. vs. Gaussian)			5.538	(0.019)	11.363	(0.023)
LR(Uncond. vs. Symmetric)					5.826	(0.120)

($\gamma_{\text{oil}}, \gamma_{\text{gold}}, \gamma_{\text{equity}}$) are negative, especially for oil and equity, suggesting more extreme dependence among returns during extreme depreciations of these assets compared with during bullish markets.

The parameters ω_0, ω_1, and ω_2, which parametrized the dynamic equation of dependence, are significant for all conditional copulas, showing strong evidence of time variation and persistence in the conditional dependence. These results regarding the estimates of the dependence functions are also consistent with the preliminary multivariate analysis of Section 2.3.1.

According to the LR test statistics reported in Table 2.5, we observe, first, that conditional copulas are preferred over their corresponding unconditional versions (p-values $\leqslant 0.05$ for the three cases). Second, the presence of tail dependence in the in-sample data is not negligible. The p-values of the LR test of the conditional and unconditional t copulas with respect to the more restrictive Gaussian copulas are always less than 0.10. Third, there is evidence of asymmetry dependence over the in-sample period, captured by the skewed t copula, but the gains from modeling this asymmetry may not make up for the penalty associated with the inclusion of more parameters in the model. These gains seem less significant than those obtained from modeling time-varying and tail dependence.

Out-of-sample parameters forecasts

To obtain the optimal portfolio decisions based on our copula models over the out-of-sample period, we need the forecasts of the different parameters at play over the 2006-2010 period. For that purpose, we recursively reestimate the marginal and copula models throughout the out-of-sample period (220 weekly observations) using a rolling window scheme that drops distant observations as more recent ones are added and therefore keeps the size of the estimation window fixed at 836 observations. Once we re-estimate the model for each point in the out-of-sample period, we construct the time-series of one-period-ahead parameter forecasts needed for the allocation stage (see Section 2.2.3 for the details of the implementation).

Figure 2.5 shows the output of the forecasts of the conditional mean, volatility, and skewness of each return process throughout the out-of-sample period. The volatility forecasts of all asset returns are relatively high, especially around October 2008. Conditional skewness is negative for equity and oil returns during the 2006-2010 period, but it is positive for gold returns during that period.

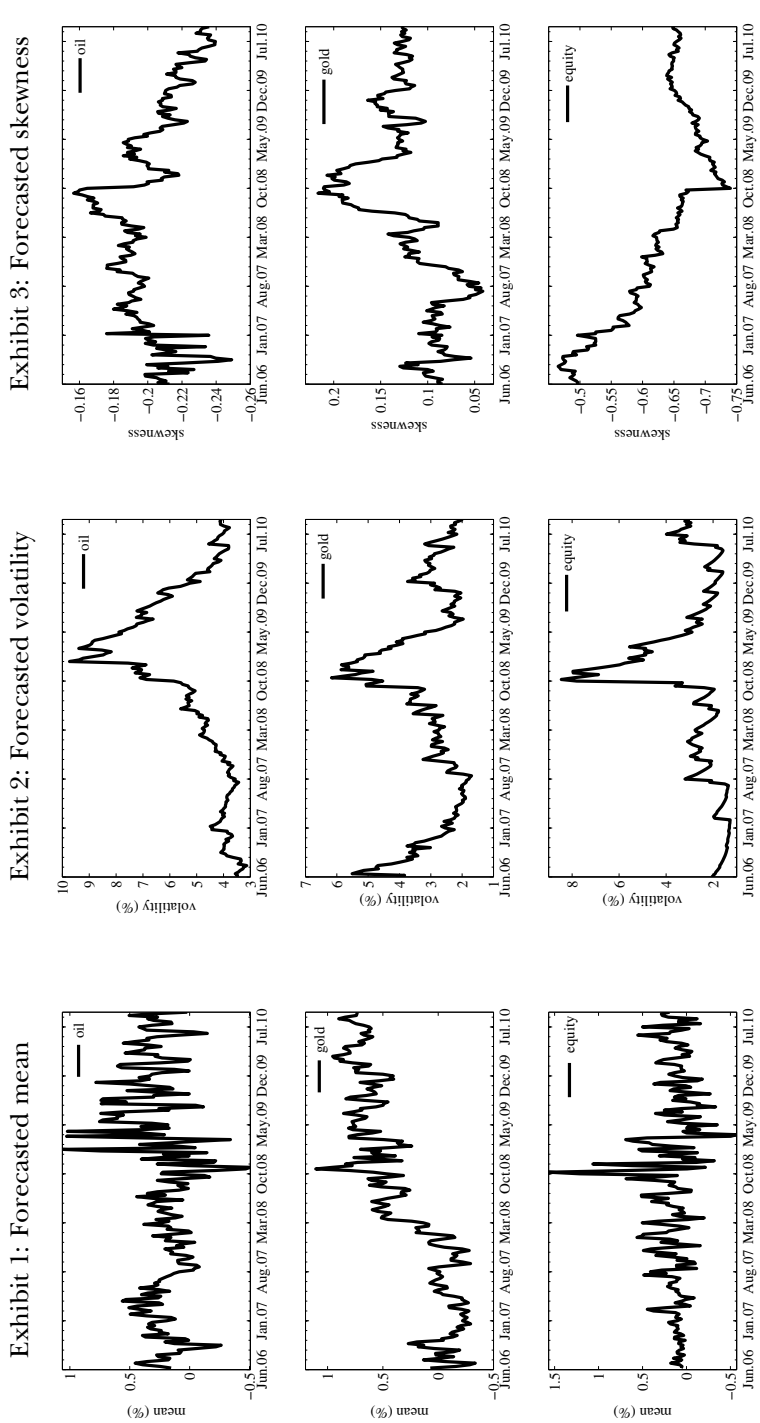

Figure 2.5. Conditional parameters of the marginal distribution model
This figure shows the one-step ahead forecasts over the out-of-sample period for the conditional mean, volatility, and skewness of the marginal distribution model with generalized Student's t distribution.

Figure 2.6 presents the forecasts of the conditional dependence parameters. It is worth noting that there is an increase in the fitted correlation coefficients among oil, gold, and equity from October 2008, especially for oil and equity returns (see Exhibit 1). In addition, the dependence coefficients seem to evolve more similarly in the latter part of the sample. The degrees-of-freedom forecasts decrease after August 2007, indicating rising tail dependence since then (see Exhibit 2). In addition, the asymmetry parameter of oil ranges between -0.6 and -0.2, which implies that extreme dependence seems to be stronger during large depreciations of oil, compared with large drops in gold or equity, whose asymmetry parameters range between -0.2 and +0.2 (see the forecast of the asymmetry parameter vector in Exhibit 3).

In general, during our re-estimation of the copula models, we find no evidence to contradict skewed and fat-tailed marginal distributions and asymmetric and extreme conditional dependence, but strong evidence indicates that Gaussian distribution and elliptical dependence are not the best-fitting models. These results over the allocation period are consistent with the sample statistics we described previously.

In summary, the skewed t copula provides a more informative measure of the dependence between commodities and equity-index returns, even taking into account that part of the tail behavior is captured by the skewed fat-tailed marginal distribution models. Therefore, possibly univariate tail behavior and asymmetric dependence are key factors not taken into account in a standard elliptical, *à la Markowitz*, approach. The extent to which these factors have a significant impact on the portfolio choice decision is addressed in the next section.

2.3.3 Optimal portfolio results

We now investigate the optimal portfolio decisions based on the copula models we estimated in the previous section, and analyze their performance over the out-of-sample period. In particular, we compare six model-driven portfolio strategies that can be analyzed from the perspective of copula models and therefore estimated using the multistage procedure from Section 2.2.3.

First, we consider the unconditional multivariate Gaussian model (Markowitz strategy), a constant Gaussian copula with unconditional Gaussian marginal distributions. Second, we generalize this case byconsidering two conditional multivariate Gaussian distributions: the constant conditional

Exhibit 1: Forecasted correlation coefficients

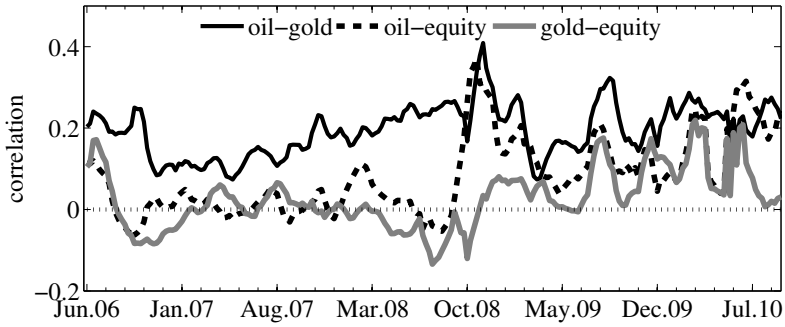

Exhibit 2: Forecasted degrees of freedom

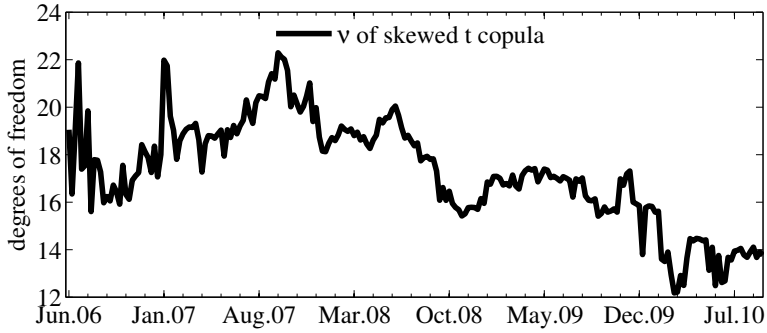

Exhibit 3: Forecasted asymmetry vector

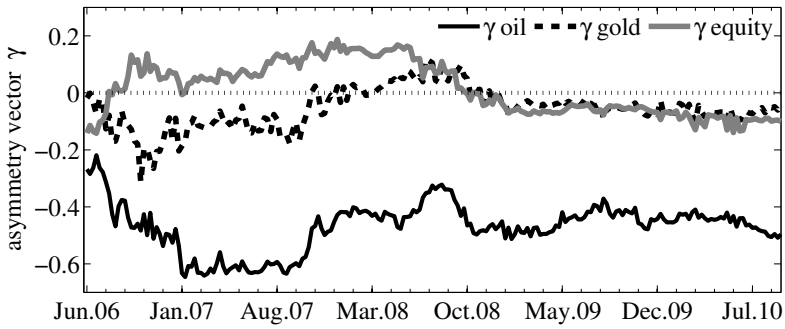

Figure 2.6. Conditional parameters of the conditional skewed t copula
This figure shows the one-step ahead forecasts over the out-of-sample period for the correlation coefficients, degrees of freedom, and asymmetry vector components of the conditional skewed t copula model.

correlation (CCC) and the dynamic conditional correlation (DCC). Both CCC and DCC specifications are formed by conditional Gaussian marginal distributions with conditional means and variances defined in equations (2.7) and (2.9). Third, we compute portfolio strategies using the conditional copula models introduced in Section 2.2. Thus, we consider the generalized Student's t distribution for the marginal models (equations 2.7 -2.10) and three types of conditional dependence functions: the Gaussian, t, and skewed t copulas (defined in equations 2.14-2.15). With this set of alternatives, we can compare the gains of including more flexible models as a means to compute portfolio decisions. In addition, we include in the analysis the equally weighted portfolio, as a common benchmark used in prior literature.

We analyze the portfolio allocations for different parameterizations of the investor's three-moment preferences, defined by φ_{V} and φ_{S}. For that purpose, we follow two complementary approaches: one where the specification of the investor's preferences is related to the third-order Taylor series expansion of an utility function with coefficient of relative risk aversion $\mathcal{A}$ (like in Guidolin and Timmermann (2008) and Jondeau and Rockinger (2012)), and other approach where the different values of φ_{V} and φ_{S} account for different arbitrary impacts of the portfolio variance and skewness on the investor's preferences (like in Harvey, Liechty, Liechty, and Müller (2010)).

Portfolio weights

In this section we analyze the time series of portfolio weights over the out-of-sample period corresponding to the portfolio allocations obtained from the six copula models described previously. For that purpose, we report in Table 2.6 the quantiles of the distribution of optimal weights for oil, gold, and equity, under various specifications (φ_{V} and φ_{S}) of the three-moment investor's preferences, characterized, in this case, by different values of the risk aversion coefficient $\mathcal{A}$. These allocation results are obtained from the unconstrained and short-sales constrained optimizations.[13] In addition, in Panel A of Figure 2.7 we plot, for two of these preferences specifications, the time-series of portfolio weights resulting from the portfolio decisions made using our most general model, the conditional skewed t copula. Panel B of Figure 2.7 shows the allocation differences between the unconditional

[13]Note that the short-sales constraint only affects the weights of spot contracts, in this case, the weights of the equity index.

Gaussian model and the conditional skewed t model for $\mathcal{A} = 5$ (i.e. for φ_{V}=5/2 and φ_{S}=5).

The results show that the bulk of the difference between portfolios strategies depends largely on the use of different marginal distribution models. The first significant discrepancies arise when using time-varying Gaussian marginal distributions (CCC and DCC models) instead of unconditional Gaussian margins (Uncond. Gaussian model). In particular, the median position in equity resulting from the CCC model decreases significantly compared with the median position of the unconditional Gaussian strategy, especially for the lowest values of $\mathcal{A}$. Accordingly, the median positions in commodity futures increases when we employ the CCC model. For example, for $\mathcal{A} = 2$ (φ_{V}=1 and φ_{S}=1), the median positions of the CCC strategy are 0.50, 0.22, and -0.22 for oil, gold, and equity, whereas for the unconditional model the median positions are 0.36, 0.10, and 0.41, respectively. We also observe relevant differences between using Gaussian (CCC and DCC models) and generalized Student's t distributions (conditional copula models) for modeling the conditional margins. The main effect of introducing fat tails and asymmetry in the marginal distributions consists in an increase of long positions in gold and a reduction of long positions in oil. For instance, comparing the DCC and conditional Gaussian copula strategies for $\mathcal{A} = 2$, we find that the median positions in oil and gold change from 0.43 and 0.21 to 0.21 and 0.46, respectively.

A second source of allocation differences is driven by the various types of dependence captured with our copula models. These discrepancies in optimal portfolio weights arise, first, from introducing a time-varying conditional dependence (e.g., CCC vs. DCC); and second, from considering tail dependence (e.g., t copula vs. Gaussian copula) and asymmetric dependence (e.g., skewed t vs. t copula). These allocation differences are significant mainly for $\mathcal{A} = 1$ (φ_{V}=1/2 and φ_{S}=1/3) and $\mathcal{A} = 2$ (φ_{V}=1 and φ_{S}=1). Specifically, when allowing for dynamic dependence, the median positions in the three assets decrease. For example, for $\mathcal{A} = 1$, the CCC strategy generates median positions in oil, gold, and equity equal to 0.88, 0.10, and -1.13; whereas for the DCC model the median weights are 0.74, 0.00, and -1.29, respectively. When capturing asymmetric dependence using the skewed t copula, we also observe that median weights diminish with respect to the median positions corresponding to the symmetric t copula strategy. Thus, for $\mathcal{A} = 1$, the median weights for the t copula model are 0.39, 0.57, and -0.82; and those obtained from the skewed t copula are equal to 0.28, 0.44, and -1.02.

Looking in more detail at the quantiles corresponding to our more flexible model, the conditional skewed t copula, we observe that the dispersion in

Table 2.6. Summary statistics of the optimal portfolio weights for different strategies and preferences

This table reports the statistics for the allocation period related to the optimal portfolio weights for different multivariate models and preference specifications parametrized by the coefficient of relative risk aversion, $\mathcal{A}$ (i.e. $\varphi_V = \mathcal{A}/2!$ and $\varphi_S = \mathcal{A}(\mathcal{A}+1)/3!$ in these cases). Panels A and B show the results for the unconstrained and short-sales constrained optimizations. ω_o, ω_g, and ω_e are the optimal portfolio weights of oil, gold, and equity, respectively.

Panel A: Unconstrained

	Uncond. Gaussian			CCC			DCC			Gaussian Copula			t copula			skewed t copula		
	ω_o	ω_g	ω_e	ω_o	ω_g	ω_e	ω_o	ω_g	ω_e	ω_o	ω_g	ω_e	ω_o	ω_g	ω_e	ω_o	ω_g	ω_e
									$\mathcal{A}=1$									
5% pct.	0.00	0.00	-0.40	0.00	-0.54	-4.85	-0.12	-1.10	-5.26	0.00	-1.31	-5.65	0.00	-1.58	-5.43	-0.08	-1.57	-5.42
Median	0.60	0.00	0.18	0.88	0.10	-1.13	0.74	0.00	-1.29	0.29	0.49	-0.90	0.39	0.57	-0.82	0.28	0.44	-1.02
95% pct.	1.11	0.91	1.00	3.87	4.14	1.00	3.86	4.46	1.00	2.81	5.64	1.00	2.83	5.34	1.00	2.89	5.38	1.00
									$\mathcal{A}=2$									
5% pct.	0.09	0.00	0.03	-0.05	-0.40	-2.16	-0.18	-0.68	-2.42	-0.09	-0.75	-2.47	-0.03	-0.85	-2.45	-0.15	-0.89	-2.43
Median	0.36	0.10	0.41	0.50	0.22	-0.22	0.43	0.21	-0.30	0.21	0.46	-0.18	0.24	0.50	-0.13	0.20	0.45	-0.18
95% pct.	0.62	0.69	0.91	2.00	2.29	1.00	1.97	2.45	1.00	1.45	2.86	1.00	1.46	2.88	1.00	1.50	2.89	1.00
									$\mathcal{A}=5$									
5% pct.	0.10	0.09	0.29	-0.17	-0.30	-0.59	-0.23	-0.37	-0.65	-0.22	-0.40	-0.71	-0.20	-0.42	-0.67	-0.22	-0.43	-0.62
Median	0.19	0.33	0.45	0.26	0.33	0.27	0.24	0.31	0.27	0.14	0.41	0.27	0.15	0.40	0.26	0.14	0.42	0.26
95% pct.	0.31	0.56	0.76	0.88	1.21	1.00	0.86	1.29	1.00	0.67	1.39	0.97	0.65	1.39	1.00	0.67	1.42	1.00
									$\mathcal{A}=10$									
5% pct.	-0.05	0.29	0.38	-0.13	-0.24	-0.04	-0.21	-0.25	-0.06	-0.22	-0.29	-0.14	-0.20	-0.31	-0.12	-0.22	-0.29	-0.11
Median	0.12	0.40	0.46	0.19	0.31	0.40	0.17	0.34	0.41	0.11	0.41	0.37	0.12	0.38	0.38	0.11	0.42	0.38
95% pct.	0.19	0.56	0.60	0.49	0.87	0.80	0.50	0.91	0.80	0.42	1.00	0.84	0.39	0.98	0.84	0.40	0.98	0.86

Table 2.6 *(continued)*

Panel B: Short-sales Constrained

	Uncond. Gaussian			CCC			DCC			Gaussian Copula			t copula			skewed t copula		
	ω_o	ω_g	ω_e	ω_o	ω_g	ω_e	ω_o	ω_g	ω_e	ω_o	ω_g	ω_e	ω_o	ω_g	ω_e	ω_o	ω_g	ω_e
									$\mathcal{A}=1$									
5% pct.	0.00	0.00	0.00	0.00	0.00	0.00	-0.03	0.00	0.00	0.00	-0.33	0.00	0.00	-0.44	0.00	0.00	-0.34	0.00
Media	0.58	0.00	0.18	0.56	0.00	0.00	0.48	0.00	0.00	0.03	0.00	0.00	0.03	0.00	0.00	0.06	0.00	0.00
95% pct.	1.00	0.62	1.00	1.00	1.00	1.00	1.00	1.00	1.00	1.00	1.00	1.00	1.00	1.00	1.00	1.00	1.00	1.00
									$\mathcal{A}=2$									
5% pct.	0.09	0.00	0.03	-0.14	-0.13	0.00	-0.16	-0.15	0.00	-0.04	-0.42	0.00	-0.06	-0.34	0.00	-0.09	-0.50	0.00
Median	0.36	0.10	0.41	0.41	0.00	0.00	0.33	0.00	0.00	0.12	0.22	0.00	0.09	0.22	0.00	0.10	0.22	0.00
95% pct.	0.62	0.67	0.91	1.00	1.00	1.00	1.00	1.00	1.00	1.00	1.00	1.00	1.00	1.00	1.00	1.00	1.00	1.00
									$\mathcal{A}=5$									
5% pct.	0.10	0.09	0.29	-0.15	-0.30	0.00	-0.23	-0.31	0.00	-0.19	-0.38	0.00	-0.18	-0.42	0.00	-0.20	-0.43	0.00
Median	0.19	0.33	0.45	0.26	0.27	0.27	0.23	0.28	0.27	0.13	0.41	0.27	0.14	0.40	0.27	0.12	0.39	0.26
95% pct.	0.31	0.56	0.76	0.86	0.90	1.00	0.87	0.99	1.00	0.61	1.00	0.99	0.58	1.00	1.00	0.61	1.00	1.00
									$\mathcal{A}=10$									
5% pct.	-0.05	0.29	0.37	-0.11	-0.23	0.00	-0.21	-0.25	0.00	-0.21	-0.29	0.00	-0.19	-0.31	0.00	-0.21	-0.29	0.00
Median	0.12	0.40	0.46	0.19	0.32	0.41	0.16	0.33	0.40	0.11	0.40	0.38	0.12	0.38	0.39	0.11	0.42	0.38
95% pct.	0.19	0.54	0.60	0.49	0.80	0.81	0.50	0.85	0.81	0.42	0.91	0.83	0.39	0.91	0.84	0.40	0.93	0.87

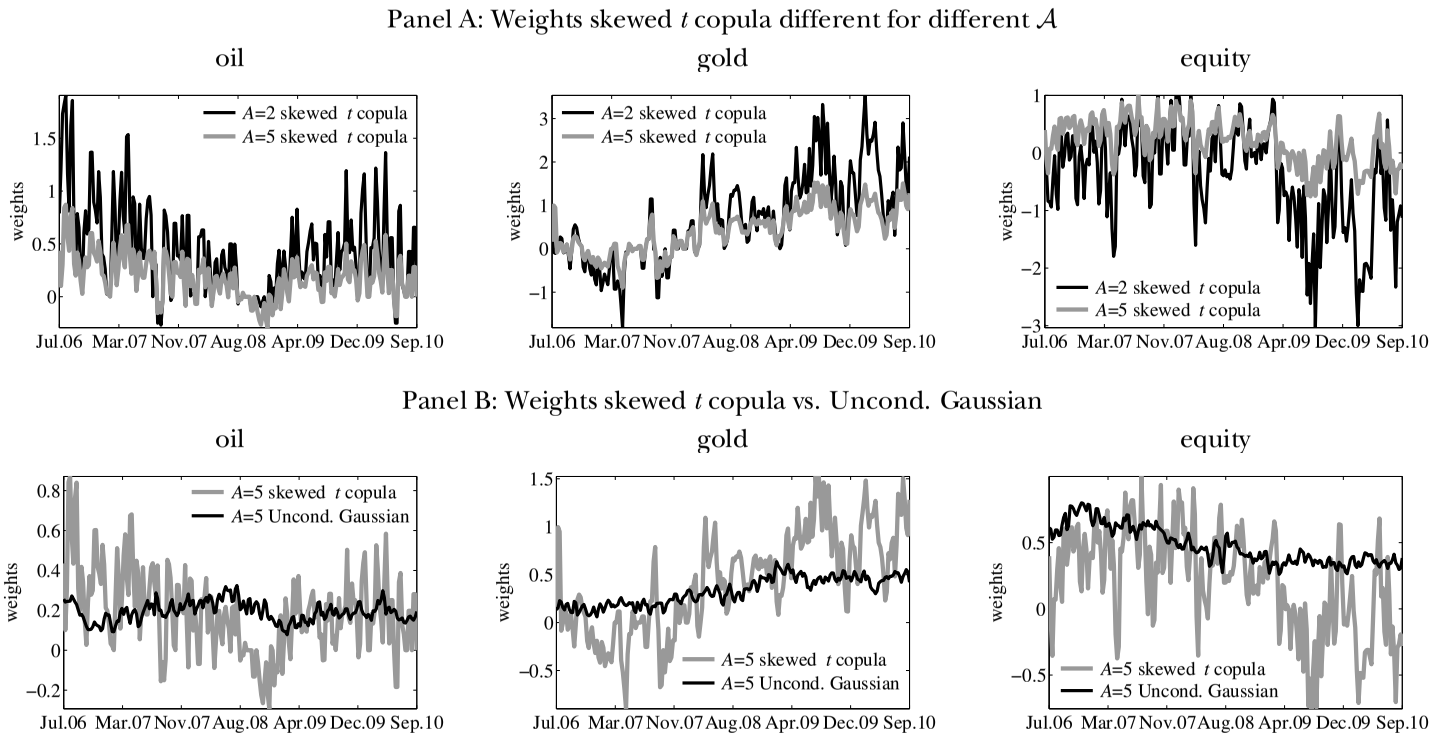

Figure 2.7. Optimal portfolio weights

Panel A shows the optimal portfolio weights over the out-of-sample period (June 2006 to September 2010) for unconstrained conditional skewed t copula for two preferences specifications characterized by relative risk aversion coefficient $\mathcal{A} = 2$ and 5. Panel B shows the optimal portfolio weights for the unconstrained conditional skewed t copula model and the unconditional Gaussian model ("a la Markowitz") for $\mathcal{A} = 5$.

the distribution of weights shrinks when increasing the value of $\mathcal{A}$ (see Figure 2.7). For the highest values of $\mathcal{A}$ considered, portfolio weights become less aggressive and there are less discrepancies among median positions of the skewed t strategy and those of less flexible models. Changes in the coefficient $\mathcal{A}$ affects to a large extent to the distribution of equity weights. Thus, under the skewed t model, the median positions in equity for values of coefficient $\mathcal{A}$ equal to 1, 2, 5, and 10 are -1.02, -0.18, 0.26, and 0.38, respectively; and the 5% percentiles are -5.42, -2.43, -0.62, and -0.11. The median weights for oil futures range from 0.28 for $\mathcal{A} = 1$ to 0.11 for $\mathcal{A} = 10$; in this case, the decline in the median is mainly given by a decrease in the presence of extreme long positions in oil futures (the 95% percentile diminishes from 2.89 to 0.40). In contrast, increasing $\mathcal{A}$ generates less extreme long and short positions in gold, and the median weight varies slightly, from 0.44 for $\mathcal{A} = 1$ to 0.42 for $\mathcal{A} = 10$.

Panel B of Table 2.6 reports the percentiles of the distribution of portfolio weights when short sales of equity are not allowed. Imposing a short-sales constraint has a strong impact on the portfolio strategies, especially for the preference specifications corresponding to values of $\mathcal{A}$ equal to 1 and 2. Only the portfolio decisions obtained from the unconditional Gaussian model are not affected by this restriction. The models that yield median positions of being short in equity under the unconstrained portfolio optimization generate median positions equal to zero under the restricted allocation. As a result, the presence of extreme positions in commodity futures is reduced, especially the long positions in gold futures. For example, for $\mathcal{A} = 2$ the 5%, 50% and 95% percentiles of the commodity positions resulting from the skewed t copula strategy under the short-sales constraint are -0.09, 0.10, and 1.00 for oil, and -0.50, 0.22, and 1.00 for gold; in contrast to the percentiles of the unrestricted portfolio decisions, which are -0.15, 0.20, and 1.50 for oil, and -0.89, 0.45, and 2.89 for gold. Therefore, for the least risk averse investors under the short-sales restriction, part of the information included in the more flexible copula models is lost.[14]

Investment ratios and portfolio performance

We now turn to analyze the moments, investment ratios, and relative performance measures of the optimal portfolio returns resulting from the different copula strategies. Results are reported in Table 2.7 for various specifications of the three-moment preferences.

[14]Patton (2004) reaches a similar conclusion for a portfolio selection problem with two stock indices.

We compute the Sharpe, Sortino, and Omega investment ratios, given respectively by

$$\text{Sharpe} = \frac{\mu_P - r_f}{\sigma_P}, \ \text{Sortino} = \frac{\mu_P - r_f}{\sqrt{q_2^l(r_f)}}, \ \text{and} \ \text{Omega} = \frac{q_1^u(r_f)}{q_1^l(r_f)}; \qquad (2.18)$$

where μ_P is the average realized portfolio return, σ_P is the realized portfolio volatility, r_f is the risk-free rate, and $q_m^l(r_f)$ and $q_m^u(r_f)$ are the lower and upper partial moments of order m with target value equal to the risk-free rate.[15] The Sortino ratio modifies the Sharpe ratio by dividing the excess return of the portfolio by the downside standard deviation or square root of semi-variance. The Omega ratio can be interpreted as the probability weighted ratio of gains to losses, relative to the risk-free rate, and it measures the combined effect of all of returns moments, rather than the individual effects of any of them. The higher the values of these ratios, the better portfolio performance.

The Sharpe, Sortino, and Omega ratios of the equally weighted portfolio are 0.05, 0.07 and 1.14 (see Table 2.7). The poor performance of equity markets and the boom of gold and oil during the 2006-2010 period reveals that these portfolios, with constant holdings in oil and gold futures, perform remarkably well compared with other strategies based on fitted distribution models. In particular, for almost all three-moment preferences considered, the investment ratios of the unconditional Gaussian model (Markowitz model) are substantially smaller than those corresponding to the equally weighted portfolio.

For the preferences considered, we find that, in general, the conditional copula models with generalized Student's t marginal distributions have larger investment ratios than the multivariate conditional Gaussian models (CCC and DCC). In addition, at least one of the t copula models (symmetric or skewed) perform better than the Gaussian copula, for most of the cases analyzed. That is, conditional copulas that capture tail or asymmetric dependence or both achieve higher investment ratios across our allocation sample. For example, the Sortino and Omega ratios of the conditional skewed t copula strategy range from 0.10 and 1.19 to 0.14 and 1.28, whereas these investment ratios for the conditional Gaussian copula model range from 0.07 and 1.15 to 0.12 and 1.23. The DCC model yields Sortino and Omega ratios varying from 0.03 and 1.06 to 0.11 and 1.20; and the unconditional Gaussian strategy has ratios ranging from -0.004 and 0.99 to 0.07 and 1.14.

[15]The lower and upper partial moments of order m for a given target θ are defined as $q_m^l(\theta) = \int_{-\infty}^{\theta}(\theta - r)^m f_p(r)\mathrm{d}r$ and $q_m^u(\theta) = \int_{\theta}^{\infty}(r - \theta)^m f_p(r)\mathrm{d}r$, where $f_p(r)$ is the probability density function of the portfolio returns.

Table 2.7. Investment ratios and relative performance measures of the realized portfolio returns

This table reports the investment ratios and relative performance measures (in basis points per week) of the realized portfolio returns over the allocation (out-of-sample) period for different strategies. We first present the Sharpe, Sortino, and Omega ratios, given respectively as $(\mu - r_f)/\sigma$, $(\mu - r_f)/\sqrt{q_2^l(r_f)}$, and $q_1^u(r_f)/q_1^l(r_f)$, where $q_m^u(\theta)$ and $q_m^l(\theta)$ are the upper and lower partial moments of order m for a given target θ. We also present the skewness (Skw) of the realized portfolio returns and two relative performance measures, the management fee (*Fee*) and the Graham-Harvey measure (*GH*), which are both calculated with respect to the equally weighted strategy. $\mathcal{A}$ is the coefficient of relative risk aversion for power utility functions. The highest value of each measure is marked in boldface.

	Unconstrained						Short-sales Constrained					
	Sharpe	Sortino	Omega	Skw	Fee	GH	Sharpe	Sortino	Omega	Skw	Fee	GH
Equally Weighted	0.050	0.071	1.142	-0.240	0.000	0.000	0.050	0.071	1.142	-0.240	0.000	0.000
Min. Variance	0.057	0.084	1.161	0.069	0.012	-0.047	0.057	0.084	1.161	0.069	0.012	-0.047
						$\mathcal{A}=1$						
Uncond. Gaussian	0.004	0.005	1.011	-0.414	-0.189	-0.132	-0.003	-0.004	0.991	-0.275	-0.207	-0.160
TARCH-CCC	0.050	0.081	1.160	0.867	-0.005	0.364	0.042	0.064	1.116	0.186	-0.032	0.018
TARCH-DCC	0.044	0.071	1.138	0.857	-0.066	0.315	0.046	0.070	1.129	**0.220**	-0.016	0.036
Gaussian Copula	0.053	0.084	1.173	0.617	0.030	0.372	0.059	0.090	1.167	0.179	0.032	0.068
t Copula	0.061	0.100	1.205	**1.191**	0.102	0.457	0.045	0.068	1.124	0.152	-0.017	0.014
skewed t Copula	**0.074**	**0.122**	**1.252**	1.146	**0.231**	**0.582**	**0.066**	**0.100**	**1.189**	0.107	**0.058**	**0.096**
						$\mathcal{A}=2$						
Uncond. Gaussian	0.018	0.024	1.051	-0.618	-0.098	-0.091	0.016	0.021	1.044	-0.629	-0.106	-0.099
TARCH-CCC	0.059	0.093	1.178	0.619	0.046	0.179	0.048	0.072	1.134	0.111	-0.007	0.030
TARCH-DCC	0.053	0.084	1.159	0.622	0.017	0.153	0.058	0.086	1.164	-0.018	0.029	0.065
Gaussian Copula	0.048	0.070	1.147	0.013	-0.015	0.110	0.067	0.100	1.188	-0.004	0.053	0.063
t Copula	**0.083**	**0.154**	**1.296**	**2.375**	**0.196**	**0.353**	0.063	0.095	1.174	**0.145**	0.040	0.050
skewed t Copula	0.078	0.127	1.249	0.861	0.147	0.265	**0.069**	**0.102**	**1.191**	-0.077	**0.058**	**0.068**

Table 2.7 *(continued)*

	Unconstrained						Short-sales Constrained					
	Sharpe	Sortino	Omega	Skw	Fee	GH	Sharpe	Sortino	Omega	Skw	Fee	GH
	$\mathcal{A} = 5$											
Uncond. Gaussian	0.042	0.058	1.119	-0.531	-0.021	-0.041	0.042	0.058	1.119	-0.531	-0.021	-0.041
TARCH-CCC	0.061	0.091	1.178	0.033	0.034	0.042	0.029	0.041	1.079	-0.212	-0.061	-0.065
TARCH-DCC	0.070	0.105	1.199	0.056	0.059	0.064	0.053	0.077	1.146	-0.165	0.008	-0.001
Gaussian Copula	0.078	0.117	1.228	0.046	0.078	0.073	0.059	0.086	1.167	-0.189	0.023	0.000
t Copula	0.072	0.108	1.208	**0.109**	0.061	0.056	0.066	0.097	1.188	**-0.080**	0.040	0.020
skewed t Copula	**0.093**	**0.142**	**1.283**	0.048	**0.125**	**0.123**	**0.082**	**0.120**	**1.238**	-0.262	**0.080**	**0.060**
	$\mathcal{A} = 10$											
Uncond. Gaussian	0.047	0.064	1.130	-0.506	-0.009	-0.036	0.051	0.071	1.144	-0.448	0.002	-0.025
TARCH-CCC	0.016	0.021	1.044	-0.493	-0.090	-0.107	0.018	0.025	1.050	-0.445	-0.083	-0.101
TARCH-DCC	0.040	0.057	1.111	-0.241	-0.024	-0.053	0.022	0.030	1.059	-0.292	-0.067	-0.096
Gaussian Copula	0.059	0.084	1.164	-0.191	0.019	-0.018	0.070	0.102	1.198	-0.226	0.043	0.005
t Copula	0.070	0.102	1.203	-0.244	0.045	0.012	0.058	0.083	1.160	**-0.174**	0.017	-0.018
skewed t Copula	**0.091**	**0.135**	**1.269**	**-0.155**	**0.091**	**0.054**	**0.088**	**0.128**	**1.254**	-0.268	**0.080**	**0.041**

We also observe in Table 2.7 that portfolio decisions made using t and skewed t copulas have generally higher skewness coefficients than do Gaussian models. That is, taking into account tail dependence in the portfolio decisions could decrease the likelihood of negative portfolio returns.

Now, we compare the six model-driven portfolios in terms of their performance with respect to a benchmark strategy: the equally-weighted portfolio. For that purpose, we employ two relative performance measures: the opportunity cost or performance fee (*Fee*) and the Graham-Harvey metric (GH). The performance fee is the amount that must be added to the return of the equally-weighted strategy, such that it leaves the investor indifferent to both portfolio decisions. The Graham and Harvey (1997) measure is the difference between the alternative portfolio returns on the volatility-matched benchmark portfolio. That is, to make both portfolios comparable in terms of volatility, we lever up/down the benchmark to match the alternative portfolio's volatility over the evaluation period. Table 2.7 reports both relative performance measures (in basis points per week) of the realized portfolio returns over the allocation period (2006-2010).

For all the preferences specifications considered, both relative performance measures coincide in indicating the same best performing strategy (see values in bold in Table 2.7). Results suggest that the investor can obtain substantial gains using the portfolio rules based on conditional t copulas with generalized t marginal distributions for most of the preference specifications we report in Table 2.7. The gains seem to be higher for the skewed t copula portfolio for the unconstrained investor when $\mathcal{A}$ is lower, although we do not observe the same monotonic relation for the t or Gaussian copula portfolios or for the short-sales constrained investor. The opportunity costs of an investor holding the equally weighted portfolio instead of the portfolio based on the skewed t copula are between 3 and 12 basis points per year, whereas the opportunity costs for the Gaussian copula strategy range from -1 to 4 basis points per year. When we use the GH measure to compare alternative strategies with different levels of risk, we also find that copula models with tail dependence outperform Gaussian dependence models. In particular, the GH measure for the skewed t copula portfolios varies between 2 and 30 basis points per year; this measure for Gaussian copula portfolios ranges from 0 to 19 basis points; and for the DCC strategy, it varies between -5 and 16 basis points.

These results suggest that the allocation differences found among the multivariate copulas portfolios imply also economical differences in terms of investment ratios and performance measures. The univariate higher moments and the tail and asymmetric dependence seem to be key features

at this respect, especially for more aggressive investors. Specifically, as variance and loss aversion increase, skewed t copula strategies are less likely to produce large performance differences. These differences are also smaller for the short-sales constrained allocation, where the investor cannot increase their exposure to commodity futures taking extreme short positions in equity. These results related to risk aversion and the performance of non-linear models is consistent with findings previously reported in portfolio choice literature (e.g., Patton (2004) for the case of asymmetric dependence and wealth allocation between small and large cap stock indices; and Das and Uppal (2004) for the case of systemic risk and international portfolio choice). In the next section, we evaluate the robustness of our results, including in the analysis other parameterizations of the three-moment preferences.

Robustness analysis

As a first robustness check, we investigate the allocation decisions made using three-moment preferences specifications with arbitrary impacts of the portfolio variance and skewness (i.e. with arbitrary values of coefficients φ_{V} and φ_{S}). Since the coefficients φ_{V} and φ_{S} may not be necessarily related with a third-order Taylor expansion of a given utility function, we have more flexibility to define ad-hoc three-moment investor's preferences; like in Harvey, Liechty, Liechty, and Müller (2010). In Table 2.8, we report the percentiles of the distributions of optimal portfolio weights for some of these preferences specifications. With respect to the allocation differences among our copula strategies, the results of this complementary approach are consistent with our previous findings. Furthermore, using arbitrary coefficients φ_{V} and φ_{S} we can do some sensitivity analysis and investigate the effect of increasing the impact of portfolio variance (φ_{V}) or skewness (φ_{S}) on the optimal allocation. More specifically, we find that when the impact of skewness (φ_{S}) increases, the median positions in equity and oil diminish, whereas long positions in gold increases.

For example, for φ_{V}=1/4 and φ_{S}=0, the skewed t copula model yields median positions equal to 0.34, 0.59, and -2.83 for oil, gold, and equity; whereas if φ_{S} rises to 1/2, the median positions are 0.09, 0.79, and -3.37. Besides, for φ_{V}=1/2, increasing φ_{S} from 1/4 to 1 modifies the median positions of oil, gold, and equity from 0.28, 0.53, and -1.02 to 0.14, 0.54, and -1.18, respectively. On the other hand, when increasing the impact of variance (φ_{V}), the median and low quantiles of equity weights rise significantly, as we observed previously in Section 2.3.3. For instance, for φ_{S}=1/2, when φ_{V}=1/4, the skewed t strategy generates median positions equal to 0.09, 0.79,

Table 2.8. Optimal portfolio weights for different preference parameterizations

This table reports the summary statistics of the optimal portfolio weights for different multivariate models and preference specifications parameterized according to Harvey, Liechty, Liechty, and Müller (2010).

	Uncond. Gaussian			CCC			DCC			Gaussian Copula			t copula			skewed t copula		
	ω_o	ω_g	ω_e	ω_o	ω_g	ω_e	ω_o	ω_g	ω_e	ω_o	ω_g	ω_e	ω_o	ω_g	ω_e	ω_o	ω_g	ω_e
	$\varphi_V = 1/4$ and $\varphi_S = 0$																	
5% pct.	0.00	0.00	-1.42	0.00	-0.90	-10.0	-0.04	-1.82	-10.0	0.00	-2.42	-10.0	0.00	-2.86	-10.0	0.00	-2.87	-10.0
Median	1.05	0.00	-0.37	1.65	0.00	-2.84	1.42	0.00	-3.31	0.44	0.71	-2.61	0.54	0.68	-2.61	0.34	0.59	-2.83
95% pct.	2.04	1.34	1.00	7.57	7.57	1.00	7.84	7.80	1.00	5.15	10.27	1.00	5.40	10.55	1.00	5.40	10.60	1.00
	$\varphi_V = 1/4$ and $\varphi_S = 1/2$																	
5% pct.	0.00	0.00	-1.44	0.00	-0.44	-10.0	-0.04	-1.84	-10.0	0.00	-2.36	-10.0	0.00	-2.85	-10.0	0.00	-2.79	-10.0
Media	1.06	0.00	-0.38	1.67	0.00	-2.97	1.44	0.00	-3.38	0.32	0.80	-3.00	0.36	0.86	-3.34	0.09	0.79	-3.37
95% pct.	2.07	1.34	1.00	8.82	7.64	1.00	8.46	7.85	1.00	5.15	11.0	1.00	5.49	11.0	1.00	5.33	11.0	1.00
	$\varphi_V = 1/2$ and $\varphi_S = 1/4$																	
5% pct.	0.00	0.00	-0.40	0.00	-0.54	-4.82	-0.13	-1.09	-5.26	0.00	-1.31	-5.56	0.00	-1.58	-5.33	-0.08	-1.59	-5.37
Media	0.60	0.00	0.18	0.88	0.11	-1.13	0.75	0.00	-1.29	0.29	0.49	-0.89	0.39	0.57	-0.84	0.28	0.53	-1.02
95% pct.	1.10	0.91	1.00	3.86	4.15	1.00	3.84	4.45	1.00	2.82	5.47	1.00	2.83	5.26	1.00	2.89	5.32	1.00
	$\varphi_V = 1/2$ and $\varphi_S = 1$																	
5% pct.	0.00	0.00	-0.41	0.00	-0.52	-4.99	-0.11	-1.10	-5.39	0.00	-1.33	-10.0	0.00	-1.54	-10.0	-0.08	-1.52	-10.0
Media	0.60	0.00	0.18	0.88	0.03	-1.14	0.77	0.00	-1.31	0.25	0.54	-1.02	0.34	0.64	-1.12	0.14	0.54	-1.18
95% pct.	1.11	0.91	1.00	4.02	4.04	1.00	3.97	4.53	1.00	2.71	9.60	1.00	2.86	10.9	1.00	2.85	11.0	1.00
	$\varphi_V = 1$ and $\varphi_S = 1/2$																	
5% pct.	0.09	0.00	0.03	-0.06	-0.40	-2.16	-0.18	-0.67	-2.42	-0.10	-0.75	-2.42	-0.11	-0.85	-2.37	-0.14	-0.90	-2.39
Media	0.36	0.10	0.41	0.50	0.22	-0.21	0.43	0.22	-0.30	0.21	0.45	-0.18	0.24	0.49	-0.13	0.20	0.45	-0.17
95% pct.	0.62	0.69	0.92	1.99	2.28	1.00	1.96	2.44	1.00	1.46	2.79	1.00	1.46	2.77	1.00	1.50	2.84	1.00

Table 2.9. Investment ratios and relative performance measures for different preference parameterizations

This table reports the investment ratios and relative performance measures (in basis points per week) of the realized portfolio returns over the allocation period for different preference specifications (φ_V and φ_S) parameterized according to Harvey, Liechty, Liechty, and Müller (2010). The highest value of each measure is marked in boldface.

	Sharpe	Sortino	Omega	Skw	Fee	GH
Equally Weighted	0.050	0.071	1.142	-0.240	0.000	0.000
Min. Variance	0.057	0.084	1.161	0.069	0.012	-0.047
	$\varphi_V = 1/4$ and $\varphi_S = 0$					
Uncond. Gaussian	0.003	0.004	1.008	-0.089	-0.302	-0.128
TARCH-CCC	0.045	0.071	1.148	0.474	-0.092	0.704
TARCH-DCC	0.045	0.072	1.144	**0.585**	-0.103	0.715
Gaussian Copula	0.070	0.112	1.235	0.459	0.330	1.044
t Copula	0.063	0.099	1.211	0.387	0.218	0.939
skewed t Copula	**0.074**	**0.119**	**1.251**	0.431	**0.407**	**1.127**
	$\varphi_V = 1/4$ and $\varphi_S = 1/2$					
Uncond. Gaussian	0,002	0,003	1,006	-0,095	-0,314	-0,134
TARCH-CCC	0,044	0,069	1,147	0,684	-0,141	0,780
TARCH-DCC	0,050	0,080	1,165	0,514	0,001	0,892
Gaussian Copula	0,041	0,065	1,136	0,576	-0,190	0,717
t Copula	0,036	0,056	1,113	0,482	-0,182	0,650
skewed t Copula	**0,076**	**0,133**	**1,289**	**1,894**	**0,614**	**1,658**
	$\varphi_V = 1/2$ and $\varphi_S = 1/4$					
Uncond. Gaussian	0.003	0.004	1.007	-0.411	-0.194	-0.137
TARCH-CCC	0.053	0.085	1.169	0.852	0.024	0.392
TARCH-DCC	0.045	0.073	1.141	0.862	-0.053	0.325
Gaussian Copula	0.055	0.087	1.178	0.675	0.044	0.383
t Copula	0.062	0.101	1.208	**1.108**	0.112	0.460
skewed t Copula	**0.079**	**0.132**	**1.271**	1.096	**0.283**	**0.630**
	$\varphi_V = 1/2$ and $\varphi_S = 1$					
Uncond. Gaussian	0.022	0.029	1.062	-0.601	-0.087	-0.080
TARCH-CCC	0.059	0.094	1.180	0.615	0.050	0.182
TARCH-DCC	0.053	0.084	1.158	0.620	0.017	0.152
Gaussian Copula	0.049	0.073	1.153	0.082	-0.006	0.118
t Copula	0.061	0.097	1.187	**0.828**	0.054	0.166
skewed t Copula	**0.080**	**0.129**	**1.253**	0.819	**0.153**	**0.267**
	$\varphi_V = 1$ and $\varphi_S = 1/2$					
Uncond. Gaussian	0.005	0.007	1.015	-0.415	-0.184	-0.126
TARCH-CCC	**0.053**	**0.085**	**1.170**	0.847	**0.023**	**0.404**
TARCH-DCC	0.046	0.074	1.144	**0.857**	-0.049	0.344
Gaussian Copula	0.006	0.008	1.018	-0.054	-0.069	-0.218
t Copula	0.038	0.059	1.107	-0.019	-0.004	0.302
skewed t Copula	0.044	0.071	1.123	0.702	0.013	0.330

and -3.37; whereas if φ_V=1, assets median positions are equal to 0.20, 0.45, and -0.17. In addition, the 5% percentile of equity weights increases from -10.0 to -2.39, and the 95% percentiles of oil and gold decrease from 5.33 and 11.0 to 1.50 and 2.84, respectively.

We also calculate the investment ratios and relative performance measures of the realized portfolio returns for these parameterizations of the three-moment preferences; see Table 2.9. The conditional t copulas outperformed the multivariate Gaussian models in 4 of the 5 comparisons, suggesting again the importance of dependence specification for asset allocation with commodity futures. The GH measures (relative to the equally weighted portfolio) obtained from the skewed t copula model ranges between 14 and 86 basis points per year, while the DCC model vary between 8 and 46 basis points per year.

Finally, using the reality check test of Hansen (2005), we compare jointly the out-of-sample performance of the different portfolio strategies. To apply this superior predictive ability test, we first need to define a metric (loss function) and then employ this metric to compute the relative performance of each model with respect to a chosen benchmark model. The null hypothesis is that the benchmark is as good as any alternative model in terms of portfolio performance. That is, the test answers if any of the models is better than the given benchmark. The stationary bootstrap of Politis and Romano (1994) is used to estimate the distribution of the test statistics under the null. Hansen (2005) proposed three p-values based on the test statistic estimates: a consistent p-value, as well as upper and lower bounds for the true p-value.

Employing the opportunity cost as our metric function (Patton (2004)), we conduct the test of superior portfolio performance for different benchmark models. The corresponding p-values are reported in Table 2.10.The null hypothesis is rejected for small p-values. We observe that the probability of rejecting the null hypothesis for the equally weighted and unconditional Gaussian portfolios is higher (p-values < 0.10) for unconstrained strategies and for low values of $\mathcal{A}$, that is, for more aggressive investors. The DCC model is outperformed by other models, with p-values < 0.15, in six of the twelve specifications we report. We are able to reject the conditional Gaussian copula model for three cases. In contrast, the conditional t copula strategy is only rejected twice, and there is little evidence that the conditional skewed t copula portfolio is outperformed by alternative models. Therefore, conditional copulas with tail dependence have generally superior out-of-sample performance for the different specifications considered.

Table 2.10. Test for superior portfolio performance

This table reports the reality check p-values of the Hansen (2005) test for superior portfolio performance for different benchmark models. Three p-values are reported: the consistent estimate (c) and the upper (u) and lower (l) bounds. We employ the opportunity cost as the performance function in this case. For small p-values, we reject the hypothesis that the benchmark model performs as well as the best competing alternative model. Those p-values below 0.15 are marked in boldface. The implementation is based on the stationary bootstrap of Politis and Romano (1994).

	Unconstrained			Short-sales Constrained			(Harvey et al., 2010)		
	l	c	u	l	c	u	l	c	u
	$\mathcal{A}=1$						$\varphi_{\mathrm{V}}=1/4$ and $\varphi_{\mathrm{S}}=0$		
Equally weighted	**0.037**	**0.049**	**0.049**	0.232	0.232	0.251	**0.104**	**0.104**	**0.104**
Uncond. Gaussian	**0.032**	**0.032**	**0.032**	**0.069**	**0.069**	**0.069**	**0.026**	**0.026**	**0.026**
CCC	**0.035**	**0.046**	**0.046**	**0.134**	**0.135**	**0.135**	**0.061**	**0.061**	**0.054**
DCC	**0.046**	**0.050**	**0.050**	**0.142**	0.153	0.153	**0.060**	**0.060**	**0.054**
Gaussian Copula	**0.137**	0.192	0.192	0.499	0.713	0.713	0.706	0.858	0.547
t Copula	0.156	0.243	0.243	**0.122**	**0.131**	**0.131**	0.275	0.275	0.200
skewed t Copula	1.000	1.000	1.000	1.000	1.000	1.000	0.837	0.895	0.895
	$\mathcal{A}=2$						$\varphi_{\mathrm{V}}=1/4$ and $\varphi_{\mathrm{S}}=1/2$		
Equally weighted	**0.086**	0.113	0.113	**0.141**	0.152	0.152	0.170	0.170	0.162
Uncond. Gaussian	**0.048**	**0.048**	**0.048**	**0.113**	**0.119**	**0.119**	**0.069**	**0.069**	**0.069**
CCC	0.167	0.278	0.278	**0.139**	0.166	0.166	**0.130**	**0.130**	**0.124**
DCC	0.155	0.198	0.198	0.565	0.782	0.782	0.179	0.179	0.163
Gaussian Copula	**0.109**	**0.111**	**0.111**	0.888	0.894	0.894	0.167	0.167	**0.089**
t Copula	1.000	1.000	1.000	0.644	0.736	0.736	**0.134**	**0.100**	**0.096**
skewed t Copula	0.531	0.572	0.792	0.902	0.902	0.902	1.000	1.000	1.000

Table 2.10 *(continued)*

	Unconstrained			Short-sales Constrained			(Harvey et al., 2010)		
	l	c	u	l	c	u	l	c	u
	$\mathcal{A} = 5$						$\varphi_{\mathrm{V}} = 1/2$ and $\varphi_{\mathrm{S}} = 1/4$		
Equally weighted	**0.128**	**0.135**	**0.135**	**0.131**	**0.133**	**0.133**	**0.137**	**0.137**	**0.128**
Uncond. Gaussian	**0.083**	**0.083**	**0.083**	**0.113**	**0.114**	**0.114**	**0.025**	**0.025**	**0.025**
CCC	0.353	0.358	0.358	**0.056**	**0.056**	**0.056**	0.237	0.237	0.233
DCC	0.463	0.470	0.470	**0.139**	**0.143**	**0.143**	0.213	0.213	0.179
Gaussian Copula	0.418	0.564	0.564	0.155	0.155	0.155	0.270	0.270	0.215
t Copula	0.366	0.441	0.441	0.155	0.319	0.319	0.314	0.314	0.256
skewed t Copula	0.880	0.887	0.887	1.000	1.000	1.000	1.000	1.000	1.000
	$\mathcal{A} = 10$						$\varphi_{\mathrm{V}} = 1$ and $\varphi_{\mathrm{S}} = 1/2$		
Equally weighted	**0.142**	0.153	0.157	**0.135**	**0.143**	**0.148**	0.261	0.261	0.249
Uncond. Gaussian	**0.113**	**0.124**	**0.124**	**0.109**	**0.141**	**0.141**	**0.105**	**0.105**	**0.104**
CCC	**0.015**	**0.015**	**0.015**	**0.063**	**0.063**	**0.063**	1.000	1.000	1.000
DCC	**0.046**	**0.046**	**0.046**	**0.036**	**0.037**	**0.037**	**0.126**	**0.126**	**0.109**
Gaussian Copula	**0.111**	**0.111**	**0.111**	**0.131**	0.214	0.235	**0.107**	**0.107**	**0.107**
t Copula	0.197	0.212	0.212	0.151	0.167	0.167	0.267	0.267	0.159
skewed t Copula	0.730	0.778	0.778	0.795	0.833	0.833	0.825	0.845	0.766

2.4 Conclusions

This chapter investigates the portfolio selection problem of an investor with time-varying three-moment preferences when commodity futures are part of the investment opportunity set. In our specification, the portfolio returns' skewness provides a measure of the investor's loss aversion. We model the joint distribution of asset returns using a flexible multivariate copula setting that can disentangle the specific properties of each asset process from its dependence structure. The more general model we posit consists of a conditional skewed t copula with generalized Student's t marginal distributions and time-varying moments. Thus we can capture the specific distributional characteristics of commodity-futures returns and focus on their implications for the portfolio selection problem.

The empirical application employs weekly data for oil and gold futures and for the S&P 500 equity index, from June 1990 to September 2010. Our preliminary analysis and in-sample estimations suggest the presence of skewness and fat tails in the univariate processes, as well as evidence of both extreme and asymmetric dependence among oil, gold, and equity. When computing the optimal portfolio weights, we find substantial discrepancies between the holdings obtained from our conditional copula models and those from more traditional Gaussian models. The key factors underlying these differences are the different specifications of the time-varying marginal distributions, the presence of dynamic conditional dependence among the univariate processes, and the modeling of tail and asymmetric dependence. The univariate higher moments and the type of tail dependence are more relevant for aggressive investors. These discrepancies translate into economical differences in terms of better investment ratios and relative performance measures for the different specifications considered. For instance, depending on the allocation specification, the gains of using the conditional t copulas range up to 86 basis points per year for the period 2006-2010. The performance differences of portfolio strategies based on more flexible copulas are smaller when variance and loss aversion increase, as well as for short-sales constrained allocations. Furthermore, we analysis the robustness of our results, confirming that conditional copulas with tail dependence have generally superior out-of-sample performance for the different specifications considered.

Finally, some extensions to our analysis can be considered. For instance, it would be interesting to study the sensitivity of the investor's portfolio decisions to parameter uncertainty. Note that some cautions with the propagation of errors between the marginal distributions and the copula function

have to be taken into account when implementing this type of analysis. Another possibility is to extend our portfolio selection problem with commodity futures to a dynamic asset allocation context. Thus, we could evaluate the hedging component of the optimal portfolio weights under the effects of skewness and asymmetric dependence.

3

Tail risk in energy portfolios

THE GROWTH OF ENERGY MARKETS has been sustained by continued deregulation processes, which have encouraged the separation of the formerly integrated value chains. This process has increased market risk exposures at every stage of the chain, including the purchase and sale of fuels, electricity generation, and obtaining gas or electricity for retail supply. In addition to the physical resource holders, financial players, such as banks and hedge funds, increasingly participate in energy markets to satisfy their customers' demands to gain or hedge energy risk exposure, as well as to trade on their own behalf. In this context, energy-related companies and financial players experience greater exposures to energy price risk, which has particular characteristics that make it different from other market risks and requires clearer explication.

In this chapter, we therefore analyze the energy price risks from a multivariate perspective. In particular, we study the aggregate tail risk of different linear energy portfolios using an asset-level approach. Accordingly, we can propose a multivariate model for the vector of energy risk factors; using the portfolio exposures to each factor, we in turn can calculate the aggregate tail behavior of the portfolio. Next, we compute the corresponding portfolio risk measures and evaluate the extent to which the tail pattern of the model is important in practice.

With this asset-level approach, we can capture the entire structure of energy risk factors in a portfolio and their interdependence relationships. This multivariate behavior (univariate and joint structure) of energy risk factors depends on the special characteristics of energy markets. In particular, the pricing of energy commodities relies largely on an equilibrium among supply, demand, and inventories, subject to various operational constraints (for example, due to infeasible or overly costly storage). These charac-

teristics cause deregulated energy markets to exhibit substantial volatility, price spikes, time-varying correlation, dependence in the extremes, and mean-reversion patterns (e.g., Cartea and Figueroa (2005), Benth, Šaltytė Benth, and Koekebakker (2008), Escribano, Peña, and Villaplana (2011), Huisman and Mahieu (2003), Pirrong (2012), and Routledge, Seppi, and Spatt (2001)).

We therefore employ a multivariate density model to depict the energy risk factors, in which we seek to include all the stylized features of the data generating process. For this purpose, we consider an econometric specification with time-varying conditional means, volatilities, and correlations, in which the innovation vector follows a multivariate generalized hyperbolic (GH) distribution. The GH class is a very flexible family of distributions that accommodates excess kurtosis, skewness, and dependence in the extremes.[1] In particular, we consider special cases included in the multivariate GH class, namely the normal inverse Gaussian (NIG) distribution, the variance-gamma (VG) distribution, the GH skewed t (skT) distribution, Student's t (T) distribution, and the Gaussian (G) distribution. These distributions differ in their dependence and tail decay patterns. In this way, we extend previous theoretical and empirical studies that employ some of these distributions to the risk analysis of energy assets (see Benth and Šaltytė Benth (2004), Börger, Cartea, Kiesel, and Schindlmayr (2009), Eberlein and Stahl (2003), Giot and Laurent (2003), and Weron (2006)).

We apply our multivariate GH specification to model the returns vector formed by the four most important commodities in the U.S. energy market: crude oil, natural gas, coal, and electricity. These commodities constitute the elements of our linear energy portfolios, which represent the exposure of any given energy company or financial player to energy price risk. We use daily data from August 2005 to March 2012 to estimate the multivariate models and evaluate the tail risk of the portfolio profit-and-loss (P&L) distribution. Then using data from March 2010 to March 2012, we conduct out-of-sample forecast evaluations of the risk measures.

We address the analysis of the aggregate tail risk by calculating two risk measures, the value at risk (VaR) and the expected shortfall (ES), for long and short trading positions in the energy portfolios. The VaR corresponds to the quantile of the portfolio loss distribution for a given probability or confidence level. The ES is defined as the conditional average loss beyond a

[1]With different parametrizations, this family of distributions has been applied in financial modeling of univariate and multivariate problems; see for example Aas and Haff (2006), Bingham and Kiesel (2002), Hu and Kercheval (2010), McNeil, Frey, and Embrechts (2005), and Prause (1999).

given quantile, and it better describes the behavior of the portfolio losses in the tail. We estimate both measures for different confidence levels, which define how far out in the tails the risk measures are calculated, as well as for several day horizons, to obtain a short-term surface of risk. Whereas most equity risk studies have focused on the left tail of long positions, the presence of positive jumps in the data generating process of energy commodities, especially for the natural gas and electricity markets, suggests that the analysis of the right tail of the possibly asymmetric P&L distribution could be relevant for traders who are worried about increases in energy prices (i.e., those with short positions).

Finally, using different backtest procedures, we monitor, for the out-of-sample period, the performance of the risk measure estimates that correspond to the GH models. In these comparative tests, we also consider several traditional approaches to calculate risk measures: the unconditional Gaussian (variance-covariance, VC) approach, the Riskmetrics model (or exponentially weighted moving average, EWMA), and non-parametric historical simulations. We pay special attention to the backtesting of the ES estimates, because this measure offers more information about aggregate tail behavior. Thus, we propose a new backtest procedure that employs the superior predictive ability (SPA) test of Hansen (2005), along with a metric function based on the ES backtesting measures of Embrechts, Kaufmann, and Patie (2005), to compare the performance of the whole set of alternative models.

The main empirical results of the chapter are as follows: With respect to the estimates of the econometric specification, we find evidence of time-varying evolution in the conditional correlations between energy markets. In particular, we observe positive asymmetry in the correlation dynamics between fuels and electricity, which has not been previously documented in this context. This result makes economic sense, in that fuel prices increase the generation costs of electricity. Regarding the conditional distribution, the results for the recursive estimations over the out-of-sample period reveal the presence of fat tails and positive skewness in the multivariate distribution of energy risk factors. These results for the estimated densities are consistent with the hypothesis of jump diffusions in the energy data generating processes. Although the VG and NIG models offer the best in-sample fit performance for the multivariate distribution of the energy returns, the T and skT models seem to estimate aggregate tail risk behavior better, especially in the case of the right tail of the portfolio's P&L distribution. The out-of-sample evaluation of the risk measure forecasts favors these findings. In general, there are more VaR violations across models for short positions

than for long ones, confirming the positive asymmetry of the P&L distribution of the energy portfolios. We also observe that the ES exceedances are quite high for (conditional and unconditional) Gaussian models, especially for the two utility portfolios. The heavy-tail models behave much better than alternative versions, with regard to the tail risk of short positions. Finally, according to the results of the SPA backtest, models with exponential tail decay (including the VG and NIG) yield inferior tail estimates for short portfolio positions compared with the T and skT models (with polynomial tail decay), especially for the far tail ($\alpha = 1\%$) of utility portfolios at short horizons. Therefore, the extent of the underestimations of the tail risk of the portfolio loss distribution depends on whether we are analyzing short or long positions in the energy portfolio, the type of portfolio, the horizon, and how far out in the tail the risk is being analyzed.

In Section 2, we begin by presenting the linear portfolios of energy commodities and the portfolio profit-and-losses function. Section 3 introduces the econometric specifications, based on the dynamic multivariate GH models, for the energy returns vector. With Section 4, we characterize the conditional risk measures, the VaR and ES, according to the multivariate models we introduced in Section 2. Next, we provide a description of the energy futures data that constitute the portfolios and the results from the empirical estimations, including a description of the tail fit of the GH models, in Section 5. After we report the results of the risk measures forecast and analyze their out-of-sample performance, in Section 6, we conclude in Section 7. A final appendix provides the technical details for the different portfolios included in the analysis, the multivariate density functions, the estimation methodologies, and the backtest measures.

3.1 Portfolios of energy commodities

We approximate a given exposure to energy price risk using a corresponding portfolio of energy futures. Thus, changes in the energy price risk factors can be mapped linearly to changes in the value of the energy futures portfolio.[2] For example, a linear portfolio could represent directly the energy futures positions of an institutional investor or the energy price exposure of an electricity producer with fuel-fired power plants. In this chapter, we consider four energy commodities: crude oil, natural gas, coal, and electric-

[2]A portfolio of futures contracts can also be considered a first-order approximation of more general energy asset portfolios with non-linear payoffs (Tseng and Barz, 2002; Cartea and González-Pedraz, 2012).

ity, identified by subscripts i equal to 1, 2, 3, and 4, respectively. These four commodities substantially represent any general exposure to energy price risk.[3]

Let $F_{i,t}$ denote the settlement price at time t of an energy futures contract i. We then assume that the value W_t of a given energy portfolio is determined by a linear combination of futures $F_{i,t}$, such that

$$W_t = \sum_{i=1}^{4} q_{i,t} F_{i,t} = \sum_{i=1}^{4} w_{i,t} = \boldsymbol{w}_t' \boldsymbol{\imath}_4 \,, \tag{3.1}$$

where the quantities $q_{i,t}$ define the size and sign of the exposure to the energy commodity i; $\boldsymbol{w}_t = (w_{1,t}, \ldots, w_{4,t})' = (q_{1,t}F_{1,t}, \ldots, q_{4,t}F_{4,t})'$ defines the portfolio weights in dollars of each energy commodity; and $\boldsymbol{\imath}_4$ is a 4×1 vector of ones.

Thus, the h-period return (in dollars) on an energy portfolio at time t is given by

$$\Delta W_t(h) = W_t - W_{t-h} = R_t(h) W_{t-h} = \boldsymbol{w}_{t-h}' (\exp(\boldsymbol{r}_t(h)) - \boldsymbol{\imath}_4) \,, \tag{3.2}$$

where $R_t(h)$ is the h-period net return on the portfolio, $\boldsymbol{r}_t(h) = \sum_{k=0}^{h-1} \boldsymbol{r}_{t-k}$ is the 4×1 vector of h-period log-returns, and $\boldsymbol{r}_t$ is the 4×1 one-period log-return vector at time t with the i-th component $r_{i,t} = \log(F_{i,t}/F_{i,t-1})$. The energy log-returns $r_{i,t}$ constitute the vector of risk factors.

According to equation (3.2), the portfolio's profit-and-loss (P&L) distribution is determined by the multivariate density model of energy risk factors $\boldsymbol{r}_t$ and the positions in the energy commodities $\boldsymbol{w}_t$. The multivariate model of risk factors describes the joint behavior of the four commodities. The different positions in energy futures define the size and sign of the exposure to each energy commodity, mapping the multivariate model onto a specific P&L distribution. In this chapter, we consider four portfolios: two related to power utilities and two others more related to financial players.

As representative portfolios of electricity producers, we include the energy portfolio of a utility with a diversified mix of generation that operates in the Pennsylvania-Jersey-Maryland (PJM) Interconnection and a linear portfolio corresponding to a gas-fired power plant. In addition, we account for two typical portfolios of financial players that seek exposure to energy

[3]Oil constitutes 33% of the world's total primary energy supply, followed by coal with a share of 27% and natural gas with 21%. In addition, coal, natural gas, and oil represent 41%, 21%, and 5%, respectively, of the world's electricity generation (International Energy Agency (2011)).

commodities: an equally weighted portfolio and the minimum variance portfolio. In Appendix A.6, we provide more details about the construction of these portfolios.

3.2 A dynamic multivariate GH model for energy returns

Using $\boldsymbol{r}_t = (r_{1,t}, \ldots, r_{4,t})'$ as the vector of the four energy assets log-returns at time t, we assume that the data generating process for $\{\boldsymbol{r}_t : t = 1, \ldots, T\}$ is given by

$$\boldsymbol{r}_t = \boldsymbol{m}_t + \boldsymbol{\varepsilon}_t \,, \text{ and} \tag{3.3}$$

$$\boldsymbol{\varepsilon}_t = \boldsymbol{H}_t^{1/2} \boldsymbol{x}_t \,, \tag{3.4}$$

where $\boldsymbol{m}_t$ and $\boldsymbol{\varepsilon}_t$ are the 4×1 vectors of conditional means and unexpected returns; $\boldsymbol{H}_t^{1/2}$ is the 4×4 Cholesky factor of the time-varying 4×4 covariance matrix $\boldsymbol{H}_t$, such that $\boldsymbol{H}_t = \boldsymbol{H}_t^{1/2}(\boldsymbol{H}_t^{1/2})'$; and $\boldsymbol{x}_t$ is the 4×1 vector of independent innovations, which follows a four-variate generalized hyperbolic (GH) distribution with zero mean and an identity covariance matrix.

To capture the possible presence of serial correlation in energy returns, we consider a diagonal vector autoregressive (VAR) process with up to 5 lags for the vector of returns.[4] Thus, the conditional mean vector is given by

$$\boldsymbol{m}_t = \mathbb{E}(\boldsymbol{r}_t | \mathcal{F}_{t-1}) = \boldsymbol{m}_0 + \sum_{j=1}^{5} \boldsymbol{\Phi}_j \boldsymbol{r}_{t-j} \,, \tag{3.5}$$

where $\boldsymbol{m}_0$ is a constant 4×1 vector, $\boldsymbol{\Phi}_j$ are 4×4 diagonal matrices, and the expectation is conditional on the history of the process up to time $t-1$, that is, $\mathcal{F}_{t-1} = \sigma(\{\boldsymbol{r}_s : s \leq t-1\})$.

At the same time, the conditional covariance matrix $\boldsymbol{H}_t$ can be decomposed as follows

$$\boldsymbol{H}_t = \mathrm{Cov}(\boldsymbol{r}_t | \mathcal{F}_{t-1}) = \boldsymbol{D}_t \boldsymbol{P}_t \boldsymbol{D}_t \,, \tag{3.6}$$

where $\boldsymbol{D}_t$ is the 4×4 diagonal matrix composed by the conditional volatilities of $\boldsymbol{r}_t$, and $\boldsymbol{P}_t$ is the 4×4 conditional correlation matrix. We want to capture possible persistence and asymmetry in conditional variances and correlations. For that purpose, we assume univariate asymmetric GARCH(1,1)

[4] In a previous empirical analysis, we determine the number of lags in the model, first, taking into account those lags that are significant and help to reduce the presence of autocorrelation in the asset returns; then, considering the values of Bayesian Information Criteria to select among the different alternative models.

processes for the conditional variances and a modified version of the asymmetric dynamic conditional correlation (ADCC) model of Cappiello, Engle, and Sheppard (2006) for the time-varying correlation matrix. That is, the elements of the diagonal volatility matrix $\boldsymbol{D}_t$, $\sqrt{h_{i,t}}$, satisfy

$$h_{i,t} = \alpha_{0,i} + \alpha_{1,i}\varepsilon_{i,t-1} + \alpha_{1,i}^{-}\varepsilon_{i,t-1}\mathbb{1}_{\{\varepsilon_{i,t-1}\leq 0\}} + \alpha_{2,i}h_{i,t-1}\,, \quad i = 1,\ldots,4\,, \tag{3.7}$$

where $\alpha_{0,i} > 0$, $\alpha_{1,i} \geq 0$, $\alpha_{1,i} + \alpha_{1,i}^{-} \geq 0$, $\alpha_{2,i} > 0$, and $\alpha_{1,i} + \alpha_{1,i}^{-}/2 + \alpha_{2,i} < 1$, which guarantees that the process is positive and covariance stationary. The dynamics of the correlation matrix in our version of the ADCC model is given by

$$\boldsymbol{P}_t = \operatorname{diag}(\boldsymbol{Q}_t)^{-1/2}\,\boldsymbol{Q}_t\,\operatorname{diag}(\boldsymbol{Q}_t)^{-1/2}\,, \tag{3.8}$$

$$\boldsymbol{Q}_t = [(1-\delta_1-\delta_2)\bar{\boldsymbol{Q}} - \delta_1^{+}\bar{\boldsymbol{N}}] + \delta_1\boldsymbol{u}_{t-1}\boldsymbol{u}_{t-1}' + \delta_1^{+}\boldsymbol{n}_{t-1}\boldsymbol{n}_{t-1}' + \delta_2\boldsymbol{Q}_{t-1}\,, \tag{3.9}$$

where $\delta_1, \delta_1^{+}, \delta_2 \geq 0$; $\boldsymbol{u}_t = \boldsymbol{D}_t^{-1}\boldsymbol{\varepsilon}_t$ is the 4×1 vector of standardized residuals; $\boldsymbol{n}_t = \boldsymbol{u}_t\mathbb{1}_{\{\boldsymbol{u}_t\geq 0\}}$; and $\bar{\boldsymbol{Q}} = \mathbb{E}(\boldsymbol{u}_{t-1}\boldsymbol{u}_{t-1}')$ and $\bar{\boldsymbol{N}} = \mathbb{E}(\boldsymbol{n}_{t-1}\boldsymbol{n}_{t-1}')$ are the unconditional covariance matrices of $\boldsymbol{u}_t$ and $\boldsymbol{n}_t$. A sufficient condition for $\boldsymbol{Q}_t$ to be positive definite is that $\delta_1 + \delta_2 + \bar{\eta}\delta_1^{+} < 1$, where $\bar{\eta}$ is the maximum eigenvalue of $\bar{\boldsymbol{Q}}^{-1/2}\bar{\boldsymbol{N}}\bar{\boldsymbol{Q}}^{-1/2}$. With this specification, we investigate, in the conditional correlation, the presence of asymmetric responses to positive shocks.

Motivated by the presence of jumps and spikes in energy prices, we employ multivariate GH distributions to model the conditional distribution of the vector of innovations $\boldsymbol{x}_t$. These GH distributions are flexible enough to accommodate different tail behaviors and types of asymmetry (e.g., thin or heavy tails, symmetric or positive/negative skewness). The GH family can be obtained using the following normal mean-variance mixture representation (see McNeil, Frey, and Embrechts, 2005):

$$\boldsymbol{x}_t \overset{\text{dist.}}{=} \boldsymbol{\mu} + \omega_t\boldsymbol{\gamma} + \omega_t^{1/2}\boldsymbol{A}\boldsymbol{z}_t\,, \quad \boldsymbol{z}_t \sim \mathrm{N}_4(\boldsymbol{0}, \boldsymbol{I}_4)\,, \tag{3.10}$$

where $\boldsymbol{\mu}$ and $\boldsymbol{\gamma}$ are the 4×1 location and skewness parameter vectors, respectively, and $\boldsymbol{\Sigma} = \boldsymbol{A}\boldsymbol{A}'$ is the 4×4 dispersion matrix. The random vector $\boldsymbol{z}_t$ follows a four-variate Gaussian distribution with zero mean and identity covariance, and $\omega_t \geq 0$ is a non-negative random variable independent of $\boldsymbol{z}_t$. The mixing random variable w_t can be understood as a shock that affects the covariance of energy assets, due to the arrival of new information in the markets (e.g., shortages in future supply, unexpected increases in demand).[5]

[5]Conditioned on ω_t, the vector of innovations $\boldsymbol{x}_t$ is normally distributed, such that $\boldsymbol{x}_t|\omega_t \sim \mathrm{N}_4(\boldsymbol{\mu} + \omega_t\boldsymbol{\gamma}, \omega_t\boldsymbol{\Sigma})$.

In the case of GH distributions, the mixing random variable ω_t follows a generalized inverse Gaussian (GIG) distribution, $\omega_t \sim N^-(\lambda, \chi, \psi)$. The very flexible GIG distribution includes as special boundary cases the gamma and inverse gamma distributions. Thus, for certain values of the parameters λ, χ, and ψ and the skewness vector $\boldsymbol{\gamma}$, we can obtain different cases of GH distributions. We consider five particular cases of multivariate GH distributions: the normal inverse Gaussian (NIG) distribution (i.e., ω_t follows an inverse Gaussian distribution, which corresponds to the case $\lambda = -1/2$), the variance-gamma (VG) distribution (i.e., ω_t follows a gamma distribution, corresponding to the parameters $\lambda > 0$ and $\chi = 0$), the skewed t (skT) distribution (i.e., ω_t follows an inverse gamma distribution, corresponding to the case in which $\lambda < 0$, $\chi = -2\lambda$, and $\psi = 0$), Student's t (T) distribution (with same mixing distribution as the skewed t but with $\boldsymbol{\gamma} = 0$), and the Gaussian (G) distribution (for which $\boldsymbol{\gamma} = 0$ and $\omega_t = 1$). In Appendix A.7, we provide more details about the density functions of these distributions.

Using the normal mean-variance specification of equation (3.10), we can compute the mean and covariance values for the vector of innovations $\boldsymbol{x}_t$ for each GH distribution, provided that the mean and variance of ω_t exist and are finite. If we assume that $\boldsymbol{x}_t$ has zero mean and unit covariance, $\mathbb{E}(\boldsymbol{x}_t) = 0$ and $\mathrm{Cov}(\boldsymbol{x}_t) = \boldsymbol{I}_4$, then the location vector and dispersion matrix of the conditional distribution must satisfy the following conditions:

$$\boldsymbol{\mu} = -\mathbb{E}(\omega_t)\boldsymbol{\gamma}\,, \text{ and} \tag{3.11}$$

$$\boldsymbol{\Sigma} = (\boldsymbol{I}_4 - \mathrm{Var}(\omega_t)\boldsymbol{\gamma}\boldsymbol{\gamma}')/\mathbb{E}(\omega_t)\,. \tag{3.12}$$

The proposed GH distributions have the advantages of exhibiting different tail patterns (Bibby and Sørensen (2003)). On the one hand, the tails of the NIG and VG distributions decay exponentially, such that their probability density functions behave, when $\boldsymbol{x}_t \to \pm\infty$, proportionally to an exponential function. This pattern is intermediate between the behavior of the Gaussian distribution, which decays more rapidly, and other, more extreme, polynomial decays. For this reason, NIG and VG distributions are sometimes referred to as semi-heavy tailed. Furthermore, when the i-th element of the asymmetry vector $\boldsymbol{\gamma}$ differs from zero (i.e., $\gamma_i \neq 0$), the two tails of the i-th innovation $x_{i,t}$ behave differently (the right tail is heavier when $\gamma_i > 0$, whereas the left tail is heavier when $\gamma_i < 0$). The tails of the T distribution instead are symmetric and behave as polynomials, such that they decay slower than those of the NIG and VG distributions. Finally, the skT distribution offers the special property of possessing, for each component of the vector of innovations, one heavy (polynomial decay) and one semi-heavy (exponential decay) tail. Thus, when $\gamma_i > 0$, the right tail ($x_{i,t} \to \infty$) is the

heaviest, while the left tail ($x_{i,t} \to -\infty$) decays exponentially; these roles switch for $\gamma_i < 0$.

3.3 Conditional risk measures

Measuring conditional risk is a natural and direct way to analyze the tail behavior of energy portfolios. In our approach, we study both long and short positions in the energy portfolios. Thus, we focus on the two tails of the P&L distribution. For short positions, the portfolio holder loses money when the portfolio value increases, so we attend to the right side of the distribution. For long positions, we focus on the left tail.

We consider two measures of risk: the value at risk (VaR) and the expected shortfall (ES). The VaR is widely used in the financial industry to monitor risk exposures for regulatory purposes and to establish trading constraints in investment decisions. In the energy industry, especially for producers, VaR is becoming more popular, with increasing relevance for corporate decisions. For example, VaR provides insights to determine hedging policies or, in the case of utilities, to obtain an optimal selection in the generation mix. Formally, for a certain horizon h and confidence level α, the VaR is defined as the α-quantile of the conditional distribution of portfolio changes $\Delta W_t(h)$. That is, the probability of incurring losses greater than a certain threshold value, called the VaR, is equal to α:

$$P(\,\Delta W_t(h) \leq \mathrm{VaR}_t(\alpha, h)\,|\,\mathcal{F}_{t-1}\,) = \alpha\,. \tag{3.13}$$

Despite its widespread use, the VaR also has been subject to substantial criticism, particularly because diversification does not always reduce risk when it is measured by VaR. In addition, the VaR ignores important information related to the tails of the loss distribution beyond the α-quantile, disregarding the risk of extreme losses. In contrast, ES measures cope well with such shortcomings and describe tail risk better (Artzner, Delbaen, Eber, and Heath (1999)). The ES is defined as the expected loss, conditional on the loss exceeding the VaR over a certain horizon h,

$$\mathrm{ES}_t(\alpha, h) = \mathbb{E}[\,(\Delta W_t(h)\,|\,\Delta W_t(h) \leq \mathrm{VaR}_t(\alpha, h))\,|\,\mathcal{F}_{t-1}\,]\,, \tag{3.14}$$

that is, the mean portfolio loss in the $\alpha\%$ of worst cases.

We describe our approach to compute VaR and ES under the dynamic econometric models proposed in the previous section for the vector of energy risk factors $\boldsymbol{r}_t$. Thus, we begin by modeling the joint distribution

of energy returns $\boldsymbol{r}_t$, then we aggregate these results for each portfolio according to its exposures to each commodity. That is, we employ an asset-level approach to measure the tail risk of the energy portfolios.

To aggregate the risk factors, it is convenient to represent the portfolio's P&L as a linear function of the individual energy log-returns. We therefore approximate the changes in the portfolio value defined in equation (3.2) as

$$\Delta W_t(h) \approx \boldsymbol{w}'_{t-h}\boldsymbol{r}_t(h) = \sum_{i=1}^{4} q_{i,t-h}F_{i,t-h}r_{i,t}(h). \tag{3.15}$$

Because the GH distributions are closed under linear transformations (see McNeil, Frey, and Embrechts (2005), their Proposition 3.13), when we aggregate the energy risk factors in a given portfolio, the linearized P&L distribution still belongs to the same class of GH distributions as does the vector of risk factors.

For the conditional mean $\boldsymbol{m}_t$ and covariance $\boldsymbol{H}_t$, and taking into account that the vector of innovations follows a four-variate GH distribution with mixing variable parameters (λ, χ, ψ) and location, dispersion, and asymmetry parameters $\boldsymbol{\mu}$, $\boldsymbol{\Sigma}$, and $\boldsymbol{\gamma}$, the linearized portfolio P&L in equation (3.15) follows a univariate GH distribution with parameters (λ, χ, ψ) unaltered and with location, dispersion, and asymmetry parameters given by:

$$\begin{aligned}
\mu_P &= \boldsymbol{w}'_{t-h}(\boldsymbol{m}_t + \boldsymbol{H}_t^{1/2}\boldsymbol{\mu})\,, \\
\Sigma_P &= \boldsymbol{w}'_{t-h}(\,\boldsymbol{H}_t^{1/2}\boldsymbol{\Sigma}(\boldsymbol{H}_t^{1/2})'\,)\boldsymbol{w}_{t-h}\,, \quad \text{and} \\
\gamma_P &= \boldsymbol{w}'_{t-h}(\boldsymbol{H}_t^{1/2}\boldsymbol{\gamma})\,.
\end{aligned} \tag{3.16}$$

Thus, we obtain the parametric distribution function for the portfolio P&L. In turn, we can analyze the tail behavior and term structure of risk directly for each portfolio P&L distribution.

Finally, we adopt two alternative numerical implementations for calculating the risk measures. We can compute VaR and ES under the GH model by solving the integrals implicit in equations (3.13) and (3.14) numerically for the portfolio P&L distribution. Alternatively, we can apply Monte Carlo simulations, which are usually more effective and preferred in this context. The latter procedure to characterize the portfolio risk measures is as follows:

1. Using our dynamic specification, defined by the conditional mean, variance, and correlation equations (3.5), (3.7), and (3.8), we simulate the $t+\tau$ vector of returns, given equations (3.3)-(3.4), as

$$\boldsymbol{r}_{t+\tau}^{(n)} = \boldsymbol{\mu}_{t+\tau} + \boldsymbol{H}_{t+\tau}^{1/2}\boldsymbol{x}_{t+\tau}^{(n)}\,, \quad n = 1, \ldots, N\,,$$

where the vector of innovations $\{\boldsymbol{x}_{t+\tau}^{(n)}\}_{n=1}^{N}$ is drawn from the appropriate GH distribution, according to the normal mixture representation in equation (3.10). Then N is the number of Monte Carlo simulations, which we set to 100,000. The h-period returns generated by the n-th simulation at time t are given by $\boldsymbol{r}_t^{(n)}(h) = \sum_{\tau=1}^{h} \boldsymbol{r}_{t+\tau}^{(n)}$.

2. We build the simulated h-period portfolio P&L, $\{\Delta W_t^{(n)}(h)\}_{n=1}^{N}$, using the energy portfolio weights at time t, $\boldsymbol{w}_t$ (see equation (3.15)). That is, $\Delta W_t^{(n)}(h) \approx \boldsymbol{w}_t \boldsymbol{r}_t^{(n)}(h)$. Alternatively, instead of implementing Steps 1 and 2, we can simulate changes in the value of the energy portfolios using the parameters of the P&L distribution that result from equation (3.16).

3. Finally, we calculate the α percentile $\widehat{\mathrm{VaR}}_t(\alpha, h)$ and expected shortfall $\widehat{\mathrm{ES}}_t(\alpha, h)$ for the simulated distribution of the h-period portfolio value changes $\{\Delta W_t^{(n)}(h)\}_{n=1}^{N}$:

$$\tfrac{1}{N}\sum_{n=1}^{N} \hat{I}_t^{(n)}(\alpha, h) = \alpha \quad \longmapsto \quad \widehat{\mathrm{VaR}}_t(\alpha, h)\,, \text{ and}$$

$$\Big(\sum_{n=1}^{N} \hat{I}_t^{(n)}(\alpha, h)\Big)^{-1} \sum_{n=1}^{N} \hat{I}_t^{(n)}(\alpha, h)\Delta W_t^{(n)}(h) \quad \longmapsto \quad \widehat{\mathrm{ES}}_t(\alpha, h)\,,$$

where $\hat{I}_t^{(n)}(\alpha, h) = \mathbb{1}_{\{\Delta W_t^{(n)}(h) \le \mathrm{VaR}_t(\alpha, h)\}}$.

3.4 Data description and model estimation

In this section, we present the data we used to build the energy portfolios, then report on the parameter estimates of the GH models presented in the previous sections and some in-sample analyses of the results.

3.4.1 Description of the energy futures data

Our energy portfolios consist of energy commodity futures for crude oil, natural gas, coal, and electricity. These four commodities effectively represent a wide range of exposures to energy price risk. In all cases, we employ daily series of one-month ahead monthly futures contracts traded on the New York Mercantile Exchange (NYMEX), which are the most liquid contracts for

Table 3.1. Descriptive statistics for energy returns

This table reports sample statistics for the daily returns for crude oil, natural gas, coal, and electricity futures. The full sample period ranges from August 2005 to March 2012 and includes 1,640 observations. The in-sample period runs from August 2005 to March 2010 (1,136 observations), and the out-of-sample period from March 2010 to March 2012 (504 observations). The *Mean, Std.Dev., Min., Max., VaR 5%, and ES 5%* are expressed in daily percentages. *JB* is the Jarque-Bera normality test statistic. *Q(m)* and *LM(m)* are the Ljung-Box and the Lagrange-Multiplier statistics, conducted using m lags to test for the presence of serial correlation in returns and squared returns, respectively. The *p*-values are reported in parentheses.

	10/08/2005-13/03/2012				10/08/2005-15/03/2010				15/03/2010-13/03/2012			
	Oil	Gas	Coal	Elec.	Oil	Gas	Coal	Elec.	Oil	Gas	Coal	Elec.
Mean	0.024 (0.669)	-0.079 (0.297)	0.001 (0.984)	0.068 (0.648)	0.027 (0.704)	-0.074 (0.451)	0.010 (0.853)	0.016 (0.924)	0.015 (0.845)	-0.090 (0.411)	-0.020 (0.677)	0.184 (0.533)
Std.Dev.	2.246	3.062	1.632	6.029	2.430	3.295	1.825	5.739	1.764	2.462	1.078	6.642
Min.	-13.07	-10.78	-10.77	-36.60	-13.07	-10.78	-10.77	-26.82	-9.038	-8.057	-4.620	-36.60
Max.	13.34	26.77	11.12	47.64	13.34	26.77	11.12	47.64	5.164	16.69	2.984	44.55
Skew.	-0.013 (0.831)	1.194 (0.000)	-0.221 (0.000)	0.945 (0.000)	0.080 (0.270)	1.241 (0.000)	-0.201 (0.006)	0.975 (0.000)	-0.573 (0.000)	0.766 (0.000)	-0.405 (0.000)	0.872 (0.000)
Kurt.	8.479 (0.000)	11.41 (0.000)	12.69 (0.000)	14.04 (0.000)	8.295 (0.000)	11.20 (0.000)	11.48 (0.000)	12.51 (0.000)	5.223 (0.000)	7.920 (0.000)	4.483 (0.000)	15.34 (0.000)
JB	2052 (0.001)	5223 (0.001)	6425 (0.001)	8576 (0.001)	1328 (0.001)	3476 (0.001)	3411 (0.001)	4464 (0.001)	131.3 (0.001)	558.6 (0.001)	60.00 (0.001)	3261 (0.001)
VaR	3.425	4.638	2.288	8.035	3.619	4.865	2.511	8.204	2.975	4.088	1.836	7.502
ES	5.323	6.260	4.116	13.84	5.693	6.661	4.697	13.32	4.414	5.114	2.666	14.99
Q(5)	4.086 (0.537)	13.14 (0.022)	74.21 (0.000)	18.89 (0.002)	3.447 (0.631)	10.43 (0.064)	48.77 (0.000)	13.58 (0.019)	6.713 (0.243)	3.919 (0.561)	37.04 (0.000)	8.135 (0.149)
LM(5)	283.2 (0.000)	17.52 (0.004)	192.5 (0.000)	14.64 (0.012)	204.8 (0.000)	11.43 (0.043)	126.4 (0.000)	6.361 (0.273)	14.24 (0.014)	3.620 (0.605)	9.555 (0.089)	8.745 (0.12)
corr(oil,j)	1.000	0.250 (0.000)	0.325 (0.000)	0.076 (0.002)	1.000	0.282 (0.000)	0.317 (0.000)	0.094 (0.001)	1.000	0.119 (0.007)	0.371 (0.000)	0.031 (0.487)
corr(gas,j)		1.000	0.211 (0.000)	0.102 (0.000)		1.000	0.193 (0.000)	0.095 (0.001)		1.000	0.310 (0.000)	0.126 (0.005)
corr(coal,j)			1.000	0.035 (0.161)			1.000	0.017 (0.561)			1.000	0.099 (0.027)

the four energy commodities analyzed.[6] For oil, we consider the light sweet crude oil futures contract, which is quoted in dollars per U.S. barrel. For natural gas, we use the futures contract for the delivery location at the Henry hub in Louisiana, which trades in dollars per million British thermal units (mmBtu) and represents the benchmark for gas prices in the United States. For coal, we employ futures written on the Central Appalachian bituminous coal, quoted in dollars per U.S. tons. Finally, for electricity, we use the PJM monthly peak electricity futures traded in dollars per MWh.

The full-sample period runs more than six years from August 2005 to March 2012, and includes 1,640 daily observations. We consider all data since the launch of the PJM electricity futures in the NYMEX (April 2003) until the day of the analysis (March 2012), but we drop the first observations (from April 2003 to August 2005), for which liquidity of electricity and coal futures was very scarce. To avoid in-sample over-fitting and spurious findings, we reserve the last two years of data, from March 2010 to March 2012 (504 observations), for the out-of-sample investigation of the tail risk. The data came from the database of Thomson Reuters Datastream.

Table 3.1 reports some summary statistics of the daily returns for crude oil, natural gas, coal, and electricity. Figure 3.1 presents the relative prices and quantile-quantile plots for the four energy commodities from August 2005 to March 2012. The table shows that no energy return shows any significant trend over either period: The means are small compared with the standard deviations of each series. Electricity has the highest volatility, kurtosis, and risk measures over the entire sample. It also shows extreme positive and negative daily moves, some larger than 30%. Oil, gas, and coal indicate high risk, though they also experience a decrease in volatility and tail risk during the 2010-2012 period compared with the 2005-2010 period.

We observe non-negligible skewness across commodity returns. Electricity and natural gas returns exhibit significantly positive skewness for all periods, suggesting that positive moves are more frequent than negative ones in these markets. The qq-plots in Figure 3.1 confirm this evidence. In contrast, coal returns show negative asymmetry, and oil returns exhibit significantly negative skewness only for the last period of the sample. Taking into account these skewness measures, as well as the Jarque-Bera (JB) statistics, we reject unconditional normality in favor of the presence of heavy tails and asymmetry. We also test serial correlation in returns and squared returns using the Ljung-Box (Q) and Lagrange Multiplier (LM) statistics, respectively.

[6]We have built the time series of the one-month ahead futures rolling over the front-month contract according to the NYMEX trading termination scheme for each futures contract (usually, between 8 to 1 business days before delivery).

Exhibit 1: Relative prices

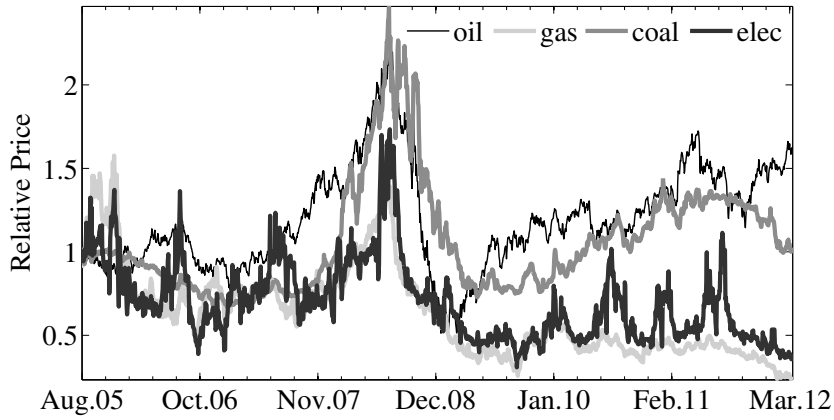

Exhibit 2: Quantile-quantile plots

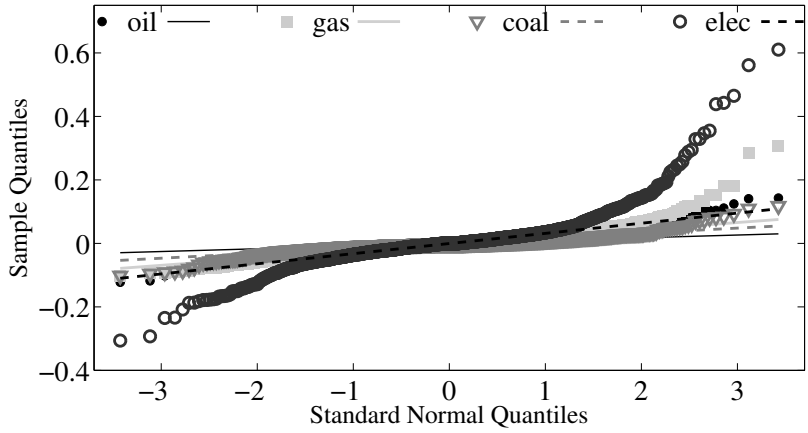

Figure 3.1. Relative prices and QQ-plots
Exhibit 1 shows the price series of the energy futures from August 2005 to March 2012 (full-sample period). Exhibit 2 presents the sample quantiles of the daily returns for the four energy commodities. The dashed lines represent the quantiles of a standard normal distribution.

The p-values in parentheses indicate that all commodities, except oil, display autocorrelation in returns, and strong evidence of temporal variation in the second moment of energy returns.

Looking at the correlation coefficients, we notice that linear dependence between energy commodities is positive and significant in general, but it varies among sample periods. The correlation coefficients between fuels (oil, gas, and coal), which to some extent represent substitute goods, range from 19% to 32% over the 2005-2010 period. In the 2010-2012 period, the correlations of oil and gas with coal increase to greater than 31%, whereas the correlation between oil and gas decreases from 28% to 12%. The linear dependence between electricity and fuels is less than 10% and only significant for oil and natural gas during 2005-2010. In the last period, correlation with coal increases to 10%.[7]

In addition to testing the univariate normality of energy returns, we conduct Mardia's test of multivariate normality (not reported here). This test is based on multivariate measures of skewness and kurtosis, defined on the bilinear form $D_{tt'} = (\boldsymbol{r}_t - \bar{\boldsymbol{r}})' \bar{\boldsymbol{H}}^{-1} (\boldsymbol{r}_{t'} - \bar{\boldsymbol{r}})$, where $\bar{\boldsymbol{r}}$ and $\bar{\boldsymbol{H}}$ are the sample mean and covariance of returns. The large values that we obtain for the test statistics, corresponding to multivariate skewness and kurtosis measures, reject the null hypothesis of joint normality of energy returns (p-values are less than 0.001 for all the sample periods).

3.4.2 Estimation results for the multivariate model

In this section, we present in two stages the estimation results of the multivariate GH models for the energy returns. The large dimension of the model prompts us to use a sequential approach to estimate the set of parameters. In the first stage, we carry out the quasi-maximum likelihood (QML) estimation of the dynamic regression model for the conditional mean and covariance, defined in equations (3.5), (3.7), and (3.8). In the second stage, we obtain the ML parameter estimates of the different multivariate GH conditional distributions. This latter estimation can be implemented using a variant of the expectation-maximization (EM) procedure presented by McNeil, Frey, and Embrechts (2005), which relies on the normal-mixture representation for GH distributions from equation (3.10). In Appendix A.8, we describe in detail the log-likelihood functions that correspond to both stages and the optimization algorithms.

[7]The electricity futures are written on peak-load power, such that we should expect a higher correlation with peak-load fuels, such as natural gas, than with coal,

Table 3.2. In-sample QML parameter estimates of the conditional model

This table reports QML parameter estimates and residual summary statistics for the conditional mean and variance equations. The *p*-values, presented in parentheses, are computed using robust standard errors. *Q(m)* and *LM(m)* are the Ljung-Box and the Lagrange-Multiplier statistics, conducted using m lags to test for the presence of serial correlation in residuals and squared residuals.

Panel A: Univariate dynamics, GJR(1,1,1)

	Crude oil	Natural gas	Coal	Electricity
Mean equation				
$m_0 \times 10^2$	0.060 (0.276)	-0.067 (0.420)	0.008 (0.831)	-0.242 (0.123)
ϕ_1	-0.033 (0.285)	-0.038 (0.204)	0.105 (0.002)	-0.042 (0.457)
ϕ_2			0.092 (0.007)	
ϕ_3				-0.077 (0.016)
ϕ_4				-0.064 (0.019)
ϕ_5		-0.073 (0.043)		
Variance equation				
$\alpha_0 \times 10^3$	0.005 (0.025)	0.008 (0.060)	0.002 (0.001)	1.941 (0.000)
α_1	0.027 (0.046)	0.024 (0.045)	0.056 (0.000)	0.394 (0.000)
α_1^-	0.060 (0.002)	0.076 (0.022)	0.007 (0.612)	0.011 (0.914)
α_2	0.933 (0.000)	0.936 (0.000)	0.935 (0.000)	0.092 (0.273)
Statistics for residuals				
Q(5)	7.394 (0.193)	1.281 (0.937)	4.024 (0.546)	7.185 (0.207)
LM(5)	14.16 (0.105)	8.596 (0.126)	6.272 (0.281)	2.817 (0.728)

Panel B: Correlation dynamics, ADCC(1,1,1) and DCC(1,1)

	Oil-Gas-Coal-Elec		Gas-Elec	
	ADCC	DCC	ADCC	DCC
δ_1	0.017 (0.042)	0.020 (0.022)	0.043 (0.120)	0.071 (0.006)
δ_1^+	0.008 (0.387)		0.099 (0.064)	
δ_2	0.894 (0.000)	0.893 (0.000)	0.663 (0.000)	0.670 (0.000)

We perform the first estimation for the period that ranges from August 2005 to March 2010, formed by 1,136 daily observations. In turn, we recursively reestimate the models throughout the out-of-sample period, using a rolling window of constant size (T=1,136), such that we obtain a full sequence of parameter estimates for each point in the out-of-sample period (504 re-estimations total). For each point in the sequence of parameter estimates, we can compute the h-period forecast density that we later use to calculate the tail risk of the energy portfolios.

QML estimates of the conditional moments

To display the outputs of the dynamics specification, in Table 3.2 we present the QML parameter estimates, robust p-values, and residual summary statistics of the conditional mean and covariance equations for the first estimation window (August 2005 to March 2010). We include in each mean equation only those autoregressive lags that have significant coefficients or cause the presence of autocorrelation to become statistically insignificant in the resulting residuals. The coefficients of lagged returns are negative, except for coal, which has significantly positive autoregressive parameters. For natural gas and electricity, some autoregressive lags are also notably significant.

We observe different patterns in the variance equation, especially with respect to the leverage effect. For crude oil and natural gas, the parameter α_1^-, corresponding to the leverage effect, is positive and significant, which suggests that negative shocks have a stronger effect on variance than do positive ones. Coal and electricity do not indicate any such asymmetry in terms of the response of volatility to negative moves, which suggests that positive shocks could have more impact on variance. Volatility persistence, measured as $\alpha_1 + \alpha_1^-/2 + \alpha_2$, also is very large (>0.95) for fossil fuels but smaller for electricity variance (around 0.50). According to the Ljung-Box (Q) and Lagrange multiplier (LM) statistics in Table 3.2, using this mean and variance specification, we can greatly reduce the presence of temporal dependence in the residuals and squared residuals.

When we consider the time-varying evolution of the correlation matrix for the vector of four energy returns, we find that dependence dynamics are strongly persistent (δ_2 = 0.89), the correlation increases when energy assets are affected by shocks of the same sign (δ_1 is small but significantly positive), and the asymmetry effect in the ADCC model is rather insignificant (δ_1^+<0.01). However, when we consider the dynamics of the correlation

which is usually a source for generating intermediate- and base-load electricity.

Exhibit 1: Volatilities

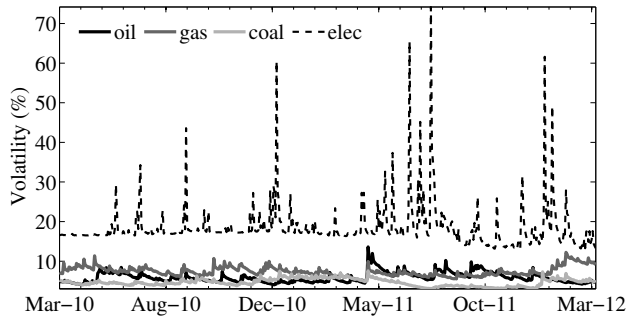

Exhibit 2: Correlations

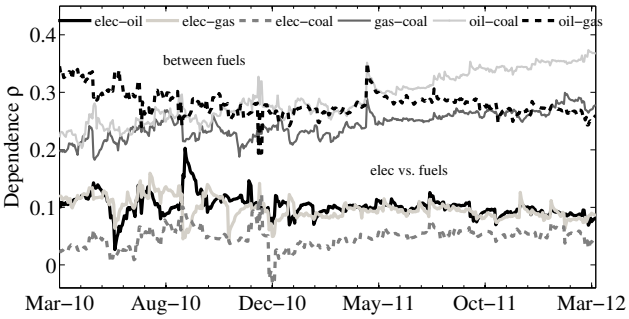

Exhibit 3: Asymmetry parameters

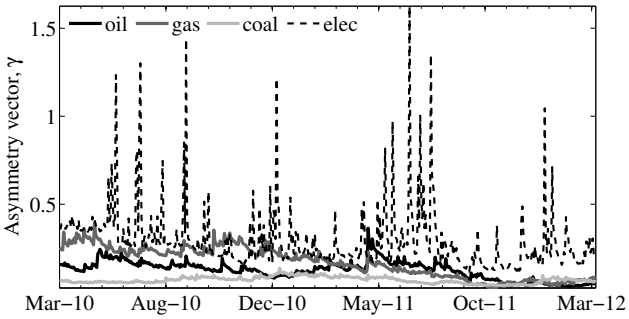

Figure 3.2. Volatility, correlation, and asymmetry parameter estimates
Exhibits 1 and 2 show the 10-day ahead forecasts of the conditional volatilities and conditional correlations over the out-of-sample period (March 2010 to March 2012). Exhibit 3 shows the asymmetry parameters vector (γ) for the multivariate VG distribution for each rolling estimation over the out-of-sample period. We employ a rolling window of constant size (T=1,136) to obtain the sequence of parameter estimates (504 re-estimations total).

between pairs of energy returns, we obtain significant, positive estimates of the asymmetry parameter δ_1^+. In particular, for natural gas and electricity, we find that $\delta_1^+ = 0.099 > \delta_1 = 0.043$, suggesting that the correlation between gas and electricity increases more after a positive co-movement ("co-boom") than after equally large negative co-movements. Although not previously documented in this context, such positive asymmetry in correlation seems sound from an economic perspective, because an increase in gas prices has a strong positive impact on the generation costs of peak-load electricity. We study this relationship between gas and electricity in depth when we analyze the tail risk of the gas-fired power plant portfolio.

When we update our parameter estimates at each point of the out-of-sample period, we obtain a time-series of the conditional moments from March 2010 to March 2012. Thus in Figure 3.2, we plot the 10-day-ahead forecasts of the conditional volatilities and correlations over the out-of-sample period. We observe several interesting features from a risk analysis perspective. As expected, electricity is highly volatile, with a strong presence of spikes, some greater than 50%. In addition, electricity volatility peaks revert to the mean quicker than those of other energy volatilities. Correlations are not very high during this period, especially between electricity and fuels. The correlation between oil and gas also decreases substantially, and only the correlations between coal and oil and between coal and gas exhibit a significant increase throughout the out-of-sample period.

Multivariate GH conditional distributions

We now fit the various conditional distributions using the vector of innovations obtained from the previous QML estimation. As we did previously, we repeat the multivariate distribution estimation for each point in the out-of-sample period. In Table 3.3, we present, for the first estimation period (August 2005 to March 2010), the ML parameter estimates and bootstrapped *p*-values of the various GH distributions. The in-sample results offer strong evidence against multivariate normality, as we expected.

First, the shape parameter estimates of the mixing distributions (λ, χ, ψ) point to the presence of fat tails in the different GH models. In particular, for the T and skT distributions, the small value of parameter χ indicates the existence of jumps and tail dependence. Similar arguments apply to the VG and NIG parameter estimates.

Second, the asymmetry parameter estimates $\boldsymbol{\gamma}$ for the three skewed GH distributions (skT, VG, and NIG) are positive for all vector components,

Table 3.3. In-sample parameter estimates of the multivariate distributions

This table presents the parameter estimates for the multivariate conditional distribution of the vector of innovations. We consider two elliptically symmetric distributions, the multivariate Gaussian (G) and Student's t (T) distributions, and three GH distributions: the multivariate skewed t (skT), variance-gamma (VG), and normal inverse Gaussian (NIG) distributions. The standard errors of these estimates are computed using a stationary bootstrap (500 samples), and their corresponding p-values appear in parentheses. The log-L, AIC, and BIC are the values at the optimum of the log-likelihood function and the Akaike and Bayesian information criteria, respectively.

	G	T	skT	VG	NIG
Parameters of the mixing r.v. W					
λ		-2.078	-2.084	1.295	-0.500
		(0.005)	(0.002)	(0.000)	
χ		4.157	4.168	0.000	0.757
		(0.002)	(0.001)		(0.001)
ψ		0.000	0.000	2.588	0.637
				(0.003)	(0.000)
Asymmetry vector $\boldsymbol{\gamma}$					
γ(oil)			0.026	0.102	0.058
			(0.117)	(0.020)	(0.042)
γ(gas)			0.037	0.106	0.078
			(0.049)	(0.018)	(0.021)
γ(coal)			0.018	0.050	0.041
			(0.263)	(0.034)	(0.050)
γ(elec)			0.015	0.078	0.039
			(0.332)	(0.028)	(0.190)
Dispersion matrix $\boldsymbol{\Sigma}$					
ρ(oil, gas)	0.347	0.367	0.365	0.360	0.364
	(0.000)	(0.000)	(0.000)	(0.000)	(0.000)
ρ(oil, coal)	0.218	0.245	0.245	0.240	0.243
	(0.000)	(0.000)	(0.000)	(0.000)	(0.000)
ρ(oil, elec)	0.109	0.118	0.117	0.119	0.118
	(0.001)	(0.000)	(0.001)	(0.000)	(0.000)
ρ(gas, coal)	0.213	0.247	0.246	0.235	0.244
	(0.000)	(0.000)	(0.000)	(0.000)	(0.000)
ρ(gas, elec)	0.118	0.222	0.220	0.207	0.219
	(0.000)	(0.000)	(0.000)	(0.000)	(0.000)
ρ(coal, elec)	0.032	0.064	0.063	0.058	0.063
	(0.105)	(0.071)	(0.077)	(0.079)	(0.075)
Information Criteria					
log-L	-5.555	-5.221	-5.220	**-5.186**	-5.200
AIC	11.134	10.469	10.473	**10.406**	10.433
BIC	11.196	10.535	10.557	**10.491**	10.517

suggesting positive skewness in the multivariate conditional distribution of daily energy returns. Only the asymmetry parameter for natural gas is statistically significant for the three GH models, whereas the parameter for electricity is significant just for the VG case.

Third, looking at the log-likelihood values (log-L), together with the Akaike and Bayesian information criteria (AIC and BIC in Table 3.3),[8] to compare the accuracy of the alternative conditional distributions, we find that the VG model is preferable over other GH alternatives for this estimation window.

We reach similar results when we reestimate the GH conditional distributions throughout the out-of-sample period. Specifically, we use a rolling window of size T=1,136, for a total of 504 re-estimations. For example, Exhibit 3 of Figure 3.2 displays the evolution of the asymmetry parameter estimates (γ) for the VG model from March 2010 to March 2012 (similar patterns are obtained for other skewed GH distributions). For all assets, the parameter estimates are always positive. In particular, the asymmetry parameter of electricity presents large positive spikes that seem to revert toward a mean value. For gas, we observe a downward trend over the sample.

In Figure 3.3, we also plot the series of shape parameters estimates for the GH distributions and the BIC values corresponding to the recursive models' fit. The sequence of re-estimation results favors the hypothesis of fat tails and positive skewness for the multivariate distribution of energy risk factors over the whole out-of-sample period. Even for the most recent estimations (i.e., the last rolling window ranges from September 2007 to March 2012), for which electricity and coal futures are less influenced by the lack of trading volume, the results suggest the presence of extreme realizations in the conditional distribution.

The front-month futures contracts may exhibit excess volatility near delivery, precisely, at the time that these contracts are rolled over. To check if some of the tail risk we find in the estimation results are due to these rollover effects near maturity, we also estimate our models for the time series of two-month ahead futures contracts.To build the generic time series of two-month ahead futures, we roll over the corresponding contract at least 22 business days before delivery. Therefore, using this time series, we limit the effects of rollover near maturity. The drawback of using two-month ahead

[8]The selection criteria shown in Table 3.3 are given by the following: log-L $= \log \mathcal{L}_2(\widehat{\theta})/T$, AIC = -2 log-L + $2k/T$, and BIC = -2 log-L + k $\log(T)/T$, where k is the number of parameters in each model, and T is the number of observations. Greater log-L, and lower AIC and BIC, values are preferred.

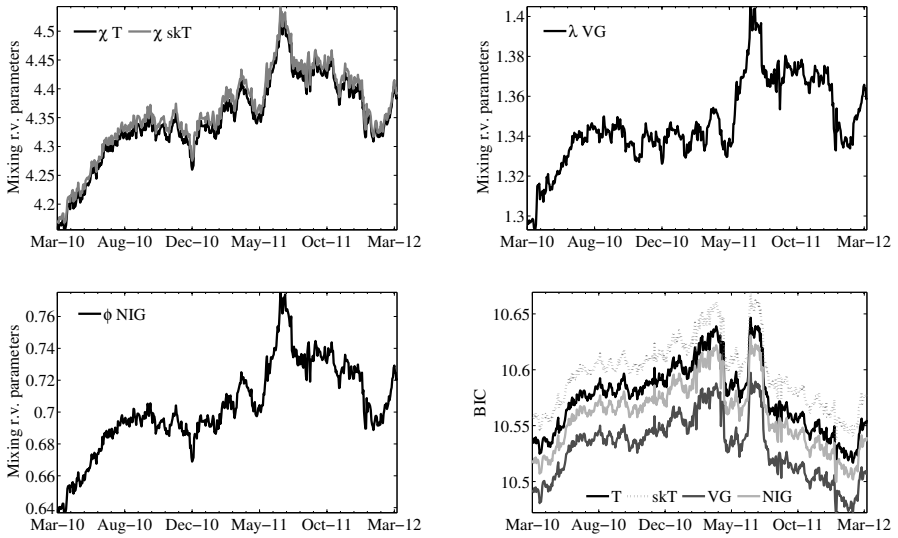

Figure 3.3. GH distribution parameters and BIC
This figure presents the representative shape parameters of the different GH distributions (χ for T and skewed T, λ for VG, and ϕ for NIG) over the out-of-sample period (March 2010 to March 2012). The Bayesian information criteria (BIC) for the non-Gaussian multivariate distributions (T, skewed T, VG, and NIG) are also reported in Exhibit 2 for the whole out-of-sample window.

contracts is that these futures are less liquid than the nearest to maturity contract, specially for coal and electricity.

The results show similar estimates for the asymmetry parameters and for the parameters of the mixing random variable W, which govern the degree of tail risk in the multivariate distribution. For example, for the VG model, the estimates of the parameters λ and ψ are 0.98 and 2.02, and the estimates of the asymmetry parameters are 0.045, 0.085, 0.055, and 0.067, for the oil, gas, coal, and electricity returns. All of them are significant at least at the 10% confidence level. Furthermore, the estimates of parameter χ for the T and skT model are around 4, showing the presence of extreme realizations in the conditional distribution.[9]

[9]We do not report all the estimates in the interest of brevity. They are available upon request. For the in-sample window, we obtain BIC values equal to 10.90, 9.32, 9.34, 9.43, and 9.35 for the G, T, skT, VG, and NIG models, respectively. Therefore, in this sample, T and skT models are preferred.

Left and right tails of the energy portfolios

To analyze the tails of the returns distribution of energy portfolios, we consider the following examples: a utility with different generation units, a gas-fired power plant, and equally weighted and minimum variance portfolios. Using the multivariate GH models previously estimated and knowing the portfolio weights, we can obtain a fitted distribution of portfolio returns for each GH model. Then, we compare the in-sample tail fit of the estimated models graphically, by plotting the estimated logarithmic density functions and the empirical log-density function of the portfolio.

The results of the multivariate estimations have shown the presence of tail asymmetry in the multivariate density functions. Now, looking at the tails of the different energy portfolios, we can analyze the joint effect of this asymmetry and the portfolio weights on the aggregate tail behavior (see equation (3.16)).

To focus on the aggregate tail risk behavior, we display in Figure 3.4 enlarged sections of the left and right tails of the energy portfolios. The circles represent the empirical probability density of portfolio return innovations. The left panel of each exhibit presents the left tail of a long position in the portfolio, and the right panel is the corresponding right tail. As expected from previous multivariate results, the distributions of portfolio returns show positive skewness and fat tails. We find that the Gaussian model (dotted line) clearly underestimates the extent of both tails, that is, the probability of extreme realizations.

Although multivariate VG and NIG models have the largest log-likelihood values and the lowest BIC values (see Table 3.3), the T and skT models better estimate the aggregate tail risk behavior, according to the plots in Figure 3.4. The slower tail decay of T and skT distributions (solid and dashed lines, respectively) causes them to outperform the tail fit of the VG and NIG models (marked with crosses and squares, respectively), especially for the right tail, which corresponds to losses of a short position in the energy portfolio.

We also observe slight differences between the tail fits of the T and skT distributions, partially due to the asymmetric tail behavior of the skT distribution. Exhibits for equally weighted and minimum variance portfolios show that the left tail of the estimated skT distribution is above the T distribution, whereas the right tail is below it.

Therefore, the extent of underestimation of the tail risk of the portfolio loss distribution strongly depends on whether we are analyzing the short or

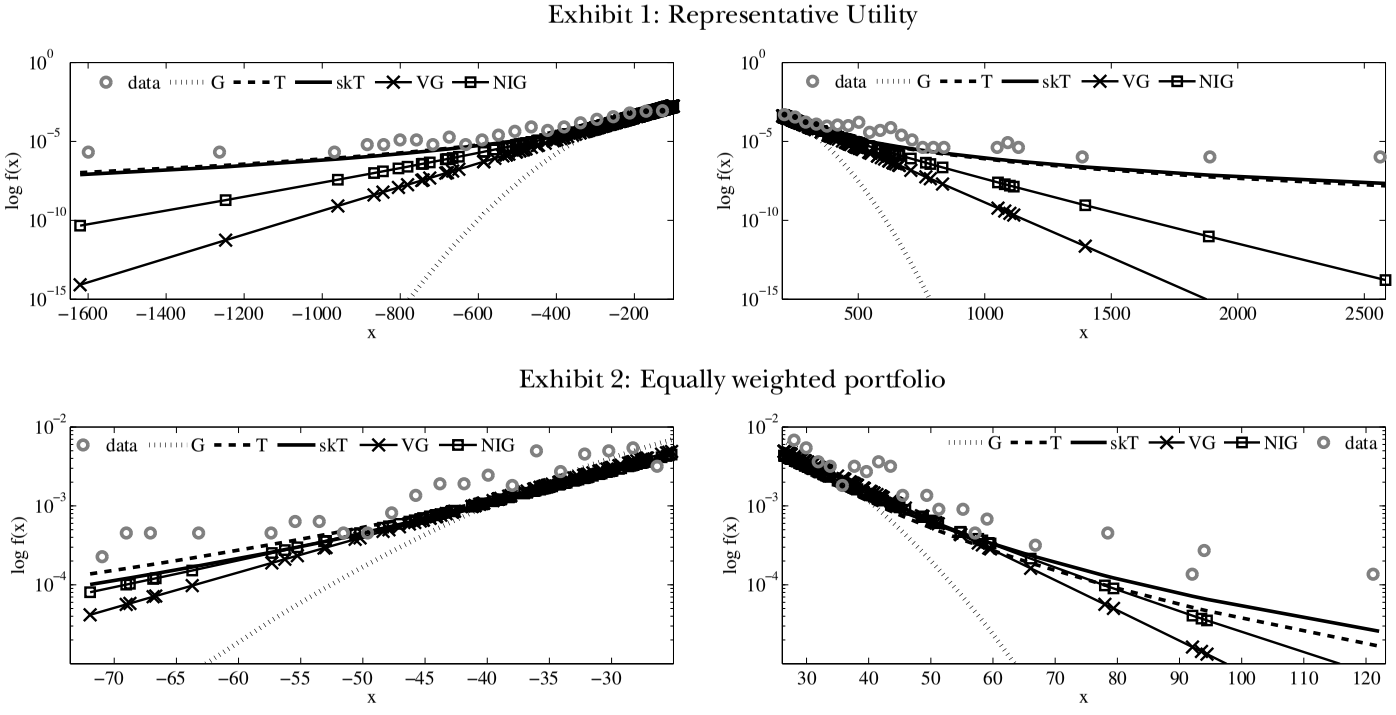

Figure 3.4. Tail plots of energy portfolios

This figure shows the left and right tail plots for the four energy portfolios. The initial exposures, in dollars, of the utility portfolio are around US$2700 for the fuels (oil, gas, and coal) and US$5016 for 57MWh of electricity. For the gas-fired power plant, the exposures corresponding to a supply of 100MWh of electricity are US$8300 and US$8800 for the natural gas and electricity contracts. While, for the the equally weighted and minimum variance portfolios, we consider an arbitrary initial investment of US$1000. The circles represent the logarithm of the empirical probability density of innovations. These figures present the estimated probability density functions of the multivariate Gaussian, T, skewed T, VG, and NIG distributions.

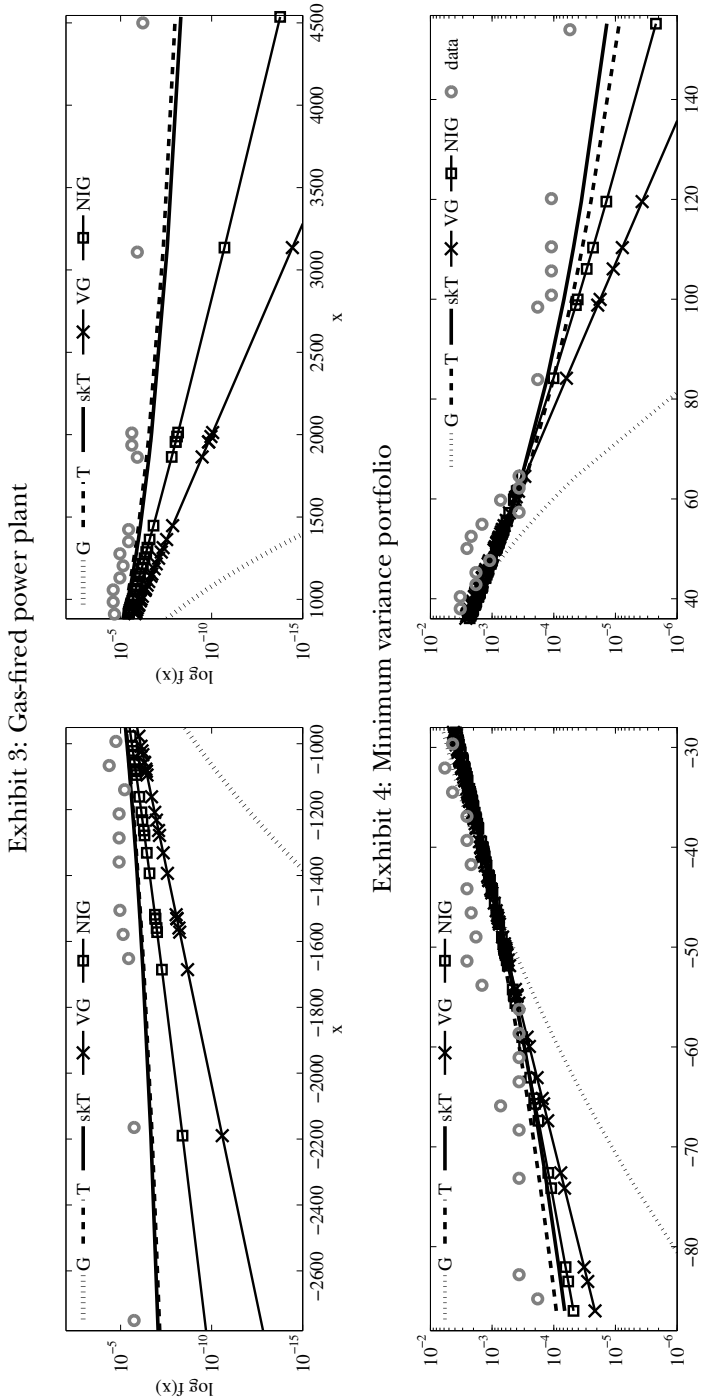

Figure 3.4 *(continued)*

long position in the energy portfolio. In the next section, we further consider the aggregate tail behavior of the energy portfolios' loss distribution, looking at the out-of-sample performance of the VaR and ES measures.

3.5 Risk measures and out-of-sample performance

We apply the procedure explained in Section 3.3 to estimate the conditional risk measures of the energy portfolios for different multivariate GH distributions. See Appendix A.6 for a detailed description of the four energy portfolios considered in the analysis. We compute VaR and ES over the out-of-sample period for different horizons and confidence levels, characterizing the term structure of these risk measures for each GH model. Then, we test the out-of-sample performance of the forecast risk measures, assessing the relative ability of the various multivariate models at hand.

3.5.1 Forecast VaR and ES

The multivariate GH models are estimated on the energy returns up to time t, and then we calculate, for a given confidence level, the out-of-sample h-horizon VaR and ES forecasts (i.e., the risk measures for the period $[t+1, t+h]$). In addition to our GH models, we also calculate the portfolio risk measures using several approaches: a traditional variance-covariance method with multivariate unconditional Gaussian distribution (VC); the Riskmetrics procedure or exponentially weighted moving average model (EWMA), as first introduced by J.P. Morgan; the multivariate Gaussian GARCH with constant conditional correlation (CCC); and the non-parametric historical simulation method (HS).

Using the various multivariate approaches, we calculate the conditional risk measures (VaR and ES) of the four energy portfolios for horizons extending from 1 to 22 days. By way of a sensitivity exercise to the cut-off point selection, we also consider in our analyses different confidence levels α: 0.1%, 0.5%, 1%, and 5%. Thus, we can analyze the possible bias in the risk measure estimates due to the fixing of the confidence level. As an example, Figure 3.5 shows the average ES of the equally weighted portfolio for different confidence levels and horizons.

The smallest ES estimates are generally produced by the EWMA or Gaussian models (CCC and VC are not reported here, in the interest of clarity). The largest ES estimates among the GH models correspond to the distributions with polynomial (slower) tail decays, that is, to the T and skT

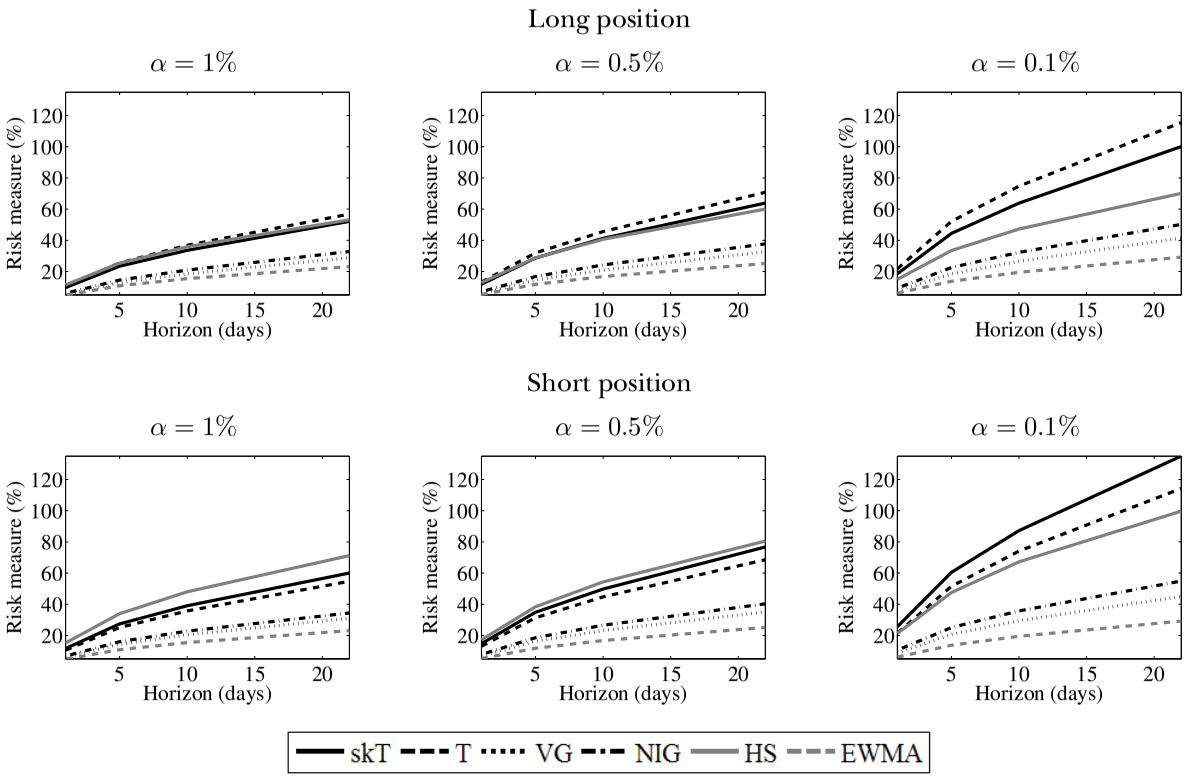

Figure 3.5. Term structure of risk: ES

This figure shows the average expected shortfall (in percentage) of the equally weighted portfolio for different day horizons and tail cut-offs (α). We use the convention of reporting risk measures as positive numbers representing a loss.

distributions. The asymmetric pattern of the skT model produces slightly larger tail risk estimates than the T model for the long positions of the energy portfolios, especially for the equally weighted and minimum variance portfolios. The ordering of the ES estimates across GH methods is invariant to the forecast horizon. In general, the tail risk estimates of the nonparametric HS are close to those of the T and skT models. The estimation windows characterized by turbulent periods of fuel returns are responsible for these large risk measure estimates of the HS approach; as we observe, only heavy-tailed distributions are able to produce similar tail risk patterns.

In practice, our interest lies in comparing (backtest) the h-horizon risk measures forecasts for long and short positions with the actual portfolio losses during the two-year out-of-sample period, from March 2010 to March 2012. As a result of this comparison and following the notation of Section 3.3, we can compute the indicator variables $\hat{I}_t(\alpha, h) = \mathbb{1}_{\{\Delta W_t(h) \leq \widehat{\mathrm{VaR}}_t(\alpha,h)\}}$, which signal the violations of the risk measure $\widehat{\mathrm{VaR}}_t(\alpha, h)$ (or $\widehat{\mathrm{ES}}_t(\alpha, h)$) of the portfolio loss distribution. In the next subsection, we use the processes $I_t(\alpha, h)$ to obtain their corresponding failure rates and develop tests of the out-of-sample performance of the estimated risk measures. In the following backtest results, we show mainly results for the 1% and 5% cut-off points. Similar conclusions to those of the 1% confidence level can be inferred for the 0.5% confidence level. For the 0.1% cut-off and for long horizons, such as 22-day or 10-day horizons, there are few observations in the tail to infer strong conclusions.

As an example of the series of forecast risk measures that we obtain, we present in Figures 3.6 and 3.7 the 1% 1-day VaR and the 5% 10-day VaR over the out-of-sample period according to three different approaches: the EWMA, VG, and skT models. In the lower side of the figure, we draw the VaR violations of each model, corresponding to the long position in the portfolio. In the upper side, we mark the VaR violations for the short position. In general, there are more violations across models for short positions than for long ones, in support of the positive asymmetry of the P&L distribution of the energy portfolios. We also observe that the VG and skT estimates (grey and black lines, respectively) respond more quickly to changing volatility than does the EWMA estimate (dashed line), which tends to be violated several times in a row during more turbulent periods (violations of the EWMA risk measure are marked with triangles). In addition, the VaR violations of the skT estimate (crosses) are fewer than those of the VG estimate (circles), suggesting again the importance of modeling the presence of heavy tails to produce conservative tail risk measures.

In the next subsection, we test if these differences are statistically and

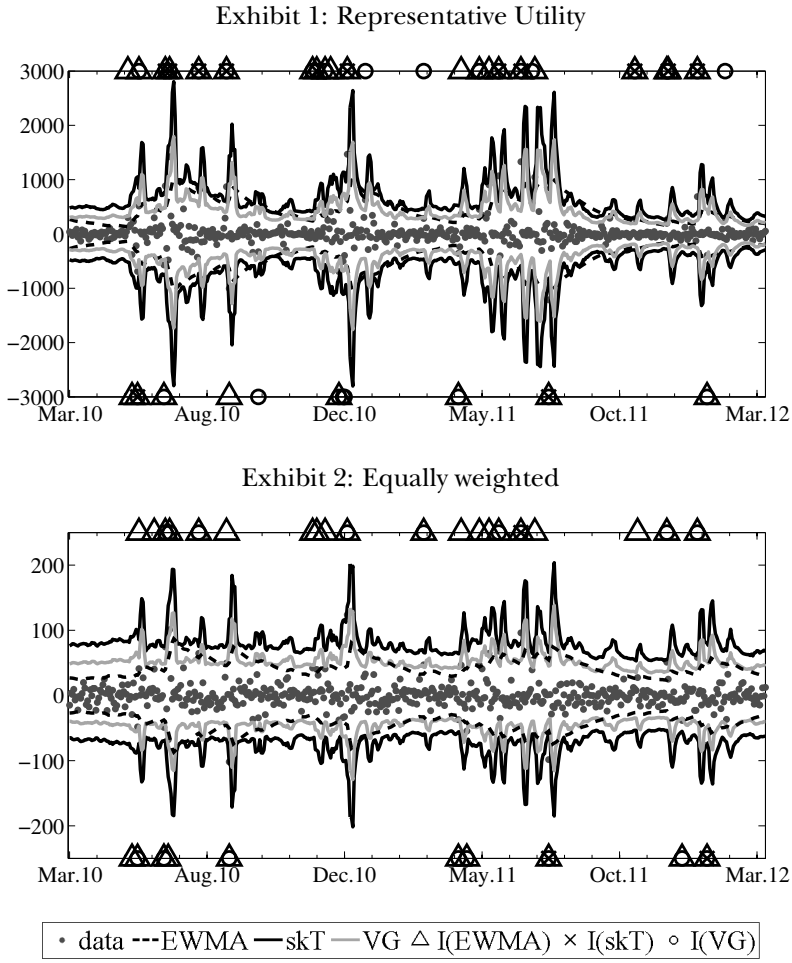

Figure 3.6. 1-day risk measures and violations
This figure presents the 1% 1-day VaR for three different approaches over the out-of-sample period. Their corresponding violations are also reported. Triangles, circles, and x-marks denote violations of the EWMA, conditional VG, and conditional skewed T models, respectively.

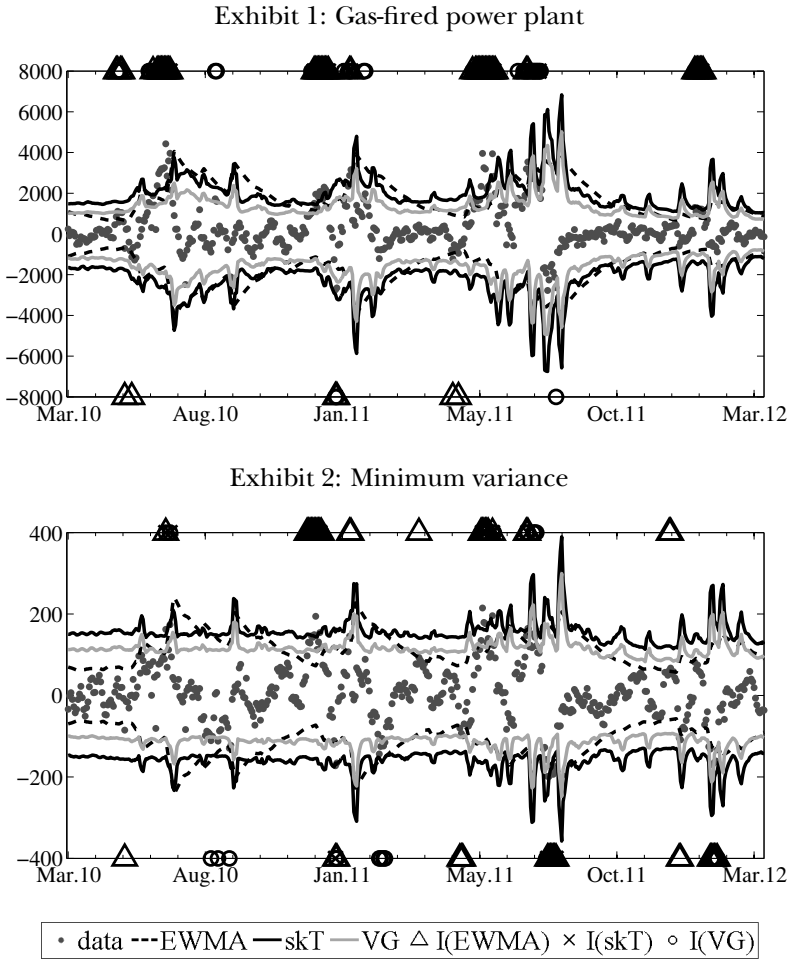

Figure 3.7. 10-day risk measures and violations
This figure presents the 5% 10-day VaR for three different approaches over the out-of-sample period. Their corresponding violations are also reported. Triangles, circles, and x-marks denote violations of the EWMA, conditional VG, and conditional skewed T models, respectively.

economically significant.

3.5.2 Tests of out-of-sample performance

In the previous subsection, we estimated, from March 2010 to March 2012, the risk measures at time t for the distribution of losses in the next h-day period $[t+1, t+h]$. Now, we backtest the risk measure estimates of the different models over time and compare their out-of-sample relative performance. Thus we can assess the differences in tail risk patterns, controlling for over-fitting and other spurious findings. In this subsection, we consider various backtests for the VaR and ES forecasts. In particular, to monitor the performance of tail risk estimates, we implement a new backtest that builds on the reality check tests of Hansen (2005) and White (2000) with a loss function based on the ES. Further details about the different backtest procedures are available in Appendix A.9.

Using the indicator variable $\hat{I}_t(\alpha, h)$, we obtain the number of VaR violations for a given confidence level α over the tested period, as well as the proportion of losses beyond that VaR estimate. By definition, the probability of incurring a VaR violation for a successful model is α. Therefore, the estimated indicator variable $\hat{I}_t(\alpha, h)$ should behave similar to realizations of a Bernoulli random variable with probability α. We first test the unconditional coverage, to check if the number of violations is correct on average, using the log-likelihood ratio (LR) statistic proposed by Christoffersen (1998) and Kupiec (1995) (see Appendix A.9 for a more detailed description).

For the five GH models and the four benchmark approaches, we report in Table 3.4 the percentage of VaR violations and the unconditional coverage LR p-values corresponding to (long and short) 1-day and 10-day VaR estimates at a 1% confidence level. The results show that the more traditional parametric approaches, such as VC, EWMA, CCC, and Gaussian-DCC models, tend to underestimate the VaR, especially for short positions and for utility portfolios. The non-parametric HS produces better coverage probabilities for these cases. The VaR estimates from the VG and NIG models are also too low for short positions, particularly at the 1-day horizon, whereas the T and skT models (i.e., those with polynomial tail decay) are generally better for these positions. For long positions, especially at the 10-day horizon, heavy-tailed models have very small and even zero coverage probabilities (i.e., there are no violations).

To backtest the success of our estimated ES, we follow the methods proposed by Embrechts, Kaufmann, and Patie (2005) and McNeil and Frey

Table 3.4. Quantiles backtest: coverage measure

This table reports the percentage of VaR violations (% viol.) and the *p*-values of the average coverage log-likelihood ratio (LR), corresponding to both 1-day and 10-day 1% VaR estimates over the out-of-sample period (March 2010 to March 2012) for different multivariate models.

	Representative utility portfolio								Equally weighted portfolio							
	Short position				Long position				Short position				Long position			
	h=1		h=10		h=1		h=10		h=1		h=10		h=1		h=10	
	% viol.	LR	% viol.	LR	% viol.	LR	% viol.	LR	% viol.	LR	% viol.	LR	% viol.	LR	% viol.	LR
VC	0.040	0.000	0.060	0.000	0.022	0.021	0.000	0.002	0.032	0.000	0.018	0.110	0.018	0.101	0.020	0.045
EWMA	0.042	0.000	0.067	0.000	0.016	0.222	0.004	0.130	0.040	0.000	0.022	0.019	0.020	0.050	0.010	0.982
CCC	0.046	0.000	0.067	0.000	0.020	0.050	0.000	0.002	0.038	0.000	0.018	0.101	0.018	0.110	0.014	0.383
G	0.046	0.000	0.067	0.000	0.020	0.050	0.000	0.002	0.036	0.000	0.020	0.045	0.018	0.110	0.014	0.383
T	0.022	0.021	0.008	0.657	0.004	0.121	0.000	0.002	0.008	0.629	0.000	0.002	0.004	0.121	0.000	0.002
skT	0.022	0.021	0.008	0.657	0.004	0.121	0.000	0.002	0.002	0.027	0.000	0.002	0.004	0.121	0.000	0.002
VG	0.040	0.000	0.042	0.000	0.018	0.110	0.000	0.002	0.018	0.110	0.002	0.030	0.016	0.222	0.012	0.646
NIG	0.038	0.000	0.034	0.000	0.012	0.677	0.000	0.002	0.018	0.110	0.002	0.030	0.010	0.986	0.004	0.130
HS	0.018	0.110	0.006	0.342	0.004	0.121	0.000	0.002	0.002	0.027	0.000	0.002	0.002	0.027	0.000	0.002
	Minimum variance portfolio								Gas-fired power plant							
	Short position				Long position				Short position				Long position			
	h=1		h=10		h=1		h=10		h=1		h=10		h=1		h=10	
	% viol.	LR	% viol.	LR	% viol.	LR	% viol.	LR	% viol.	LR	% viol.	LR	% viol.	LR	% viol.	LR
VC	0.034	0.000	0.012	0.646	0.020	0.050	0.016	0.206	0.038	0.000	0.053	0.000	0.026	0.003	0.000	0.002
EWMA	0.036	0.000	0.024	0.007	0.022	0.021	0.004	0.130	0.042	0.000	0.059	0.000	0.020	0.050	0.004	0.130
CCC	0.040	0.000	0.020	0.045	0.026	0.003	0.012	0.646	0.042	0.000	0.067	0.000	0.022	0.021	0.000	0.002
G	0.042	0.000	0.022	0.019	0.024	0.008	0.012	0.646	0.042	0.000	0.067	0.000	0.024	0.008	0.000	0.002
T	0.012	0.677	0.000	0.002	0.004	0.121	0.000	0.002	0.020	0.050	0.008	0.657	0.004	0.121	0.000	0.002
skT	0.010	0.986	0.000	0.002	0.004	0.121	0.000	0.002	0.020	0.050	0.008	0.657	0.004	0.121	0.000	0.002
VG	0.024	0.008	0.004	0.130	0.014	0.407	0.006	0.342	0.034	0.000	0.044	0.000	0.016	0.222	0.000	0.002
NIG	0.022	0.021	0.004	0.130	0.012	0.677	0.004	0.130	0.032	0.000	0.034	0.000	0.006	0.323	0.000	0.002
HS	0.006	0.323	0.000	0.002	0.004	0.121	0.000	0.002	0.016	0.222	0.004	0.130	0.002	0.027	0.000	0.002

(2000). In both approaches, we evaluate the discrepancies between losses and ES estimates, defined by $\hat{D}_t(\alpha, h) = \Delta W_t(h) - \widehat{\mathrm{ES}}_t(\alpha, h)$, on those points at which the VaR estimate is violated, that is, when $\hat{I}_t(\alpha, h) = 1$. Ideally, we would expect that the variable $[\hat{D}_t(\alpha, h)\hat{I}_t(\alpha, h)]$ behaves similar to realizations of a distribution with mean close to zero.

Thus in Table 3.5, we present, for the 1-day and 10-day 1% ES estimates of the various multivariate models, the backtest measure V_1, defined as the conditional average of excesses $\hat{D}_t(\alpha, h)$ conditioned on the indicator variable $\hat{I}_t(\alpha, h)$, and the p-value (MF) corresponding to a bootstrap test that checks if ES values are systematically underestimated. We observe that ES exceedances are quite high for (conditional and unconditional) Gaussian models, especially for the two utility portfolios. Semi-heavy-tailed models (VG and NIG) behave reasonably well for long positions in the utility portfolios and for both short and long positions in the equally weighted and minimum variance portfolios, but they underestimate the 1-day tail risk of short positions in utility portfolios. The T and skT models produce average exceedances that are generally positive or at most slightly negative. These heavy-tailed models behave better than alternative versions with regard to the tail risk of short positions.

A more appropriate test would compare all models jointly, to determine whether the differences in the tail patterns are statistically significant. Thus, we next compare the performance of the tail risk estimates using the superior predictive ability (SPA) test of Hansen (2005), which requires the stationary bootstrap of Politis and Romano (1994) to implement. In our application of the SPA test, we generate $B = 10,000$ bootstrap resamples. This test is designed to assess whether a particular model is significantly outperformed by others, while also controlling for the set of models being compared. Thus, over the out-of-sample (validation) period, we evaluate the risk measure forecasts using a prespecified loss function. The preferred model produces the smallest expected loss (see Appendix A.10 for more details).

Because the ES measure describes overall tail risk behavior better, we decide here to focus on an ES-based loss function.[10] In particular, we consider a linear-linear (or "lin-lin") loss function $L(\widehat{\mathrm{ES}}_t(\alpha, h))$ that penalizes events below the ES estimate more than those for which actual losses do not exceed the ES forecast, such that

$$L(\widehat{\mathrm{ES}}_t(\alpha, h)) = \left(\alpha - \mathbb{1}_{\{V_1(\widehat{\mathrm{ES}}_t(\alpha,h))<0\}}\right) V_1(\widehat{\mathrm{ES}}_t(\alpha, h)), \tag{3.17}$$

[10]We also take into account other loss functions, based on both VaR and ES forecasts, but we do not report them here.

Table 3.5. Expected shortfall (ES) backtests

This table reports the Embrechts, Kaufmann, and Patie (2005) backtest measure V_1 and the p-value of McNeil and Frey's (2000) test (MF). Both are calculated for the 1-day and 10-day 1% ES forecasts of various multivariate models over the out-of-sample period.

	Representative utility portfolio								Equally weighted portfolio							
	Short position				Long position				Short position				Long position			
	h=1		h=10		h=1		h=10		h=1		h=10		h=1		h=10	
	V_1	MF	V_1	MF	V_1	MF	V_1	MF	V_1	MF	V_1	MF	V_1	MF	V_1	MF
VC	-349.2	0.000	-294.5	0.182	-137.7	0.090	0.000	1.000	-19.05	0.104	8.168	1.000	-23.95	0.160	4.869	1.000
EWMA	-214.2	0.000	-193.4	0.000	-175.1	0.000	-112.9	0.121	-11.18	0.000	-10.03	0.090	-14.23	0.000	6.873	1.000
CCC	-268.2	0.000	-232.0	0.230	-121.7	0.060	0.000	1.000	-11.57	0.010	8.544	1.000	-10.72	0.200	-2.352	1.000
G	-267.7	0.000	-229.2	0.200	-120.1	0.060	0.000	1.000	-12.88	0.020	8.388	0.980	-11.28	0.190	-2.143	1.000
T	-15.39	1.000	629.9	1.000	195.2	1.000	0.000	1.000	27.90	1.000	0.000	1.000	5.812	1.000	0.000	1.000
skT	-9.851	0.990	693.8	1.000	197.8	1.000	0.000	1.000	20.68	1.000	0.000	1.000	0.276	1.000	0.000	1.000
VG	-212.4	0.020	-27.83	0.990	-50.62	0.310	0.000	1.000	-8.834	0.950	29.64	1.000	-4.014	0.580	20.52	1.000
NIG	-182.9	0.100	62.24	1.000	-43.70	0.410	0.000	1.000	-1.254	1.000	49.66	1.000	-7.710	0.740	15.54	1.000
HS	-161.8	0.170	319.5	1.000	144.5	1.000	0.000	1.000	24.21	1.000	0.000	1.000	7.883	1.000	0.000	1.000
	Minimum variance portfolio								Gas-fired power plant							
	Short position				Long position				Short position				Long position			
	h=1		h=10		h=1		h=10		h=1		h=10		h=1		h=10	
	V_1	MF	V_1	MF	V_1	MF	V_1	MF	V_1	MF	V_1	MF	V_1	MF	V_1	MF
VC	-23.89	0.010	-2.360	0.679	-28.87	0.045	12.79	1.000	-652.3	0.000	-430.6	0.176	-224.0	0.107	0.000	1.000
EWMA	-18.14	0.000	-18.55	0.000	-16.54	0.000	16.30	1.000	-370.1	0.000	-331.0	0.090	-231.6	0.000	93.60	1.000
CCC	-17.62	0.000	-1.472	0.850	-9.401	0.140	2.233	1.000	-491.5	0.000	-351.3	0.160	-191.5	0.070	0.000	1.000
G	-16.60	0.010	1.001	0.870	-11.08	0.130	1.413	1.000	-486.4	0.000	-343.9	0.228	-162.3	0.160	0.000	1.000
T	24.60	1.000	0.000	1.000	3.043	1.000	0.000	1.000	117.1	1.000	677.9	1.000	548.1	1.000	0.000	1.000
skT	32.49	1.000	0.000	1.000	-3.146	1.000	0.000	1.000	5.656	1.000	586.7	1.000	511.5	1.000	0.000	1.000
VG	-10.22	0.400	28.47	1.000	-12.83	0.320	17.29	1.000	-453.2	0.020	-88.02	0.595	-50.40	0.479	0.000	1.000
NIG	-4.12	0.750	55.46	1.000	-9.026	0.540	32.40	1.000	-364.7	0.122	248.7	1.000	-231.8	0.188	0.000	1.000
HS	24.61	1.000	0.000	1.000	1.716	1.000	0.000	1.000	-242.7	0.198	451.9	1.000	218.1	1.000	0.000	1.000

where $V_1(\widehat{\mathrm{ES}}_t(\alpha, h))$ represents the backtesting measure of Embrechts, Kaufmann, and Patie (2005).

Employing the loss function proposed in equation (3.17), we report in Table 3.6 the consistent *p*-values corresponding to the SPA tests of the 1% and 5% ES estimates for 1-day and 10-day (long and short) portfolio losses. We include in the analysis the GH models and the parametric benchmark models. Any *p*-values greater than 0.20 are highlighted in bold, which indicates that the null hypothesis for the corresponding benchmark is not rejected. According to these results, we reject the claim that the (conditional and unconditional) Gaussian models, such as VC, EWMA, CCC, and G, perform as well as the best competing alternative model, with the possible exception of the long portfolio positions at 10-day horizons. The SPA tests support our previous findings, namely that models with exponential tail decay (i.e., VG and NIG models) yield inferior tail estimates for short portfolio positions, especially for the far tail ($\alpha = 1\%$) of utility portfolios at the 1-day horizon. The *p*-values of the T and skT models are close to one for most portfolio positions,[11] so we know that the polynomial tail decay is not outperformed by other tail patterns we have considered. In addition, for short positions, $\alpha = 1\%$, and a 1-day horizon, these models are the only SPA benchmarks for which we do not reject the null hypothesis. In particular, at both confidence levels ($\alpha = 5\%, 1\%$), we cannot reject the skT model for any short or long position.

3.6 Conclusions

In this chapter, we have characterized the tail behavior of energy price risk using a dynamic multivariate model. We approximated exposure to energy price risk for physical and financial players using linear combinations (portfolios) of crude oil, natural gas, coal, and electricity futures. To model the stylized features of the vector of energy risk factors, we have proposed a flexible econometric specification with time-varying conditional mean, variance, and correlation, which accommodate the possible presence of serial dependence in returns, heteroskedasticity, and leverage effects. With respect to the conditional distribution, we considered the possibility that the vector of innovations may be generated by a multivariate GH distribution, which contains as particular cases some popular distributions, such as the NIG, the VG, the skewed t, Student's t, and the Gaussian distribution.

[11] If the SPA statistic is greater than or equal to zero, there is no evidence against the null hypothesis, and *p*-value = 1.00 by convention.

Table 3.6. Superior Predictive Ability (SPA) backtests

This table presents the results of SPA tests of 1% and 5% ES estimates for 1-day and 10-day portfolio returns over the out-of-sample period (March 2010 to March 2012) for different parametric multivariate models. Consistent p-values above 0.20 are highlighted in bold.

	Representative utility portfolio								Equally weighted portfolio							
	Short position				Long position				Short position				Long position			
	h=1		h=10		h=1		h=10		h=1		h=10		h=1		h=10	
	5%	1%	5%	1%	5%	1%	5%	1%	5%	1%	5%	1%	5%	1%	5%	1%
VC	0.064	0.010	0.013	0.018	0.047	0.049	0.117	0.153	0.014	0.023	0.108	0.151	0.132	0.133	0.124	0.146
EWMA	**0.202**	0.043	0.035	0.061	0.014	0.013	0.119	0.188	0.004	0.017	0.105	0.115	**0.256**	**0.217**	**0.376**	**0.250**
CCC	0.051	0.004	0.008	0.024	0.067	0.053	**0.579**	**0.426**	0.001	0.009	0.084	**0.247**	0.142	**0.464**	0.172	0.128
G	0.023	0.005	0.007	0.026	0.065	0.054	**0.577**	**0.432**	0.000	0.008	0.068	**0.249**	**0.180**	**0.429**	0.170	0.141
T	**1.000**	**0.571**	0.112	**1.000**	**1.000**	**1.000**	**0.749**	**0.435**	0.033	**0.693**	**0.915**	**0.746**	**0.670**	**1.000**	**0.885**	**0.773**
skT	**0.830**	**1.000**	**1.000**	**0.716**	**0.426**	**0.852**	**0.740**	**0.438**	**1.000**	**1.000**	**0.840**	**0.751**	**1.000**	**0.463**	**1.000**	**0.776**
VG	**0.251**	0.009	0.014	0.047	0.162	0.084	**0.510**	**0.434**	0.008	0.045	**0.822**	**0.715**	**0.667**	**0.708**	**0.197**	**0.546**
NIG	**0.551**	0.020	0.032	0.119	**0.270**	0.102	**0.499**	**0.424**	0.007	0.103	**1.000**	**0.723**	**0.814**	**0.331**	**0.297**	**0.608**
	Minimum variance portfolio								Gas-fired power plant							
	Short position				Long position				Short position				Long position			
	h=1		h=10		h=1		h=10		h=1		h=10		h=1		h=10	
	5%	1%	5%	1%	5%	1%	5%	1%	5%	1%	5%	1%	5%	1%	5%	1%
VC	0.012	0.016	0.138	**0.246**	0.062	0.152	0.129	0.158	0.028	0.012	0.014	0.021	0.022	0.066	0.144	0.142
EWMA	0.005	0.007	0.087	0.092	0.045	**0.449**	**0.455**	**0.510**	**0.201**	0.041	0.040	0.082	0.010	0.034	0.108	0.101
CCC	0.001	0.006	0.053	**0.272**	0.034	**0.789**	0.180	0.153	0.002	0.004	0.011	0.030	0.005	0.054	**0.618**	**0.422**
G	0.000	0.005	0.055	**0.276**	0.030	**0.794**	0.174	0.160	0.003	0.004	0.012	0.031	0.006	0.076	**0.617**	**0.415**
T	0.032	**0.219**	**1.000**	**0.708**	**1.000**	**1.000**	**0.840**	**0.713**	**0.516**	**1.000**	**1.000**	**0.763**	**1.000**	**0.683**	**0.676**	**0.420**
skT	**1.000**	**1.000**	**0.776**	**0.700**	**0.666**	**0.452**	**1.000**	**0.709**	**1.000**	**0.419**	0.158	**1.000**	**0.376**	**1.000**	**0.686**	**0.420**
VG	0.002	0.023	**0.619**	**0.735**	0.154	**0.627**	**0.188**	**0.657**	0.169	0.006	0.019	0.052	0.014	0.108	**0.502**	**0.428**
NIG	0.008	0.065	**0.726**	**0.747**	**0.313**	**0.709**	**0.417**	**0.583**	**0.263**	0.012	0.054	**0.261**	0.126	0.102	**0.476**	**0.431**

With these distributions, we can model different dependence patterns (e.g., dependence in the extremes, positive or negative skewness) and tail decays (e.g., exponential vs. polynomial).

Our empirical application featured daily data from August 2005 to March 2012 related to energy futures traded in the NYMEX. We reserved the observations from March 2010 to March 2012 for our out-of-sample analysis. Thus, using the recursive estimates of the multivariate GH models, we calculated the conditional risk measures corresponding to four prespecified energy portfolios. Then, we evaluated the performance of those sequences of risk measures forecast over the out-of-sample period. Our in-sample and out-of-sample results showed the importance of fat tails and positive skewness in the multivariate distribution of energy risk factors. We also proposed comparing the tail risk estimates corresponding to the GH models and other more traditional procedures, by applying a test of superior predictive ability (SPA). Regarding the tail risk of short positions, our SPA backtest results confirmed that distributions with polynomial tail decay (heavy-tailed) outperformed alternative versions, especially for the utility portfolios. The distributions with exponential tail decays (Gaussian and semi-heavy-tailed) behaved reasonably well for long positions and longer horizons. Ultimately, the extent to which we underestimate the tail risk of the portfolio loss distribution depends on the portfolio weights of the different energy commodities, whether we are analyzing the short or long trading position, and the horizon and confidence level considered.

It is worth mentioning that many power firms in liberalized markets have two main lines of business: electricity generation and electricity distribution. These days, and given the chronic generation overcapacity afflicting many developed markets (United States, Europe) most firms tend to focus more on the distribution business which implies an aggregate short position in electricity. The evidence we present suggests that conventional market risk measures (Gaussian VaR and ES) severely underestimate market risk under these circumstances. This fact should be taken into account not only by the company's shareholders and creditors but also by market regulators and supervisors.

Some questions arise for further research. First, we did not consider the effects of parameter uncertainty in the calculations of the tail risk measures, and it would be interesting, albeit computationally intensive, to study the impacts on the results if we were to take such uncertainty into account. Second, we characterized the aggregate tail risk using prespecified energy price risk exposures, given by the portfolio weights, of various representative energy-market players. However, an advantage of our asset-level approach is

that we can analyze the sensitivity of the tail risk measures to changes in the weights of the energy portfolio. Furthermore, we can use these multivariate approaches to determine how the risk measures we have analyzed might be used to construct an optimal energy portfolio. Finally, it would be interesting to compare the GH models with other parametric and semi-parametric multivariate approaches, such as those related to multivariate extreme value theories (e.g., Poon, Rockinger, and Tawn (2004)). We leave these questions for future analysis.

II

Asset pricing and derivatives valuation in continuous time

4

Interconnecting electricity markets: A real options approach

ELECTRICITY MARKETS have undergone a series of fundamental changes sparked by the liberalization of this industry. The first stage of liberalization required privatization of all or most of the generation assets, as well as privatization of the transmission grid which transports electricity from the generation points to the end consumer. Another important step in the development of the wholesale electricity markets is to exploit price differentials between locations by building interconnectors which are bi-directional transmission lines connecting the grids of two locations or the grids of two countries. Although interconnecting different grids is at the top of the political agenda in many countries, the decision to build them depends on their financial value.[1]

Electricity prices are characterized by exhibiting extreme volatility and by undergoing abrupt changes (large upward spikes and large downward jumps), as well as fast mean reversion to a seasonal trend. This extreme behavior is also present in the difference between prices of two locations and explains why interconnecting two markets could be profitable. The main question we address in this chapter is how to value an interconnector. One of the key features that drives the financial value of an interconnector is that the owner has the right, but not the obligation, to transmit electricity between two locations. Therefore, once it has been built, the financial value of an interconnector is given by a series of real options which are written on the price differential between two electricity markets.

[1]For example, see Department of Energy (2002) and European Commission (2008) for the policy steps towards interconnecting grids in the US and European Union.

In this chapter we propose a valuation tool that uses real options theory to consider the problem and we employ market data of five pairs of European neighboring countries to value hypothetical interconnectors under realistic assumptions. The value of an interconnector is given by a strip of European-style options (Bull Call Spreads) written on the spread between the two markets and the valuation formula is in closed-form and is quick to implement. Our model for the spread captures the main characteristics of the dynamics of price differentials: jumps in both directions, high seasonal volatility, and fast mean reversion to a seasonal trend. We propose an algorithm to detect jumps where the emphasis is placed on avoiding misclassifying mean reversion as jumps. We estimate the parameters of the spread model and find that the introduction of jumps in the model delivers gains in the in-sample performance of between 20% and 48% with respect to a misspecified or "naive" model in which jumps are not included.

We show valuations under different liquidity caps, which proxy for the depth of the interconnected power markets. We also derive no-arbitrage lower bounds for the value of the interconnector in terms of electricity futures contracts of the respective power markets. We find that most of the time these bounds are satisfied, but there are days where the value of the interconnector is given by the no-arbitrage bound instead of the price delivered by the sum of the prices of real options. We find that, depending on the depth of the market, the jumps in the spread can account for between 1% and 40% of the total value of the interconnector. The two markets where an interconnector would be most (resp. least) valuable are Germany and the Netherlands (resp. France and Germany). The markets where off-peak transmission between the two countries is more valuable than transmission during peak times are: France and Germany, France and UK, and the Netherlands and UK. We also provide "rules of thumb" to summarize the different drivers of the interconnector value.

The rest of this chapter is organized as follows. Section 4.1 reviews the literature on real options in commodity markets, electricity price models, and spread options. Section 4.2 discusses the data and why interconnectors are valuable. Section 4.3 frames the financial value of interconnector leases as a strip of European Bull Call Spread options and Section 4.4 derives no-arbitrage bounds for the lease based on traded assets such as electricity forwards and futures. Section 4.5 presents a model for the spread and derives valuation formulae. Section 4.6 describes how the model parameters are estimated and describes the algorithm that we propose to detect jumps and disentangle mean-reversion from jumps. Section 4.7 shows values of a one-year interconnection lease for five pairs of European neighboring

markets and discusses the no-arbitrage bounds using futures data. Section 4.8 concludes.

4.1 Literature Review

In energy markets there are many projects whose value depends on the flexibility of being able to delay decision-making until more information becomes available. These decisions can include delaying or accelerating production, postponing entry, scaling production, changing technology, etc, see Trigeorgis (1996), Brennan and Trigeorgis (2000), and Keppo and Lu (2003). In many cases the flexibility embedded in some types of project is what drives most of their value. For example, some electricity plants are only economically viable to operate when market prices are very high, otherwise they must be "switched off". Moreover, gas-fired plants are very valuable because relative to other plants (for instance nuclear and coal-fired ones) it is easier to ramp up or ramp down according to the level of market prices. Neglecting these embedded real options may seriously undervalue some projects to the extent that they might seem to deliver a negative NPV when in fact they are viable.

In the natural gas and liquified natural gas (LNG) industry, the value of some assets and financial instruments principally depends on the flexibility that these assets provide to their management. For example, the market value of a natural gas storage facility depends on the ability to store gas during times of low prices, and the ability to bring the stored gas to market at times of high prices, see Chen and Forsyth (2007), Boogert and De Jong (2008), and Carmona and Ludkovski (2010). The value of natural gas supply contracts depends on the flexibility of the shipper to interrupt delivery during the life of the contract, see Jaillet, Ronn, and Tompaidis (2004), and Cartea and Williams (2008).

Real options in electricity markets are also key components in project valuation. Power plants that offer operational flexibility derive most of their value from the option to produce electricity when prices are high. These options are valuable because wholesale electricity prices are extremely volatile, but the extreme behavior of power prices makes electricity prices a difficult commodity to model. Modeling electricity interruptible supply contracts and electricity swing contracts has been undertaken by Kamat and Oren (2002), Keppo (2004), and Hambly, Howison, and Kluge (2009). Modeling power prices, and other contracts such as futures and forwards, can be found in Roncoroni (2002), Cartea and Figueroa (2005), Weron (2006),

Pirrong and Jermakyan (2008), Cartea and Villaplana (2008), Hikspoors and Jaimungal (2008), Borak and Weron (2008), Coulon and Howison (2009), Kiesel, Schindlmayr, and Börger (2009), and Escribano, Peña, and Villaplana (2011).

The other literature that is relevant to our approach of valuing electricity interconnectors is that related to spread options in energy commodities: Dempster, Medova, and Tang (2008), Hikspoors and Jaimungal (2007), Benth and Šaltytė Benth (2006), Marckhoff and Muck (2009),and for a thorough and extensive survey on the topic see Carmona and Durrleman (2003).

4.2 The market for interconnectors and data

An important feature common to all energy commodities is that their market value depends on the location and the date that the delivery of the commodity takes place. This is particularly important for electricity where date and location are crucial determinants of market clearing prices because electricity must be consumed immediately upon delivery, while consumption of other energy commodities such as gas and oil can be deferred by either postponing delivery or by storing them. In fact, as a consequence of the non-storability of electricity, one can think of electricity delivered over different intervals of the day, or throughout periods of the year, as different goods.[2]

A further consequence of not being able to store electricity is that, strictly speaking, there are no electricity spot prices as commonly understood. Market clearing prices must be agreed prior to delivery at a time when production and demand are not known for sure; this uncertainty is resolved at the time when the physical transaction occurs. In addition, for this market clearing process to function, it is necessary for the system operator to ensure that there is sufficient capacity in the grid to secure transmission from generators to both retailers and consumers. Therefore, the convention in the market and the literature is to treat the day-ahead prices as the spot prices, although their structure is more akin to that of a forward contract. Depending on the market one can find different day-ahead quotes (prices today for next-day delivery) for contracts that dispatch electricity over fixed-time intervals during the delivery day. For example, in the UK it is possible to individually trade each of the 48 half-hours one day prior to delivery, while

[2]Due to its non-storability, electricity is considered a non-traded asset, see Schwartz (1997).

in the Nord Pool it is possible to individually trade each of the 24 hours one day prior to delivery. Another standard way in which blocks of electricity are bundled is peak and off-peak. Peak hours correspond to a fixed interval of hours for business days characterized by high electricity demand, normally between 8am and 8pm. Off-peak hours belong to the interval between the end of a peak block and the beginning of the next one, and include the 24 hours of weekends' days and holidays. The day-ahead peak and off-peak contracts specify delivery of 1 MWh for every hour of their corresponding time interval.

The owner of the interconnector capacity needs to schedule the flows according to prevailing market prices and the transmission costs in the two interconnected locations. In practice these decisions are generally taken on the day-ahead market. Thus, we assume that the decision to use the interconnector to dispatch electricity from A to B, or vice versa, is based on the peak and off-peak market prices observed in the day-ahead market, net of transmission costs.[3] Therefore, every day the owner of the interconnector capacity faces various alternatives. To commit to dispatching electricity the following day from A to B, or from B to A, during the peak and off-peak hours. To decide not to dispatch electricity in any direction during the peak and/or off-peak period.

4.2.1 Data

European energy markets are undergoing important changes in the way they function and in how integration between them is evolving. Bunn and Gianfreda (2010) employ electricity forward and spot data to show that the degree of market integration between the French, German, British, Dutch and Spanish markets is increasing. Here we look at five electricity markets: Powernext (France), UKPX (the United Kingdom), EEX (Germany and Austria), APX (the Netherlands) and Nord Pool (Norway, Sweden, Finland and Denmark). Table 4.1 summarizes the data we use in this chapter. For all markets, peak and off-peak day-ahead prices for weekdays are available.[4]

[3]In spite of that, inefficient arbitrage transmission can occur. Bunn and Zachmann (2010) have shown that, under the presence of a dominant generator in one location, there might be electricity flows from high to low price area, even whilst most players trade in the opposite (efficient arbitrage) direction.

[4]In addition, for France, UK, and Nord Pool, we have data for weekends. The definition of peak hours differs across markets. For example, peak hours for France are between 9am and 8pm, Germany from 7am to 7pm, UK from 8am to 8pm, and Nord Pool from 7am to 10pm.

Table 4.1. Summary statistics

Summary statistics (mean, standard deviation, minimum, maximum, in Euros/MWh, and skewness and kurtosis) of spot prices and spreads. *Corr* is the sample correlation coefficient between the spot prices used to calculate the spread, all are significant at the 5% level. We perform an Augmented Dickey-Fuller test (ADF) on the prices using 21 lags. The null hypothesis is a unit root with constant trend in the null hypothesis, whose critical values are equal to -3.49, -2.87 and -2.59 for 1%, 5% and 10% confidence levels, respectively. The unit root hypothesis is always rejected in favor of the mean reverting alternative at 1% significance. Normality in the spreads is rejected in all cases at a 1% level according to the Jarque-Bera statistic (*JB stat*). In this table, we only take into account working days. For the markets where we have weekend data, main statistics do not change significantly, neither do the results of the tests of normality nor the unit root tests.

Panel A: Spot Prices

	France		UK		Germany		Nord Pool		Netherlands	
Period	11/2001 – 07/2009		06/2000 – 07/2009		01/2002 – 04/2009		01/2000 – 07/2009		01/2000 – 07/2009	
# Obs.	2,776		2,359		2,676		3,473		2,479	
	Peak	Off-Peak	Peak	Off-Peak	Peak	Off-Peak	Peak	Off-Peak	Peak	Off-Peak
Mean	52.75	32.82	50.09	44.33	48.39	32.06	34.97	31.08	58.77	27.32
Std. Dev.	33.10	16.18	30.32	25.34	30.58	21.74	14.45	13.56	41.76	14.53
Min	5.06	4.79	14.78	15.97	0.80	-342.24	5.71	3.7883	1.78	1.93
Max	551.41	123.10	265.28	214.05	543.72	293.82	119.32	112.42	944.61	119.97
Skew.	3.93	1.12	1.99	2.01	4.18	-0.91	1.31	1.35	6.74	1.82
Kurt.	40.65	3.79	8.67	8.86	45.09	71.78	6.18	6.57	105.36	7.29
ADF	-14.62	-7.42	-12.14	-6.62	-24.28	-40.72	-5.70	-4.16	-22.25	-9.58

Panel B: Spread Prices

	France-Germany		France-UK		Nord Pool-Germany		Germany-Netherlands		Netherlands-UK	
	Peak	Off-Peak	Peak	Off-Peak	Peak	Off-Peak	Peak	Off-Peak	Peak	Off-Peak
Mean	0.27	-1.71	2.84	-9.75	-13.42	-0.98	-10.41	4.76	10.77	-15.56
Std Dev	17.88	19.03	25.57	18.15	27.00	21.50	40.75	18.80	39.53	17.76
Min	-222.09	-256.51	-169.94	-166.53	-489.02	-270.45	-901.42	-389.92	-169.49	-165.90
Max	305.56	396.85	419.41	286.81	94.07	393.42	323.67	263.47	915.88	36.61
Skew.	2.50	3.26	3.74	0.21	-4.59	3.24	-6.34	-2.37	8.79	-2.67
Kurt.	110.71	158.34	64.80	40.97	60.76	101.67	121.81	139.59	166.90	16.05
ADF	-49.48	-51.77	-28.78	-27.45	-30.21	-42.01	-34.39	-49.66	-24.46	-13.41
Corr.	0.848	0.561	0.677	0.671	0.470	0.330	0.400	0.527	0.441	0.721
JB stat. ($\times 10^5$)	9.6	19	3.1	1.6	3.3	9.6	14	18	21	16

Panel A in Table 4.1 shows statistics for peak and off-peak prices for these five markets. Panel B in Table 4.1 hints at why interconnecting neighboring markets might be desirable. If we assume that transmission costs are around 5 Euros/MWh and if the price paid for interconnector capacity is seen as a sunk cost, then from a mean price point of view it would be profitable to transmit electricity across the different locations. For example, by looking at the mean of the historical spreads it seems that in the off-peak segment of the day it would be profitable to use the interconnector between France and the UK, and between the Netherlands and the UK. Similarly, in the peak segment, electricity would flow from Germany to Nord Pool, from the Netherlands to Germany, and from the UK to the Netherlands.

As Table 4.1 shows, the correlation between the prices used to calculate the locational spreads in Panel B are in all cases significant and relatively high. Spreads range from a minimum of 0.33 for off-peak hours between Nord Pool and Germany, to a maximum of 0.85 for peak hours between France and Germany; two markets that are already partially interconnected.

We perform an Augmented Dickey-Fuller (ADF) test on the prices and spreads using 21 lags. Although the power of this type of test is sensitive to heteroscedasticity and outliers, statistics suggest the rejection of the unit root hypothesis in favor of mean-reverting alternatives in all cases. This pattern is even stronger for spread prices than for the price levels. The Jarque-Bera statistics show that spreads are far from being Gaussian. Moreover, spreads present a significant non-zero skewness and larger kurtosis than the prices.

Other important statistics shown in Panel B of Table 4.1 are the maxima and minima of the spreads. For example, the minimum peak spread between Germany and the Netherlands is -901 Euros/MWh. The maximum spread is between the Netherlands and UK at 915 Euros/MWh. Although these are the extreme cases observable in the data and although they are not frequent occurrences in these markets, it prompts a very important question. Will it be possible for the owner of the interconnector capacity to take simultaneous short and long positions in the two locations when the market is undergoing such remarkable price differentials? Although there seems to be insufficient public information about the depth of these markets, market participants agree that these represent situations where liquidity in at least one of the two locations is too thin. Consequently, it does not seem plausible to assume that the owner of the interconnector capacity will be able to take advantage of such extreme situations; something that will need to be taken into account when valuing the real option held by the owner of the interconnector capacity. We will return to this issue in Section 4.3 below.

4.3 Valuing interconnection capacity: a strip of real options

Writing contracts on the difference between two or more assets has a long tradition in commodity markets. In the exchanges, all of the commonly traded energy spread options have the difference between a linear combination of energy *futures* contracts as the underlying. These standard spread option contracts are written on the difference of futures contracts between: electricity and natural gas (the spark spread), electricity and coal (the dark spread), electricity and a fuel including emission allowance costs (the clean spread), crude oil and one of its derivative products (the crack spread), and others.[5]

We note that all energy spread options that are traded in exchanges have payoffs based on futures contracts. Consequently, models proposed in the literature to price options on spreads are designed to capture the stylized features of the underlying futures. Compared to more traditional asset classes such as equity, modeling commodities futures is relatively more involved due to the fact that energy futures have delivery periods (which can range from one day to years) rather than spot or instantaneous delivery, see Benth and Koekebakker (2008), Fusai, Marena, and Roncoroni (2008), Borak and Weron (2008), and Fusai and Roncoroni (2008).

Our objective is to price the optionality provided by an interconnector that can exploit the wholesale electricity spot price differential between two markets.[6] There are two crucial features that differentiate our problem from the more traditional spread options studied in the literature. First, for the owner of the interconnector capacity, the underlying "asset" of the real option is MWh of electricity and not futures or forwards written on electricity.

Second, the value of interconnection capacity between two locations, for instance locations A and B, is equivalent to holding a strip of European-style options. The decision to use the interconnector to dispatch or not to dispatch electricity in any direction, at peak and off-peak hours, is based on the day-ahead market. That is, every day the owner of the interconnector exercises the right to use the capacity to simultaneously buy electricity in market A, to sell the same quantity of electricity in market B, or vice versa. In other words, the owner of the capacity holds four daily European options:

[5]See www.nymex.com for more information on the exchange traded spread options in energy commodities.

[6]Bunn and Martoccia (2010) show that such optionality is exhibited by some of the established transmission auction prices for inter-country electricity trading in Europe.

two options on the spread between A and B; and two options on the spread between B and A (one option for peak and the other for off-peak). Since each individual option is only for one day, we cannot cast the valuation problem in terms of futures contracts since the delivery period for these will be at least one month. Nevertheless the information provided by futures contracts can be used to determine no-arbitrage bounds for the European options on the spread; this is discussed in detail below in Section 4.4.

A further assumption we make is that the capacity of the interconnector is small relative to that of the markets it is connecting. This is the same as assuming that the presence of the interconnector does not alter the price dynamics in either market; a plausible assumption for the cases we study below. Although our model does not endogenize the impact that the interconnector might have on the spread dynamics, our framework allows us to analyze different scenarios and look at the sensitivity of the value of the interconnector to: price volatility; price spikes; speed of mean reversion; and liquidity constraints when two markets are interconnected.[7]

In Panel B of Table 4.1 we showed the maxima and minima of the spread for different locations and argued that in these extreme conditions markets were too thin; in Figure 4.2 we can also appreciate some of the extreme prices in the spread. In at least one of the locations it does not seem plausible to take long or short positions at the prices that produced such large spreads. Here we assume that during times of extreme price deviations, the owner of the interconnector capacity can take positions in both markets but we limit the extent to which he can profit from the situation. We do this by capping the amount of profit that can be extracted from in-the-money options upon exercise, when valuing interconnection capacity. We denote the maximum spread level, at which it is feasible for the owner of the interconnector capacity to take positions in both locations, by M and for simplicity assume that this liquidity cap is the same regardless of whether it is an option on the peak or off-peak spread.

The valuation problem thus reduces to being able to price European capped options. For ease of presentation let us focus on the spread between A and B, which we denote $S^{\mathrm{A,B}}(t)$, and assume that it is for peak electricity, without specifying the particular hour during the peak segment. Let $C_p^{\mathrm{A,B}}\left(S^{\mathrm{A,B}}, M, t; T, K^{\mathrm{A,B}}\right)$ denote the price of a European call at time t, written on the spread $S^{\mathrm{A,B}}(t)$ during peak time, but capping the maximum value at $M > 0$, and expiring at a future date T with strike price $K^{\mathrm{A,B}} < M$. The

[7]Keppo and Lu (2003) consider the impact that market entry of a large electricity producer has on equilibrium prices.

pay-off of such option is given by $\max\left(\min\{S^{\mathrm{A,B}}(T), M\} - K^{\mathrm{A,B}}, 0\right)$. The option gives the right to transmit 1 MWh of electricity, during a designated hour of the day, but for ease of notation we do not specify the particular hour of the day.[8] The strike price represents the transmission costs between locations A and B, and time T represents the time in future periods when the decision will be made whether to use the interconnector capacity. Then, the price of the call is given by

$$C_p^{\mathrm{A,B}}(S^{\mathrm{A,B}}, M, t; T, K^{\mathrm{A,B}}) = \mathrm{e}^{-\rho(T-t)}\mathbb{E}_t\left[\max\left(\min\{S^{\mathrm{A,B}}(T), M\} - K^{\mathrm{A,B}}, 0\right)\right] \tag{4.1}$$

where ρ is the risk-adjusted discount rate, $\mathbb{E}_t$ denotes the expectation operator with information up until time t, $\max(a, b)$ denotes the maximum of the quantities a and b, and $\min\{a, b\}$ denotes the minimum of the quantities a and b.

The valuation problem of the capped European call (4.1) is also known in the literature as a Bull Call Spread. Note that capping the states of nature where the value of the call exceeds the cap M is equivalent to being long a standard European call option with strike $K^{\mathrm{A,B}}$ and short a standard European call option with strike M written on the underlying $S^{\mathrm{A,B}}(t)$. Hence

$$\begin{aligned} C_p^{\mathrm{A,B}}(S^{\mathrm{A,B}}, M, t; T, K^{\mathrm{A,B}}) = {} & C_p^{\mathrm{A,B}}(S^{\mathrm{A,B}}, \infty, t; T, K^{\mathrm{A,B}}) \\ & - C_p^{\mathrm{A,B}}(S^{\mathrm{A,B}}, \infty, t; T, M), \end{aligned} \tag{4.2}$$

where the standard European call $C^{\cdot,\cdot}(S^{\cdot,\cdot}, \infty, t; T, K^{\cdot,\cdot}) = \mathrm{e}^{-\rho(T-t)}\,\mathbb{E}_t[\max(S^{\cdot,\cdot}(T) - K^{\cdot,\cdot}, 0)]$, i.e. is given by equation (4.1) with $M = \infty$.

Generally, rights to interconnector capacity are sold over a period of time that covers a number of years and represents a significant proportion of the life of the interconnection assets. For expository purposes we will assume that the rights are in the form of a one-year lease and we value a lease for capacity of 1 MWh during peak times and 1 MWh during off-peak times. The value of the interconnector lease is given by the sum of all the capped European call options (one for every day of transmission from A to B and from B to A) between time t and expiry of the lease contract. Denoting by $V(t)$ the value of the interconnector lease with 1 MWh of capacity at time t for one hour during peak and one hour during off-peak we have that

$$V(t) = V^{\text{peak}}(t) + V^{\text{off-peak}}(t) \tag{4.3}$$

[8] If the peak time is 12 hours then the owner of the interconnector capacity holds 12 call options $C_p^{\mathrm{A,B}}$ for the peak time and 12 options for the off-peak time $C_{op}^{\mathrm{A,B}}$ where the subscript *op* stands for off-peak.

where

$$V^{\text{peak}}(t) = \sum_{i=1}^{365} C_p^{\text{A,B}}\big(S^{\text{A,B}}, M, t; t + i/365, K^{\text{A,B}}\big) + \sum_{i=1}^{365} C_p^{\text{B,A}}\big(S^{\text{B,A}}, M, t; t + i/365, K^{\text{B,A}}\big) \tag{4.4}$$

is the value of the strip of peak real options, and

$$V^{\text{off-peak}}(t) = \sum_{i=1}^{365} C_{op}^{\text{A,B}}\big(S^{\text{A,B}}, M, t; t + i/365, K^{\text{A,B}}\big) + \sum_{i=1}^{365} C_{op}^{\text{B,A}}\big(S^{\text{B,A}}, M, t; t + i/365, K^{\text{B,A}}\big) \tag{4.5}$$

is the value of the strip of off-peak real options. Here the notations C_p and C_{op} denote the capped calls on the peak and off-peak segments of every day respectively and the sum is from day 1 until day 365. Hence the one-year lease consists of 1,460 options, of which 730 are for a one-hour slot during peak times and 730 are for a one-hour slot during off-peak times.[9] Are the values (4.4) and (4.5) arbitrage free? We know that storing electricity in an economical way is not possible, therefore the four strips of 365 options described here cannot be arbitraged using a buy-and-hold argument. Below we show that by setting a simple strategy based on forward contracts, one can derive lower bounds for the four options discussed here.

4.4 No-arbitrage bounds

Although the real option valuation of the interconnector requires knowledge of the distribution of the difference between peak and off-peak prices under the statistical measure and the risk-adjusted rate ρ in order to discount the risky cash-flows, one can check whether the strip of call options being used in the valuation satisfies no-arbitrage lower bounds given by the forward or futures markets in both locations.

Assume that the lessor sells capacity for each hour of the day. For example, one can purchase interconnector capacity for the hour 8am to 9am for as many days as desired, or one can purchase the entire peak segment for as many days as desired. Now, let us focus on the no-arbitrage bound

[9]The value of a one-year lease for the 12 peak and 12 off-peak hourly slots of the day is given by $12\left(V^{\text{peak}}(t) + V^{\text{off-peak}}(t)\right)$.

satisfied by interconnector capacity on peak electricity. Denote an electricity future for peak electricity in location $i = \{\text{A,B}\}$ by $F_p^i(t, T_1, T_2)$ where t is the current time, T_1 is the expiry of the contract, delivery of electricity starts at time $T_1 + 1$, and T_2 is the last day of delivery. Below we show that at time t the price of interconnector capacity between dates $T_1 + 1$ and T_2, inclusive, must satisfy

$$\sum_{j=T_1+1}^{T_2} C_p^{\text{A,B}}(t; j) + C_p^{\text{B,A}}(t; j) \geq \sum_{j=T_1+1}^{T_2} \mathrm{e}^{-r(j-t)} \Big(F_p^{\text{B}}(t, T_1, T_2) - F_p^{\text{A}}(t, T_1, T_2) - K^{\text{A,B}} \Big) \tag{4.6}$$

where $C_p^{\text{A,B}}(t; j) = C_p^{\text{A,B}}(S^{\text{A,B}}, M, t; T, K^{\text{A,B}})$ and $C_p^{\text{B,A}}(t; j) = C_p^{\text{B,A}}(S^{\text{B,A}}, M, t; T, K^{\text{B,A}})$ are the prices of the capped options at time t that give the holder the right, but not the obligation, to use the interconnector to deliver 1 MWh of peak electricity from location A to B, or from B to A, at time T. r is the risk-free rate, and $K^{\text{A,B}}$ and $K^{\text{B,A}}$ are the transmission costs incurred when dispatching the 1 MWh of electricity.

Inequality (4.6) is a no-arbitrage bound because if it is not satisfied the following set of trades produces a riskless profit. First, assume that market quotes reveal that $F_p^{\text{B}}(t, T_1, T_2) - F_p^{\text{A}}(t, T_1, T_2) - K^{\text{A,B}} > 0$; the interconnector capacity between locations A and B for peak electricity costs

$$\sum_{j=T_1+1}^{T_2} C_p^{\text{A,B}}(t; j) + C_p^{\text{B,A}}(t; j)\,; \tag{4.7}$$

and inequality (4.6) is not satisfied. Second, pay (4.7) for the strip of calls on the interconnector capacity for the peak hours between $T_1 + 1$ and T_2 and, at the same time, go long a forward contract in location A and short a forward contract in location B (both with expiry T_1 and end of delivery T_2 for peak electricity). Every day, from $T_1 + 1$ to T_2, collect the 1 MWh bought at price $F_p^{\text{A}}(t, T_1, T_2)$ in location A, send the power to B via the interconnector, sell it in B for $F_p^{\text{B}}(t, T_1, T_2)$, and pay transmission charges of $K^{\text{A,B}}$. Therefore the present value of the net profits, where we include the cost of the interconnector capacity, is given by

$$\sum_{j=T_1+1}^{T_2} \mathrm{e}^{-r(j-t)} \Big(F_p^{\text{B}}(t, T_1, T_2) - F_p^{\text{A}}(t, T_1, T_2) - K^{\text{A,B}} \Big) - \sum_{j=T_1+1}^{T_2} C_p^{\text{A,B}}(t; j) + C_p^{\text{B,A}}(t; j) > 0, \tag{4.8}$$

which is greater than zero and represents a riskless profit, i.e. an arbitrage.

One of the points we clarify in the arbitrage strategy above is that although we assume that electricity is bought in market A and sold in market B, the arbitrageur's strategy requires him to purchase options to send peak electricity from both A to B, and also from B to A, even if he never transmits power from B to A. His arbitrage strategy commits him to using all the capacity every day during peak hours in only one direction, and the seller of the capacity charges the amount (4.7) regardless. This explains why we include the strip of options $\sum_{j=T_1+1}^{T_2} C_p^{\mathrm{B,A}}(t;j)$ as part of the cost of using the interconnector.

Therefore, given two peak forward contracts in locations A and B with the same T_1 and T_2, the following bounds must be obeyed for $t < T_1$:

$$\sum_{j=T_1+1}^{T_2} \mathrm{e}^{-r(j-t)}\Big(F_p^{\mathrm{B}}(t,T_1,T_2) - F_p^{\mathrm{A}}(t,T_1,T_2) - K^{\mathrm{A,B}}\Big) \leq \sum_{j=T_1+1}^{T_2} C_p^{\mathrm{A,B}}(t;j) + C_p^{\mathrm{B,A}}(t;j)\,, \tag{4.9}$$

and

$$\sum_{j=T_1+1}^{T_2} \mathrm{e}^{-r(j-t)}\Big(F_p^{\mathrm{A}}(t,T_1,T_2) - F_p^{\mathrm{B}}(t,T_1,T_2) - K^{\mathrm{B,A}}\Big) \leq \sum_{j=T_1+1}^{T_2} C_p^{\mathrm{A,B}}(t;j) + C_p^{\mathrm{B,A}}(t;j)\,, \tag{4.10}$$

for peak hours. Similarly, given off-peak forward contracts in locations A and B, F_{op}^{A} and F_{op}^{B}, we can obtain no-arbitrage lower bounds for the off-peak real options, $C_{op}^{\mathrm{A,B}}(t;j)$ and $C_{op}^{\mathrm{B,A}}(t;j)$.

4.5 A model for the electricity spot price differentials

Modeling electricity prices, and other financial instruments related to this market, is quite recent in the academic literature. For instance, the work of Schwartz (1997) and Schwartz and Smith (2000) which considered storable commodities served as a platform for a number of articles that proposed no-arbitrage models for the dynamics of electricity prices, see Roncoroni (2010). Examples of no-arbitrage models are found in Lucía and Schwartz (2002) and Cartea and Figueroa (2005). Other models examined in the

literature are the so-called equilibrium and hybrid models, see for example: Bessembinder and Lemmon (2002), Barlow (2002), Pirrong and Jermakyan (2008), and Cartea and Villaplana (2008), among others.

Since the valuation of the call options embedded in the interconnector capacity is cast within the real options framework, the emphasis must be placed on a model that is specified under the statistical measure. Instead of estimating the parameters for the two markets A and B, we can value the interconnector capacity by modeling the difference in prices directly. Therefore, we can estimate the parameters of the spread model and use it as the departure point to value the European call options on the spread.[10]

Here we propose a model for the spread in the spirit of the no-arbitrage spot price models which captures the most important features of the price dynamics, that is: large price spikes or jumps, strong mean reversion of large deviations and the presence of a seasonal component. In addition, we obtain the following three desired properties. First, the spread model also exhibits the stylized characteristics observed in the price difference between two locations, specifically large positive and negative deviations that mean revert very quickly to a seasonal trend. Second, the estimation of the spread model parameters can be achieved with the usual techniques. Third, the spread model specification enables us to calculate the price of European-style options by employing standard tools.

Let $S^{\mathrm{A,B}}(t) = S^{\mathrm{A}}(t) - S^{\mathrm{B}}(t)$ denote the spread in wholesale prices at time t between locations A and B. We propose, under the statistical measure, the following arithmetic model for the price differences between locations A and B, $S^{\mathrm{A,B}}(t)$, at time T:

$$S^{\mathrm{A,B}}(T) = f(T) + X(T) + Y(T) \tag{4.11}$$

where $f(T)$ is a deterministic seasonal pattern (i.e. the long term trend of the spot) evaluated at time T, $X(T)$ is a mean reverting stochastic process at time T given by

$$X(T) = X(t)\mathrm{e}^{-\alpha(T-t)} + \int_t^T \mathrm{e}^{-\alpha(T-u)}\sigma(u)\mathrm{d}W(u), \tag{4.12}$$

and $Y(T)$ is a zero-mean reverting pure jump process at time T expressed as

$$Y(T) = Y(t)\mathrm{e}^{-\beta(T-t)} + \int_t^T \mathrm{e}^{-\beta(T-u)}\mathrm{d}J^{+}(u) + \int_t^T \mathrm{e}^{-\beta(T-u)}\mathrm{d}J^{-}(u)\,, \tag{4.13}$$

[10]Models for the spread can also be found in Benth and Šaltytė Benth (2006) and Benth and Kufakunesu (2009).

where α and β are the speeds of mean reversion for the Gaussian diffusion and the jump process, respectively; $\sigma(t)$ is the time-dependent deterministic volatility; $\mathrm{d}W(u)$ are the increments of a standard Brownian motion; and $\mathrm{d}J^{+}(u)$ and $\mathrm{d}J^{-}(u)$ are the increments of a compound Poisson process defined as

$$J^{s}(t) = \sum_{n=1}^{N^{s}(t)} j_{n}^{s}, \quad s = +, - , \tag{4.14}$$

where $N^{s}(t)$ denotes an inhomogeneous Poisson process with time-dependent intensity $\lambda^{s}(t)$. The random variables $\{j_1^s, j_2^s, \ldots, j_n^s\}$ represent the size of the jumps in the spread process, which are i.i.d. and exponentially distributed with parameter η^s so that the expected size of the jump is $1/\eta^s$.

The spread between B and A is given by $S^{\mathrm{B,A}}(T) = -S^{\mathrm{A,B}}(T)$. Once we have the model for the price differences, we can proceed to value the European call options on the spread.

4.5.1 Call option with jumps

In this subsection we describe how to price the real option (4.1) when the spread follows (4.11), with OU component (4.12), and jump component (4.13) with exponentially distributed jumps. The value of the call option is expressed in closed-form in Fourier space (see Appendix for details). The value of a European-style option to transmit electricity from market B to market A is given by evaluating

$$C^{\mathrm{A,B}}(S^{\mathrm{A,B}}, t; T, K^{\mathrm{A,B}}) = \frac{\mathrm{e}^{-r(T-t)}}{2\pi} \int_{-\infty+i\xi_i}^{\infty+i\xi_i} \Psi_{S}^{\mathrm{A,B}}(-\xi)\Pi^{\mathrm{A,B}}(\xi)\,\mathrm{d}\xi \tag{4.15}$$

where the transform variable $\xi = \xi_r + i\xi_i$, with ξ_r, $\xi_i \in \mathbb{R}$, $i = \sqrt{-1}$, and $\Pi^{\mathrm{A,B}}(\xi)$ is the Fourier transform of the call option payoff between locations A and B:

$$\Pi^{\mathrm{A,B}}(\xi) = \int_{-\infty}^{\infty} \mathrm{e}^{i\xi x} \max(x - K^{\mathrm{A,B}}, 0)\mathrm{d}x = -\frac{\mathrm{e}^{i\xi K^{A,B}}}{\xi^2}, \quad \text{for } \xi_i > 0\,. \tag{4.16}$$

To calculate the inversion in (4.15) we also require the characteristic function of $S^{\mathrm{A,B}}(T)$ (see Appendix for the proof):

$$\begin{aligned}\Psi_{S}^{\mathrm{A,B}}(\xi) = {} & \mathrm{e}^{i\xi h(T) - \frac{1}{2}\xi^2 \int_t^T \mathrm{e}^{-2\alpha(T-u)}\sigma^2(u)\mathrm{d}u} \, \mathrm{e}^{\int_t^T \left(\frac{\eta_1}{\eta_1 - i\xi \mathrm{e}^{-\beta(T-u)}} - 1\right)\lambda^{+}(u)\mathrm{d}u} \\ & \times \mathrm{e}^{\int_t^T \left(\frac{\eta_2}{\eta_2 + i\xi e^{-\beta(T-u)}} - 1\right)\lambda^{-}(u)\mathrm{d}u},\end{aligned} \tag{4.17}$$

where $h(T) = f(T) + X(t)e^{-\alpha(T-t)} + Y(t)e^{-\beta(T-t)}$, $\lambda^+(t)$ and $\lambda^-(t)$ are the time-dependent intensities of the Poisson arrival of positive and negative jumps respectively, and we require $-\eta_2 < \xi_i < \eta_1$.

Note that if we make the assumption that there are no jumps in the spread, the value of the capped European option to transmit electricity from location B to A is given by (see Appendix for the proof):

$$\begin{aligned} C^{\mathrm{A,B}} = &\mathrm{e}^{-\rho(T-t)}\Big[\Big(\mu(t,T) - K^{\mathrm{A,B}} + \tfrac{v(t,T)\phi(\beta_1)}{1-\Phi(\beta_1)}\Big)\Phi(-\beta_1) \\ &- \Big(\mu(t,T) - M + \tfrac{v(t,T)\phi(\beta_2)}{1-\Phi(\beta_2)}\Big)\Phi(-\beta_2)\Big], \end{aligned} \tag{4.18}$$

where

$$\begin{aligned} \mu(t,T) =& f(T) + X(t)\mathrm{e}^{-\alpha(T-t)} \quad \text{and} \\ v^2(t,T) =& \int_t^T \mathrm{e}^{-2\alpha(T-u)}\sigma^2(u)\mathrm{d}u\,, \end{aligned} \tag{4.19}$$

$C^{\mathrm{A,B}} = C^{\mathrm{A,B}}(S^{\mathrm{A,B}}, M, t; T, K^{\mathrm{A,B}})$, $\phi(x)$ and $\Phi(x)$ denote the probability density and distribution functions of a standard normal random variable. $\beta_1 = (K^{\mathrm{A,B}} - \mu(t,T))/v(t,T)$, $\beta_2 = (M - \mu(t,T))/v(t,T)$ and M is the liquidity cap. The price of the option to transmit electricity from A to B is calculated in the same way.

4.6 Estimation of model parameters

In this section, we discuss how we estimate the underlying structural parameters of the state variables $X(t)$ and $Y(t)$, as well as the deterministic seasonal factor, $f(t)$. The estimation procedure requires the following steps. First, find the deterministic seasonal trend $f(t)$ using an OLS regression and compute the detrended spread. Second, detect the positive and negative jumps in the detrended spread series considering mean reversion in the jumps. The jump detection algorithm we employ is designed to cope with the problem of miss-identifying mean reversion as jumps. Third, find the MLE of the (possibly time-dependent) intensity of positive and negative jumps. Finally, estimate the parameters of the state variables $X(t)$ and $Y(t)$.

equations (4.11), (4.12) and (4.13) describe the continuous-time model for the spread $S^{\mathrm{A,B}}(t)$ between locations A and B. We estimate the parameters of the discrete-time versions of the continuous-time equations (4.12) and (4.13) employing daily electricity data. For ease of notation we use time t in subscript to denote the discrete version of the continuous time variables,

for example the discrete versions of $X(t)$ and $Y(t)$ are denoted by X_t and Y_t respectively. To estimate the parameters of the Gaussian process $X(t)$ we use the discrete model

$$X_t = \mathrm{e}^{-\alpha\Delta t}\, X_{t-\Delta t} + \varepsilon_t \qquad t = 1, 2, \ldots, N \tag{4.20}$$

where ε_t satisfies

$$\mathbb{E}[\varepsilon_t^2] = \sigma_{\varepsilon,\,t}^2 = \frac{\sigma_t^2}{2\alpha}\,(1 - \mathrm{e}^{-2\alpha\Delta t}) \qquad \text{and} \qquad \mathbb{E}[\varepsilon_t] = 0\,, \tag{4.21}$$

and we specify the discrete-time version of the jump factor $Y(t)$ as

$$Y_t = \mathrm{e}^{-\beta\Delta t}\, Y_{t-\Delta t} + \Delta J^+ + \Delta J^-\,, \tag{4.22}$$

where $\Delta J^{+,-} = J^{+,-}\,\Delta N^{+,-}$. Here ΔN^+ and ΔN^+ are the increments of the discrete-time counting process for positive and negative jumps with arrival frequency $\lambda_t^+\Delta t$ and $\lambda_t^-\Delta t$. The random variables J^+ and J^- are positive and negative exponentially i.i.d. jump sizes with parameters η_+ and η_-. Hence, their means are $\mathbb{E}[J^+] = 1/\eta_+$ and $\mathbb{E}[J^-] = 1/\eta_-$.

We use these discrete schemes to estimate the set of parameters of the Gaussian, $\{\alpha, \sigma(t)\}$, and jump processes, $\{\beta, \lambda_t^+(t), \lambda_t^-(t), \eta^+, \eta^-\}$. Before determining these parameters, we proceed with the analysis of the seasonal behavior of spreads and prices.

4.6.1 The deterministic function f(t) and other seasonal features.

We follow the approach developed in Manoliu and Tompaidis (2002) and Jaillet, Ronn, and Tompaidis (2004) to model the seasonal component $f(t)$ of the spread of electricity spot prices. The discrete-time version of $f(t)$ takes the form:

$$f_t = f_0 + f_1\, t + \sum_{m=1}^{11} F_m\, D_t^m \tag{4.23}$$

where f_0 is a constant, f_1 is the coefficient for the time trend, F_m, for $m = 1, \ldots, 11$, are constant parameters and D_t^m are monthly dummies taking the value 1 if t belongs to the m-th month and 0 otherwise. Table 4.2 shows the estimates and Figure 4.1 depicts some examples of the seasonal function (4.23) for individual peak and off-peak spreads.

One of the features that we explore is whether there is a seasonal pattern in the volatility of the spread innovations which can emerge from a seasonal pattern in the diffusion coefficient $\sigma_{\varepsilon,t}$ of the X_t process; and/or in the

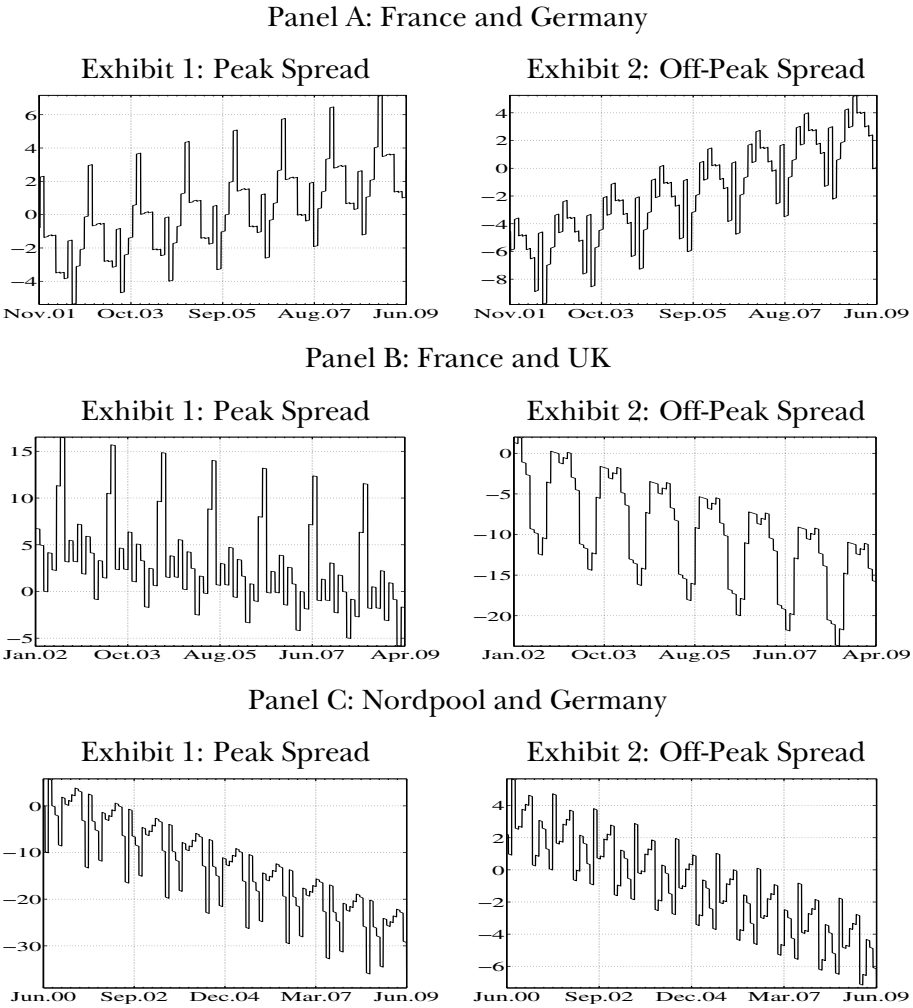

Figure 4.1. Examples of interconnection's deterministic component for peak and off-peak load

This figure shows the deterministic component of the peak and off-peak spread $S^{i,j}$ between the respective locations (black solid line in Exhibits 1 and 2 of each Panel). Table 4.2 reports the parameters employed to depict the seasonal components. In all graphs the y-axis is in Euros/MWh.

Table 4.2. Coefficients of the deterministic component

In this table we report the OLS estimates parameters of the time-dependent deterministic component of equation (4.23): $f_t = f_0 + f_1 t + \sum_{m=1}^{11} F_m D_t^m$, where f_0 is a constant, f_1 is the coefficient for the time trend, F_m for $m = 1, \ldots, 11$ are constant parameters, and D_t^m are monthly dummies, taking the value 1 if t belongs to the mth month and 0 otherwise. R^2 shows the goodness of fit of the linear regression, the F-statistic and its p-value, in parentheses, show the overall significance of the model. *DW* stands for the Durbin-Watson statistic (p-value in parentheses), and is used to test the presence of autocorrelation in the residuals.

	France-Germany				France-UK				Nord Pool-Germany			
	Peak		Off-Peak		Peak		Off-Peak		Peak		Off-Peak	
	Coeff	t-stat	Coeff	t-stat	Coeff	t-stat	Coeff	t-stat	Coeff	t-stat	Coeff	t-stat
f_0	2.24	1.51	-5.94	-3.77	2.67	1.17	0.56	0.42	3.36	1.67	4.51	2.65
$f_1 (\times 10^2)$	0.19	3.81	0.35	6.56	-0.23	-3.03	-0.51	-11.89	-0.89	-16.18	-0.25	-5.47
Jan	-3.68	-1.95	2.12	1.06	4.07	1.47	0.79	0.50	-1.22	-0.48	0.64	0.30
Feb	-3.63	-1.88	0.82	0.40	2.37	0.84	1.60	0.98	-0.15	-0.06	-3.62	-1.64
Mar	-3.70	-1.95	0.70	0.35	-2.51	-0.91	-1.32	-0.83	1.33	0.52	-2.94	-1.37
Apr	-5.98	-3.14	-0.38	-0.19	1.68	0.60	-2.69	-1.67	3.04	1.19	-0.69	-0.32
May	-6.05	-3.20	-1.14	-0.57	-0.08	-0.03	-9.21	-5.59	2.71	1.07	-1.11	-0.52
Jun	-6.45	-3.38	-3.61	-1.79	9.00	3.11	-9.54	-5.75	-3.32	-1.31	-2.29	-1.07
Jul	-4.24	-2.17	0.49	0.24	14.26	4.98	-12.02	-7.30	-13.04	-5.13	-3.48	-1.62
Aug	-8.10	-4.14	-4.74	-2.29	1.02	0.36	-9.86	-5.99	2.83	1.11	1.27	0.59
Sep	-5.89	-2.98	-2.03	-0.97	3.36	1.16	-2.84	-1.71	-2.62	-1.02	-1.72	-0.79
Oct	-4.93	-2.53	-0.89	-0.43	1.18	0.41	1.10	0.67	-4.31	-1.70	-1.52	-0.71
Nov	-3.03	-1.55	1.36	0.66	5.23	1.81	1.11	0.67	-10.50	-4.09	-0.39	-0.18
R^2	0.019		0.031		0.034		0.113		0.126		0.018	
F-stat	3.207 (0.000)		5.192 (0.000)		5.538 (0.000)		28.262 (0.000)		28.110 (0.000)		3.543 (0.000)	
DW	2.167 (0.001)		2.197 (0.000)		1.394 (0.000)		1.105 (0.000)		1.028 (0.000)		1.407 (0.000)	

Table 4.2 *(continued)*

	Germany-Netherlands				Netherlands-UK			
	Peak		Off-Peak		Peak		Off-Peak	
	Coeff	t-stat	Coeff	t-stat	Coeff	t-stat	Coeff	t-stat
f_0	-30.12	-9.35	7.68	5.07	24.05	6.82	-7.51	-4.99
$f_1(\times 10^2)$	0.76	8.71	0.07	1.82	-1.17	-10.24	-0.65	-13.42
Jan	12.03	2.97	-4.85	-2.54	-1.72	-0.40	5.26	2.89
Feb	14.29	3.45	-6.41	-3.29	-5.25	-1.21	8.80	4.75
Mar	12.69	3.11	-6.45	-3.37	-8.74	-2.04	5.71	3.13
Apr	12.65	3.07	-6.13	-3.17	-1.63	-0.38	5.72	3.09
May	9.94	2.44	-3.71	-1.94	-1.86	-0.42	-3.81	-2.03
Jun	6.18	1.53	-3.62	-1.91	11.56	2.60	-4.97	-2.63
Jul	8.70	2.15	-5.55	-2.91	4.33	0.98	-10.62	-5.66
Aug	3.98	0.98	-5.47	-2.88	9.25	2.11	-3.79	-2.02
Sep	1.25	0.30	-2.91	-1.51	3.30	0.75	0.25	0.13
Oct	2.51	0.62	-2.52	-1.33	10.10	2.31	2.87	1.54
Nov	3.43	0.84	-2.22	-1.16	9.97	2.25	-0.25	-0.13
R^2	0.048		0.012		0.078		0.168	
F-stat	9.630 (0.000)		2.247 (0.000)		13.115 (0.000)		31.486 (0.000)	
DW	1.420 (0.000)		1.885 (0.002)		1.173 (0.000)		0.563 (0.000)	

intensity of the jumps, λ_t^+ and λ_t^-. To test for seasonality in the parameters that drive the conditional variance, we assume a time-dependent seasonal functional form for the volatility $\sigma_{\varepsilon,t}$, and for the intensity parameters λ_t^+ and λ_t^-.

In order for the number of parameters in the model to be tractable, and for us to have sufficient observations for each case, we model the periodicity with seasonal dummies as follows:

$$\sigma_{\varepsilon,t} = \sigma_{\varepsilon,\text{winter}} D_t^{\text{winter}} + \sigma_{\varepsilon,\text{spring}} D_t^{\text{spring}} + \sigma_{\varepsilon,\text{summer}} D_t^{\text{summer}} + \sigma_{\varepsilon,\text{autumn}} D_t^{\text{autumn}} \tag{4.24}$$

for the volatility, and

$$\lambda_t^{+,-} = \lambda_{\text{winter}}^{+,-} D_t^{\text{winter}} + \lambda_{\text{spring}}^{+,-} D_t^{\text{spring}} + \lambda_{\text{summer}}^{+,-} D_t^{\text{summer}} + \lambda_{\text{autumn}}^{+,-} D_t^{\text{autumn}} \tag{4.25}$$

for the intensity parameters of the positive and negative jumps. D_t^i are seasonal dummies which take the values 0 or 1. That is, December, January, and February correspond to the dummy variable D_t^{winter}; March, April, and May to D_t^{spring}; June, July, and August to D_t^{summer}; and, finally, September, October, and November to D_t^{spring}.

In the next section we show how to deal with these seasonal patterns in trend, volatility and intensity and their relation with the filtering of jumps and the estimation of the state-variables.

4.6.2 Methodology to deal with the jump process and parameter estimates

Here we discuss how to estimate the underlying structural parameters of the Gaussian variable $X(t)$ and the jump factor $Y(t)$ described by the discrete-time models (4.20) and (4.22). The estimation consists of the next steps:

i) Remove the fitted seasonal component from the spread and calculate the detrended spread denoted by $\tilde{S}_t^{\mathrm{A,B}} = S_t^{\mathrm{A,B}} - f_t$.

ii) Detect the arrival of jumps (positive or negative) in the detrended spread series $\tilde{S}_t^{\mathrm{A,B}}$ and avoid classifying fast mean-reversion as jumps.

iii) Estimate the jump intensities allowing for seasonal dependence in the arrival of the jumps.

iv) Estimate the parameters of the exponential distributions for positive and negative jumps.

v) Estimate the mean-reversion rates of the Gaussian and jump factors of the spread model and the volatility of the Gaussian process.

The first step is straightforward, we discuss the others below.

Detecting jumps. We apply a recursive semi-parametric filter to identify the calendar position of the jumps in the spread. The procedure identifies a hypothetical arrival of a jump when the detrended spread difference deviates, in absolute value, by more than three standard deviations from its mean. In our framework, these standard deviations might be time-dependent, so we compute them taking into account the possible seasonal pattern in the variance of the spread, see equation (4.24). We remove the observations identified as possible jumps, recalculate the mean, and proceed to filter again. We iterate until no jumps are found. However, in highly mean-reverting time series, for instance electricity prices, some of these hypothetical jumps could correspond to the mean-reversion effect and not to the arrival of jumps of opposite sign. As we can see in equation (4.22), the mean-reversion effect with rate β is always present in the discrete-time dynamics of the jump process Y_t.

Disentangling jumps from mean reversion. Our methodology is designed to cope with the problem of miss-identifying mean reversion as jumps as follows. Assume that at time t spread prices are above the estimated seasonal trend $S_t^{\mathrm{A,B}} > \widehat{f}_t$. Suppose that the next price innovation is negative, i.e. $S_{t+1}^{\mathrm{A,B}} - S_t^{\mathrm{A,B}} < 0$, and that it is flagged as a possible jump because in absolute terms the innovation is larger than three standard deviations from the mean.

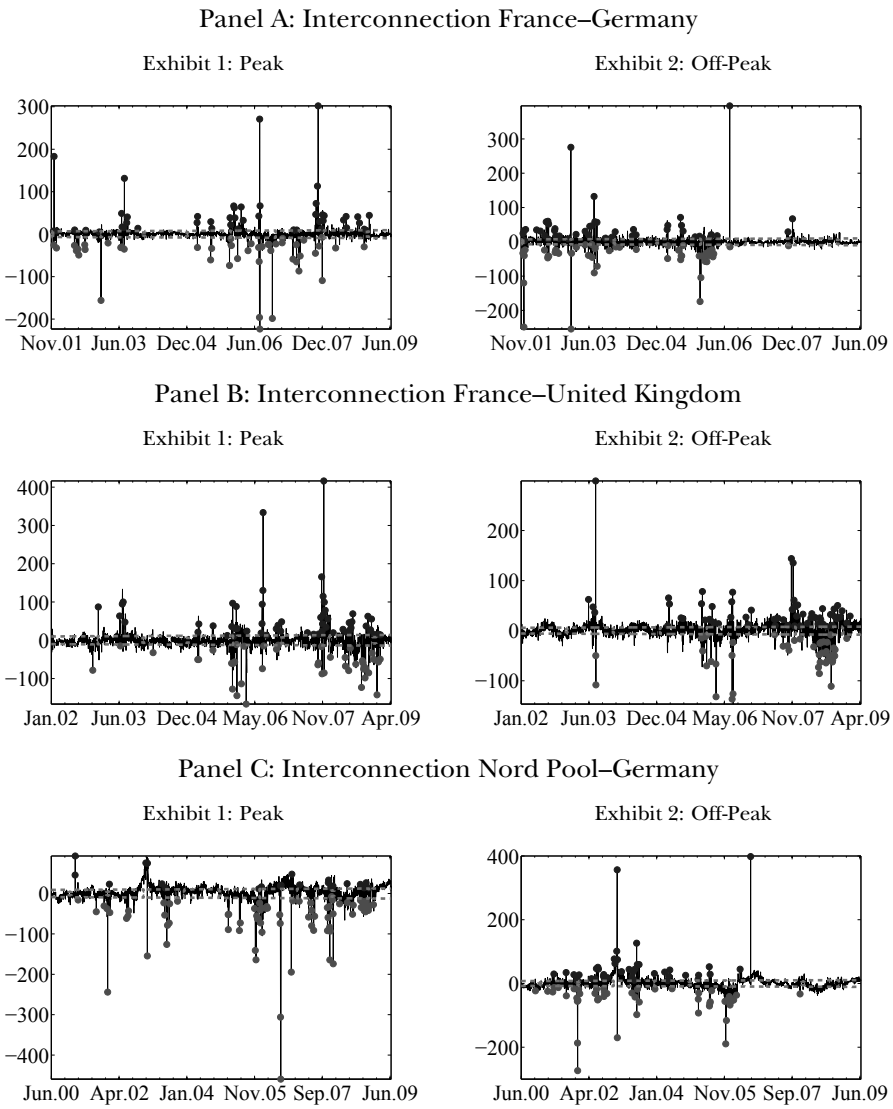

Figure 4.2. Examples of detecting jumps from the jump diffusion process

This figure shows the spread series $S^{i,j}$ (Euros/MWh) for the two possible load regimes, peak and off-peak, for three examples of interconnection. The dashed line represents the 95% confidence intervals for the deterministic component for each series. The gray circles below the lower confidence bound mark the presence of a negative jump, while the black circles above the upper confidence bound show the position of a positive jump.

Now, before labeling it as a downward jump, we check "how close" the new value $S_{t+1}^{\text{A,B}}$ is to $\widehat{f}_{t+1}$. If it is close to the seasonal component then it cannot be a downward jump, it must be mean reversion. If it is sufficiently below $\widehat{f}_{t+1}$, then it is a downward jump, that is, it diverges from the long-term trend. The metric used here to assess proximity to the seasonal trend is based on the confidence bounds for the estimates of $\widehat{f}_t$. Spread prices that after a large negative innovation fall within 95% of the confidence bounds of the estimated seasonal trend, $\widehat{f}_t$, or above are not considered negative jumps, but are due to mean reversion. Only innovations that take the spread below the lower 95% confidence interval are considered a downward jump. Similarly, large upward shocks to the spread are considered positive jumps if they satisfy two requirements: the innovation is larger than three standard deviations from the mean; and the resulting spread at time $t+1$ is above the upper 95% confidence interval of the estimated seasonal trend, $\widehat{f}_t$.

With the advent of high-frequency financial data, jump detection in equity returns has received a considerable amount of attention. Perhaps the first non-parametric filter designed to detect the arrival (including position) of Poisson jumps is that of Lee and Mykland (2008). In order to appreciate the performance of our jump filter we use Monte Carlo simulations and compare our results to those given by the Lee-Mykland (L-M) test. For example, we simulate 500 paths of the discrete version of (4.11) where we use the seasonal component estimated for the peak spread between France and Germany.[11] We compare the performance of the two tests by looking at the probability that the test fails to detect a jump, and the probability of spurious detection. We find that our jump detection filter performs better than the L-M test on both counts. In this example, the probability of not detecting an actual jump (resp. detecting a spurious jump) with our filter is 0.17 (resp. 0.03), whereas for the L-M is 0.48 (resp. 0.44).[12]

Estimating jump intensities. Once we have identified the jumps, we estimate their intensity by maximum likelihood. We analyze two scenarios,

[11]The parameters we employ are: $\alpha = 250$, $\beta = 150$, λ's are seasonal, being $\lambda^+ = [8, 2, 8, 7]$ and $\lambda^- = [5, 4, 10, 4]$ (that is, one $\lambda^\pm$ for each season: winter, spring, summer, and autumn), $\eta^+ = 1/70$, $\eta^- = 1/50$, $\sigma = 10$, and the length of the time series is $N = 2,774$. We chose these parameters based on the estimation results reported below.

[12]We note that the L-M test is designed to perform better the higher the frequency of the data and in this case we have used daily observations which is the frequency available for the our electricity data. Moreover, other filters have been proposed in the literature, however, although they are designed to tell whether there is a non-Gaussian component in the price process, they are not capable of detecting the position of the possible jump.

Table 4.3. Intensity parameter of the jumps

This table reports the intensities of jump arrivals λ. We model positive and negative jumps assuming two cases, one where the two intensities are constant throughout the year, and the other with time-dependent intensities $\lambda(t)$ which vary with the season of the year, i.e. $\lambda_t^{+,-} = \lambda_{\text{winter}}^{+,-} D_t^{\text{winter}} + \lambda_{\text{spring}}^{+,-} D_t^{\text{spring}} + \lambda_{\text{summer}}^{+,-} D_t^{\text{summer}} + \lambda_{\text{autumn}}^{+,-} D_t^{\text{autumn}}$, where D_t^{winter}, D_t^{spring}, D_t^{summer} and D_t^{autumn} are seasonal dummies. *p-val (+,-)* are the *p*-values of likelihood ratio tests, where the unrestricted model is the one with seasonal lambda. *p*-values under 0.050 indicate rejection of the constant (restricted) model at a 5% level of significance. For example, we see that for peak spread between France and Germany, we reject the constant model in favor of a seasonal intensity for both positive (5% significance) and negative jumps (10% significance).

	France-Germany				France-UK				Nord Pool-Germany			
	Peak		Off-Peak		Peak		Off-Peak		Peak		Off-Peak	
	Coeff	t-stat	Coeff	t-stat	Coeff	t-stat	Coeff	t-stat	Coeff	t-stat	Coeff	t-stat
λ^+	5.976	5.943	5.976	5.943	7.520	6.630	5.560	6.760	2.458	3.916	4.382	5.496
λ^-	5.849	5.871	6.230	6.086	5.673	5.648	4.241	5.797	8.015	7.731	5.237	6.086
$\lambda^+_{\text{winter}}$	7.814	3.141	6.837	2.892	7.127	2.892	4.741	2.760	3.910	2.182	4.345	2.336
$\lambda^+_{\text{spring}}$	1.924	1.256	4.328	2.182	2.515	1.470	3.231	2.182	0.854	0.750	4.698	2.483
$\lambda^+_{\text{summer}}$	7.842	3.018	8.888	3.261	9.882	3.377	7.435	3.490	1.254	1.020	6.687	3.141
$\lambda^+_{\text{autumn}}$	6.574	2.624	3.835	1.848	11.077	3.600	7.121	3.377	3.877	2.182	1.723	1.256
$\lambda^-_{\text{winter}}$	5.372	2.483	9.279	3.490	6.109	2.624	2.188	1.666	8.690	3.600	6.952	3.141
$\lambda^-_{\text{spring}}$	3.847	2.020	3.366	1.848	3.018	1.666	1.436	1.256	5.125	2.624	3.417	2.020
$\lambda^-_{\text{summer}}$	9.934	3.490	8.888	3.261	3.294	1.666	8.217	3.708	8.358	3.600	7.522	3.377
$\lambda^-_{\text{autumn}}$	4.383	2.020	3.287	1.666	10.523	3.490	5.538	2.892	9.908	3.916	3.015	1.848
p-val (+)	0.019		0.154		0.005		0.110		0.040		0.060	
p-val (-)	0.074		0.012		0.011		0.000		0.270		0.056	

Table 4.3 *(continued)*

	Germany-Netherlands				Netherlands-UK			
	Peak		Off-Peak		Peak		Off-Peak	
	Coeff	t-stat	Coeff	t-stat	Coeff	t-stat	Coeff	t-stat
λ^+	7.030	7.138	6.706	6.951	8.431	7.014	2.007	3.018
λ^-	7.138	7.199	3.461	4.761	6.558	6.086	8.833	7.199
$\lambda^+_{\text{winter}}$	6.655	3.018	8.873	3.600	6.783	2.760	1.043	0.750
$\lambda^+_{\text{spring}}$	2.184	1.470	4.804	2.483	3.098	1.666	0.516	0.429
$\lambda^+_{\text{summer}}$	7.140	3.261	7.980	3.490	9.374	3.261	2.757	1.470
$\lambda^+_{\text{autumn}}$	12.062	4.402	5.169	2.624	14.954	4.308	3.877	1.848
$\lambda^-_{\text{winter}}$	4.880	2.483	3.106	1.848	7.304	2.892	5.217	2.336
$\lambda^-_{\text{spring}}$	1.747	1.256	3.057	1.848	3.098	1.666	5.680	2.483
$\lambda^-_{\text{summer}}$	7.980	3.490	6.300	3.018	3.860	1.848	15.440	4.402
$\lambda^-_{\text{autumn}}$	13.785	4.761	1.292	1.020	12.185	3.813	9.415	3.261
p-val (+)	0.001		0.237		0.001		0.070	
p-val (-)	0.000		0.032		0.003		0.004	

one where intensities are constant, and the other where intensities are time-dependent and may exhibit a seasonal pattern as described in equation (4.25). MLE results for the positive and negative intensities $\lambda^+(t)$ and $\lambda^-(t)$ are shown in Table 4.3. In the table we also report the p-values of the likelihood ratio test, which compares the unrestricted model for the jump intensities (seasonal $\lambda^{+,-}(t)$) with the restricted model of constant intensities. p-values under 0.10 indicate rejection of the constant (restricted) model with a 10% significance level. In 16 out of 20 cases, we reject the model with constant intensity at a 10% significance level. For example, for peak spread between France and Germany, we reject the constant model in favor of a seasonal intensity for both positive (5% significance) and negative jumps (10% significance). Results in Table 4.3 show that the estimated number of jumps for spreads ranges from 2 to 9 per year. In Figure 4.2, we show the positions of negative and positive jumps for some of the markets we study.

Estimating jump size parameters. One of the advantages of being able to locate jumps is that we also know their sizes and signages. We use this information to fit an exponential distribution to the jump data and to obtain the average sizes of positive and negative jumps given by $1/\eta^+$ and $1/\eta^-$.[13]

[13]We do this in the following way. Once we have located the positive and negative jumps, we estimate the sizes using the differences between the spread $\tilde{S}^{\text{A,B}}_t$ of the observation and the previous value of the spread, $\tilde{S}^{\text{A,B}}_{t-1}$. This approach performs well when the mean-reversion rates of jumps and OU processes are large, which is the case in electricity prices and the spread.

Table 4.4. Estimates of seasonal volatility, mean reversion rates and jumps sizes

This table reports the parameters estimates of seasonal volatility $\sigma(t)$ of the diffusion process, the jumps sizes mean $1/\eta^+$ and $1/\eta^-$, and the mean reversion rates α and β of the diffusion and the jump component. All parameters are expressed in annual terms and in Euros/MWh, to be consistent with the arithmetic model for the spread. We show $t-$statistics and the RMSE of the model.

	France-Germany				France-UK				Nord Pool-Germany			
	Peak		Off-Peak		Peak		Off-Peak		Peak		Off-Peak	
	Coeff	t-stat	Coeff	t-stat	Coeff	t-stat	Coeff	t-stat	Coeff	t-stat	Coeff	t-stat
α	273.07	14.02	108.02	14.19	122.05	15.41	109.06	18.58	66.54	16.23	70.21	16.38
σ_{winter}	230.17	19.36	300.22	20.89	341.70	21.48	162.47	27.36	288.27	25.63	237.22	25.38
σ_{spring}	132.57	19.48	188.81	21.24	245.19	21.59	165.48	27.47	179.57	25.77	181.76	25.70
σ_{summer}	289.95	18.84	244.60	20.89	321.42	20.95	239.16	26.67	241.30	25.96	290.71	25.87
σ_{autumn}	218.22	18.68	211.21	20.48	370.60	20.89	193.47	26.53	257.66	25.71	190.03	25.63
β	183.90	30.12	96.46	21.10	167.14	21.68	121.68	21.38	206.85	25.11	100.45	20.67
$1/\eta^+$	72.72	5.43	67.77	5.43	86.35	6.12	53.12	6.25	56.14	3.39	74.68	4.98
$1/\eta^-$	59.24	5.36	80.87	5.57	76.82	5.13	53.27	5.28	71.48	7.22	72.44	5.57
RMSE	9.10		10.94		14.89		9.93		12.91		11.92	

Table 4.4 *(continued)*

	Germany-Netherlands				Netherlands-UK			
	Peak		Off-Peak		Peak		Off-Peak	
	Coeff	t-stat	Coeff	t-stat	Coeff	t-stat	Coeff	t-stat
α	5.37	7.57	1.42	4.06	194.44	15.75	50.45	13.95
σ_{winter}	353.00	30.30	275.56	24.67	331.83	20.61	117.53	24.38
σ_{spring}	308.88	30.50	186.01	25.25	277.81	20.72	128.01	24.51
σ_{summer}	785.73	31.02	205.20	25.58	620.57	20.15	180.54	23.83
σ_{autumn}	444.71	30.65	204.41	25.29	458.49	20.26	137.28	23.86
β	10.34	21.43	52.65	15.22	231.53	22.84	120.37	14.12
$1/\eta^+$	106.25	6.63	71.45	6.44	100.57	6.50	28.44	2.49
$1/\eta^-$	135.45	6.69	79.70	4.24	74.19	5.57	33.35	6.69
RMSE	30.35		12.42		20.25		7.86	

The estimates are shown in Table 4.4.

Estimating mean-reversion parameters and the volatility of the OU process. For each time series we estimate the mean-reversion rates of the Gaussian process X_t and jump process Y_t, and the volatility parameters of X_t by minimizing the mean-squared errors which are given by the average of the squared differences between the observed and the modeled spreads. Using the model specification of equations (11), (12) and (13), we have that the differences between observed spreads and the proposed jump dynamics follows an autoregressive process of order one, that is, $\tilde{S}_t^{\text{A,B}} - \mathrm{e}^{-\beta} Y_{t-1} - \hat{J}_t^+ - \hat{J}_t^- = X_t$, where $X_t = \mathrm{e}^{-\alpha} X_{t-1} + \varepsilon_t$ and $\varepsilon_t \sim N(0, \sigma^2_{\varepsilon,t})$. Hence, the estimates of both mean-reversion rates β and α, as well as the volatility of the OU process can be simultaneously obtained by means of nonlinear least squares. We report the results in Table 4.4 where we see that spreads show significant mean reversion in jumps and in the Gaussian deviations. The half-life of the jumps ranges between 1 and 15 days approximately.

As a specific case we study a "naive" or misspecified version of the spread model where we do not include the jump process $Y(t)$. In the interest of space, the estimates of the model without jumps are not reported, however, results show that the introduction of jumps in the model delivers gains in the in-sample performance of between 20% and 48% compared to the "naive" version.

4.7 The market value of interconnectors

In this section we discuss the results of valuing interconnection capacity in neighboring European countries. Based on the market data described

above, we calculate the market value of a one-year lease of an interconnector that gives the lessee the right, but not the obligation, to transmit 1 MWh of electricity between two markets during peak and off-peak times. The lease contract starts on January 1, 2010 and ends on December 31, 2010 and we assume that the initial condition of the OU and jump processes are both zero: $X(t) = Y(t) = 0$ and $t =$ January 1, 2010. We estimate the spread model with electricity prices data available until July 2009. Using these estimates, we value the interconnector lease that starts on January 1, 2010. Since the estimation is done in July 2009, the values for $X(t)$ and $Y(t)$ in January 1, 2010 are unknown. Hence, we take as initial values of the OU and jump processes the expected value of both variables, which is zero for both. We use the valuation formulae (4.4) and (4.5) to calculate prices for the four strips of options that total the value of the one-year lease of 1 MWh capacity for a one-hour slot during peak time and a one-hour slot during off-peak time. We assume that the cash-flows are discounted at the risk-adjusted rate $\rho = 10\%$.

Initially we do not check whether the option values that we obtain are equal or above the no-arbitrage bounds derived in Section 4.4. We do this below in Subsection 4.7.1, where we calculate the lower bounds using futures data. Our assumption is that the lessor will price the real options and calculate the lower bounds (4.9) and (4.10) for peak-hours, and the corresponding bounds for off-peak hours, but for clarity we show the results of the option valuation first and then where necessary we amend the values in the light of the no-arbitrage bounds.[14]

We provide different values of the interconnector, which result from different assumptions about: the seasonal function of the spread; the liquidity and depth in both markets; and how jumps affect the extrinsic value of the real options used to calculate the value of the interconnector. We discuss how these three assumptions affect the value of the interconnector:

Seasonal component. One of the points that we scrutinize is how the seasonal component affects the value of the interconnector. In this chapter we have assumed that the seasonal component is deterministic and that the historical seasonal trend will repeat itself at future dates when forecasting the spread. Although this assumption is consistent with that of the literature, care must be taken when producing forecasts and pricing options written on

[14]If one or more lower bounds are not satisfied, the lessor will set the price according to the bound instead of the price indicated by the value of the strip of options. Alternatively, if a bound is not satisfied, one expects that market participants will bid the price of the lease up until the price reaches the no-arbitrage bound.

electricity price spreads. Indeed, inspecting Figure 4.1 prompts the question of whether it is plausible to expect that the seasonal component will in the future be broadly the same as it was in the past. The answer is probably not, but until now there has been no better alternative in the literature. Therefore, to appreciate the contribution of the seasonal component to the value of the interconnector, we look at different scenarios where we assume that for future dates the seasonal component is as in Figure 4.1, and for comparative purposes we also assume that the seasonal component is $f(T) = 0$ for all T. To assume that the seasonal trend is zero is an extreme case because the markets that we are considering have their idiosyncrasies and this makes it reasonable to expect predictable patterns in the average price differentials between them.

Liquidity constraints. As discussed above, it does not seem plausible to exploit large price differentials due to liquidity reasons in the two markets. We cap the maximum price differentials that can be profited from at different levels: $M \in \{10, 20, 30, 40, 50, \infty\}$ Euros/MWh, where we allow $M = \infty$ to include the hypothetical case where there are no liquidity constraints in the day-ahead market.In all examples we assume that the transmission costs from A to B, and from B to A, for both peak and off-peak times, are $K = 5$ Euros/MWh, which seems a plausible figure for the interconnection costs according to some market participants. Nevertheless, these costs could vary across different markets and the value of the interconnector will be affected by changes in K: the higher is K the lower the value of the interconnector.

Jumps and extrinsic value. Both the volatility of the OU component of the spread model and the jumps increase the value of the interconnector. We can isolate the contribution of the jumps to the value of the interconnector in the following way. Estimate the model parameters and value the interconnector with the jumps in the spread and then compare it to the valuation obtained if we "switch off" the jump factor, by setting the jump intensities of the positive and negative jumps to zero.

We address the three points discussed above and report the values of the interconnector in Tables 4.5 and 4.6. In the tables the values of the one year-lease are broken into the four options available to the manager of the lease: transmit electricity from A to B and from B to A for both on-peak and off-peak segments of the day. Note that these values are for the use of the interconnector during the 365 days of the one-year lease. The total value of the lease is given by the sum of the four options.

Table 4.5 shows the value of a one-year interconnector lease for both peak and off-peak use. In the first column we show the different assumptions for the value of the liquidity cap M. The second and third columns show

Table 4.5. Value of one-year interconnector lease

The model for the spread, $S(T)$, is (4.11), (4.12), and (4.13). The parameters of the seasonal component $f(T)$ are given in Table 4.2; the parameter estimates of the OU, $X(T)$, are in Panel B of Table 4.4; the parameters of the jump component, $Y(T)$, are at the bottom of Panel B in Table 4.4 and in Panel B of Table 4.3. In columns 3 and 4 the intensity parameters, $\lambda^{\pm}_{\text{season}}$, of the positive and negative jumps are set to zero.

	Seasonality, OU, and Jumps $f(T)+X(T)+Y(T)$		Seasonality and OU $f(T)+X(T)$		Seasonality, OU, and Jumps $f(T)+X(T)+Y(T)$		Seasonality and OU $f(T)+X(T)$	
	Peak France and Germany				Off-Peak France and Germany			
M	Ger → Fr	Fr → Ger	Ger → Fr	Fr → Ger	Ger → Fr	Fr → Ger	Ger → Fr	Fr → Ger
10	601	251	572	209	737	459	728	397
20	1,136	467	1,002	337	1,697	1,023	1,605	805
30	1,312	554	1,074	355	2,177	1,316	1,960	939
40	1,398	605	1,081	357	2,416	1,488	2,077	975
50	1,457	641	1,082	357	2,550	1,604	2,110	984
∞	1,681	761	1,082	357	2,949	2,095	2,120	985
	Peak France and UK				Off-Peak France and UK			
M	UK → Fr	Fr → UK	UK → Fr	Fr → UK	UK → Fr	Fr → UK	UK → Fr	Fr → UK
10	616	661	580	662	89	1,333	41	1,382
20	1,472	1,568	1,339	1,540	187	3,354	62	3,461
30	1,960	2,058	1,717	1,975	243	4,472	64	4,565
40	2,229	2,304	1,880	2,159	282	4,969	64	5,004
50	2,382	2,430	1,940	2,2256	310	5,174	64	5,143
∞	2,850	2,725	1,967	2,255	401	5,441	64	5,189
	Peak Nord Pool and Germany				Off-Peak Nord Pool and Germany			
M	Ger → NP	NP → Ger	Ger → NP	NP → Ger	Ger → NP	NP → Ger	Ger → NP	NP → Ger
10	66	1,512	61	1,508	432	829	403	815
20	135	4,226	120	4,199	972	1,997	864	1,915
30	165	6,391	140	6,313	1,246	2,651	1,052	2,465
40	178	7,935	146	7,779	1,392	2,993	1,121	2,697
50	186	8,920	147	8,671	1,478	3,177	1,143	2,784
∞	206	10,302	148	9,510	1,762	3,628	1,153	2,826

Table 4.5 *(continued)*

	Seasonality, OU, and Jumps $f(T)+X(T)+Y(T)$		Seasonality and OU $f(T)+X(T)$		Seasonality, OU, and Jumps $f(T)+X(T)+Y(T)$		Seasonality and OU $f(T)+X(T)$	
	Peak Germany and Netherlands				Off-Peak Germany and Netherlands			
M	Ne → Ger	Ger → Ne	Ne → Ger	Ger → Ne	Ne → Ger	Ger → Ne	Ne → Ger	Ger → Ne
10	816	848	860	788	881	752	858	771
20	2,377	2,475	2,491	2,279	2,540	2,156	2,465	2,210
30	3,842	4,011	4,006	3,659	4,062	3,432	3,932	3,515
40	5,215	5,459	5,407	4,932	5,455	4,585	5,265	4,692
50	6,498	6,824	6,699	6,104	6,720	5,624	6,469	5,749
∞	22,461	27,929	19,424	17,788	15,895	12,564	14,623	12,551
	Peak Netherlands and UK				Off-Peak Netherlands and UK			
M	UK → Ne	Ne → UK	UK → Ne	Ne → UK	UK → Ne	Ne → UK	UK → Ne	Ne → UK
10	390	971	347	993	18	1,586	14	1,582
20	939	2,438	803	2,471	31	4,364	21	4,320
30	1,283	3,313	1,054	3,321	37	6,351	22	6,214
40	1,501	3,770	1,187	3,732	39	7,506	22	7,239
50	1,641	3,996	1,254	3,909	41	8,074	22	7,676
∞	2,112	4,359	1,308	4,033	44	8,606	22	7,892

values of the flow from one market to the other during peak time when the model includes the seasonal trend $f(T)$, the OU Gaussian shocks $X(T)$, and the jumps $Y(T)$. For example, if $M = 10$ Euros/MWh, the value of the 365 options to send 1 MWh of peak electricity from Germany to France (France to Germany) during peak times is 601 Euros (251 Euros), and if the cap is $M = 50$ the 365 options are worth 1,457 Euros (641 Euros). In the same table, columns 4 and 5, show the value of the interconnector for peak time if the jump intensities are set to zero. In this case, if $M = 10$ Euros/MWh, the 365 options to send peak electricity from Germany to France (France to Germany) is 572 Euros (209 Euros), or if the cap is $M = 50$ Euros/MWh the value of the options is 1,082 Euros (357 Euros).[15] Hence, if we use this example as a proxy for the value added by the jumps, then the difference between columns 2 and 4 (3 and 5) indicates how much value can be extracted from using the interconnector when there are jumps in the spread between Germany and France during peak hours. Columns 6 through 9 can be interpreted in the same way, but they refer to electricity flows during off-peak hours.

From Table 4.5 we see that the effect of the liquidity cap is different across the markets we study. For example, if the cap between Germany and the Netherlands is reduced from $M = \infty$ to $M = 50$ Euros/MWh, the value of the interconnector decreases by almost 75%. If we draw the same comparison in the UK–Netherlands market, the value of the interconnector only decreases by 8%. These different effects of the liquidity cap are due to the particular characteristics of the spread in each market: seasonal component, volatility of the OU process, jump intensities and jump sizes. For example, the cap has an important effect on the markets where the spread undergoes frequent and large jumps which is the case for Germany–Netherlands. And in general, depending on the depth of the market, the results of Table 4.5 show that the jumps in the spread can account for between 1% and 40% of the total value of the interconnector.

Moreover, Table 4.5 shows that the peak and off-peak value of interconnection can also be different even within the same market, hence there are markets where most of the value of the interconnector is derived from flows in one direction and for a particular segment of the day. For instance, most of the value of the interconnection between the Netherlands and the United Kingdom is provided by off-peak hours, while most of the value between Germany and Nord Pool is during peak hours.

In Table 4.6 we investigate the case when the seasonal trend is set to zero

[15]These values are calculated employing equation (4.4), where location A is France and location B is Germany.

for all T. The table gives an indication of what happens to the value of the interconnector if it is assumed that for future dates the parameters of the OU and jump component are the same, but that the deterministic seasonal trend of the spread between the locations is zero. By comparing these values to those of Table 4.5, we can see that the seasonal trend adds considerable value to the interconnector, especially for cases with high liquidity cap M. For example, if the spread is modeled with $f(T) + X(T) + Y(T)$, then the value of an interconnector between France and Germany is 6,252 Euros ($M = 50$ Euros/MWh), but if we assume that the seasonal function is set to zero, $f(T) = 0$, then the value drops to 5,904 Euros.[16] Moreover, Table 4.6 also shows that the cases in Table 4.5 where the interconnector was mostly a uni-directional flow are mainly due to the seasonal component.

Finally, based on the statistics and estimates in Tables 4.1-4.4, we provide some rules of thumb that help to interpret and provide a qualitative summary of the results in Tables 4.5 and 4.6.

First, as in financial options, high volatilities in the underlying spread means higher interconnector values. This feature is clearly exhibited by the peak-hour interconnections in Germany-Netherlands, Netherlands-UK, and Germany-Nordpool, where the standard deviations of the spread of the peak-hours are the largest and so are their interconnector values (see summary statistics in Table 4.1). As discussed above, the variance of the spread process depends on four elements: the variance of the diffusion process, the size and arrival intensity of jumps, the mean-reversion rate of the diffusion, and the mean reversion rate of the jumps. Each one of these elements affects the value of the interconnector.

Similar to the effect of volatility of the underlying asset of financial options, the higher the volatility of the diffusion part of the spread, the higher is the value of the interconnector. By inspecting Table 4.6 (columns 4 and 5 for peak hours, and 8 and 9 for off-peak hours) where we turn off the effect of the seasonal trend and the jumps in the spread, we can see how the diffusion component of the spread model affects the value of the interconnector. For example, if we look at the peak-hour and the off-peak-hour spreads of Germany-Nordpool we see that they have similar mean-reversion rates, but the volatility of the diffusion component of the peak spread is slightly higher than that of the off-peak spread. Thus, as

[16]These figures are obtained from adding up the values of the peak and off-peak of the flows between Germany and France. Note that the lessee owns the four options: Germany to France, France to Germany during peak time as well as off-peak time.

Table 4.6. Value of one-year interconnector lease without including the seasonal component

The model for the spread, $S(T)$, is (4.11), (4.12), and (4.13). The parameters of the seasonal component $f(T)$ are given in Table 4.2; the parameter estimates of the OU, $X(T)$, are in Panel B of Table 4.4; and we set all intensities λ of Table 4.3 to zero. Although the estimation of the parameters is performed including the seasonal component $f(T)$ we value the one-year lease without including the seasonal component $f(T)$. Not including the predictable component $f(T)$ allows us to quantify how much of the value of the interconnector is derived from the deterministic seasonal level by comparing these results with those of Table 4.5.

	OU and Jumps $X(T)+Y(T)$		OU $X(T)$		OU and Jumps $X(T)+Y(T)$		OU $X(T)$	
	Peak France and Germany				Off-Peak France and Germany			
M	Ger → Fr	Fr → Ger	Ger → Fr	Fr → Ger	Ger → Fr	Fr → Ger	Ger → Fr	Fr → Ger
10	397	386	352	352	579	596	549	549
20	735	703	579	579	1,294	1,347	1,157	1,157
30	862	811	611	611	1,642	1,729	1,376	1,376
40	935	869	614	614	1,823	1,941	1,441	1,441
50	987	909	614	614	1,932	2,076	1,458	1,458
∞	1,194	1,039	614	614	2,290	2,613	1,463	1,463
	Peak France and UK				Off-Peak France and UK			
M	UK → Fr	Fr → UK	UK → Fr	Fr → UK	UK → Fr	Fr → UK	UK → Fr	Fr → UK
10	649	615	614	614	522	495	481	481
20	1,542	1,443	1,411	1,411	1,063	993	916	916
30	2,039	1,885	1,798	1,798	1,267	1,170	1,024	1,024
40	2,306	2,108	1,959	1,959	1,360	1,246	1,044	1,044
50	2,456	2,223	2,017	2,017	1,415	1,289	1,047	1,047
∞	2,921	2,506	2,041	2,041	1,569	1,408	1,048	1,048
	Peak Nord Pool and Germany				Off-Peak Nord Pool and Germany			
M	Ger → NP	NP → Ger	Ger → NP	NP → Ger	Ger → NP	NP → Ger	Ger → NP	NP → Ger
10	594	663	618	618	608	625	593	593
20	1,379	1,572	1,429	1,429	1,405	1,454	1,328	1,328
30	1,777	2,071	1,832	1,832	1,819	1,893	1,657	1,657
40	1,957	2,330	2,005	2,005	2,030	2,124	1,785	1,785
50	2,034	2,465	2,071	2,071	2,147	2,255	1,829	1,829
∞	2,111	2,765	2,102	2,102	2,478	2,633	1,849	1,849

Table 4.6 *(continued)*

	OU and Jumps $X(T)+Y(T)$		OU $X(T)$		OU and Jumps $X(T)+Y(T)$		OU $X(T)$	
	Peak Germany and Netherlands				Off-Peak Germany and Netherlands			
M	Ne → Ger	Ger → Ne	Ne → Ger	Ger → Ne	Ne → Ger	Ger → Ne	Ne → Ger	Ger → Ne
10	786	878	824	824	840	793	814	814
20	2,287	2,563	2,384	2,384	2,416	2,277	2,337	2,337
30	3,694	4,154	3,830	3,830	3,859	3,630	3,722	3,722
40	5,011	5,655	5,165	5,165	5,173	4,857	4,975	4,975
50	6,242	7,069	6,396	6,396	6,365	5,965	6,105	6,105
∞	21,622	28,738	18,575	18,575	14,800	13,544	13,559	13,559
	Peak Netherlands and UK				Off-Peak Netherlands and UK			
M	UK → Ne	Ne → UK	UK → Ne	Ne → UK	UK → Ne	Ne → UK	UK → Ne	Ne → UK
10	641	609	610	610	473	578	507	507
20	1,520	1,427	1,403	1,403	944	1,219	1,006	1,006
30	2,024	1,875	1,809	1,809	1,088	1,475	1,151	1,151
40	2,316	2,119	2,006	2,006	1,128	1,583	1,185	1,185
50	2,495	2,255	2,101	2,101	1,141	1,637	1,191	1,191
∞	3,042	2,528	2,178	2,178	1,153	1,727	1,193	1,193

expected, the interconnector values for peak hours are higher than those for off-peak hours.

The largest values of the interconnector correspond to markets where the size and frequency of jumps is significantly large (e.g. Germany-Netherlands peak hours in Table 4.5). The effect of the jump component depends on the depth of the market; increases in the liquidity cap M imply significant increases in the value of the interconnectors.

At the same time, for similar levels of variance in the diffusion process of the spread, a larger rate of mean reversion of the diffusion component decreases the value of the interconnector. An example of this effect can be found in the results for the France-Germany interconnector values when the jump component is "switched off" (see Table 4.6, columns 4 and 5 for peak hours, and 8 and 9 for off-peak hours). There we observe that the off-peak interconnector values are larger than the corresponding peak interconnector values while the diffusion volatilities of peak and off-peak spreads are similar. Thus, this difference in the option values can be attributed mainly to the difference in the speed of mean reversion between the diffusion processes of the peak and off-peak spreads.

If we take into account the jump component, we also observe that, when the arrival intensities and jump sizes are similar, the speeds of mean reversion of the jump and diffusive component, become important drivers of the interconnector value. Thus, spreads with higher mean reversion rates of the jump processes have the lowest interconnector value.

4.7.1 No-arbitrage bounds

The values in Tables 4.5 and 4.6 do not take into account the arbitrage bounds that forward or futures prices could impose on the valuation of the interconnector. In this subsection we use the prices shown in Table 4.5 for the benchmark model $S(T) = f(T) + X(T) + Y(T)$ in columns 2, 3 (peak) and columns 6, 7 (off-peak) as a reference. For a fixed liquidity cap M, the no-arbitrage bounds require that the sum of the values in columns 2 and 3 obey the peak electricity bounds (4.9) and (4.10). Similarly, for a given cap M the sum of values in columns 6 and 7 must obey the no-arbitrage bounds for off-peak hours.

To verify whether the prices reported in the valuation tables are arbitrage-free, we look at a particular example. Recall that the values reported in the tables are for a one-year lease between January 1 2010 and December 31 2010 and that these values were calculated employing data that ended

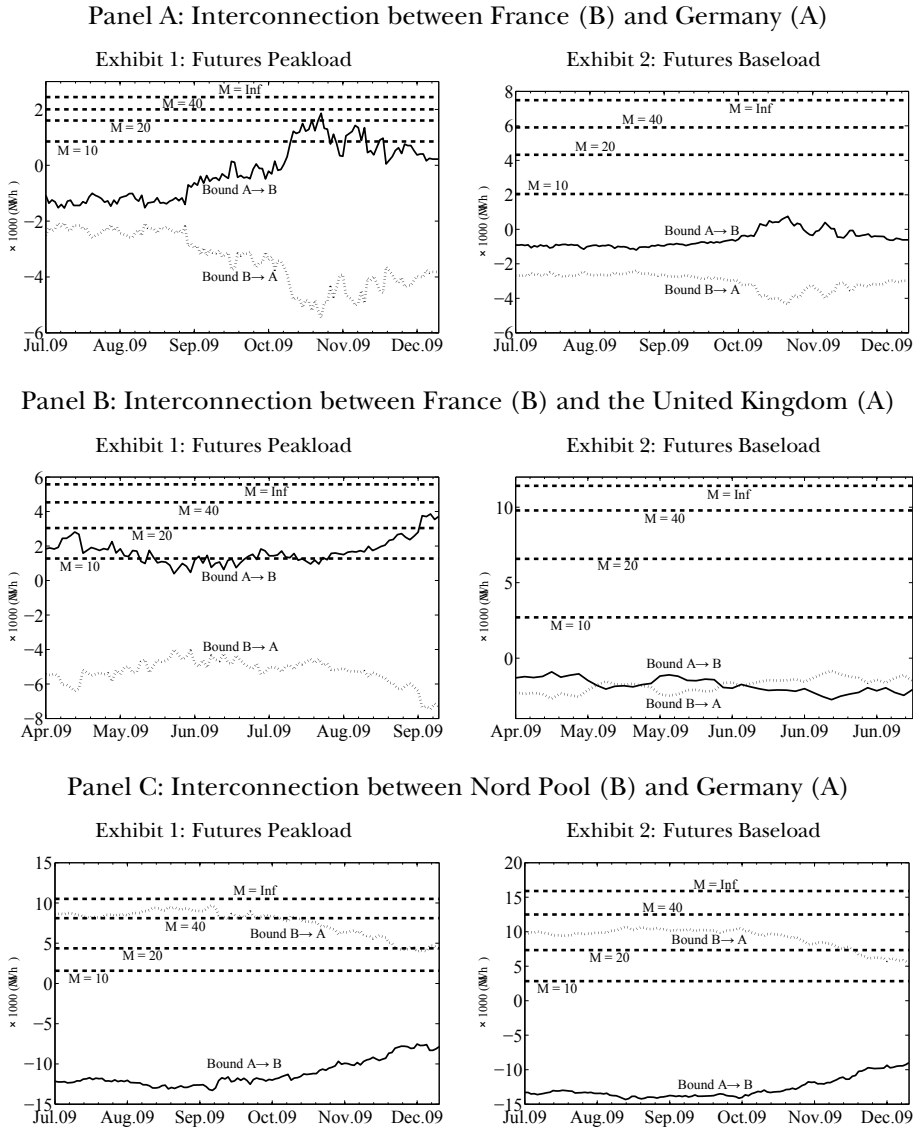

Figure 4.3. Empirical no-arbitrage bounds

Dashed, straight lines show the corresponding interconnector value of Table 4.5 for different liquidity constraints $M = 10, 20, 40$ and ∞. Figure also shows the bounds (Eur/MWh) computed from equations (4.9) and (4.10) for peak hours and the respective ones for off-peak hours. The no-arbitrage bounds resulting from buying a forward contract in location B, and shorting a forward contract for location A (bound A→B) are depicted by a solid line. Similarly, the dotted line represents the bound resulting from being long a forward contract in location A, and short a forward in location B (bound B→A).

in June 2009 (below we show in detail how the bound for peak time on October 29 2009 between Germany and France is calculated). The no-arbitrage bounds will depend on the market data on the day the calculation is performed; here it can be any day between July 1 2009 and December 31 2009. Figure 4.3 shows the bounds for every day during this period for France and Germany, France and UK, and Nord Pool and Germany. We can observe that the bounds exhibit considerable variation over time. These pronounced changes in the bounds are a reflection of changes in futures prices due to changes in: market expectations, fuel prices, changes in risk-premia, weather predictions, etc.

For example, the no-arbitrage bound for peak electricity between France and Germany on October 29 2009 is calculated in the following way. Assume that $M = 20$, and the price for a one-year lease of 1 MWh capacity, for a one-hour slot during the peak time between Germany and France, is 1,603 Euros (1,136 Euros for transmission from Germany to France plus 467 Euros for transmission from France to Germany; see Table 4.5). On October 29 2009, yearly peak-load futures (delivering electricity during peak time throughout 2010) are trading at 77.63 Euros/MWh in France and 68.15 Euros/MWh in Germany. Now, consider the following strategy: 1) Purchase the yearly peak-load forward in Germany and sell a yearly peak-load forward in France; 2) Purchase interconnector capacity for 2010, during peak time at 1,603 Euros (4.40 Euros/MWh during 365 days); 3) Every day during 2010, transmit 1 MWh from Germany to France and pay transmission costs of 5 Euros/MWh. Following equation (4.9), the no-arbitrage lower bound is 1,611 Euros, and the net present value of this arbitrage strategy is 8 Euros (i.e. the difference between the no-arbitrage bound and the value of the interconnector capacity).[17] Therefore, the valuation in Table 4.5 does not satisfy the no-arbitrage bound and if the lessor is selling capacity on October 29 2009, he should increase the price from 1,603 Euros to at least 1,611. However, if the same arbitrage strategy is considered on October 30 2009, the non-arbitrage bound is equal to 1,236 Euros, which is below the value charged by the lessor, and there are no opportunities to arbitrage the price. Exhibit 1 of Panel A in Figure 4.3 illustrates this example.

[17]That is, $\sum_{t=1}^{365} \mathrm{e}^{-rt}$ (77.63 - 68.15 - 5) = 1,611 Euros/MWh; the risk-free rate employed in the calculations is 3%. Note that this profit is for 1 MWh but could be much more if we consider that an interconnector may have a capacity of 1,000 MWh (or more) and that there are 12 peak hourly slots every day. In this case the total profit is 96,000 Euros.

4.8 Conclusions

In this chapter we show how to value an electricity interconnector as an asset that gives the owner the optionality to manage electricity flows between two markets. In financial terms, the value of the interconnector is the same as a strip of real options written on the spread between the power prices of two markets. We model the spread prices based on a: seasonal trend, mean-reverting Gaussian process, and mean-reverting jump process.

As a first contribution, we express the value of these real options in closed-form in the presence of mean-reverting jumps processes. We also propose a methodology to detect jumps in the spread that addresses the possible miss-classification of mean reversion as jumps. We estimate the parameters of the spread model and find that the introduction of jumps in the model delivers gains in the in-sample performance of between 20% and 48% with respect to a misspecified or "naive" model in which jumps are not included.

We value a hypothetical one-year lease of the interconnector between five pairs of European neighboring markets. The total value of the lease is the sum of the premia of 1,460 (4 times 365) real options on the spread: 365 options to transmit electricity from market A to B during on-peak hours; 365 to transmit electricity from A to B during off-peak hours; and the same number for transmitting both on- and off-peak power from market B to A. We show valuations under different assumptions about the seasonal component of the spread and different liquidity caps, which proxy for the depth of the interconnected power markets. Finally, we provide some rules of thumb to interpret the different interconnector values.

Although we cast the problem in terms of real options, where the statistical distribution of the spread and the risk-adjusted discount rate are key ingredients in the valuation, we also derive no-arbitrage lower bounds for the value of the interconnector in terms of electricity futures contracts. We show that most of the time these bounds are satisfied, but there are days where the value of the interconnector is given by the no-arbitrage bound instead of the price delivered by the sum of the prices of real options.

We find that the seasonal component is an important factor that determines the direction of the interconnector value. We also show that the variance of the diffusion process, the size of the jumps, and the mean-reversion rates of the diffusion and jump processes are key elements to determine the final value of the interconnector. Some of our valuation findings indicate that, depending on the depth of the market, the jumps in the spread can

account for between 1% and 40% of the total value of the interconnector. The presence of a liquidity constraint reduces the value of interconnectors specially for those interconnected markets where the jump component plays a key role in the variance of the spread price. The two markets where an interconnector would be most (least) valuable is between Germany and the Netherlands (between France and Germany). The markets where off-peak transmission between the two countries is more valuable than transmission during the peak times are: France and Germany, France and UK, and the Netherlands and UK.

5

Mean-reversion rate and risk premium in commodity markets

TRYING TO UNDERSTAND THE PRICE BEHAVIOR of commodities has a long tradition in the finance literature and is a long standing issue for stakeholders in commodity markets. On the one hand, there are market participants with exposure to spot price risks because they produce or consume the commodity. On the other hand, there are those that have no need to purchase or sell the commodity, but enter the market for speculative purposes. Either way, both types need to understand not only the behavior of spot prices but also the dynamics of the financial instruments written on the commodities so that decisions about bearing spot price risk, hedging, and speculation can be made.

From a reduced-form modeling perspective there are two possible ways to model price behavior. One way is first to build a model for commodity prices that tries to capture the main features of the price dynamics under both the data generating measure and risk-adjusted measure. The alternative way is to specify a reduced-form model under the risk-adjusted measure and place less importance on the dynamics of the commodity under the data generating measure. This second approach, although desirable in some cases, is built at the expense of not capturing some of the characteristics exhibited by price dynamics of the commodity under the data generating measure which in some cases, such as in energy commodities, might be an undesirable feature.

Our departure point in this chapter is that an important proportion of market participants are exposed to spot price commodity risk and it is their needs to hedge their positions the key factor which brings them to market to trade derivatives instruments to manage their exposures. Therefore,

understanding the dynamics of commodities under the data generating measure is as important as understanding the dynamics of prices under the risk-adjusted measure. The main questions we set out to answer here are: how are the data generating and risk-adjusted measures related? How can we reconcile the behavior of the physical dynamics of spot prices with those of the different forwards with different expiries?

To answer this question we first need to understand: what are the key elements that market participants price according to their risk preferences? What are the main risks that different stakeholder wish to offload? What happens to the risks that are being managed across different time horizons? What are futures contracts insurance for? Although our discussion could be applied to a wide variety of commodities, especially those whose prices tend to show a degree of mean reversion, we focus on two energy commodities: gas and electricity.

In general, establishing the link between the data generating measure and the risk-neutral measure in asset pricing is a difficult task because of market incompleteness. In energy markets in particular, the connection between these two measures is less well understood and has been overlooked in most cases, especially in electricity. So far, most of the reduced-form models for gas and electricity lack either a more realistic representation of prices under the data generating measure, or a better specification of the risk-adjusted measure to reconcile the dynamics of derivative instruments, for instance futures or forward contracts across different maturities.

This chapter contributes to the literature on the pricing of risk in commodities by proposing a parsimonious reduced-form model that can capture the main characteristics of commodity prices under the data generating measure and show that there is a family of risk-adjusted measures capable of capturing the fact that market participants may overstate (understate) the probability of occurrence of undesirable (desirable) events.

In particular we show that participants in energy markets price financial instruments under the risk-adjusted measure by modifying how long deviations from the seasonal component may last. In the most general version of our model there are three factors out of which two are mean reverting: one factor is an Ornstein-Uhlenbeck (OU) driven by Brownian motion and the other factor is a mean reverting jump process with positive and negative jumps.

Until now, all reduced-form models that specify jumps in prices under the data generating measure assume that under the risk-adjusted measure the jump component has all or most of the following characteristics: a) jumps

are non-systematic or that the market-price of jump risk is zero; b) jumps have the same arrival structure under both measures; c) the distribution of jump sizes is the same under both measures; and d) the speed at which jumps mean revert is the same under both the data generating and risk-adjusted measures.

Assumptions a) to d) are at odds with the evidence observed in gas and power markets because forward contracts are in most cases bought (resp. sold) by consumers (resp. producers) of the commodity as insurance against large upward (resp. downward) price deviations that would have an adverse effect on their profits. For instance, assuming that jumps are non-systematic implies that in the cross section of futures prices the presence of jumps does not affect futures prices.

Assuming that spot prices mean revert at the same speed under both measures makes it difficult to reconcile the spot and forwards model dynamics with observed market prices. The family of risk-adjusted measures that we propose allow for the mean reversion of the jump component of spot prices to be different between the two measures.

In the empirical part, we estimate our model using the Bayesian inference for two types of energy commodities, natural gas and power. Specifically, we implement a Markov Chain Monte Carlo (MCMC) estimation scheme, which accounts for parameter uncertainty. Our results suggest that the degree of mean reversion under the physical and the risk-adjusted measures differ. Under the Q measure, the estimates of the speed of mean-reversion of the Gaussian factor decrease for all models. On the contrary, the estimates of the mean-reversion rate corresponding to the jump factor are much higher under Q than under the physical measure P.

The rest of the chapter is organized as follows. Section 5.1 relates the chapter to previous literature of commodity modeling. Section 5.2 describes the arithmetic model and presents the new change of measure that we propose. Section 5.3 summarize the inference methodology and the MCMC estimation. Section 5.4 presents the data and develops the empirical application. Finally, in Section 5.5 we conclude.

5.1 Background

In this section we review some of the models that have been proposed in the commodities literature. The common characteristic shared by most commodities is mean reversion in spot prices. Reduced-form models for

storable commodities have been around for a long time. Gibson and Schwartz (1990) propose a two-factor model where spot prices follow a geometric Brownian motion and the stochastic convenience yield follows an OU mean reverting process under the data generating measure. They propose a risk-adjusted measure which results from introducing a market-price of convenience yield risk in the form of a linear shift in the distribution of the convenience yield under the data generating measure. In their model the mean reversion of spot prices under both the data generating and risk-adjusted measure is induced by the mean reversion in the convenience yield. The model is applied to oil spot and forward prices. This model is extended in Schwartz (1997) and applied to oil, gold an copper. Miltersen and Schwartz (1998) allow for both stochastic convenience yield and stochastic interest rates and Hilliard and Reis (1998) further extend the model to include jumps in the spot price process. Another common feature to all these models is that when one of the factors of the model is mean reverting then the speed of mean reversion will be the same under both the data generating and risk-adjusted measure.

Furthermore, Schwartz and Smith (2000) propose a two-factor model for oil prices In this model one of the factors is an OU process where the under the risk-adjusted measure is obtained by introducing a state dependent market price of risk which allows for the mean reversion speed under the pricing measure to be slower than under the data generating measure.

Casassus and Collin-Dufresne (2005) propose a three-factor model of spot prices, convenience yields and interest rates. The factor dynamics are driven by OU Brownian motion processes. The connection between the data generating measure and the risk-adjusted measure is introduced via a state dependent market price of risk for each factor. The immediate implication is that under the data generating measure the speed of mean reversion of spot prices, convenience yields, and interest rates can be different from the speed of mean reversion under the risk-adjusted measure. They estimate the model parameters to futures prices of: crude oil, copper, gold, and silver, and show that risk-premia are varying and negatively correlated with the spot price. One of their findings is that in the four commodities they study the speed of mean reversion of spot prices is higher under the data generating measure than under the risk-adjusted measure. Furthermore, the authors present an extension to their Gaussian model to include jumps in the spot prices. They assume that jump-size risk is not priced and that jump intensities are the same under both the data generating and risk-adjusted measure which implies that forward prices are not affected by the inclusion of jumps.

Furthermore, electricity is the only commodity that is either impossible or too uneconomical to store at a relevant scale. The literature proposes to model wholesale electricity prices by employing reduced-form models or equilibrium models. Examples of the reduced form models include those of Lucía and Schwartz (2002) and Cartea and Figueroa (2005). Alternatives to the reduced-form models are the so-called equilibrium and hybrid models that, given the particular characteristics of electricity, explain price formation based on state variables that are mainly associated to supply and demand, see for example Bessembinder and Lemmon (2002), Pirrong and Jermakyan (2008), and Benth, Cartea, and Kiesel (2008). In the next sections, we propose a reduced-form, arithmetic model for commodity spot prices; and a new, more flexible change of measure, for which pricing and calibration of basic building blocks such as futures contracts can be performed analytically.

5.2 An arithmetic jump-diffusion model for the spot

Let $X(t)$ be the vector of state variables $(X_1(t), X_2(t), X_3(t))'$. The evolution of the state variables $X(t)$ under the real probability measure P is given by

$$\mathrm{d}X(t) = -A_P X(t)\mathrm{d}t + C_P\,\mathrm{d}L(t)\,, \tag{5.1}$$

where $\mathrm{d}L(t) = (\mathrm{d}L_1(t), \mathrm{d}L_2(t), \mathrm{d}L_3(t))'$. $L_1(t)$ and $L_2(t)$ are independent Brownian motions and $L_3(t)$ is an independent compound Poisson process with intensity parameter λ and jump sizes distributed as $\mathrm{N}(\mu_Z, \sigma_Z)$. Here, A_P is a 3×3 diagonal matrix that reflects the mean-reversion rates of the state variables under the physical measure P,

$$A_P = \mathrm{diag}(\alpha_1, 0, \alpha_3)\,. \tag{5.2}$$

Note that we are considering the case where $\alpha_2 = 0$, that is $X_2(t)$ is an arithmetic Brownian motion while $X_1(t)$ is a Gaussian OU process. The 3×3 lower triangular matrix C_P defines the dependence between state variables and is given by

$$C_P = \begin{pmatrix} \Sigma & 0 \\ 0 & 1 \end{pmatrix}, \tag{5.3}$$

where Σ is the Cholesky factorization for the 2×2 variance-covariance matrix under P of the Gaussian state variables $X_1(t)$ and $X_2(t)$; that is

$$\Sigma = \begin{pmatrix} \sigma_1 & 0 \\ \sigma_2\rho_{12} & \sigma_2\sqrt{1-\rho_{12}^2} \end{pmatrix}. \tag{5.4}$$

Under the physical measure P, the spot price process $S(t)$ can be decomposed into a stochastic component defined by the state variables in $X(t)$ and a deterministic component $\mu(t)$.[1] That is:

$$S(t) = \mu(t) + \imath' X(t)\,, \tag{5.5}$$

where $\imath$ is a 3×1 vector of ones. In the empirical application, we will consider the following seasonal deterministic function $\mu(t) = \mu_0 + \mu_1 t + \mu_2 d_t^{\text{winter}} + \mu_3 d_t^{\text{spring}} + \mu_4 d_t^{\text{summer}}$, where $\mu_0, \ldots, \mu_4$ are constant parameters and d_t^{winter}, d_t^{spring}, and d_t^{summer} are deterministic dummy variables for winter, spring, and summer, correspondingly.

5.2.1 An alternative change of measure: Reversion rate can vary

We now consider the following change of measure Q:

$$\mathrm{d}L(t) = \mathrm{d}L^Q(t) + \Lambda(t)\mathrm{d}t \tag{5.6}$$

with

$$\Lambda(t) = \Phi_Q + C_P^{-1} B_Q X(t). \tag{5.7}$$

Here, $\mathrm{d}L^Q(t) = (\mathrm{d}L_1^Q(t), \mathrm{d}L_2^Q(t), \mathrm{d}L_3^Q(t))'$ and Φ_Q is defined as

$$\Phi_Q = (\theta_1,\, \theta_2, \phi_3'(\theta_3))'\,, \tag{5.8}$$

where $\phi_i'(\theta)$ is the derivative of the logarithm of the moment generating function of $L_i(t)$. B_Q is a 3×3 diagonal matrix of parameters:

$$B_Q = \mathrm{diag}(\beta_1, 0, \beta_3)\,, \tag{5.9}$$

where we are considering possible changes in the mean-reversion rate under Q for the mean-reverting processes $X_1(t)$ and $X_3(t)$. Then, under the Q-measure, the dynamics of state variable vector $X(t)$ is given by

$$\mathrm{d}X(t) = (C_P\Phi_Q - A_Q X(t))\mathrm{d}t + C_P \mathrm{d}L^Q(t) \tag{5.10}$$

where $A_Q = A_P - B_Q$.

To obtain the change of measure Q, we define for each component i of $X(t)$ the following process

$$Y_i(t,z) = \left(\mathrm{e}^{\theta_i z} + \frac{\beta_i}{\phi_i'(0)} X_i(t)\right)\,. \tag{5.11}$$

[1]Notice that the model is arithmetic and allows eventually for possible negative prices in the spot. A first specification of this type can be traced back to Ross (1997).

Note that, for the validity of this change of measure, we need to assume exponential integrability conditions for the Lévy measure of L_i, ℓ_i, that is,

$$\int_{-\infty}^{\infty} \mathrm{e}^{\theta_i z} \ell_i(\mathrm{d}z) < \infty. \tag{5.12}$$

The exponential integrability condition of the Lévy measure ensures the existence of moments of all orders, and makes the measure change valid in the case of $\beta_i = 0$. Furthermore, Nicolato and Venardos (2003, Theorem 3.1.) specifies a necessary condition for Y_i to give an equivalent measure change:

$$\int_0^T \int_{\mathbb{R}_+} (\sqrt{Y_i(s,x)} - 1)^2 \ell_i(\mathrm{d}z)\mathrm{d}s < \infty \text{ a.s.}. \tag{5.13}$$

Using the triangle inequality, and requiring that $\ell_i(\mathbb{R}_+) < \infty$, shows that condition (5.13) is satisfied:

$$\begin{aligned}\int_0^T (\sqrt{Y_i(s)} - 1)^2 \mathrm{d}s &\le c \int_0^T \int_0^\infty Y_i(s,z)\ell_i(\mathrm{d}z)\mathrm{d}s + T\ell_i(\mathbb{R}_+) \\ &\le c\Big(\int_0^T X_i(s)\mathrm{d}s\, \ell_i(\mathbb{R}_+) + T\int_0^\infty \mathrm{e}^{\theta_i z}\ell_i(\mathrm{d}z) + \ell_i(\mathbb{R}_+)\Big) \\ &< \infty\,,\end{aligned}$$

since $X_i(s)$ is a cadlag process and c is an appropriate constant value. Then, we have that Q is an equivalent measure, for which the compensator measure of L_i is given by

$$\ell_i^Q(\mathrm{d}t, \mathrm{d}z) = Y_i(t)\ell_i(\mathrm{d}z)\mathrm{d}t\,. \tag{5.14}$$

Specifically for the compound Poisson process $X_3(t)$, we can therefore write the dynamics with respect to Q as

$$\begin{aligned}\mathrm{d}X_3(t) &= -\alpha_3 X_3(t)\mathrm{d}t + \int_{-\infty}^{\infty} z\, N^Q(\mathrm{d}z, \mathrm{d}t) + \int_{-\infty}^{\infty} zY_3(t,z)\ell_3(\mathrm{d}z)\mathrm{d}t \\ &= \Big(-\alpha_3 X_3(t) + \int_{-\infty}^{\infty} z\mathrm{e}^{\theta_3 z}\ell_3(\mathrm{d}z) + \frac{\beta_3}{\phi_3'(0)}\int_{-\infty}^{\infty} z\ell_3(\mathrm{d}z)\Big)\mathrm{d}t + \mathrm{d}L_3^Q(t) \\ &= (\phi_3'(\theta_3) - (\alpha_3 - \beta_3)X_3(t))\mathrm{d}t + \mathrm{d}L_3^Q(t)\,,\end{aligned}$$

where N^Q is the compensated Poisson random measure associated to L_3; $\mathrm{d}L_3^Q(t)$ is a Q-martingale with the compensator measure of equation (5.14); and

$$\phi_3'(\theta_3) = \int_{-\infty}^{\infty} z\mathrm{e}^{\theta_3 z}\ell_3(\mathrm{d}z)\,,$$

which is the expectation of L_3 under P when $\theta_3 = 0$. When $L_i(t)$ is a Brownian motion, such as in $X_1(t)$ and $X_2(t)$, the above derivation is still

valid, since the measure change (5.6) works on each factor independently, but in this case we have $\phi_j'(\theta_j) = \theta_j$, for $j = 1, 2$.[2]

The effect of the stochastic term $X_i(t)$ in the measure change (5.14) can be seen as a complete shift by a *constant*. When $X_i(t)$ is low or for $\beta_i = 0$, we essentially have the usual transform rescaling, a re-weighting of the Lévy measure. But if, for example, the process X_i exhibits large shocks, we shift the whole compensator measure by a factor. In the case of X_3, this shift could be interpreted as if we rescale the jump intensity in the compound Poisson process. For instance, if $\theta_3 = 0$, we have under Q a compound Poisson process with a stochastic intensity $\lambda(1 + \beta_3 X_3(t)/\phi_i'(0))$, where λ is the intensity under P. That is, if this is a negative (positive) rescaling, we *lessen* (*intensify*) the compound Poisson process under Q.

5.2.2 The futures price and the risk premium

The futures price $f(t,T)$ at time t of a contract to deliver one unit of commodity at time $T > t$ is defined as the expected spot price under the risk-adjusted probability measure Q

$$f(t,T) = \mathbb{E}_t^Q[S(T)]\,, \quad t \in [0,T]. \tag{5.15}$$

For energy's futures contracts, instead of a single maturity time, every contract specifies a delivery period, which are typically a month, quarter, season, or even year. Hence, if $F(t,T_1,T_2)$ denotes the market price for an energy's futures contract with time T_1 until maturity and delivery period $[T_1,T_2]$, then

$$F(t,T_1,T_2) = \frac{1}{T_2 - T_1}\mathbb{E}_t^Q\Big[\int_{T_1}^{T_2} S(u)\mathrm{d}u\Big] \tag{5.16}$$

where $t < u$ and $T_1 \leq u \leq T_2$. Therefore, by definition, we have that $S(t) = f(t,t) = F(t,t,t+1)$.

Considering the dynamics of $X(t)$ under Q in equation (5.10) and that the Lévy measures ℓ_i^Q are Q-martingales, we compute the expectation in equation (5.16) and find the following expression for the futures price

$$\begin{aligned} F(t,T_1,T_2) = {} & \bar{\mu}(T_1,T_2) + \bar{\alpha}_{Q,1}(t,T_1,T_2)X_1(t) + \frac{\vartheta_1}{\alpha_{Q,1}}\left(1 - \bar{\alpha}_{Q,1}(t,T_1,T_2)\right) \\ & + X_2(t) + \widetilde{\vartheta}_2\bar{\tau}(t,T_1,T_2) + \bar{\alpha}_{Q,3}(t,T_1,T_2)X_3(t) \\ & + \frac{\phi'(\theta_3)}{\alpha_{Q,3}}\left(1 - \bar{\alpha}_{Q,3}(t,T_1,T_2)\right)\,, \end{aligned} \tag{5.17}$$

[2]Note that the Gaussian cumulant function is given by $\phi(\theta) = \theta^2/2$

where $\widetilde{\vartheta}_2 = \vartheta_1\rho_{12} + \vartheta_2\sqrt{1-\rho_{12}^2}$, $\vartheta_1 = \theta_1\sigma_1$, and $\vartheta_2 = \theta_2\sigma_2$. The functions $\bar{\mu}(T_1,T_2)$, $\bar{\alpha}_{Q,i}(t,T_1,T_2)$, and $\bar{\tau}(t,T_1,T_2)$ are respectively the average of $\mu(u)$, $\mathrm{e}^{-\alpha_{Q,i}(u-t)}$, and $(u-t)$ over the interval $[T_1,T_2]$, that is

$$\bar{\mu}(T_1,T_2) = \frac{1}{T_2-T_1}\int_{T_1}^{T_2}\mu(u)\,\mathrm{d}u\,, \tag{5.18}$$

$$\bar{\alpha}_{Q,i}(t,T_1,T_2) = \frac{\mathrm{e}^{-\alpha_{Q,i}(T_1-t)} - \mathrm{e}^{-\alpha_{Q,i}(T_2-t)}}{\alpha_{Q,i}(T_2-T_1)}\,,\ \text{and} \tag{5.19}$$

$$\bar{\tau}(t,T_1,T_2) = ((T_2-t)+(T_1-t))/2\,. \tag{5.20}$$

Furthermore, lets define the risk premium for Q as the difference between the futures price and the predicted spot price,

$$\Pi_Q(t,T_1,T_2) = F(t,T_1,T_2) - \frac{1}{T_2-T_1}\,\mathbb{E}_t^P\left[\int_{T_1}^{T_2} S(u)\,\mathrm{d}u\right]. \tag{5.21}$$

The theory of normal backwardation says that producers are willing to pay a premium for having their production hedged, implying that $\Pi_Q < 0$. In electricity, there is some empirical evidence for $\Pi_Q > 0$ in the short end, that is, for contracts close to maturity. Under our specification, we may observe a change in the sign of the risk premium, for example, from positive to negative along the forward curve, a change which is stochastically dependent on the price factor $X_i(t)$.

5.3 Econometric methodology

This section describes the estimation problem when both spot and futures prices are observed. Our implementation is based on an MCMC simulation that provides inference for unobserved state variables and model parameters given information under the probability measures P and Q. We follow here Eraker, Johannes, and Polson (2003), Eraker (2004), Jacquier, Johannes, and Polson (2007), Johannes and Polson (2009), Johannes and Polson (2010), and Polson and Stroud (2003) mainly.

Consider the observations of spot prices $\widetilde{S}_t$ and monthly futures prices $\widetilde{F}_{t,n}$ for maturities $T_{1,n}-t$, where $n = 1,\ldots,N$. For each discrete, integer time $t \in [0,L]$, we have the panel $Y_t = \{Y_{t,j}\}_{j=1}^{N+1} = [\widetilde{S}_t, \widetilde{F}_{t,1},\ldots,\widetilde{F}_{t,N}]$. That is, there are observations available for $N+1$ assets over a period $[0,L]$ obtaining a total of $N+1\times L$ data points. We assume that market prices $Y_{t,j}$ are observed with independent pricing errors $\varepsilon_{t,j} \sim \mathcal{N}(0,\sigma_{\varepsilon,j}^2)$,

$$Y_{t,j} = H(t,T_{1,j},T_{2,j},X_t,\Theta) + \varepsilon_{t,j}\,,\quad j = 1,\ldots,N+1\,, \tag{5.22}$$

where $H(t, T_{1,j}, T_{2,j}, X_t, \Theta)$ represents the theoretical value of spot and futures prices, $S(t)$ (for $j = 1$) and $F(t, T_{1,j}, T_{2,j})$ (for $j = 2, \ldots, N+1$); which, in our model specification, are determined by the vector of state variables X_t and a parameter vector Θ through the functions defined in equations (5.5) and (5.17), respectively. There are mainly two motivations for adding an additive pricing error: to consider the possibility that the model can be misspecified and that there can be measure errors related with noisy price observations.

5.3.1 Bayesian inference

The specification of the pricing errors allows us to describe the conditional likelihood of the set of observations $Y = \{Y_{t,j} : t = 1, \ldots, L;\ j = 1, \ldots, N+1\}$ as the function

$$p(Y|X, \Theta) \propto \prod_{t=1}^{L} \prod_{j=1}^{N+1} \psi(Y_{t,j}; H(t, T_{1,j}, T_{2,j}, X_t, \Theta), \sigma^2_{\varepsilon,j}) \,, \tag{5.23}$$

where $\psi(x; m, s^2)$ is the Gaussian density function with mean m and variance s^2 evaluated at x. The parameter vector Θ can be decomposed into the parameter vector under P and the parameter vector under the risk-adjusted probability measure Q, that is, $\Theta = \{\Theta^P, \Theta^Q\}$. Furthermore, the dynamics of the spot prices can be determined using the likelihood $p(S|X, \Theta^P)$, where the state variables X evolve according to the dynamics defined in equation (5.1) and $\Theta^P = \{\alpha_1, \alpha_2, \sigma_1, \sigma_2, \rho_{12}, \lambda, \mu_Z, \sigma_Z\}$. The parameter vector Θ^Q denotes the market price of risk parameters, $\Theta^Q = \{\theta_1, \theta_2, \theta_3, \beta_1, \beta_3\}$, which are used in the derivative pricing, but do not affect the dynamics under P of the state variable vector X.

Then, the inference problem consists of the computation of the joint posterior density of latent variables and parameters given by

$$p(X, \Theta^P, \Theta^Q|Y) \propto p(Y|X, \Theta^P, \Theta^Q) p(X|\Theta^P) p(\Theta^P) p(\Theta^Q) \,, \tag{5.24}$$

where $p(X|\Theta^P)$ denotes the density corresponding to the state variable dynamics, and $p(\Theta^P)$ and $p(\Theta^Q)$ denotes priors on the parameters under P and Q, respectively. Furthermore, the likelihood $p(Y|X, \Theta^P, \Theta^Q)$, described in equation (5.23), can be decomposed in two factors $p(S|X, \Theta^P)$ corresponding to the underlying spot price, and $p(F|S, X, \Theta^Q)$ corresponding to the panel of futures prices.

The joint posterior density $p(X, \Theta^P, \Theta^Q|Y)$ summarizes the sample information concerning the parameters and latent variables combining the

likelihood and the prior information. Unfortunately, this posterior density is an unknown, non-standard, and highly dimensional density function, and, therefore, difficult to sample directly.

5.3.2 MCMC implementation

The MCMC approach provides a method to sample parameters Θ^P and Θ^Q and latent variables X_t from their joint posterior density $p(X, \Theta^P, \Theta^Q|Y)$. We first employ a time discretization of the continuous time model to compute the likelihood $p(Y|X, \Theta^P, \Theta^Q)$ and the latent state distribution $p(X|\Theta^P)$, assuming that the time interval matches the observed frequency (one day). The discretization bias is small because we are using daily data.

The MCMC method consists in constructing a Markov chain that has as stationary distribution the joint posterior density. To handle the dimensionality problem and the presence of nonstandard conditional densities, we employ a hybrid Gibbs sampler. The Gibbs sampler allows to simulate iteratively, in sub-sets, all the variables of the joint posterior distribution, obtaining a sequence that converges to $p(Y|X, \Theta^P, \Theta^Q)$. Gibbs sampling makes use of the close-form derivation of conditional posterior densities for some sub-sets of parameters and latent variables. However, there are some elements of the set of values we want to estimate, $\{\Theta, X\}$, that do not have standard, closed form posterior densities. In this case, we implement a Metropolis algorithm, i.e. an accept-reject procedure, to draw from these random variables.

Thus, our MCMC simulation generates samples iteratively, for $g = 1, \ldots, G$, from the following set of conditional posteriors:

i) Sub-set i of parameters at iteration g, $\Theta_i^{(g)}$, from $p(\Theta_i|\Theta_{-i}^{(g-1)}, X^{(g-1)}, Y)$, where Θ_{-i} denotes the elements of the parameter vector except Θ_i.

ii) State variable j at time t, $X_{j,t}^{(g)}$, from $p(X_{j,t}|\Theta_i^{(g)}, X_{j,-t}^{(g-1)}, Y)$, where $X_{j,-t}$ denotes all the values of the state variable j in the sample interval $[0, L]$ except the value at t.

For $g = 0$, we initialize the recursive scheme using an appropriate set of starting values. The conditional posteriors of the parameters under P, Θ^P, the variance matrix of the pricing errors, Σ_ε, and the market price of risk parameters θ_1 and θ_2 are known in closed form and can be sampled directly using standard distributions. Note that we employ diffusive priors for the density specification $p(\Theta)$. In contrast, the conditionals for the

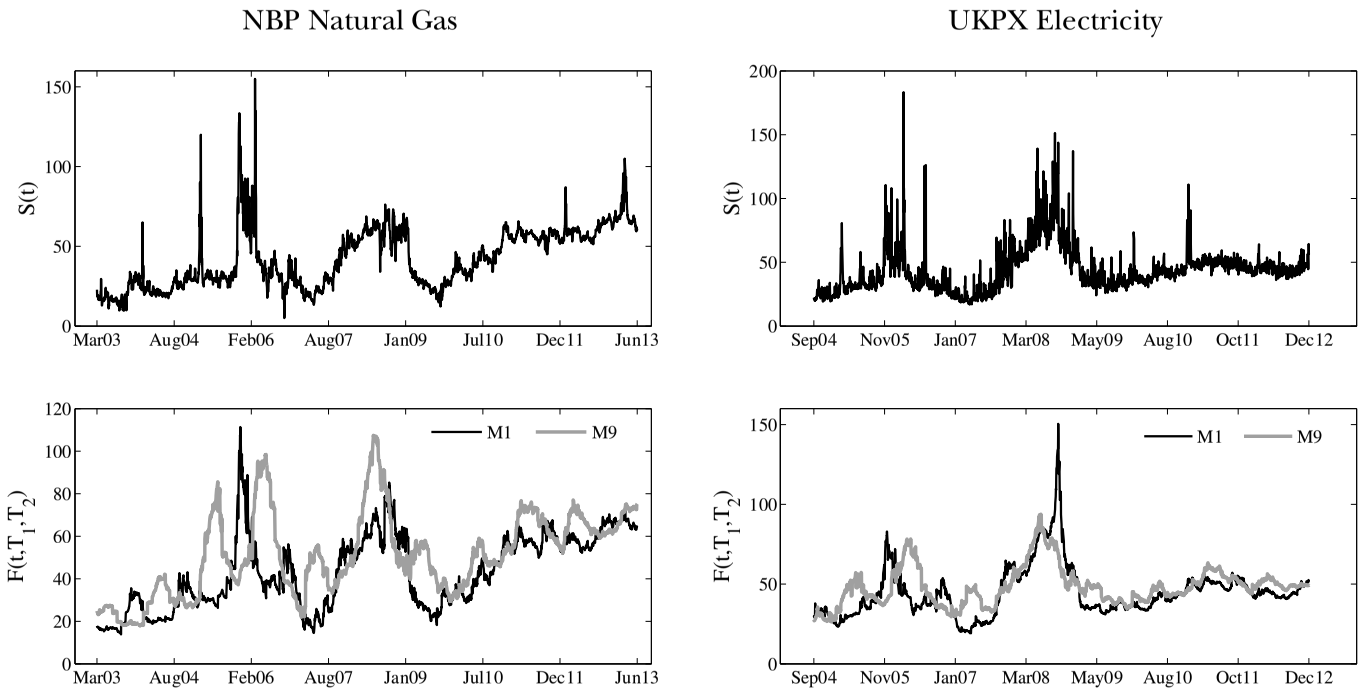

Figure 5.1. Spot and futures prices

The figure shows, in the first column, the series of spot prices ($S(t)$) and, in the second column, the 1-month and 9-month (M1 and M9) futures contracts ($F(t, T_1, T_2)$) on the NBP Natural Gas and UKPX Electricity. The samples range from March 13, 2003 to June 17, 2013 and September 14, 2004 to December 7, 2012, respectively. Natural gas prices are in GB pence per Therm, and electricity prices are in GB pounds per MWh.

mean-reversion rated under Q, α_1^Q and α_3^Q, and the market price of risk for jumps θ_3 are not standard due to the nonlinear form in which these parameters enter into the futures pricing function. We therefore use a fat-tailed random walk Metropolis algorithm to sample these parameters. For the state variables, for each iteration, $2L$ latent variables (jump times and sizes) have to be drawn for the mean-reverting jump diffusion $X_{3,t}$, and L variables for each of the two correlated Gaussian processes $X_{1,t}$ and $X_{2,t}$. The conditional posterior for the jump times is Bernoulli since the jump indicator is a binary random variable, can only take two values (0 or 1). Finally, conditional on the jump indicators, the model is a linear, Gaussian state-space model, and it is possible to use the Kalman filter to obtain a direct block draw of the L-dimensional state variables (X_1, X_2). The block sampling procedure is as follows: first, we run the usual Kalman filter algorithm (forward-filtering step), then we move backward to unwind the conditioning information (backward-sampling step).

5.4 Data and empirical application

We estimate the model for two types of energy commodities, natural gas and power, using the Bayesian inference described in the previous section. We first introduce the data sample, then we describe and discuss our results.

5.4.1 Description of the data

The empirical analysis of this chapter is based on a sample of spot (day ahead) and futures prices of natural gas and electricity. In particular, we use daily data of monthly futures contracts for physical delivery through the transfer of rights in respect of natural gas at the National Balancing Point (NBP) and electricity on a continuous baseload basis, i.e. 23:00 - 22:59 Monday - Sunday; both operated by National Grid, the transmission system operator in Great Britain and traded at the Intercontinental Exchange (ICE) in pence/therm and pounds/MWh, respectively. We consider contracts with maturities 1, 3, 6, and 9 months (labeled from M1 to M9), having a panel of 5 asset prices (4 futures and 1 spot prices) at each time period. Delivery is made equally each day throughout delivery period, in this case, one month. Our sample of natural gas prices ranges from March 13, 2003 to June 17, 2013; containing 2,592 trading days and 10,368 futures prices. The sample of electricity prices ranges from September 14, 2004 to December 7, 2012, that is, 2,107 trading days and 8,428 futures prices. Table 5.1 shows the summary

Table 5.1. Descriptive statistics for spot and futures prices

The table reports mean and standard deviation (S.D.) for daily observations of spot and futures contracts of NBP Natural Gas and UKPX Electricity from March 13, 2003 to June 17, 2013 and September 14, 2004 to December 7, 2012, respectively. Natural gas prices are in GB pence per Therm, electricity prices are in GB pounds per MWh, and maturities (Maturity = $T_1 - t$) are in days. The contract denominations (M1, M3, M6, and M9) specify the number of months to maturity. Backwardation is defined as the relative difference between the futures price and the spot price, i.e. Backwardation = $F(t, T_1, T_2)/S(t) - 1$. The two final rows show the auto-correlation coefficients (AC) corresponding to 1 and 22 lags, respectively.

	NBP Natural Gas					UKPX Electrcity				
	Sample: 13/03/2003 - 17/06/2013					Sample: 14/09/2004 - 7/12/2012				
	Spot	M1	M3	M6	M9	Spot	M1	M3	M6	M9
Mean Price	42.15	43.28	47.34	50.36	51.38	43.82	44.72	46.70	47.67	48.44
S.D.	18.57	17.49	18.99	20.21	19.37	17.70	16.07	14.99	14.04	12.03
Maturity	-	15.85	76.75	168.1	229.0	-	15.75	76.64	167.9	259.2
S.D.	-	8.715	8.741	8.770	8.757	-	8.762	8.783	8.823	8.803
Backwardation	-	0.061	0.201	0.315	0.341	-	0.054	0.123	0.165	0.190
S.D.	-	0.311	0.547	0.588	0.553	-	0.201	0.288	0.344	0.326
AC(1)	0.972	0.994	0.996	0.996	0.997	0.849	0.995	0.996	0.995	0.994
AC(22)	0.769	0.888	0.897	0.904	0.911	0.623	0.855	0.900	0.888	0.884

statistics for both commodities. Figure 5.1 exhibits the price of spot, M1, and M9 contracts on natural gal and electricity over their respective sample periods.

5.4.2 Empirical results

Given the samples of the posterior distributions for the parameter vector Θ and the state variables X_t, we can obtain straightforward the Monte Carlo estimate of the mean of parameters and latent variables, for example, the mean of parameter $\Theta_i \subset \Theta$ is $\mathbb{E}[\Theta_i|Y] \approx \frac{1}{G}\sum_{g=1}^{G}\Theta_i^{(g)}$. Our estimates take into account parameter uncertainty, when we estimate the mean of the posterior state-variable distribution, we are considering the fact that parameter estimates are random variables. In this section, we compute posterior estimates of the different parameters and state variables employed in our model specification using the NBP natural gas and UKPX electricity futures data described above. In this empirical application, we also compare the more general model with other nested specifications with less state variables.

Tables 5.2 and 5.3 reports the posterior means, posterior standard deviations (in parentheses), and the posterior 5 and 95 percentiles (in square brackets) of the different model parameters for the NBP natural gas and UKPX electricity, respectively. For each commodity we present the parameters governing the seasonal trend $(\mu_1, \ldots, \mu_4)$, the mean reversion under the physical measure P (α_1), the variance matrix of the Gaussian factors, $(\sigma_1$, σ_2, and $\rho_{12})$, the market price of risk parameters for the different factors $(\theta_1$ and $\theta_2)$, the mean-reversion rate under the risk-adjusted measure Q (α_1^Q). For the jump diffusion models, we also report the jump intensity (λ) and the mean and standard deviation of jump sizes (μ_Z and σ_Z), as well as, the mean-reversion of jumps under P and Q (α_3 and α_3^Q) and the market price of risk parameter for jumps (θ_3). Finally, for each model considered, we also present in Tables 5.2 and 5.3 the standard deviation diagonal matrix $(\sigma_{\varepsilon,1}, \ldots, \sigma_{\varepsilon,5})$ of the independent pricing error vector ε_t. Columns 1 and 2 reports the one-factor and two-factor Gaussian Models (OU model and OU-AB model, respectively). Columns 3 and 4 (OU-MRJ and OU-AB-MRJ models) shows the previous two Gaussian models plus a mean-reverting jump diffusion factor, which consists in a mean-reverting compound Poisson process with Gaussian jump sizes.

Furthermore, Figure 5.2 shows the estimated jump times for the OU-AB-MRJ model, and Figure 5.3 exhibits the inferred state-variable paths for this model and the 95% confidence intervals for these paths.

Table 5.2. Parameter estimates for NBP natural gas

The table reports posterior means, standard deviation (in parenthesis), and 95% confidence intervals (in square brackets) for the the model most general model described in Section 5.2, OU-AB-MRJD, and other nested models: OU is the arithmetic model with one mean-reverting Gaussian factor, OU-AB is the two-factor arithmetic model composed by a mean-reverting Gaussian process and an arithmetic Brownian process; and OU-MRJ is the OU model plus a mean-reverting jump diffusion. The estimates correspond to a unit of time defined to be one day. The estimation sample ranges from March 13, 2003 to June 17, 2013.

	OU	OU-AB	OU-MRJ	OU-AB-MRJ
μ_0	22.65 (2.695) [18.68, 27.58]	25.16 (1.882) [22.20, 28.05]	15.17 (1.520) [12.89, 17.80]	26.03 (1.381) [24.03, 28.66]
μ_1	3.086 (0.376) [2.527, 3.778]	3.487 (0.371) [3.002, 4.005]	3.528 (0.159) [3.220, 3.767]	3.650 (0.225) [3.279, 3.986]
μ_2	0.235 (1.182) [-1.692, 2.242]	0.057 (1.166) [-1.913, 1.931]	0.278 (0.627) [-0.753, 1.245]	0.312 (0.717) [-0.994, 1.351]
μ_3	0.178 (1.325) [-2.015, 2.332]	0.045 (1.409) [-2.500, 2.336]	-0.391 (0.708) [-1.568, 0.756]	-0.281 (0.832) [-1.681, 1.125]
μ_4	-1.437 (1.200) [-3.342, 0.653]	-1.254 (1.143) [-3.106, 0.612]	-1.515 (0.586) [-2.526, -0.541]	-1.361 (0.725) [-2.578, -0.150]
α_1	0.027 (0.006) [0.017, 0.035]	0.175 (0.059) [0.101, 0.2753]	0.0092 (0.0027) [0.0048, 0.0137]	0.720 (0.196) [0.420, 1.059]
α_3			1.435 (0.119) [1.244, 1.645]	1.532 (0.127) [1.344, 1.755]
σ_1	3.467 (0.089) [3.319, 3.617]	3.232 (0.334) [2.653, 3.772]	1.749 (0.041) [1.683, 1.817]	1.905 (0.137) [1.688, 2.142]
σ_2		2.451 (0.225) [2.113, 2.845]		2.379 (0.099) [2.225, 2.554]
ρ_{12}		-0.239 (0.140) [-0.462, -0.004]		-0.781 (0.026) [-0.820, -0.736]

Table 5.2 *(continued)*

	OU	OU-AB	OU-MRJ	OU-AB-MRJ
λ			0.051 (0.005) [0.042, 0.060]	0.047 (0.005) [0.038, 0.056]
μ_Z			9.655 (2.470) [5.763, 13.77]	10.46 (2.540) [6.436, 14.82]
σ_Z			17.26 (1.173) [15.45, 19.29]	16.76 (1.187) [14.90, 18.80]
θ_1	6.905 (2.628) [3.085, 10.77]	2.882 (5.764) [-1.324, 17.10]	8.603 (11.75) [7.110, 10.53]	1.792 (10.93) [-1.025, 8.433]
θ_2		6.478 (2.204) [1.487, 8.565]		9.092 (11.10) [2.034, 12.72]
θ_3			-0.189 (0.042) [-0.235, -0.098]	0.210 (0.010) [0.194, 0.226]
$\alpha_{Q,1}$	0.0033 (0.0003) [0.0026, 0.0038]	0.012 (0.003) [0.007, 0.018]	0.0011 (0.0002) [0.0008, 0.0013]	0.0034 (0.0013) [0.0016, 0.0056]
$\alpha_{Q,3}$			6.634 (0.162) [6.306, 6.851]	84.12 (3.796) [78.68, 90.89]
$\sigma_{\varepsilon,1}$	1.999 (0.088) [1.856, 2.147]	1.868 (0.095) [1.709, 2.022]	0.922 (0.031) [0.873, 0.974]	0.918 (0.032) [0.867, 0.971]
$\sigma_{\varepsilon,2}$	7.182 (0.1447) [6.955, 7.427]	7.055 (0.224) [6.687, 7.426]	5.982 (2.836) [5.726, 6.107]	6.749 (5.872) [5.862, 8.085]
$\sigma_{\varepsilon,3}$	12.75 (0.4244) [12.10, 13.46]	13.02 (0.536) [12.13, 13.89]	11.79 (0.785) [11.37, 12.21]	12.32 (3.874) [11.54, 12.76]
$\sigma_{\varepsilon,4}$	16.34 (0.513) [15.56, 17.23]	17.65 (0.730) [16.42, 18.84]	15.89 (3.082) [15.32, 16.38]	16.50 (1.253) [15.75, 17.21]
$\sigma_{\varepsilon,5}$	15.02 (0.462) [14.31, 15.84]	16.38 (0.679) [15.23, 17.48]	14.87 (5.231) [14.27, 15.27]	15.48 (1.129) [14.81, 16.14]

Regarding the variance matrix of the Gaussian components, we find that the volatility of the mean-reverting variable $X_{1,t}$ (short-term factor), σ_1, for the OU and OU-AB models, is relatively high, 3.47 and 3.23 for natural gas, and 4.44 and 6.31 for electricity. For the OU-MRJ and OU-AB-MRJ models, the estimates of σ_1 are much smaller (1.75 and 1.90, for NBP natural gas; and 2.13 and 2.39, for UKPX), suggesting that the jump factor is explaining a significant part of the unconditional price variations. The correlation coefficient ρ_{12} between the Gaussian state-variables is negative and large in magnitude, especially when the jumps are included in the model specification. The estimates of ρ_{12} for the OU-AB-MRJ model are -0.78 and -0.25, for NBP gas and UKPX electricity, respectively.

Next, we examine the jump intensity λ and the jump size parameters, μ_Z and σ_Z, for both commodities. We observe that jumps are more frequent than in other asset classes, such as equity. The intensity estimates show that on average we can expect around 5 jumps in 100 trading days for NBP natural gas, and about 15 jumps for UKPX electricity. The estimates of the mean jump size are largely positive and significant. According to OU-AB-MRJ estimates, the average jump size μ_Z is in the range [6.4, 14.8] with 95% probability for natural gas, and in the range [11.7, 16.5] for electricity; while the posterior mean of the standard deviation of jump sizes σ_Z is 16.8 and 16.9 for gas and electricity, respectively. These results indicates that, when jumps occur, positive size jumps are more common than negative ones.

We now turn to discuss the mean-reversion rate parameters of the Gaussian OU variable and the jump factor under the physical and risk-adjusted measures: α_1 and α_1^Q, and α_3 and α_3^Q, respectively. The mean reversion rates under the physical measure are significant for both commodities and for all models. The estimates of speed of mean reversion of the jump factor under P for the OU-MRJ and OU-AB-MRJ are around 1.44 and 1.53 for natural gas, and 1.69 and 1.70 for electricity. That means the observed half-life of the price deviations corresponding to the jump factor is less than 1 day. For both jump models, the estimates of the mean-reversion rate of the Gaussian state-variable are 0.009 and 0.72 for natural gas, and 0.01 and 0.60 for electricity; which corresponds to an estimated half-life of 75 and 1.0 days, and 57 and 1.2 days, respectively. Under the Q measure, the estimates of the speed of mean-reversion of the Gaussian factor decrease for all models. For the jump diffusion models OU-MRJ and OU-AB-MRJ, the expected half lives in days corresponding to the α_1^Q estimates for natural gas are 630 and 204. The 95%-probability ranges are [533, 866] and [124, 433] for each model. For electricity, the expected half lives are 1,155 and 4.10 days, respectively. Therefore, under the risk-adjusted measure, the degree of mean reversion of

Table 5.3. Parameter estimates for UKPX electricity

The table reports posterior means, standard deviation (in parenthesis), and 95% confidence intervals (in square brackets) for the the model most general model described in Section 5.2, OU-AB-MRJD, and other nested models: OU is the arithmetic model with one mean-reverting Gaussian factor, OU-AB is the two-factor arithmetic model composed by a mean-reverting Gaussian process and an arithmetic Brownian process; and OU-MRJ is the OU model plus a mean-reverting jump diffusion. The estimates correspond to a unit of time defined to be one day. The estimation sample ranges from September 14, 2004 to December 7, 2012.

	OU	OU-AB	OU-MRJ	OU-AB-MRJ
μ_0	32.77 (4.645) [24.66, 40.37]	19.49 (8.965) [7.261, 37.19]	25.85 (7.029) [16.76, 36.03]	10.28 (4.847) [0.902, 17.47]
μ_1	1.632 (0.611) [0.735, 2.797]	1.107 (1.735) [-1.883, 3.592]	2.378 (0.720) [1.195, 3.320]	7.288 (0.768) [5.842, 8.427]
μ_2	-0.795 (2.303) [-4.516, 3.095]	-0.560 (1.972) [-3.753, 2.766]	-0.617 (1.174) [-2.551, 1.273]	-0.746 (1.233) [-2.796, 1.319]
μ_3	-0.474 (2.575) [-4.743, 3.854]	-0.234 (2.354) [-4.280, 3.534]	-0.460 (1.391) [-2.702, 1.815]	-1.046 (1.572) [-3.561, 1.542]
μ_4	1.790 (2.163) [-1.773, 5.299]	1.145 (2.117) [-2.397, 4.714]	-0.276 (1.159) [-2.107, 1.617]	-0.477 (1.406) [-2.693, 1.900]
α_1	0.037 (0.008) [0.025, 0.050]	0.667 (0.111) [0.488, 0.852]	0.0122 (0.0041) [0.0057, 0.0193]	0.599 (0.236) [0.301, 1.030]
α_3			1.693 (0.127) [1.497, 1.919]	1.697 (0.124) [1.515, 1.916]
σ_1	4.444 (0.268) [4.015, 4.888]	6.309 (0.501) [5.441, 7.086]	2.127 (0.138) [1.904, 2.358]	2.388 (0.180) [2.104, 2.692]
σ_2		2.485 (0.202) [2.171, 2.836]		1.930 (0.148) [1.695, 2.188]
ρ_{12}		0.009 (0.169) [-0.268, 0.291]		-0.249 (0.096) [-0.403, -0.088]

Table 5.3 *(continued)*

	OU	OU-AB	OU-MRJ	OU-AB-MRJ
λ			0.153 (0.013) [0.133, 0.175]	0.138 (0.013) [0.118, 0.159]
μ_Z			13.10 (1.295) [11.03, 15.27]	14.03 (1.458) [11.74, 16.50]
σ_Z			16.48 (0.746) [15.32, 17.75]	16.92 (0.815) [15.64, 18.32]
θ_1	4.943 (2.243) [1.296, 8.578]	1.837 (11.27) [-17.23, 20.88]	-0.732 (8.825) [-11.76, 4.622]	8.589 (42.65) [-15.41, 60.08]
θ_2		2.776 (1.764) [0.213, 5.952]		-3.809 (1.201) [-5.206, -2.155]
θ_3			0.247 (0.007) [0.233, 0.258]	0.226 (0.006) [0.217, 0.236]
$\alpha_{Q,1}$	0.0027 (0.0003) [0.0022, 0.0031]	0.0879 (0.0359) [0.0265, 0.1407]	0.0006 (0.0003) [0.0002, 0.0011]	0.169 (0.002) [0.167, 0.171]
$\alpha_{Q,3}$			167.9 (77.08) [56.77, 295.0]	453.7 (19.88) [429.9, 492.3]
$\sigma_{\varepsilon,1}$	6.352 (0.201) [6.023, 6.679]	4.243 (0.458) [3.498, 4.999]	2.264 (0.129) [2.058, 2.476]	1.953 (0.119) [1.763, 2.155]
$\sigma_{\varepsilon,2}$	8.605 (0.287) [8.159, 9.094]	7.791 (0.363) [7.225, 8.409]	8.565 (3.351) [7.628, 10.54]	8.893 (4.570) [7.457, 13.33]
$\sigma_{\varepsilon,3}$	10.36 (0.733) [9.248, 11.62]	10.09 (0.735) [8.916, 11.32]	9.362 (1.573) [8.533, 10.15]	9.637 (2.874) [8.405, 11.42]
$\sigma_{\varepsilon,4}$	11.86 (0.964) [10.39, 13.58]	12.77 (1.023) [11.17, 14.55]	10.72 (0.620) [9.852, 11.67]	11.01 (1.111) [9.844, 12.28]
$\sigma_{\varepsilon,5}$	9.659 (0.706) [8.621, 10.92]	11.17 (0.701) [10.06, 12.38]	9.026 (2.110) [8.122, 10.03]	9.208 (0.671) [8.392, 10.11]

the Gaussian factor is extremely reduced in most of the models, and the risk premium $\alpha_1 - \alpha_1^Q$, which is associated with the volatility risk, is estimated to be always positive. On the contrary, the estimates of the mean-reversion rate corresponding to the jump factor are much higher under Q than under the physical measure P. For natural gas, the posterior means of α_3^Q are 6.63 for the OU-MRJ model and 84.1 for the OU-AB-MRJ model. For electricity, the observed half-life values are even closer to zero. These results suggest that the presence of a jump is largely vanished under the risk-adjusted measure right after the jump occurs.

The significance of the market price of risk parameters differs among models and commodities, however we can observe some common patterns. For natural gas, the θ_1 estimates, i.e. the coefficient related to the Gaussian OU factor, are not estimated with much accuracy, are only significant and positive for the OU and OU-MRJ models, but not when we include the AB factor (i.e. the long-term state variable) in the model specification. For electricity, it is only significant in the OU model. In contrast, the θ_2 and θ_3 estimates, i.e. the risk premia related to the AB and the MRJ factors, are in general significant for both commodities, although their expected sign and magnitude vary across the different model specifications.

Finally, regarding the measure error variances Σ_ε, we find that the inclusion of mean-reverting jumps reduce on average the estimates of Σ_ε related to the futures and spot prices. In particular, for NBP natural gas, the pricing error variances of the spot prices diminish 54% and 51% when using the OU-MRJ and OU-AB-MRJ models instead of the OU and OU-AB models. For UKPX electricity, this reduction is even greater, 64% and 54%, respectively.

5.5 Conclusions

In this chapter, we propose a new way of thinking about the market price of risk so that market participants bearing spot commodity risk are compensated for: jump arrival risk; jump size risk; and speed of mean reversion risk of both diffusion and/or jumps. When pricing under the risk-adjusted measure agents will: over-state the time it takes to return to the seasonal trend; alter the mean of the process; and change the intensity of the jumps and their average size. Our approach can also be viewed as a special case of stochastic discount factors that not only affect the mean of the process but also its variance via the persistence of shocks to the economy.

Using a panel data on natural gas and electricity futures, we empirically

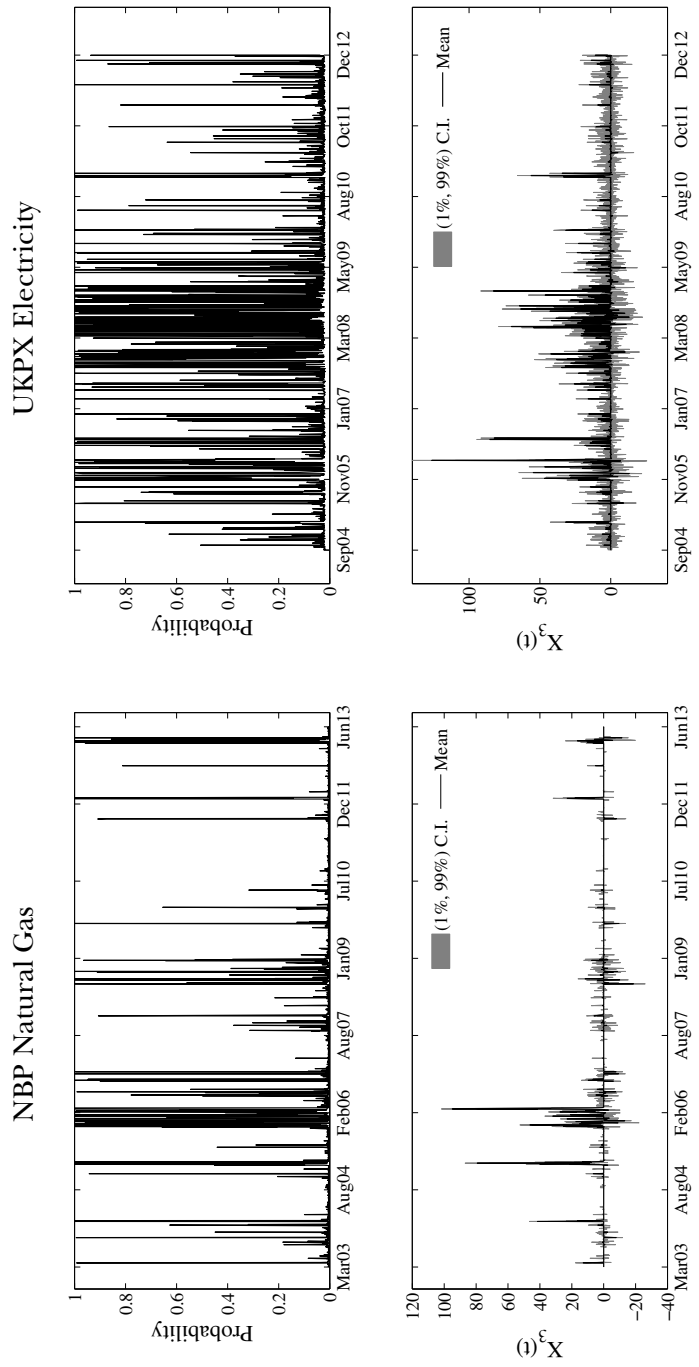

Figure 5.2. Estimated jump probabilities
The figure shows the inferred jump times and the jump paths $(X_{3,t})$ for the OU-AB-MRJ model.

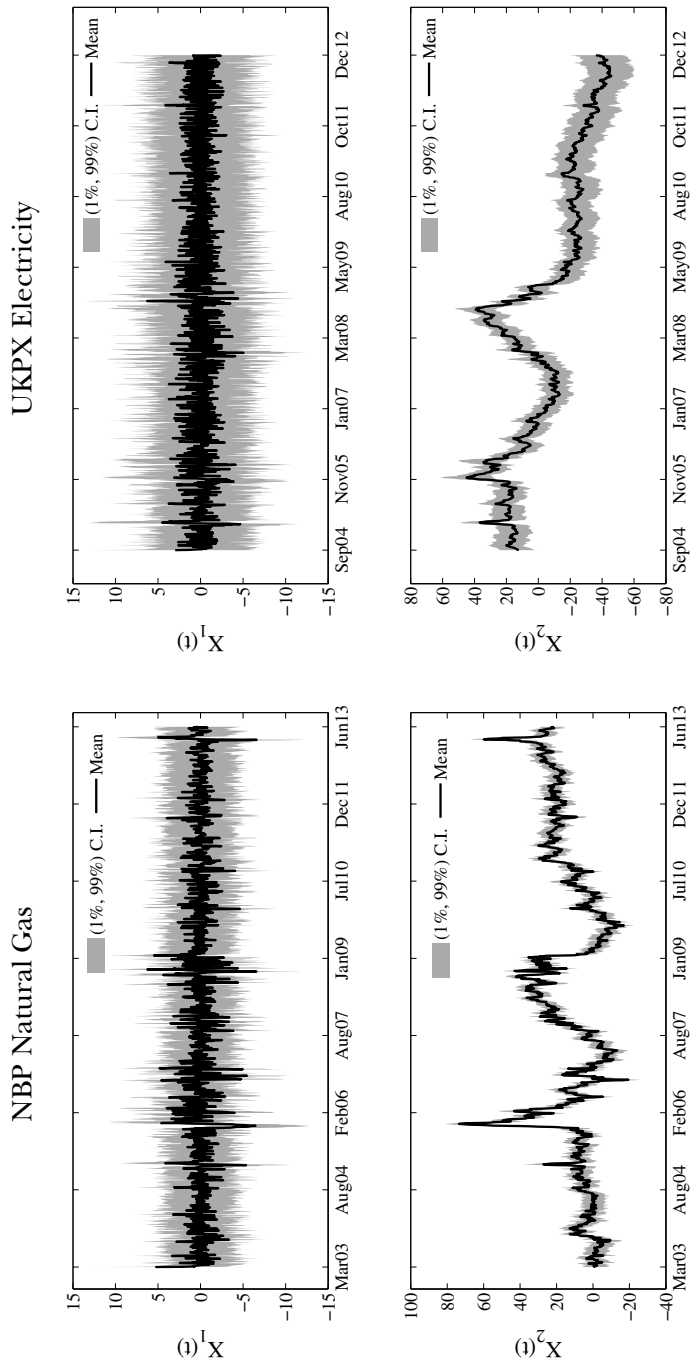

Figure 5.3. Estimated state variable paths
The figure shows the inferred state variable paths ($X_{1,t}$ and $X_{2,t}$) for the OU-AB-MRJ model.

estimate the model using a MCMC methodology. We find evidence of the different degree of mean reversion under the physical and the risk-adjusted measures. We also report the features of a mean-reverting jump component under both probability measures.

Although our specification does not include specifically a dynamics for the convenience yield, we can infer from the instantaneous interest rate dynamics the stochastic process for the convenience yield or, in terms of market price of risk, we can infer an implicit stochastic market price of risk.

6

General conclusions and further research

THE INCREASING PRESENCE OF INVESTORS and financial intermediaries in commodity markets, together with the huge increase in the volatility of commodity prices, have renewed the interest in commodities and commodity derivatives. In the last decade, a better understanding of the behavior of commodity prices and their idiosyncratic statistical features has emerged as a relevant financial and policy topic. This thesis provides new insights, first, to analyze the multivariate distribution of commodity returns and its impact on portfolio selection and tail risk measures; and, second, to price commodity derivatives under the presence of non-Gaussian shocks in a continuous time framework.

To conclude this thesis, we summarize the main findings and contributions along these lines and provide some extensions for future research. We divide our following exposition into theoretical or methodological contributions and empirical results; let us start with the former.

6.1 Summary of methodological contributions

In Chapter 2, supported by different empirical analyses of the statistical features of commodity returns, we propose a new multivariate conditional skewed t copula model for the joint distribution of oil, gold, and equity returns that allows for time-varying moments and state-dependent tail behavior.

We also solve numerically the portfolio selection problem of an investor with three-moment preferences when commodity futures are part of the

investment opportunity set. In our specification, we consider the investor's loss aversion, in the form of the portfolio returns' skewness, and we modify the budget constraint of the investor's problem to take the collateral of commodity futures contracts into account (Chapter 2).

We also contribute to understand the tail behavior of energy price risk using a dynamic multivariate model, in which the vector of innovations is generated by different multivariate GH distributions (Chapter 3). Specifically, we consider the NIG, the VG, the skewed t, Student's t, and the Gaussian distributions; we model different dependence patterns (e.g., dependence in the extremes, positive or negative skewness) and tail decays (e.g., exponential vs. polynomial). Due to the normal mean-variance mixture structure of GH distributions, we can apply the powerful EM algorithm for parameter estimation. In our specification, we approximate the exposure of physical and financial players to energy price risk using portfolios of crude oil, natural gas, coal, and electricity futures.

In Chapter 4, we address the question of how to value an electricity interconnector, using a strip of real options written on the price differential between two power markets . Our model for the dynamics of spread prices captures: jumps in both directions, high seasonal volatility, and fast mean reversion to a seasonal trend. We also derive no-arbitrage lower bounds for the value of the interconnector in terms of electricity futures contracts of the respective power markets. To estimate the jump diffusion parameters, we propose a methodology to detect spikes where the emphasis is placed on avoiding misclassifying mean reversion as jumps.

Chapter 5 contributes to literature on the pricing of risk in commodities by proposing a parsimonious reduced-form model that can capture the main characteristics of commodity prices under the data generating measure and show that there is a family of risk-adjusted measures capable of capturing the fact that market participants may overstate (understate) the probability of occurrence of undesirable (desirable) events. We propose an arithmetic model, instead of exponential, because the pricing and calibration of basic building blocks such as futures contracts can be performed analytically. Our model consists of three factors: an arithmetic Brownian factor, which describes a long-term component; an Ornstein-Uhlenbeck (OU) driven by a Brownian motion, for short-term Gaussian shocks; and a mean-reverting jump process with positive and negative jumps. The family of risk-adjusted measures that we propose allows for the mean reversion of the jump component of spot prices to be different between the two measures. Now, we turn to summarizing the main empirical findings.

6.2 Summary of empirical results

Our first empirical application analyzes 20 years of weekly data of oil and gold futures and, using a rolling window scheme, computes the time series of portfolio weights corresponding to various copula models (Chapter 2). We find that the different specifications of the time-varying marginal distributions, the presence of dynamic conditional dependence among the univariate processes, and the modeling of tail and asymmetric dependence are the main factors behind the differences between the allocation strategies. Results suggest that both marginal distribution modeling and copula modeling have important implications for out-of-sample portfolio performance (as in Patton (2004)). Overall, conditional t copulas yield better portfolio decisions in terms of investment ratios and relative performance than Gaussian models, especially when variance and loss aversion decrease.

In a posterior empirical analysis over a seven-year sample of NYMEX energy futures prices, we calculate recursively the conditional tail risk measures, in a multivariate approach, of different exposures to energy market risk (Chapter 3). Our in-sample and out-of-sample results suggest the importance of fat tails and positive skewness in the multivariate distribution of energy risk factors. Regarding the tail risk of short positions, distributions with polynomial tail decay (heavy-tailed) outperformed alternative versions with exponential tail decays, especially for the utility portfolios. The extent to which the tail risk of the portfolio loss distribution is underestimated depends on the portfolio weights of the different energy commodities, whether we analyze the short or long trading position, and the horizon and confidence level considered.

In the empirical application of Chapter 4, we employed nine years of electricity prices for five pairs of European neighboring markets to value hypothetical interconnectors under different assumptions about the seasonal component of the spread and under different liquidity caps, which proxy for the depth of the interconnected power markets. Our valuation findings indicate that the jumps in the spread can account for between 1% and 40% of the total value of the interconnector, depending on the depth of the market. Some “rules of thumb" summarize the different drivers of the interconnector value: the variance of the diffusion process, the size of the jumps, and the mean-reversion rates of the diffusion and jump processes, all of which are key elements to determine the final value of the interconnector.

Finally, in the empirical part of Chapter 5, we considered two energy commodities: natural gas and electricity traded in United Kingdom, over a period of 10 and 8 years. For the model estimation, we implement a

MCMC scheme, which accounts for parameter uncertainty. We show that participants in energy markets price financial instruments under the risk-adjusted measure by overstating how long deviations from the seasonal component may last. Assuming that spot prices mean revert at the same speed under both measures makes it difficult to reconcile the spot and forwards model dynamics with observed market prices. Furthermore, results suggest that the presence of jumps in spot prices under the data generating measure becomes an important contributing factor to the prices of futures written on the commodity.

6.3 Extensions and further research

To conclude, some extensions to our different analysis can be considered. With respect to Chapter 2, it would be interesting to study the sensitivity of the investor's portfolio decisions to parameter uncertainty using Bayesian analysis. Note that some cautions with the propagation of errors between the marginal distributions and the copula function must be taken into account when implementing this type of analysis. Another possibility is to extend our portfolio selection problem with commodity futures to a dynamic asset allocation context (in a manner similar to Stefanova (2009)). Thus, we could evaluate the hedging component of the optimal portfolio weights under the effects of skewness and asymmetric dependence.

Turning to Chapter 3, some questions also arise for further research. First, we did not consider the effects of parameter uncertainty in the calculations of the tail risk measures, and it would be interesting, albeit computationally intensive, to study the impacts on the results if we were to take such uncertainty into account. Second, we characterized the aggregate tail risk using prespecified energy price risk exposures, given by the portfolio weights, of various representative energy-market players. However, an advantage of our asset-level approach is that we can analyze the sensitivity of the tail risk measures to changes in the weights of the energy portfolio. Furthermore, we can use these multivariate approaches to determine how the risk measures we have analyzed might be used to construct an optimal energy portfolio. Finally, it would be interesting to compare the GH models with other parametric and semi-parametric multivariate approaches, such as those related to multivariate extreme value theories (e.g., Poon, Rockinger, and Tawn (2004)).

Regarding the interconnector valuation (Chapter 4), several extensions might be considered for future analysis. Using a string of spread options

may not capture the full flexibility in the contract. More complete valuation could be based on the formulation of the problem as a stochastic control or optimal switching problem (as in Carmona and Ludkovski (2010)), for which the optimal transmission strategy would be a function of time and the random scenarios of the time evolution of the difference between the spot prices. Moreover, taking control of the transmission, the agent could hedge the risk exposure associated with the transmission decision with a financial position in the futures markets. We leave these questions for future analysis.

In Chapter 4 and Chapter 5 we used reduced form models based on latent variables to describe the dynamics of prices. It also would be interesting to relate the presence of jumps and the risk-adjusted dynamics, proposed in Chapter 5, with commodity market fundamentals (see Bessembinder and Lemmon (2002)). Thus, new structural models, at substantial computational cost, might incorporate the underlying factors that drive commodity prices and might be used to value contingent claims on commodities.

Incorporating jump clustering under the data generating measure would be a desirable property, but it would come at the expense of parsimony. Although we do not model jump clustering under the data generating measure, the family of risk-adjusted measures in Chapter 5 can allow for jump clustering, which is precisely a feature that some market participants consider insuring against.

Assuming a diffusion process for the instantaneous interest rate and using no-arbitrage relationships, we can infer the stochastic process for the convenience yield; alternatively, we could infer an implicit stochastic dynamics for market price of risk.

A
Appendix

A.1 The generalized *t* univariate distribution

In this appendix, we summarize some useful results related to the generalized t distribution introduced by Hansen (1994) and posteriorly analyzed by Jondeau and Rockinger (2003), among others. The following presentation is based on these works. Consider a random variable z that follows a generalized t distribution. Its probability density function $g(z;\,\nu,\lambda)$ is defined as

$$g(z;\,\nu,\lambda) = \begin{cases} b\,c\left[1+\frac{1}{\nu-2}\left(\frac{b\,z+a}{1-\lambda}\right)^2\right]^{-(\nu+1)/2} & z < -a/b \\ b\,c\left[1+\frac{1}{\nu-2}\left(\frac{b\,z+a}{1+\lambda}\right)^2\right]^{-(\nu+1)/2} & z \geqslant -a/b \end{cases}, \quad \text{(A.1)}$$

where $2 < \nu < +\infty$ and $-1 < \lambda < 1$, and the constants a, b and, c are given by

$$a = 4\,\lambda\,c\,(\nu-2)/(\nu-1), \quad b^2 = 1+3\lambda^2-a^2, \quad \text{and} \quad c = \frac{\Gamma\left((\nu+1)/2\right)}{\sqrt{\pi(\nu-2)}\,\Gamma\left(\nu/2\right)}. \quad \text{(A.2)}$$

Furthermore, $\Gamma(y)$ denotes the Gamma function, defined as

$$\Gamma(y) = \int_0^\infty t^{y-1}\mathrm{e}^{-t}\mathrm{d}t$$

for $\Re(y) > 0$ (see (Abramowitz and Stegun, 1965)).

The first three moments of the standardized innovations Z are defined as:

$$\mathbb{E}(Z) = 0; \quad \mathbb{E}(Z^2) = \mathrm{Var}(Z) = 1; \quad \text{and} \tag{A.3}$$

$$\mathbb{E}(Z^3) = \mathrm{Skew}(Z) = \frac{m_3 - 3am_2 + 2a^3}{b^3} \tag{A.4}$$

where $m_2 = b^2 + a^2$ and $m_3 = 16c\lambda(1+\lambda^2)(\nu-2)^2/((\nu-1)(\nu-3))$ if $\nu > 3$ (see Jondeau and Rockinger (2003)).

According to Jondeau and Rockinger (2003, Proposition 1), we can express the the generalized t cumulative distribution function, $G(p\,;\nu,\lambda)$, as a function of the standard Student's t distribution with ν degrees of freedom, $T(p;\,\nu)$, as follows

$$G(p;\,\nu,\lambda) = \begin{cases} (1-\lambda)\,T\left(\sqrt{\frac{\nu}{\nu-2}}\,\frac{bp+a}{1-\lambda}\,;\,\nu\right) & p < -a/b \\ (1+\lambda)\,T\left(\sqrt{\frac{\nu}{\nu-2}}\,\frac{bp+a}{1+\lambda}\,;\,\nu\right) & p \geqslant -a/b \end{cases}, \tag{A.5}$$

where the standard Student's t distribution is defined as

$$T(p;\,\nu) = \int_{-\infty}^{p} \frac{\Gamma\left((\nu+1)/2\right)}{\sqrt{\pi\nu}\,\Gamma\left(\nu/2\right)} \left(1 + x^2/\nu\right)^{-(\nu+1)/2} \mathrm{d}x. \tag{A.6}$$

Finally, the inverse function of the generalized t distribution can be obtained by inverting the standard Student's t distribution, such that

$$G^{-1}(u;\,\nu,\lambda) = \begin{cases} \frac{1}{b}\left[(1-\lambda)\sqrt{\frac{\nu-2}{\nu}}T^{-1}\left(\frac{u}{1-\lambda};\,\nu\right) - a\right] & u < \frac{1-\lambda}{2} \\ \frac{1}{b}\left[(1+\lambda)\sqrt{\frac{\nu-2}{\nu}}T^{-1}\left(\frac{u+\lambda}{1+\lambda};\,\nu\right) - a\right] & u \geq \frac{1-\lambda}{2} \end{cases}, \tag{A.7}$$

where $u \in [0,1]$.

A.2 Explanatory variables for the mean equation

We include the following explanatory factors in the conditional mean equation of our marginal distribution model: short rate, default spread, momentum, basis, and growth in open interest.

- The short rate is a proxy for the expected shocks in the economy. We use the weekly average yield of the three-month T-bills.
- The default spread is the difference between Moody's Baa and Aaa corporate bond yields and should capture the variation in the risk premium. We also employ the weekly average of this variable.

- Momentum is computed as the moving average of previous returns, and it is employed to measure the market sentiment. In our empirical application, we compute it using the weekly returns of previous eight weeks.

- The basis is the relative difference between the six-month-maturity future prices and the month-ahead futures prices; the basis measures the futures curve slope with respect to a six-month delivery horizon. For the empirical application, we employ the weekly average of this measure.

- The dollar open interest is the month-ahead futures price multiplied by the number of contracts outstanding; thus, growth in open interest measures the capital flow into commodity markets. Again, to reduce the noise in the measure, we use the weekly average of this variable.

Although all these variables are considered for the mean equation, we ultimately just select the exogenous regressors that are statistically significant in our time-series analysis.

A.3 Copula functions

This section describes the three implicit copulas we propose as dependence functions of our multivariate model: the Gaussian, t, and skewed t copulas (see Section 2.2). These three copulas correspond to the dependence functions contained in three multivariate normal mixture distributions (see McNeil, Frey, and Embrechts (2005)). This class of distributions adopts the following representation:

$$\boldsymbol{X} = \boldsymbol{\mu} + W\boldsymbol{\gamma} + \sqrt{W}\boldsymbol{Z} \tag{A.8}$$

where $\boldsymbol{\mu}$ and $\boldsymbol{\gamma}$ are parameter vectors in $\mathbb{R}^d$, $\boldsymbol{Z} \sim N(\mathbf{0}, \boldsymbol{\Sigma})$, and W is a random variable independent of $\boldsymbol{Z}$. When the mixing random variable W satisfies $\nu/W \sim \chi^2(\nu)$, then the resulting mixture distribution of the random vector $\boldsymbol{X}$ is denoted as the asymmetric or skewed t distribution, $H(\boldsymbol{\mu}, \boldsymbol{\Sigma}, \nu, \boldsymbol{\gamma})$, which belongs to the the wider family of multivariate generalized hyperbolic distributions.

Applying Sklar's theorem in equation (2.6), we can obtain the skewed t copula function from the generalized hyperbolic skewed t distribution,

$H(\mathbf{0}, \boldsymbol{P}, \nu, \boldsymbol{\gamma})$, defined by $\boldsymbol{\mu} = \mathbf{0}$, and the correlation matrix $\boldsymbol{P}$ implied by the dispersion matrix $\boldsymbol{\Sigma}$.[1]Then, the skewed t copula is defined as

$$C^{\mathrm{SK}}(\boldsymbol{u}; \boldsymbol{P}, \nu, \boldsymbol{\gamma}) = H(\, H_1^{-1}(u_1\,; \nu, \gamma_1),\, \ldots,\, H_d^{-1}(u_d\,; \nu, \gamma_d)\,; \boldsymbol{P}, \nu, \boldsymbol{\gamma}\,), \tag{A.9}$$

where the $H_i(\cdot\,;\, \nu, \gamma_i)$ are the d univariate skewed t distribution functions, the H_i^{-1} are the corresponding quantile functions, and $\boldsymbol{u} = (u_1, \ldots, u_d)'$ is the probability transformed vector.

Special cases can be obtained from the normal mixture representation in equation (A.8). When $\boldsymbol{\gamma} = \mathbf{0}$, we have the multivariate Student's t distribution; obviously, when W is constant, we obtain the multivariate Gaussian distribution. Thus, the unique t copula of a d-variate Student's t distribution can be expressed as

$$C^{\mathrm{T}}(\boldsymbol{u}; \boldsymbol{P}, \nu) = T(\, T^{-1}(u_1;\, \nu),\, \ldots,\, T^{-1}(u_d; \nu)\,;\, \boldsymbol{P}, \nu)\,, \tag{A.10}$$

where $T(\cdot\,;\, \boldsymbol{P}, \nu)$ is the joint distribution function of a d-variate Student's t distribution with ν degrees of freedom and correlation matrix $\boldsymbol{P}$, and $T^{-1}(u_i; \nu)$ is the inverse function of the univariate Student's t distribution with ν degrees of freedom. In the same way, we can define the d-variate Gaussian copula as

$$C^{\mathrm{G}}(\boldsymbol{u};\, \boldsymbol{P}) = \Phi(\Phi^{-1}(u_1),\, \ldots,\, \Phi^{-1}(u_d)\,;\, \boldsymbol{P})\,, \tag{A.11}$$

where $\Phi(\cdot\,;\, \boldsymbol{P})$ denotes the joint distribution function of the d-variate standard normal distribution with correlation matrix $\boldsymbol{P}$, and Φ^{-1} denotes the inverse of the univariate standard normal distribution.

We proceed to compute the density functions of the three copulas. The density function of a parametric copula that is absolutely continuous is given by

$$c(\boldsymbol{u}) = \frac{\partial^d C(u_1, \ldots, u_d)}{\partial u_1 \cdots \partial u_d}. \tag{A.12}$$

For the case of the three implicit copulas we consider here, the density functions can be obtained from differentiating equations (A.9), (A.10), and (A.11). Thus, the density function of the d-variate skewed t copula can be expressed as

$$c^{\mathrm{SK}}(\boldsymbol{u};\, \boldsymbol{P}, \nu, \boldsymbol{\gamma}) = \frac{h(\, H_1^{-1}(u_1;\, \nu, \gamma_1),\, \ldots,\, H_d^{-1}(u_d;\, \nu, \gamma_d)\,;\, \boldsymbol{P}, \nu, \boldsymbol{\gamma}\,)}{h_1(H_1^{-1}(u_1;\, \nu, \gamma_1);\, \nu, \gamma_1) \cdots h_d(H_d^{-1}(u_d;\, \nu, \gamma_d);\, \nu, \gamma_d)}. \tag{A.13}$$

[1]The copula function is invariant under any strictly increasing transformation of the marginal distributions, including the standardization of the components of the random vector $\boldsymbol{X}$.

where $h(\cdot;\, \boldsymbol{P}, \nu, \boldsymbol{\gamma})$ is the joint density of the multivariate skewed t distribution H, and the $h_i(\cdot;\, \nu, \gamma_i)$ are its corresponding marginal density functions. Using the results from McNeil, Frey, and Embrechts (2005, Section 3.2.3) for the density functions of generalized hyperbolic distributions, and some algebra, we explicitly obtain the density function of the d-variate skewed t copula, given by

$$\begin{aligned} c^{\mathrm{SK}}(\boldsymbol{u};\, \boldsymbol{P}, \nu, \boldsymbol{\gamma}) = |\boldsymbol{P}|^{-1/2} \left(\frac{\Gamma(\frac{\nu}{2})}{2^{1-\nu/2}} \right)^{d-1} & \frac{\prod_{i=1}^{d} \left(1 + \frac{x_i^2}{\nu}\right)^{(\nu+1)/2}}{\left(1 + \frac{\boldsymbol{x}'\boldsymbol{P}^{-1}\boldsymbol{x}}{\nu}\right)^{(\nu+d)/2}} \\ & \times 1/\Big(\prod_{i=1}^{d} K_{\frac{\nu+1}{2}}\Big(\sqrt{(\nu + x_i^2)\gamma_i^2}\Big) \Big(\sqrt{(\nu + x_i^2)\gamma_i^2}\Big)^{\frac{\nu+1}{2}} \mathrm{e}^{x_i\gamma_i} \Big) \\ & \times K_{\frac{\nu+d}{2}}\Big(\sqrt{(\nu + \boldsymbol{x}'\boldsymbol{P}^{-1}\boldsymbol{x})\boldsymbol{\gamma}'\boldsymbol{P}^{-1}\boldsymbol{\gamma}}\Big) \\ & \times \Big(\sqrt{(\nu + \boldsymbol{x}'\boldsymbol{P}^{-1}\boldsymbol{x})\boldsymbol{\gamma}'\boldsymbol{P}^{-1}\boldsymbol{\gamma}}\Big)^{\frac{\nu+d}{2}} \mathrm{e}^{\boldsymbol{x}'\boldsymbol{P}^{-1}\boldsymbol{\gamma}} \end{aligned} \tag{A.14}$$

where $\boldsymbol{x} = (x_1, \ldots, x_d)'$ and $x_i = H_i^{-1}(u_i\,;\, \nu, \gamma_i)$.

In addition, $\Gamma(\cdot)$ denotes the Gamma function and K_η is the modified Bessel function of the second kind with order η, which can be implemented numerically (see Abramowitz and Stegun (1965) for more details about these functions and their properties). A similar expression to that in equation (A.12) can be derived for the t and Gaussian copulas from their respective joint and marginal density functions. Thus the density function of the d-variate t copula is given by

$$c^{\mathrm{T}}(\boldsymbol{u}; \boldsymbol{P}, \nu) = |\boldsymbol{P}|^{-1/2} \frac{\Gamma\left(\frac{\nu+d}{2}\right) \Gamma\left(\frac{\nu}{2}\right)^{d-1}}{\Gamma\left(\frac{\nu+1}{2}\right)^{d}} \frac{\prod_{i=1}^{d} \left(1 + \frac{x_i^2}{\nu}\right)^{(\nu+1)/2}}{\left(1 + \frac{\boldsymbol{x}'\boldsymbol{P}^{-1}\boldsymbol{x}}{\nu}\right)^{(\nu+d)/2}}, \tag{A.15}$$

where $x_i = T^{-1}(u_i; \nu)$. Finally, the density function of the d-variate Gaussian copula is expressed as

$$c^{\mathrm{G}}(\boldsymbol{u}; \boldsymbol{P}) = |\boldsymbol{P}|^{-1/2} \exp\left(-\frac{1}{2}\, \boldsymbol{x}' \left(\boldsymbol{P}^{-1} - \mathbb{I}_d \right) \boldsymbol{x} \right), \tag{A.16}$$

where $x_i = \Phi^{-1}(u_i)$ and $\mathbb{I}_d$ denotes the unit matrix of size d.

A.4 The two-stage log-likelihood function

Following Nelsen (2006, Theorem 2.10.9) and Patton (2006b, Theorem 1), equation (2.6) presents a multivariate and conditional extension to

Sklar's theorem. Then, according to equation (2.6), the conditional density function of the joint distribution $F_t(r_{1,t+1}, \ldots, r_{d,t+1};\, \boldsymbol{\theta})$ is given by

$$\begin{aligned} f_t(\boldsymbol{r}_{t+1}; \boldsymbol{\theta}) &= \frac{\partial^d F_t(\boldsymbol{r}_{t+1}; \boldsymbol{\theta})}{\partial r_{1,t+1} \cdots \partial r_{d,t+1}} \\ &= \prod_{i=1}^{d} f_{i,t}(r_{i,t+1}\,; \boldsymbol{\theta}_{i,M}) \cdot c_t(u_{i,t+1}, \ldots, u_{i,t+1}\,; \boldsymbol{\theta}_C), \end{aligned} \tag{A.17}$$

where the $u_{i,t+1} = F_{i,t}(r_{i,t+1}\,; \boldsymbol{\theta}_{i,M})$ are the marginal conditional distributions; $f_{i,t}(r_{i,t+1}\,; \boldsymbol{\theta}_{i,M})$ are the marginal conditional density functions; and $c_t(u_{1,t+1}, \ldots, u^d_{d,t+1}\,; \boldsymbol{\theta}_C)$ is the conditional copula density function (defined in equation (A.12)).

Taking logarithms in equation (A.17) and summing for all observations in the sample, $\bar{\boldsymbol{r}}_T = \{\boldsymbol{r}_1, \ldots, \boldsymbol{r}_T\}$, we determine that the log-likelihood function of the joint model $\mathcal{L}(\boldsymbol{\theta}\,; \bar{\boldsymbol{r}}_T)$ in equation (2.16) can be divided in two terms, as follows:

$$\begin{aligned} \mathcal{L}(\boldsymbol{\theta}\,; \bar{\boldsymbol{r}}_T) &= \sum_{i=1}^{d} \sum_{t=1}^{T} \log f_{i,t}(r_{i,t+1}\,; \boldsymbol{\theta}_{i,M}) + \sum_{t=1}^{T} \log c_t(u_{1,t+1}, \ldots, u_{d,t+1}\,; \boldsymbol{\theta}_C) \\ &= \sum_{i=1}^{d} \mathcal{L}_i(\boldsymbol{\theta}_{i,M}; \bar{\boldsymbol{r}}_T) + \mathcal{L}_C(\boldsymbol{\theta}_C; \boldsymbol{\theta}_M, \bar{\boldsymbol{r}}_T)\,, \end{aligned} \tag{A.18}$$

where $\mathcal{L}_i$ and $\mathcal{L}_C$ are the log-likelihood functions for the i-th marginal model and for the copula function, respectively. Moreover, $\boldsymbol{\theta}_M = (\boldsymbol{\theta}_{1,M} \ldots \boldsymbol{\theta}_{d,M})'$ is the parameter set of the d marginal conditional distributions, and $\boldsymbol{\theta}_C$ is the parameter set of the conditional copula.

A.5 Multivariate tests

Engle and Sheppard (2001) test for constant correlation Panel B of Table 2.2 presents the results of Engle and Sheppard (2001) test for constant correlation for 5, 10, and 20 lags. This test requires a consistent estimate of the constant conditional correlation and a vector autoregression. We use the standardized residuals of GARCH(1,1) processes to estimate the correlation matrix, $\boldsymbol{P}$, and the diagonal matrix of standard deviations, $\boldsymbol{D}_{t+1}$. Then, under the null hypothesis of constant correlation, all the coefficients in

$$\text{vech}^{\text{u}}(\boldsymbol{Y}_{t+1}) = \alpha + \beta_1 \text{vech}^{\text{u}}(\boldsymbol{Y}_{t+1-1}) + \ldots + \beta_s \text{vech}^{\text{u}}(\boldsymbol{Y}_{t+1-s}) + \eta_t \tag{A.19}$$

should be 0; vech^{u} is an operator that selects the upper off-diagonal elements, and $\boldsymbol{Y}_{t+1}$ is a symmetric matrix defined by

$$(\boldsymbol{P}^{-1/2}\boldsymbol{D}_{t+1}^{-1}\boldsymbol{r}_{t+1})(\boldsymbol{P}^{-1/2}\boldsymbol{D}_{t+1}^{-1}\boldsymbol{r}_{t+1})' - \mathbb{I}.$$

Under the null hypothesis, the statistic $\frac{\hat{\boldsymbol{\beta}}\boldsymbol{X}'\boldsymbol{X}\hat{\boldsymbol{\beta}}'}{\hat{\sigma}_\eta^2}$ is asymptotically distributed as χ_{s+1}^2, where $\boldsymbol{X}$ is the vector of regressors, $\boldsymbol{\beta}$ is the vector of coefficients in the latter regression equation (A.19), and $\hat{\sigma}_\eta^2$ is the unbiased sample variance of the estimated residuals $\hat{\eta}_t$. All test p-values, which represent the probability of constant correlation, are all less than 0.05; we reject the hypothesis of constant correlation for all lags considered and for all sample periods.

Mardia (1970) test of multivariate normality We implement the Mardia (1970) test of multivariate normality, based on d-variate measures for the skewness and kurtosis of the vector of returns. These measures are computed using the so-called *Mahalanobis angle*, defined as

$$D_{tt'} = (\boldsymbol{r}_t - \bar{\boldsymbol{r}})'\bar{\boldsymbol{S}}^{-1}(\boldsymbol{r}_{t'} - \bar{\boldsymbol{r}}),$$

where $\bar{\boldsymbol{r}}$ and $\bar{\boldsymbol{S}}$ are the sample mean and covariance estimators. Under this framework, d-variate skewness and kurtosis are computed as

$$s_d = 1/T^2 \sum_{t=1}^{T}\sum_{t'=1}^{T} D_{tt'}^3 \quad \text{and} \quad k_d = 1/T \sum_{t=1}^{T} (D_{tt}^{1/2})^4 .$$

Under the null hypothesis of multivariate normality, $1/6Ts_d$ and k_d are asymptotically distributed as a $\chi^2(d(d+1)(d+2)/6)$ and a $N(d(d+2), 8d(d+2)/T)$, respectively. Panel C of Table 2.2 reports these multivariate measures, s_d and k_d, for our three-dimensional vector of returns and their corresponding statistics, rejecting the null hypothesis of multivariate normality for the three sample periods considered.

Test of ellipticity of the vector of returns Following McNeil, Frey, and Embrechts (2005), we test for the ellipticity of the vector of returns. This test considers if standardized returns are consistent with a spherical distribution. Standardized returns $\boldsymbol{z}_t$ are defined by the sample mean and covariance as follows

$$\boldsymbol{z}_t = \bar{\boldsymbol{S}}^{-1/2}(\boldsymbol{r}_t - \bar{\boldsymbol{r}})$$

If $\boldsymbol{z}_t$ is consistent with the spherical assumption, then the statistic T_{ellip} will be distributed according to a Beta distribution; that is,

$$T_{ellip} = \sum_{i=1}^{k} z_i^2 / \sum_{i=1}^{d} z_i^2 \sim \text{Beta}(k/2, (d-k)/2)\,,$$

where d is the dimension of the returns vector (i.e. $d = 3$), and k is chosen to roughly equal $d - k$ (see McNeil, Frey, and Embrechts (2005)). We analyze the results of this test graphically, through the qq-plot in Exhibit 2 of Figure 2.2, and numerically, implementing a Kolmogorov-Smirnov (KS) test with the data, whose results are reported in Panel C of Table 2.2. The curvature in the qq-plot suggests that the vector of returns is not elliptically distributed for any of the sample periods considered (we just report the plot for the full-sample period). For the full-sample period, the KS test statistic equals 0.174, above the critical value (0.048). Therefore, we reject the elliptical hypothesis. The same conclusion is inferred for the other subsamples.

Exceedance correlation The exceedance correlation is defined as the correlation between the returns above or below a given quantile. Following Longin and Solnik (2001), Ang and Chen (2002), and Patton (2004), we use exceedance correlation to investigate the dependence structure among commodities and equity returns, checking for the presence of possibly asymmetric interactions. The exceedance correlation at a threshold level q is given by

$$\varrho(q) = \begin{cases} \text{Corr}\left[r_i, r_j \,|\, r_i \leqslant Q_i(q) \bigcap r_j \leqslant Q_j(q)\right] & \text{if } q \leqslant 0.5 \\ \text{Corr}\left[r_i, r_j \,|\, r_i > Q_i(q) \bigcap r_j > Q_j(q)\right] & \text{if } q > 0.5 \end{cases},$$

where $Q_i(q)$ and $Q_j(q)$ are the q-th quantiles of returns r_i and r_j. Figure 2.3 plots exceedence correlation as a function of returns quantiles. The shape of the exceedance correlation function depends on the bivariate distribution between each pair of returns; it provides a means to measure the degree of asymmetry in the joint distribution of these returns. The exceedance correlation for the extreme returns is 0 for a bivariate normal distribution.

Patton (2006b)'s Symmetrized Joe-Clayton copula To attend to the tail dependence of the returns vector, we fit the symmetrized Joe-Clayton (SJC) copula proposed by Patton (2006b) to our unfiltered sample of returns.

The SJC copula is given by:

$$C^{\mathrm{SJC}}(u_1, u_2; \tau^U, \tau^L) = 1/2 \Big(u_1 + u_2 - 1 + C^{\mathrm{JC}}(u_1, u_2; \tau^U, \tau^L) + C^{\mathrm{JC}}(1-u_1, 1-u_2; \tau^L, \tau^U) \Big).$$

This copula is a modification of the Joe-Clayton copula C^{JC}:

$$C^{\mathrm{JC}}(u_1, u_2; \tau^U, \tau^L) = 1 - \left(1 - \Big(\frac{1}{[1-(1-u_1)^\kappa]^\xi} + \frac{1}{[1-(1-u_2)^\kappa]^\xi} - 1 \Big)^{-1/\xi} \right)^{1/\kappa}$$

where $\kappa = 1/\log_2(2-\tau^U)$, $\xi = -1/\log_2(\tau^L)$, and $\tau^U, \tau^L \in (0,1)$. The parameters τ^U and τ^D are measure of dependence in the extremes, that is,

$$\lim_{\epsilon \to 0} \mathbb{P}[U_1 \leq \epsilon; U_2 \leq \epsilon] = \tau^L \quad \text{and} \quad \lim_{\epsilon \to 1} \mathbb{P}[U_1 > \epsilon; U_2 > \epsilon] = \tau^U$$

By construction, the SJC copula is symmetric when $\tau^U = \tau^L$ and exhibits no upper tail dependence if $\tau^U = 0$, or no lower tail dependence if $\tau^L = 0$. In Panel D of Table 2.2, we report the estimates of the upper and lower tail dependence parameters, τ^U and τ^D, corresponding to the SJC copula.

A.6 Description of energy portfolios

We consider two groups of typical energy portfolios. One group represents the exposures to energy price risk that we can find in the power industry. In this case, the energy futures portfolio approximates the utility's future payoffs. A second group represents the typical financial positions of investors trading in energy commodities.

In each of these groups, we account for two example portfolios, providing a total of four representative portfolios, for which we analyze tail behavior and compute risk measures.

Portfolios of utility companies: Consider an arbitrary utility whose mix of generation consists of coal-fired plants, which represents intermediate-load generators, and peak-load power plants, which are fired mainly by natural gas and marginally with oil.

Each fuel-fired power plant involves two marketed commodities: the electricity and the fuel used to produce that electricity. Thus, the payoffs of the utility can be modeled as a function of the difference between the electricity price (in \$/MWh) and the fuel price (in \$/fuel units), multiplied by the heat rate of the power plant (in fuel units/MWh). The heat rate determines the efficiency of the power plant and is defined as the conversion ratio between the electricity and the fuel used for generation.

Therefore, the exposure of the utility to energy price risk can be approximated by an energy futures portfolio composed of long (short) positions in electricity and short (long) positions in coal, gas, and oil. The size of the exposure to each fuel is determined by the amount of electricity produced by that source. Thus, the weight (in dollars) of each fuel in the utility portfolio is given by

$$\begin{aligned} w_{i,t} &= q_{i,0}F_{i,t} = (\mp C_i \cdot \mathcal{H}_i)F_{i,t}\,, \quad \text{for } i = 1,2,3\,(\text{oil, gas, coal})\,, \text{ and} \\ w_{4,t} &= q_{4,0}F_{4,t} = (\pm C)F_{4,t}\,, \quad \text{for electricity}\,, \end{aligned} \tag{A.20}$$

where C (in MWh) is the total electricity capacity/production generated by coal, gas, and oil; C_i (in MWh) is the amount of power generated by fuel i; $\mathcal{H}_i$ is the heat rate of fuel i expressed in units of fuel per MWh; and $F_{i,t}$ is the futures price at time t (in \$ per units of fuel).

As a practical example, we analyze the energy risk exposure of an utility operating in the Pennsylvania-Jersey-Maryland (PJM) Interconnection. We first calculate the amounts of power C_i using the production capacity by source of generation data observed in the PJM. In this market, 57 of 100 MWh are generated using some of the three fuels. In particular, coal, natural gas, and oil are used to produce the 36%, 19%, and 2%, respectively, of the total load. Then, we calculate the average operating heat rates for each fuel by dividing the energy consumed for generation (in mmBtu) by the MWh of generated power. To convert the heat rates in mmBtu to the fuel units employed in the futures contract price, we apply the corresponding conversion factors.[2]

In a second example, we analyze only a gas-fired power plant. In this case, the total amount of electricity is generated by natural gas, and therefore,

[2]According to the data reported by the U.S. EIA, the average operating heat rates for petroleum, coal, and natural gas are (in mmBtu/MWh): 11.02, 10.38, and 8.31, respectively. The conversion factors that we employ also come from the EIA, and they are as follows: 1 barrel of oil = 5.8 mmBtu, and 1 U.S. ton of coal = 24 mmBtu. Natural gas is traded directly in mmBtu.

we just have two energy commodities in the portfolio. That is, $w_{\text{gas},t} = (\mp C \cdot \mathcal{H}_{\text{gas}})F_{\text{gas},t}$ and $w_{\text{elec},t} = (\pm C)F_{\text{elec},t}$.

In both examples, these portfolios behave as "let-it-run" portfolios, because the quantities $q_{i,0}$ are assumed to be fixed (capacity is assumed to remain constant throughout the sample). The relative weight of a fuel within the portfolio thus varies, due to changes in its futures prices. That is, the initial value of the portfolios depends on the futures prices at the initial observation and the generated capacity. For our sample, the initial exposures, in dollars, of the utility portfolio are around US$2700 for the fuels (oil, gas, and coal) and US$5016 for 57MWh of electricity. For the gas-fired power plant, the exposures corresponding to a supply of 100MWh of electricity are US$8300 and US$8800 for the natural gas and electricity contracts, respectively.

Portfolios of financial players: Within this group, we first consider an equally weighted portfolio, built with the four energy commodities at hand, as a simple, direct way to gain exposure to energy commodities. This portfolio can represent investments in an energy index, as well as the behavior of the energy commodities asset class. For this strategy, the portfolio weight in dollars for energy futures i at time $t = 0$ is given by $w_{i,0} = W_0/4$, where W_0 is the initial wealth. If we keep weights constant and equal to $1/4$ along the life of the portfolio, such that $w_{i,t} = q_{i,t}F_{i,t} = W_t/4$, we must rebalance the positions in each commodity,

$$q_{i,t} = W_t/(4F_{i,t}) = \sum_{j=1}^{4} w_{j,t-1}F_{j,t}/(4F_{i,t})\,. \tag{A.21}$$

Therefore, an equally weighted portfolio with rebalancing implies the embedded trading strategy of buying "losers" and selling "winners" at the end of the day. This trading characteristic could be very attractive for investors, due to the mean-reverting pattern of energy commodity prices. Furthermore, the performance of the equally weighted portfolio approximates the average return of the aggregate energy futures market.

In the second example, we consider the minimum variance portfolio of an investor trading in energy markets. In general, investors (e.g., banks, asset managers) maximize the expected returns of their portfolios, subject to some risk constraint. When variance is an adequate measure of risk, this problem is equivalent to solving the optimal mean-variance portfolio,

$$\boldsymbol{w}_t^* = \arg\min_{\boldsymbol{w}_t} 1/2\,\mathrm{Var}(\Delta W_t) \quad \text{s.t.} \quad \mathbb{E}(\Delta W_t) \geq \mathcal{R}\,.$$

Across the entire spectrum of solutions, which depend on how much risk the investor accepts to reach a higher expected return $\mathcal{R}$, we focus on the minimum variance solution. Thus, when we omit the expected return constraint in the optimization problem, the solution is given by

$$\boldsymbol{w}_t^* = (\bar{\boldsymbol{H}}^{-1}\,\boldsymbol{\imath}_4)/(\boldsymbol{\imath}_4'\bar{\boldsymbol{H}}^{-1}\boldsymbol{\imath}_4)\,, \tag{A.22}$$

where $\bar{\boldsymbol{H}}$ is the sample covariance matrix of the energy returns, and $\boldsymbol{\imath}_4$ is a 4×1 vector of ones.

To measure the portfolio weights and the risk measures estimates in dollars, we consider for both portfolios an initial investment of US$1000.

A.7 Generalized hyperbolic distributions

In this appendix, we present some details on the GH distribution functions that we employ as conditional distributions of our dynamic multivariate model for the vector of energy returns. The GH distributions are presented in equation (3.10) as normal mean-variance mixtures, for which the mixture random variable follows a generalized inverse Gaussian (GIG) distribution, $N^-(\lambda,\chi,\psi)$, with the following density function:

$$h(\omega) = \frac{\chi^{-\lambda}(\sqrt{\chi\psi})^{\lambda}}{2K_\lambda(\sqrt{\chi\psi})}\omega^{\lambda-1}\,\exp\big(-(\chi\omega^{-1}+\psi\omega)/2\big)\,,\quad \omega>0\,. \tag{A.23}$$

Here, $K_\lambda(y)$ is the modified Bessel function of the second kind, with order $\lambda\in\mathbb{R}$, defined by the integral representation:

$$K_\lambda(y) = 1/2\int_0^\infty u^{\lambda-1}\exp\big(-y(u+u^{-1})/2\big)\mathrm{d}u\,.$$

The parameter domain of $N^-(\lambda,\chi,\psi)$ satisfies that $\chi>0$, $\psi\geqslant 0$ if $\lambda<0$; $\chi>0$, $\psi>0$ if $\lambda=0$; and $\chi\geqslant 0$, $\psi>0$ if $\lambda>0$. Then, according to equation (3.10), the joint density function of a d-variate GH distribution is

$$g(\boldsymbol{x}) = \int_{\mathbb{R}^+}\frac{\mathrm{e}^{(\boldsymbol{x}-\boldsymbol{\mu})\boldsymbol{\Sigma}^{-1}\boldsymbol{\gamma}}}{\det(\boldsymbol{\Sigma})^{1/2}(2\pi w)^{d/2}}\,\exp\Big(-\frac{\mathcal{Q}(\boldsymbol{x})}{2w}-\frac{\boldsymbol{\gamma}'\boldsymbol{\Sigma}^{-1}\boldsymbol{\gamma}}{2/w}\Big)h(\omega)\mathrm{d}\omega\,, \tag{A.24}$$

where $\mathcal{Q}(\boldsymbol{x})\equiv(\boldsymbol{x}-\boldsymbol{\mu})'\boldsymbol{\Sigma}^{-1}(\boldsymbol{x}-\boldsymbol{\mu})$.

We form several subclasses of GH distributions by evaluating this integral for different boundary cases of the GIG density function $h(\omega)$. In the following, we detail the various cases of GH distributions used in this chapter.

Normal inverse Gaussian (NIG) distribution: When $\lambda = -1/2$, and $\chi, \psi > 0$, the resulting mixing GIG distribution in (A.23) is known as inverse Gaussian. Integrating in (A.24) and taking into account several properties of the modified Bessel functions, namely, that $K_{-\lambda}(y) = K_\lambda(y)$ and $K_{1/2}(y) = (\pi/2y)^{1/2}\,\mathrm{e}^{-y}$, we obtain the density function of the multivariate NIG distribution:

$$\begin{aligned} g(\boldsymbol{x}) = & C\, K_{(d+1)/2}\Big((\chi + \mathcal{Q}(\boldsymbol{x}))^{1/2}(\psi + \boldsymbol{\gamma}'\boldsymbol{\Sigma}^{-1}\boldsymbol{\gamma})^{1/2}\Big) \\ & \times \Big(\chi + \mathcal{Q}(\boldsymbol{x})\Big)^{-(d+1)/4} \mathrm{e}^{(\boldsymbol{x}-\boldsymbol{\mu})'\boldsymbol{\Sigma}^{-1}\boldsymbol{\gamma}}\,, \end{aligned} \tag{A.25}$$

where C is the normalizing constant

$$C = \frac{\chi^{1/2}(\psi + \boldsymbol{\gamma}'\boldsymbol{\Sigma}^{-1}\boldsymbol{\gamma})^{(d+1)/4}}{(2\pi)^{d/2}\det(\boldsymbol{\Sigma})^{1/2}(\pi/2)} \mathrm{e}^{\sqrt{\chi\psi}}\,.$$

If the random variable $\boldsymbol{x}$ follows a NIG distribution, then its mean and covariance are given by

$$\begin{aligned} \mathbb{E}(\boldsymbol{x}) &= \boldsymbol{\mu} + (\chi/\psi)^{1/2}\boldsymbol{\gamma}\,, \text{ and} \\ \mathrm{Cov}(\boldsymbol{x}) &= (\chi/\psi)^{1/2}\boldsymbol{\Sigma} + (\chi/\psi^3)^{1/2}\boldsymbol{\gamma}\boldsymbol{\gamma}'\,. \end{aligned}$$

Variance-gamma (VG) distribution: The VG distribution is obtained when $\lambda > 0$ and $\chi = 0$. In this case, the mixing random variable follows a gamma distribution, with density function $h(\omega) = (\psi/2)^\lambda\, \omega^{\lambda-1}\, \mathrm{e}^{-\psi\omega/2}/\Gamma(\lambda)$, where $\Gamma(\cdot)$ is the gamma function (limiting case corresponding to $\chi \to 0$ in (A.23)). Integrating in (A.24) and taking into account that $K_\lambda(y) \simeq \Gamma(\lambda)\, 2^{\lambda-1} y^{-\lambda}$ when $y \to 0^+$ and for $\lambda > 0$, we determine that the VG density function is

$$\begin{aligned} g(\boldsymbol{x}) = & C\, K_{\lambda-d/2}\Big((\chi + \mathcal{Q}(\boldsymbol{x}))^{1/2}(\psi + \boldsymbol{\gamma}'\boldsymbol{\Sigma}^{-1}\boldsymbol{\gamma})^{1/2}\Big) \\ & \times \Big(\chi + \mathcal{Q}(\boldsymbol{x})\Big)^{\lambda/2-d/4} \mathrm{e}^{(\boldsymbol{x}-\boldsymbol{\mu})'\boldsymbol{\Sigma}^{-1}\boldsymbol{\gamma}}\,, \end{aligned} \tag{A.26}$$

where the constant C is

$$C = \frac{\psi^\lambda(\psi + \boldsymbol{\gamma}'\boldsymbol{\Sigma}^{-1}\boldsymbol{\gamma})^{d/4-\lambda/2}}{(2\pi)^{d/2}\det(\boldsymbol{\Sigma})^{1/2}\Gamma(\lambda)2^{\lambda-1}}\,.$$

The mean and covariance of a VG random variable $\boldsymbol{x}$ are

$$\begin{aligned} \mathbb{E}(\boldsymbol{x}) &= \boldsymbol{\mu} + (2\lambda/\psi)\boldsymbol{\gamma}\,, \text{ and} \\ \mathrm{Cov}(\boldsymbol{x}) &= (2\lambda/\psi)\boldsymbol{\Sigma} + (4\lambda/\psi^2)\boldsymbol{\gamma}\boldsymbol{\gamma}'\,. \end{aligned}$$

GH skewed t (skT) distribution: In this case, $\lambda = -\chi/2$ and $\psi = 0$, and the mixing random variable follows an inverse gamma distribution with density function $h(\omega) = (\chi/2)^{\chi/2}/\Gamma(\chi/2)\ \omega^{-(\chi/2+1)}\mathrm{e}^{-\omega\chi/2}$, which is the limiting case of density (A.23) when $\psi \to 0$. If we integrate ω in (A.24) and apply $K_\lambda(y) \simeq \Gamma(-\lambda)2^{-\lambda-1}y^\lambda$ as $y \to 0^+$ for $\lambda < 0$, we obtain the skT density function

$$\begin{aligned} g(\boldsymbol{x}) = & C\, K_{(\chi+d)/2}\Big((\chi + \mathcal{Q}(\boldsymbol{x}))^{1/2}(\boldsymbol{\gamma}'\boldsymbol{\Sigma}^{-1}\boldsymbol{\gamma})^{1/2}\Big) \\ & \times \Big(\chi + \mathcal{Q}(\boldsymbol{x})\Big)^{-(\chi+d)/4} \mathrm{e}^{(\boldsymbol{x}-\boldsymbol{\mu})'\boldsymbol{\Sigma}^{-1}\boldsymbol{\gamma}}\,, \end{aligned} \tag{A.27}$$

with constant C

$$C = \frac{\chi^{\chi/2}(\boldsymbol{\gamma}'\boldsymbol{\Sigma}^{-1}\boldsymbol{\gamma})^{(\chi+d)/4}}{(2\pi)^{d/2}\det(\boldsymbol{\Sigma})^{1/2}\Gamma(\chi/2)2^{\chi/2-1}}\,.$$

The mean and covariance of a skT random variable $\boldsymbol{x}$ are

$$\begin{aligned} \mathbb{E}(\boldsymbol{x}) &= \boldsymbol{\mu} + (\chi/(\chi-2))\boldsymbol{\gamma}\,, \text{ and} \\ \mathrm{Cov}(\boldsymbol{x}) &= (\chi/(\chi-2))\boldsymbol{\Sigma} + [2\chi^2/((\chi-2)^2(\chi-4))]\boldsymbol{\gamma}\boldsymbol{\gamma}'\,. \end{aligned}$$

The mean and variance of the skT distribution are finite only if $\chi > 2$ and $\chi > 4$, respectively. For this distribution, χ corresponds to the degrees-of-freedom parameter.

Student's t (T) distribution: If the vector of asymmetry parameters $\boldsymbol{\gamma}$ tends to zero, the mixture representation in equation (3.10) generates symmetric GH distributions. In particular, when the mixing random variable follows the inverse gamma distribution defined previously for the skT case (i.e., when $\psi \to 0$, $\lambda = -\chi/2$, and $\chi > 0$), we obtain the multivariate Student's t (T) distribution with degrees of freedom χ. Then, the T density function is given by

$$g(\boldsymbol{x}) = \frac{\chi^{-d/2}\Gamma((\chi+d)/2)}{\pi^{d/2}\det(\boldsymbol{\Sigma})^{d/2}\Gamma(\chi/2)}\Big(1 + \mathcal{Q}(\boldsymbol{x})/\chi\Big)^{-(\chi+d)/2}. \tag{A.28}$$

For this symmetric T case, the mean and covariance are $\mathbb{E}(\boldsymbol{x}) = \boldsymbol{\mu}$ and $\mathrm{Cov}(\boldsymbol{x}) = (\chi/(\chi-2))\boldsymbol{\Sigma}$, and therefore, the covariance matrix is finite when $\chi > 2$.

Multivariate Gaussian (G) distribution: When $\boldsymbol{\gamma} = 0$ and $\omega = 1$, that is, when the distribution is symmetric and the mixing variable is constant, we

obtain in equation (A.24) the density function of the multivariate Gaussian distribution,

$$g(\boldsymbol{x}) = \frac{1}{(2\pi)^{d/2}\det(\boldsymbol{\Sigma})^{1/2}} \exp\Big(-\frac{\mathcal{Q}(\boldsymbol{x})}{2}\Big), \tag{A.29}$$

with mean vector $\mathbb{E}(\boldsymbol{x}) = \boldsymbol{\mu}$ and covariance matrix $\mathrm{Cov}(\boldsymbol{x}) = \boldsymbol{\Sigma}$.

A.8 Estimation methodology: QML and EM

We can split the total number of parameters in the model into two subsets. The first subset $\boldsymbol{\vartheta}$ consists of parameters related to the dynamic specification of the model, which is defined in equations (3.5), (3.7), and (3.8). That is, $\boldsymbol{\vartheta} = (\boldsymbol{\vartheta}_1, \ldots, \boldsymbol{\vartheta}_4, \delta_1, \delta_1^+, \delta_2)'$, where $\boldsymbol{\vartheta}_i = (m_{0,i}, \boldsymbol{\Phi}_{1,i}, \ldots, \boldsymbol{\Phi}_{5,i}, \alpha_{0,i}, \alpha_{1,i}, \alpha_{1,i}^-, \alpha_{2,i})'$. Even if the true conditional distribution is not Gaussian, the set of parameters $\boldsymbol{\vartheta}$ can be consistently estimated by maximizing the following Gaussian log-likelihood function:

$$\log \mathcal{L}_1(\boldsymbol{\vartheta}|\boldsymbol{r}_1, \ldots, \boldsymbol{r}_T) = -\tfrac{T}{2}\log(\det(\boldsymbol{H}_t(\boldsymbol{\vartheta}))) - \tfrac{1}{2}\sum_{t=1}^{T} \boldsymbol{\varepsilon}_t(\boldsymbol{\vartheta})'\boldsymbol{H}_t^{-1}(\boldsymbol{\vartheta})\boldsymbol{\varepsilon}_t(\boldsymbol{\vartheta}), \tag{A.30}$$

where the residual vector $\boldsymbol{\varepsilon}_t$ and the conditional covariance $\boldsymbol{H}_t$ are given by equations (3.4) and (3.6). This method is known as quasi-maximum likelihood (QML) estimation and yields consistent and asymptotically Gaussian estimators $\widehat{\boldsymbol{\vartheta}}$ of the dynamics equations, which we use to forecast the h-period mean and covariance. Because normality is not assumed, the standard errors of the QML estimator $\widehat{\boldsymbol{\vartheta}}$ must be "robustified."

In the second step, assuming we have obtained i.i.d. innovations $\widehat{\boldsymbol{x}}_t$ from the QML estimation, we proceed to estimate the subset of parameters $\boldsymbol{\theta}$ corresponding to the GH conditional distribution, such that $\boldsymbol{\theta} = (\lambda, \chi, \psi, \boldsymbol{\mu}, \mathrm{vech}(\boldsymbol{\Sigma}), \boldsymbol{\gamma})'$. Thus, we need to find the parameters $\boldsymbol{\theta}$ that maximize the log-likelihood function:

$$\log \mathcal{L}_2(\boldsymbol{\theta}|\boldsymbol{x}_1, \ldots, \boldsymbol{x}_T) = \sum_{t=1}^{T} \log g(\boldsymbol{x}_t\,; \boldsymbol{\theta}), \tag{A.31}$$

where $g(\boldsymbol{x}_t\,; \boldsymbol{\theta})$ is the density function of the GH distribution at hand, parametrized by $\boldsymbol{\theta}$. Due to the number of parameters and how they enter the structure of the objective function, the direct maximization of the latter log-likelihood function is not flexible. For that reason, using the normal mixture representation of the GH distributions in equation (3.10) and for a

given mixing of random variables $(\omega_1, \ldots, \omega_T)$, we can divide $\log \mathcal{L}_2$ into two components:

$$\log \widetilde{\mathcal{L}}_2(\boldsymbol{\theta}|\boldsymbol{x}_1, \ldots, \boldsymbol{x}_T; \omega_1, \ldots, \omega_T) = \sum_{t=1}^{T} \log g(\boldsymbol{x}_t|\omega_t\,; \boldsymbol{\mu}, \boldsymbol{\Sigma}, \boldsymbol{\gamma}) + \sum_{t=1}^{T} \log h(\omega_t\,; \lambda, \chi, \psi)\,, \tag{A.32}$$

where $h(\omega_t\,; \lambda, \chi, \psi)$ is the density function of ω_t featured by the GIG parameters (λ, χ, ψ), and $g(\boldsymbol{x}_t|\omega_t\,; \boldsymbol{\mu}, \boldsymbol{\Sigma}, \boldsymbol{\gamma})$ is the conditional density of $\boldsymbol{x}_t$ given ω_t and parameterized by $(\boldsymbol{\mu}, \boldsymbol{\Sigma}, \boldsymbol{\gamma})$. The two terms can be maximized separately. Furthermore, if we suppose that the mixing random variables $(\omega_1, \ldots, \omega_T)$ are observable, then $g(\boldsymbol{x}_t|\omega_t)$ is Gaussian.

However, we are not able to observe the random variables $(\omega_1, \ldots, \omega_T)$ in practice. To deal with this latency of $(\omega_1, \ldots, \omega_T)$, we employ an estimation procedure based on the so-called expectation-maximization (EM) algorithm (see Protassov (2004)). The EM algorithm is an iterative method that consists of two steps. In the first stage, or expectation step, the mixing variables are replaced by an estimate, given the observed data and current parameter estimates, and an expected log-likelihood function is calculated. Then, in a second, maximization step, we maximize this log-likelihood function and update the parameter estimates. We repeat these two steps, increasing the log-likelihood value in each iteration, until the process converges to the optimal parameter estimates.

Following Hu and Kercheval (2010) and McNeil, Frey, and Embrechts (2005), we can detail the implementation of the EM procedure to the particular problem of the estimation of our GH distributions:

1. Select the starting values for the the first guess ($k = 1$) of the set of parameters, $\boldsymbol{\theta}^{[k]}$. In this case, reasonable values for $\boldsymbol{\mu}$, $\boldsymbol{\Sigma}$, and $\boldsymbol{\gamma}$ are the sample mean of the innovations $\bar{\boldsymbol{x}}$, the sample covariance matrix $\bar{\boldsymbol{H}}$, and the zero vector, respectively.

2. Compute the conditional expectation of the log-likelihood in equation (A.32), given the data $\boldsymbol{x}_1, \ldots, \boldsymbol{x}_T$ and the parameters $\boldsymbol{\theta}^{[k]}$, such that

$$\begin{aligned} Q(\boldsymbol{\theta}; \boldsymbol{\theta}^{[k]}) &= \mathbb{E}[\widetilde{\mathcal{L}}_2(\boldsymbol{\theta}; \boldsymbol{x}_1, \ldots, \boldsymbol{x}_T, \omega_1, \ldots, \omega_T)|\boldsymbol{x}_1, \ldots, \boldsymbol{x}_T; \boldsymbol{\theta}^{[k]}] \\ &= Q_1(\boldsymbol{\mu}, \boldsymbol{\Sigma}, \boldsymbol{\gamma}; \boldsymbol{\theta}^{[k]}) + Q_2(\lambda, \chi, \psi; \boldsymbol{\theta}^{[k]})\,. \end{aligned}$$

   For the first term Q_1, we consider that the distribution of $\boldsymbol{x}_t$ conditioned on ω_t is Gaussian. The second term Q_2 refers to the conditional expectation of the logarithm of the GIG density function in

equation (A.23). To compute this second term, we must calculate some conditional expectations of the functions of ω_t that appear in Q_2. In particular, $\eta_t^{[k]} = \mathbb{E}[\omega_t|\boldsymbol{x}_t;\boldsymbol{\theta}^{[k]}]$, $\delta_t^{[k]} = \mathbb{E}[1/\omega_t|\boldsymbol{x}_t;\boldsymbol{\theta}^{[k]}]$, and $\xi_t^{[k]} = \mathbb{E}[\log(\omega_t)|\boldsymbol{x}_t;\boldsymbol{\theta}^{[k]}]$.

3. Maximize the objective function $Q(\boldsymbol{\theta};\boldsymbol{\theta}^{[k]})$ with respect to the parameters $\boldsymbol{\theta}$ to obtain the updated estimates $\boldsymbol{\theta}^{[k+1]}$. The optimized values for $\boldsymbol{\mu}$, $\boldsymbol{\Sigma}$, and $\boldsymbol{\gamma}$ can be derived analytically from the first order conditions corresponding to the first term Q_1, to obtain the next updates of the estimates:

$$\boldsymbol{\gamma}^{[k+1]} = \frac{\frac{1}{T}\sum_{t=1}^{T}\delta_t^{[k]}(\bar{\boldsymbol{x}} - \boldsymbol{x}_t)}{\bar{\delta}^{[k]}\,\bar{\eta}^{[k]} - 1};$$

$$\boldsymbol{\mu}^{[k+1]} = \frac{\frac{1}{T}\sum_{t=1}^{T}\delta_t^{[k]}\boldsymbol{x}_t - \boldsymbol{\gamma}^{[k+1]}}{\bar{\delta}^{[k]}}; \quad \text{and}$$

$$\boldsymbol{\Sigma}^{[k+1]} = |\bar{\boldsymbol{H}}|^{\frac{1}{d}}\frac{1}{T}\sum_{t=1}^{T}\delta_t^{[k]}(\boldsymbol{x}_t - \boldsymbol{\mu}^{[k+1]})(\boldsymbol{x}_t - \boldsymbol{\mu}^{[k+1]})' - \bar{\eta}^{[k]}\boldsymbol{\gamma}^{[k+1]}\boldsymbol{\gamma}^{[k+1]\prime}$$
$$\left|\frac{1}{T}\sum_{t=1}^{T}\delta_t^{[k]}(\boldsymbol{x}_t - \boldsymbol{\mu}^{[k+1]})(\boldsymbol{x}_t - \boldsymbol{\mu}^{[k+1]})' - \bar{\eta}^{[k]}\boldsymbol{\gamma}^{[k+1]}\boldsymbol{\gamma}^{[k+1]\prime}\right|^{-\frac{1}{d}};$$

where $\bar{\delta}^{[k]} = \frac{1}{T}\sum_{t=1}^{T}\delta_t^{[k]}$, and the other average functions $\bar{\eta}^{[k]}$ and $\bar{\xi}^{[k]}$ are defined in the same way. For the T distribution, we use a simplified version, in which $\boldsymbol{\gamma}^{[k]} = \boldsymbol{\gamma}^{[k+1]} = \mathbf{0}$. To complete the calculation of $\boldsymbol{\theta}^{[k+1]}$, we maximize with respect to λ, χ, and ψ the following function:

$$Q_2(\lambda,\chi,\psi\,;\boldsymbol{\theta}^{[k]}) = (\lambda-1)T\bar{\xi}^{[k]} - \tfrac{1}{2}T(\chi\,\bar{\delta}^{[k]} + \psi\,\bar{\eta}^{[k]}) + \tfrac{1}{2}T\lambda\log\left(\frac{\psi}{\chi}\right) - T\log(2K_\lambda(\sqrt{\chi\psi})).$$

This maximization can be implemented numerically.[3]

4. Calculate the increment in the log-likelihood function obtained from the updated parameters $\theta^{[k+1]}$. The algorithm stops when the relative increment of the log-likelihood is small enough; otherwise, we set the counter from k to $k+1$ and repeat the process from Step 2.

[3]For T and skT distributions, the optimization is simplified to the computation of the degrees of freedom $\chi^{[k+1]}$ by solving the equation $-\Psi(\frac{\chi}{2}) + \log(\frac{\chi}{2}) + 1 - \bar{\xi}^{[k]} - \bar{\delta}^{[k]} = 0$ (see Hu and Kercheval (2010)), where $\Psi(x)$ is the so-called digamma function, defined as the derivative of the logarithm of the gamma function: $\Psi(x) \equiv \mathrm{d}(\log(\Gamma(x)))/\mathrm{d}x$.

Finally, we calculate the standard errors of the parameter estimates of the GH distribution using a block bootstrap. We generate 500 bootstrap samples to estimate the confidence intervals.

A.9 Backtests

In this appendix, we present the different backtest measures and methodologies that we apply to obtain the results in Tables 3.4, 3.5, and 3.6.

Christoffersen (1998) unconditional coverage LR test: The number of VaR violations over the out-of-sample period $(T+1,\ldots,T+L)$ is given by the sum $\hat{n}(\alpha,h)=\sum_{t=T+1}^{T+L}\hat{I}_t(\alpha,h)$. Therefore, the proportion of VaR violations can be calculated as $\hat{n}(\alpha,h)/L$. If the proposed model is reasonable, the indicator series $\hat{I}_t(\alpha,h)$ should behave as realizations of a Bernoulli distribution with violation (success) probability α. To test the null hypothesis that expected proportion of violations should be α, we consider the following log-likelihood ratio (LR) statistic:

$$\mathrm{LR}=2\log\left((n_\alpha/L)^{n_\alpha}(1-n_\alpha/L)^{L-n_\alpha}\right)-2\log\left((1-\alpha)^{n_\alpha}\alpha^{L-n_\alpha}\right), \quad \text{(A.33)}$$

where $n_\alpha\equiv\hat{n}(\alpha,h)$, and L is the number of observations in the validation (out-of-sample) period. Under the null hypothesis, the LR statistic should be asymptotically distributed as $\chi^2(1)$.

Embrechts, Kaufmann, and Patie (2005) measures: As a first backtesting measure of the ES forecast, we calculate the conditional average of the difference between the observed losses and the estimated ES, $\hat{D}_t(\alpha,h)$, conditioned on the VaR-violation indicator $\hat{I}_t(\alpha,h)$. That is,

$$V_1=\sum_{t=T+1}^{T+L}\hat{D}_t(\alpha,h)\hat{I}_t(\alpha,h)/\hat{n}(\alpha,h)\,. \quad \text{(A.34)}$$

Therefore, a good estimation of the ES leads to a non-negative and low value of the backtest measure V_1.

McNeil and Frey (2000) test: We define the forecast violation residuals as

$$\hat{s}_t(\alpha,h)=\hat{D}_t(\alpha,h)/\hat{\sigma}_{P,\,t+h}\,, \quad \text{(A.35)}$$

where $\hat{D}_t(\alpha,h)$ is the difference between actual losses and the ES forecast, and $\hat{\sigma}_{P,\,t+h}$ is the estimated volatility of the portfolio losses.

The expected value of the difference process $D_t(\alpha, h)$, conditional on the indicator variable $I_t(\alpha, h)$ (i.e., on a quantile violation), is zero, such that $\mathbb{E}(D_t(\alpha, h)I_t(\alpha, h)) = 0$. Therefore, if we define the model for the energy portfolio returns correctly, the residuals $\hat{s}_t(\alpha, h)$ in the event of a VaR violation ($\hat{I}_t(\alpha, h) = 1$) should be i.i.d. distributed with mean zero. We are more worried about the negative values of the differences $D_t(\alpha, h)$ than about the positive ones though, so we test the null hypothesis of a non-negative mean against the alternative of a mean less than zero. That is, we check if the ES is systematically underestimated. For that purpose, following McNeil and Frey (2000), we apply a one-sided bootstrap test that makes no assumption about the violation residuals' distribution.

A.10 Superior predictive ability test

The SPA test of Hansen (2005), based on the previous reality check of White (2000), is designed to compare the performance of a set of forecasting models. Let $L(S_t, \hat{S}_t)$ denote the loss of prediction $\hat{S}_t$ when the actual value is S_t. The performance of model k at time t relative to a benchmark model, denoted by $k = 0$, is given by

$$d_{k,t} = L(S_t, \hat{S}_{0,t}) - L(S_t, \hat{S}_{k,t}), \tag{A.36}$$

where $k = 1, \dots K$, and $t = T+1, \dots, T+L$, such that L is the length of the time series of forecasts $\hat{S}_{k,t}$. To check if any of the K models are better than the benchmark model ($k = 0$), we formulate the testable hypothesis that the benchmark is the best forecasting model in terms of the loss function $L(S_t, \hat{S}_t)$. This hypothesis can be expressed as

$$H_0 : \ \mathbb{E}(d_{k,t}) \leqslant 0, \quad k = 1, \dots, K\,. \tag{A.37}$$

According to Hansen (2005), one way to test this hypothesis consists of considering the test statistic:

$$T^{\mathrm{SPA}} = \max_{k=1,\dots K} L^{1/2}\, \bar{d}_k / \hat{\varsigma}_k^2, \tag{A.38}$$

where $\bar{d}_k = L^{-1} \sum_{t=T+1}^{T+L} d_{k,t}$, and $\hat{\varsigma}_k^2$ is a consistent estimator of the asymptotic variance ς_k^2, such that $\hat{\varsigma}_k^2 = \widehat{\mathrm{Var}}(L^{1/2}\, \bar{d}_k)$. That is, the test statistics T^{SPA} represents the largest t-statistic of relative performance.[4]

[4]The reality check of White (2000) employs the non-standardized test statistic $T^{\mathrm{RC}} = \max_{k=1,\dots,K} \bar{d}_k$.

It is convenient to use a bootstrap implementation of the SPA test that does not require an explicit estimator of the variance ς_k^2. For that purpose, we employ the stationary bootstrap of Politis and Romano (1994).[5] From the B bootstrap resamples $(\boldsymbol{d}_{b,1}^*, \ldots, \boldsymbol{d}_{b,L}^*)$, where $\boldsymbol{d}_{b,j}^* \in \mathbb{R}^K$ and $b = 1, \ldots, B$, we construct an estimate of the variance ς_k^2 and estimates of the distribution of the statistic T^{SPA} under the null hypothesis. Hansen (2005) proposes a procedure to approximate the distribution of T^{SPA} and derives consistent estimates of the p-values for the SPA test p^{SPA}. With this consistent p-value, as reported in Table 3.6, the test asymptotically determines which models are worse than the benchmark, preventing them from affecting the distribution of the test statistics. The null hypothesis is rejected for small p-values.

A.11 Prices of Call Options on the Spread

To calculate European option prices using transform techniques we need the Fourier transform of the payoff of the option and the characteristic function (cf) of the process for the spread. We start from the result that for a Lévy process $L(t)$ and a deterministic function $h(t)$

$$\mathbb{E}\left[\mathrm{e}^{i\xi\int_t^T h(u)\mathrm{d}L_u}\right] = \mathrm{e}^{\int_t^T \Psi(h(u)\xi)\mathrm{d}u}, \quad \xi = \xi_r + i\xi_i \quad \text{and} \quad \xi_r,\, \xi_i \in \mathbb{R}\,.$$

Hence, for a compound Poisson process with time-dependent intensity $\lambda(t)$ and $h(u) = \mathrm{e}^{-\beta(T-u)}$

$$\mathbb{E}\left[\mathrm{e}^{i\xi\int_t^T h(u)J\mathrm{d}N_u}\right] = \mathrm{e}^{\int_t^T \left(\Psi_J(\mathrm{e}^{-\beta(T-u)}\xi)-1\right)\lambda(u)\mathrm{d}u}$$

where $\Psi_J(\xi)$ is the cf of the jump random variable J.

In the particular case where jump sizes are exponentially distributed the cfs are

$$\begin{aligned}\mathbb{E}\left[\mathrm{e}^{i\xi J}\right] &= \frac{\eta_1}{\eta_1 - i\xi} \quad \text{with} \quad \xi_i > -\eta_1 \quad \text{and}\\ \mathbb{E}\left[\mathrm{e}^{i\xi J}\right] &= \frac{\eta_2}{\eta_2 + i\xi} \quad \text{with} \quad \xi_i < \eta_2\,.\end{aligned}$$

Since we assume that the intensity parameters of the inhomogeneous Poisson processes are either constant or piecewise constant, we must calculate the integrals $\int_t^T \Psi_J(\mathrm{e}^{-\beta(T-u)}\xi)\mathrm{d}u$, over a time interval $(t, T]$, for the

[5] To choose the block length of the bootstrap resampling, we follow the procedure presented by Patton, Politis, and White (2009).

positive and negative jumps, respectively:

$$\int_t^T \Big(\frac{\eta_1}{\eta_1 - i\xi \mathrm{e}^{-\beta(T-u)}} - 1\Big)\mathrm{d}u = \frac{1}{\beta}\ln\Big(\frac{i\xi \mathrm{e}^{-\beta(T-t)} - \eta_1}{i\xi - \eta_1}\Big),$$

and

$$\int_t^T \Big(\frac{\eta_2}{\eta_2 + i\xi \mathrm{e}^{-\beta(T-u)}} - 1\Big)\mathrm{d}u = \frac{1}{\beta}\ln\Big(\frac{i\xi \mathrm{e}^{-\beta(T-t)} + \eta_2}{i\xi + \eta_2}\Big).$$

Thus, the cf of $S^{\mathrm{A,B}}(T)$, conditioned on information up until time t, and assuming constant intensity parameters for the jump processes between $(t, T]$, is given by

$$\begin{aligned}\Psi_S^{\mathrm{A,B}}(\xi) = \mathbb{E}[\mathrm{e}^{i\xi S(T)}] = \mathrm{e}^{i\xi h(T) - \frac{1}{2}\xi^2 \int_t^T \mathrm{e}^{-2\alpha(T-u)}\sigma^2(u)\mathrm{d}u} \\ \times \Big(\frac{i\xi \mathrm{e}^{-\beta(T-t)} - \eta_1}{i\xi - \eta_1}\Big)^{\frac{\lambda^+}{\beta}} \Big(\frac{\eta_2 + i\xi \mathrm{e}^{-\beta(T-t)}}{\eta_2 + i\xi}\Big)^{\frac{\lambda^-}{\beta}}\end{aligned} \tag{A.39}$$

where $h(T) = f(T) + X(t)\mathrm{e}^{-\alpha(T-t)} + Y(t)\mathrm{e}^{-\beta(T-t)}$, $-\eta_1 < \xi_i < \eta_2$, and λ^+ and λ^- are the intensities of the Poisson arrival of positive and negative jumps respectively.

Therefore, the price of European options on the spread $S^{\mathrm{A,B}}(T)$, with expiry T and strike $K^{\mathrm{A,B}}$ is given by an integral along a straight line in $\mathbb{C}$ parallel to $\mathbb{R}$, with $-\eta_2 < \xi_i < \eta_1$,

$$C^{\mathrm{A,B}}(S, \infty, t; T, K^{\mathrm{A,B}}) = \frac{\mathrm{e}^{-r(T-t)}}{2\pi}\int_{-\infty+i\xi_i}^{\infty+i\xi_i} \Psi_S(-\xi)\Pi^{\mathrm{A,B}}(\xi)\mathrm{d}\xi \tag{A.40}$$

and $\Pi^{\mathrm{A,B}}(\xi)$ is the Fourier transform of the call option payoff:

$$\Pi^{\mathrm{A,B}}(\xi) = \int_{-\infty}^{\infty} \mathrm{e}^{i\xi x}\max(x - K^{\mathrm{A,B}}, 0)\mathrm{d}x = -\frac{\mathrm{e}^{i\xi K^{A,B}}}{\xi^2} \tag{A.41}$$

for $\xi_i > 0$. $\Pi^{\mathrm{B,A}}(\xi)$ is obtained in the same way.

Proof of equation (4.18)**.** Let $Y = S^{\mathrm{A,B}}(T)$ and let $f(y)$ the pdf of the normal random variable Y and recall that $\mu(t, T)$ and $v^2(t, T)$ are as in

(4.19). Then,

$$\begin{aligned} C^{\mathrm{A,B}}(S^{\mathrm{A,B}}, M, t; T, K^{\mathrm{A,B}}) &= \mathrm{e}^{-\rho(T-t)}\Big[\int_{K^{\mathrm{A,B}}}^{\infty} Yf(y)\mathrm{d}y - K^{\mathrm{A,B}}\int_{\beta_1}^{\infty}\phi(x)\mathrm{d}x \\ &\quad - \int_{M}^{\infty} Yf(y)\mathrm{d}y - M\int_{\beta_2}^{\infty}\phi(x)\mathrm{d}x\Big] \\ &= \mathrm{e}^{-\rho(T-t)}\Big[\int_{K^{\mathrm{A,B}}}^{\infty} Yf(y)\mathrm{d}y - K^{\mathrm{A,B}}\Phi(-\beta_1) - \\ &\quad \int_{K^{\mathrm{A,B}}}^{\infty} Yf(y)\mathrm{d}y - M\Phi(-\beta_2)\Big] \\ &= \mathrm{e}^{-\rho(T-t)}\Big[\Big(\mu(t,T) - K^{\mathrm{A,B}} + \tfrac{v(t,T)\phi(\beta_1)}{1-\Phi(\beta_1)}\Big)\Phi(-\beta_1) \\ &\quad - \Big(\mu(t,T) - M + \tfrac{v(t,T)\phi(\beta_2)}{1-\Phi(\beta_2)}\Big)\Phi(-\beta_2)\Big], \quad \text{(A.42)} \end{aligned}$$

where $\beta_1 = (K^{\mathrm{A,B}} - \mu(t,T))/v(t,T)$ and $\beta_2 = (M - \mu(t,T))/v(t,T)$.

Moreover, note that to evaluate the integrals that are of the form

$$\int_{K^{\mathrm{A,B}}}^{\infty} yf(y)\mathrm{d}y, \tag{A.43}$$

in equation (A.42), where $f(y)$ and $F(Y)$ are the pdf and cdf of the random variable $Y \sim N(\mu(t,T),\, v^2(t,T))$, we use Bayes' theorem to obtain

$$\begin{aligned} \int_{K^{\mathrm{A,B}}}^{\infty} yf(y \mid y > K^{\mathrm{A,B}})\mathrm{d}y &= \int_{K^{\mathrm{A,B}}}^{\infty} y\frac{f(y)}{(1-F(K^{\mathrm{A,B}}))}\mathrm{d}y \\ &= \mu(t,T) + v(t,T)\frac{\phi\Big(\frac{K^{\mathrm{A,B}}-\mu(t,T)}{v(t,T)}\Big)}{1-\Phi\Big(\frac{K^{\mathrm{A,B}}-\mu(t,T)}{v(t,T)}\Big)}, \end{aligned}$$

and for the last equality we use the fact that for a constant K

$$\mathbb{E}[Y \mid K < Y] = \mu(t,T) + v(t,T)\frac{\phi\Big(\frac{K-\mu(t,T)}{v(t,T)}\Big)}{1-\Phi\Big(\frac{K-\mu(t,T)}{v(t,T)}\Big)} \tag{A.44}$$

and

$$\mathbb{E}[Y \mid Y < K] = \mu(t,T) - v(t,T)\frac{\phi\Big(\frac{K-\mu(t,T)}{v(t,T)}\Big)}{\Phi\Big(\frac{K-\mu(t,T)}{v(t,T)}\Big)}. \tag{A.45}$$

Therefore, the truncated integral

$$\int_{K^{\mathrm{A,B}}}^{\infty} yf\,(y)\,\mathrm{d}y = \mu(t,T)\Big(1-\Phi\Big(\tfrac{K^{\mathrm{A,B}}-\mu(t,T)}{v(t,T)}\Big)\Big) + v(t,T)\frac{\phi\Big(\tfrac{K^{\mathrm{A,B}}-\mu(t,T)}{v(t,T)}\Big)}{1-\Phi\Big(\tfrac{K^{\mathrm{A,B}}-\mu(t,T)}{v(t,T)}\Big)}(1-\Phi\Big(\tfrac{K^{\mathrm{A,B}}-\mu(t,T)}{v(t,T)}\Big)).$$

References

Aas, K., and I. H. Haff (2006): "The generalized hyperbolic skew Student's t-distribution," *Journal of Financial Econometrics*, 4(2), 275–309.

Abramowitz, M., and I. A. Stegun (1965): *Handbook of mathematical functions with formulas, graphs, and mathematical tables*. Dover Publications, New York, NY.

Ang, A., and J. Chen (2002): "Asymmetric correlations of equity returns," *Journal of Financial Economics*, 63(3), 443–494.

Artzner, P., F. Delbaen, J. M. Eber, and D. Heath (1999): "Coherent risk measures," *Mathematical Finance*, 9(3), 203–228.

Barberis, N. C., and M. Huang (2008): "Stocks as lotteries: The implications of probability weighting for security prices," *The American Economic Review*, 98(5), 2066–2100.

Barlow, M. (2002): "A diffusion model for electricity prices," *Mathematical Finance*, 12(4), 287–298.

Benth, F., and R. Kufakunesu (2009): "Pricing of exotic energy derivatives based on arithmetic spot models," *International Journal of Theoretical and Applied Finance*, 12(04), 491–506.

Benth, F., and J. Šaltytė Benth (2004): "The normal inverse Gaussian distribution and spot price modelling in energy markets," *International Journal of Theoretical and Applied Finance*, 7(2), 177–192.

——— (2006): "Analytical approximation for the price dynamics of spark spread options," *Studies in Nonlinear Dynamics and Econometrics*, 10(3), 1355–1355.

Benth, F., J. Šaltytė Benth, and S. Koekebakker (2008): *Stochastic modelling of electricity and related markets*. World Scientific Publishing, New York, NY.

Benth, F. E., Á. Cartea, and R. Kiesel (2008): "Pricing forward contracts in power markets by the certainty equivalence principle: Explaining the sign of the market risk premium," *Journal of Banking and Finance*, 32(10), 2006–2021.

Benth, F. E., and S. Koekebakker (2008): "Stochastic modeling of financial electricity contracts," *Energy Economics*, 30(3), 1116–1157.

Bessembinder, H., and M. Lemmon (2002): "Equilibrium pricing and optimal hedging in electricity forward markets," *Journal of Finance*, 57(3), 1347–1382.

Bibby, B., and M. Sørensen (2003): "Hyperbolic processes in finance," in *Handbook of Heavy Tailed Distributions in Finance*, ed. by S. Rachev, pp. 211–248. Elsevier, Amsterdam.

Bingham, N., and R. Kiesel (2002): "Semi-parametric modelling in finance: theoretical foundations," *Quantitative Finance*, 2(4), 241–250.

Boogert, A., and C. De Jong (2008): "Gas storage valuation using a Monte Carlo method," *Journal of Derivatives*, 15(3), 81–98.

Borak, S., and R. Weron (2008): "A semiparametric factor model for electricity forward curve dynamics," *Journal of Energy Markets*, 1(3), 3–16.

Börger, R. H., Á. Cartea, R. Kiesel, and G. Schindlmayr (2009): "Cross-commodity analysis and applications to risk management," *Journal of Futures Markets*, 29(3), 197–217.

Brennan, M., and L. Trigeorgis (2000): *Project flexibility, agency, and competition: New developments in the theory and application of real options*. Oxford University Press, Oxford.

Bunn, D., and A. Gianfreda (2010): "Integration and shock transmissions across European electricity forward markets," *Energy Economics*, 32(2), 278 – 291.

Bunn, D., and M. Martoccia (2010): "The efficiency of network transmission rights as derivatives on energy supply chains," *Journal of Derivatives*, 18(2), 46–57.

Bunn, D., and G. Zachmann (2010): "Inefficient arbitrage in inter-regional electricity transmission," *Journal of Regulatory Economics*, 37(3), 243–265.

Büyükşahin, B., and M. Robe (2010): "Speculators, commodities, and cross-market linkages," *Working paper, Commodity Futures Trading Commission.*

Büyükşahin, B., M. Haigh, and M. Robe (2010): "Commodities and equities: ever a "Market of One"?," *Journal of Alternative Investments*, 12(3), 76–95.

Campbell, J., and L. Hentschel (1992): "No news is good news:: An asymmetric model of changing volatility in stock returns," *Journal of Financial Economics*, 31(3), 281–318.

Cappiello, L., R. Engle, and K. Sheppard (2006): "Asymmetric dynamics in the correlations of global equity and bond returns," *Journal of Financial Econometrics*, 4(4), 537–572.

Carmona, R., and V. Durrleman (2003): "Pricing and Hedging Spread Options," *SIAM Review*, 45(4), 627–685.

Carmona, R., and M. Ludkovski (2006): "Energy trading," *SIAM News*, 32(5).

——— (2010): "Valuation of energy storage: an optimal switching approach," *Quantitative Finance*, 10(4), 359 – 374.

Cartea, Á., and M. G. Figueroa (2005): "Pricing in electricity markets: a mean reverting jump diffusion model with seasonality," *Applied Mathematical Finance*, 12(4), 313–335.

Cartea, Á., and C. González-Pedraz (2012): "How much should we pay for interconnecting electricity markets? A real options approach," *Energy Economics*, 34(1), 14–30.

Cartea, Á., and P. Villaplana (2008): "Spot price modeling and the valuation of electricity forward contracts: The role of demand and capacity," *Journal of Banking and Finance*, 32(12), 2502–2519.

CARTEA, Á., AND T. WILLIAMS (2008): "UK gas markets: The market price of risk and applications to multiple interruptible supply contracts," *Energy Economics*, 30(3), 829–846.

CASASSUS, J., AND P. COLLIN-DUFRESNE (2005): "Stochastic convenience yield implied from commodity futures and interest rates," *Journal of Finance*, 60(5), 2283–2331.

CASASSUS, J., P. LIU, AND K. TANG (2013): "Economic linkages, relative scarcity, and commodity futures returns," *Review of Financial Studies*, 26(5), 1324–1362.

CHEN, Z., AND P. FORSYTH (2007): "A semi-Lagrangian approach for natural gas storage valuation and optimal operation," *SIAM Journal on Scientific Computing*, 30(1), 339–368.

CHRISTOFFERSEN, P. F. (1998): "Evaluating interval forecasts," *International Economic Review*, 39(4), 841–862.

COULON, M., AND S. HOWISON (2009): "Stochastic behaviour of the electricity bid stack: from fundamental drivers to power prices," *Journal of Energy Markets*, 2(1), 29–69.

DAS, S. R., AND R. UPPAL (2004): "Systemic risk and international portfolio choice," *Journal of Finance*, 59(6), 2809–2834.

DASKALAKI, C., AND G. SKIADOPOULOS (2011): "Should investors include commodities in their portfolios after all? New evidence," *Journal of Banking and Finance*, 35(10), 2606–2626.

DEMARTA, S., AND A. J. MCNEIL (2005): "The t copula and related copulas," *International Statistical Review*, 73(1), 111–130.

DEMPSTER, M., E. MEDOVA, AND K. TANG (2008): "Long term spread option valuation and hedging," *Journal of Banking and Finance*, 32(12), 2530–2540.

DEPARTMENT OF ENERGY (2002): *National Transmission Grid Study*. Secretary of Energy, Washington DC.

DIEBOLD, F. X., T. A. GUNTHER, AND A. S. TAY (1998): "Evaluating density forecasts with applications to financial risk management," *International Economic Review*, 39(4), 863–883.

DUFFIE, D. (1989): *Futures markets*. Prentice Hall, Englewood Cliffs, NJ.

DUSAK, K. (1973): "Futures trading and investor returns: An investigation of commodity market risk premiums," *Journal of Political Economy*, 81(6), 1387–1406.

EBERLEIN, E., AND G. STAHL (2003): "Both sides of the fence: A statistical and regulatory view of electricity risk," *Energy and Power Risk Management*, 8(6), 32–36.

EMBRECHTS, P., R. KAUFMANN, AND P. PATIE (2005): "Strategic long-term financial risks: Single risk factors," *Computational optimization and applications*, 32(1), 61–90.

EMBRECHTS, P., F. LINDSKOG, AND A. MCNEIL (2003): "Modelling dependence with copulas and applications to risk management," in *Handbook of heavy tailed distributions in finance*, ed. by S. T. Rachev, pp. 329–384. Elsevier, Amsterdam.

ENGLE, R. F. (2002): "Dynamic conditional correlation: a simple class of multivariate generalized autoregressive conditional heteroskedasticity models," *Journal of Business and Economic Statistics*, 20(3), 339–350.

ENGLE, R. F., AND K. SHEPPARD (2001): "Theoretical and empirical properties of dynamic conditional correlation multivariate GARCH," *NBER Working Paper*.

ERAKER, B. (2004): "Do stock prices and volatility jump? Reconciling evidence from spot and option prices," *Journal of Finance*, 59(3), 1367–1403.

ERAKER, B., M. JOHANNES, AND N. POLSON (2003): "The impact of jumps in volatility and returns," *Journal of Finance*, 58(3), 1269–1300.

ERB, C. B., AND C. R. HARVEY (2006): "The strategic and tactical value of commodity futures," *Financial Analysts Journal*, 62(2), 69–97.

ESCRIBANO, A., J. I. PEÑA, AND P. VILLAPLANA (2011): "Modelling electricity prices: International evidence," *Oxford Bulletin of Economics and Statistics*, 73(5), 622–650.

ETULA, E. (2013): "Broker-dealer risk appetite and commodity returns," *Journal of Financial Econometrics*, 11(3), 486–521.

EUROPEAN COMMISSION (2008): *Interconnecting Europe. New perspectives for trans-European energy networks*. Official Publications of the European Communities, Luxembourg.

Fusai, G., M. Marena, and A. Roncoroni (2008): "Analytical pricing of discretely monitored Asian-style options: Theory and application to commodity markets," *Journal of Banking and Finance*, 32(10), 2033–2045.

Fusai, G., and A. Roncoroni (2008): *Implementing models in quantitative finance: Methods and cases*. Springer Verlag, Berlin.

Geman, H. (2005): *Commodities and commodity derivatives: Modelling and pricing for agriculturals, metals, and energy*. Wiley, New York, NY.

Gibson, R., and E. Schwartz (1990): "Stochastic convenience yield and the pricing of oil contingent claims," *Journal of Finance*, 45(3), 959–976.

Giot, P., and S. Laurent (2003): "Market risk in commodity markets: A VaR approach," *Energy Economics*, 25(5), 435–457.

Goffe, W., G. Ferrier, and J. Rogers (1994): "Global optimization of statistical functions with simulated annealing," *Journal of Econometrics*, 60(1-2), 65–99.

Goldman Sachs (2004): "The case for commodities as an asset class," Technical presentation.

Gorton, G., and K. G. Rouwenhorst (2006): "Facts and fantasies about commodity futures," *Financial Analysts Journal*, 62(2), 47–68.

Graham, J. R., and C. R. Harvey (1997): "Grading the performance of market-timing newsletters," *Financial Analysts Journal*, 53(6), 54–66.

Guidolin, M., and A. Timmermann (2008): "International asset allocation under regime switching, skew, and kurtosis preferences," *Review of Financial Studies*, 21(2), 889–935.

Hambly, B., S. Howison, and T. Kluge (2009): "Modelling spikes and pricing swing options in electricity markets," *Quantitative Finance*, 9(8), 937–949.

Hansen, B. E. (1994): "Autoregressive conditional density estimation," *International Economic Review*, 35(3), 705–730.

Hansen, P. R. (2005): "A test for superior predictive ability," *Journal of Business and Economic Statistics*, 23(4), 365–380.

Harvey, C. R., J. C. Liechty, M. W. Liechty, and P. Müller (2010): "Portfolio selection with higher moments," *Quantitative Finance*, 10(5), 469–485.

HARVEY, C. R., AND A. SIDDIQUE (1999): "Autoregressive conditional skewness," *Journal of Financial and Quantitative Analysis*, 34(4), 465–487.

——— (2000): "Conditional skewness in asset pricing tests," *Journal of Finance*, 55(3), 1263–1295.

HIKSPOORS, S., AND S. JAIMUNGAL (2007): "Energy spot price models and spread options pricing," *International Journal of Theoretical and Applied Finance*, 10(07), 1111–1135.

HIKSPOORS, S., AND S. JAIMUNGAL (2008): "Asymptotic pricing of commodity derivatives for stochastic volatility spot models," *Applied Mathematical Finance*, 15(5), 449–477.

HILLIARD, J., AND J. REIS (1998): "Valuation of commodity futures and options under stochastic convenience yields, interest rates, and jump diffusions in the spot," *Journal of Financial and Quantitative Analysis*, 33(1), 61–86.

HONG, H., AND M. YOGO (2012): "What does futures market interest tell us about the macro-economy and asset prices?," *Journal of Financial Economics*, 105(3), 473–490.

HU, W., AND A. N. KERCHEVAL (2010): "Portfolio optimization for t and skewed-t returns," *Quantitative Finance*, 10(1), 91–105.

HUISMAN, R., AND R. MAHIEU (2003): "Regime jumps in electricity prices," *Energy Economics*, 25(5), 425–434.

INTERNATIONAL ENERGY AGENCY (2011): *Key world energy statistics*. OECD, Paris.

IRWIN, S., AND D. SANDERS (2011): "Index funds, financialization, and commodity futures markets," *Applied Economic Perspectives and Policy*, 33(1), 1–31.

JACQUIER, E., M. JOHANNES, AND N. POLSON (2007): "MCMC maximum likelihood for latent state models," *Journal of Econometrics*, 137(2), 615–640.

JAILLET, J., E. RONN, AND S. TOMPAIDIS (2004): "Valuation of commodity-based swing options," *Management Science*, 50(7), 909–921.

JOHANNES, M., AND N. POLSON (2009): "Markov chain Monte Carlo," in *Handbook of Financial Time Series*, ed. by T. Mikosch, J.-P. Kreiß, R. Davis, and T. Andersen, pp. 1001–1013. Springer Verlag, Berlin.

——— (2010): "MCMC methods for continuous-time financial econometrics," in *Handbook of financial econometrics: Applications*, ed. by Y. Ait-Sahalia, and L. Hansen, pp. 1–72. North Holland, Amsterdam.

Jondeau, E., and M. Rockinger (2003): "Conditional volatility, skewness, and kurtosis: existence, persistence, and comovements," *Journal of Economic Dynamics and Control*, 27(10), 1699–1737.

——— (2006): "The copula-GARCH model of conditional dependencies: An international stock market application," *Journal of International Money and Finance*, 25(5), 827–853.

——— (2012): "On the importance of time variability in higher moments for asset allocation," *Journal of Financial Econometrics*, 10(1), 84–123.

Kamat, R., and S. Oren (2002): "Exotic options for interruptible electricity supply contracts," *Operations Research*, 50(5), 835–850.

Kat, H. M., and R. C. A. Oomen (2007a): "What every investor should know about commodities. Part I: Univariate return analysis," *Journal of Investment Management*, 5(1), 4–28.

——— (2007b): "What every investor should know about commodities. Part II: Multivariate return analysis," *Journal of Investment Management*, 5(3), 16–40.

Keppo, J. (2004): "Pricing of electricity swing options," *Journal of Derivatives*, 11(3), 26–43.

Keppo, J., and H. Lu (2003): "Real options and a large producer: The case of electricity markets," *Energy Economics*, 25(5), 459 – 472.

Kiesel, R., G. Schindlmayr, and R. Börger (2009): "A two-factor model for the electricity forward market," *Quantitative Finance*, 9(3), 279 – 287.

Kraus, A., and R. H. Litzenberger (1976): "Skewness preference and the valuation of risk assets," *Journal of Finance*, 31(4), 1085–1100.

Kupiec, P. (1995): "Techniques for Verifying the Accuracy of Risk Measurement Models," *Journal of Derivatives*, 3, 73–84.

Lee, S. S., and P. A. Mykland (2008): "Jumps in financial markets: A new nonparametric test and jump dynamics," *Review of Financial Studies*, 21(6), 2535–2563.

LONGIN, F., AND B. SOLNIK (2001): "Extreme correlation of international equity markets," *Journal of Finance*, 56(2), 649–676.

LUCÍA, J., AND E. S. SCHWARTZ (2002): "Electricity prices and power derivatives: Evidence from the Nordic power exchange," *Review of Derivatives Research*, 5(1), 5–50.

MANOLIU, M., AND S. TOMPAIDIS (2002): "Energy futures prices: term structure models with Kalman filter estimation," *Applied Mathematical Finance*, 9(1), 21–43.

MARCKHOFF, J., AND M. MUCK (2009): "Locational price spreads and the pricing of contracts for difference: Evidence from the Nordic market," *Energy Economics*, 31(2), 257–268.

MARDIA, K. (1970): "Measures of multivariate skewness and kurtosis with applications," *Biometrika*, 57(3), 519–530.

MCNEIL, A. J., AND R. FREY (2000): "Estimation of tail-related risk measures for heteroscedastic financial time series: An extreme value approach," *Journal of Empirical Finance*, 7(3), 271–300.

MCNEIL, A. J., R. FREY, AND P. EMBRECHTS (2005): *Quantitative risk management: Concepts, techniques, and tools*. Princeton University Press, Princeton, NJ.

MILTERSEN, K., AND E. SCHWARTZ (1998): "Pricing of options on commodity futures with stochastic term structures of convenience yields and interest rates," *Journal of Finance*, 33(1), 33–59.

MITTON, T., AND K. VORKINK (2007): "Equilibrium underdiversification and the preference for skewness," *Review of Financial Studies*, 20(4), 1255–1288.

NELSEN, R. B. (2006): *An introduction to copulas*. Springer, New York, NY.

NICOLATO, E., AND E. VENARDOS (2003): "Option pricing in stochastic volatility models of the Ornstein-Uhlenbeck type," *Mathematical Finance*, 13(4), 445–466.

PATTON, A. J. (2004): "On the out-of-sample importance of skewness and asymmetric dependence for asset allocation," *Journal of Financial Econometrics*, 2(1), 130–168.

——— (2006a): "Estimation of multivariate models for time series of possibly different lengths," *Journal of Applied Econometrics*, 21(2), 147–173.

——— (2006b): "Modelling asymmetric exchange rate dependence," *International Economic Review*, 47(2), 527–556.

PATTON, A. J., D. POLITIS, AND H. WHITE (2009): "Correction to "Automatic block-length selection for the dependent bootstrap" by D. Politis and H. White," *Econometric Reviews*, 28(4), 372–375.

PIRRONG, C. (2012): *Commodity price dynamics: A structural approach*. Cambridge University Press, New York, NY.

PIRRONG, C., AND M. JERMAKYAN (2008): "The price of power: The valuation of power and weather derivatives," *Journal of Banking and Finance*, 32(12), 2520–2529.

POLITIS, D., AND J. ROMANO (1994): "The stationary bootstrap," *Journal of the American Statistical Association*, 89(428), 1303–1313.

POLSON, N., AND J. STROUD (2003): "Bayesian inference for derivatives prices," *Bayesian Statistics*, 7, 641–650.

POON, S. H., M. ROCKINGER, AND J. TAWN (2004): "Extreme value dependence in financial markets: Diagnostics, models, and financial implications," *Review of Financial Studies*, 17(2), 581–610.

PRAUSE, K. (1999): "The generalized hyperbolic model: Estimation, financial derivatives, and risk measures," Doctoral thesis, University of Freiburg.

PROTASSOV, R. S. (2004): "EM-based maximum likelihood parameter estimation for multivariate generalized hyperbolic distributions with fixed λ," *Statistics and Computing*, 14(1), 67–77.

RONCORONI, A. (2002): "A class of marked point processes for modeling electricity prices," Doctoral thesis, Université Paris IX Dauphine.

——— (2010): "Commodity Price Models," in *Encyclopedia of quantitative finance*, ed. by R. Cont, pp. 298–303. John Wiley and Sons, New York, NY.

ROSS, S. (1997): "Hedging long run commitments: Exercises in incomplete market pricing," *Economic Notes*, 26(5), 385–420.

ROUTLEDGE, B. R., D. J. SEPPI, AND C. S. SPATT (2000): "Equilibrium forward curves for commodities," *Journal of Finance*, 55(3), 1297–1338.

——— (2001): "The spark spread: An equilibrium model of cross-commodity price relationships in electricity," Working paper, Carnegie Mellon University.

SAMUELSON, P. A. (1970): "The fundamental approximation theorem of portfolio analysis in terms of means, variances and higher moments," *Review of Economic Studies*, 37(4), 537–542.

SCHWARTZ, E. S. (1997): "The stochastic behavior of commodity prices: Implications for valuation and hedging," *Journal of Finance*, 52(3), 923–973.

SCHWARTZ, E. S., AND J. E. SMITH (2000): "Short-term variations and long-term dynamics in commodity prices," *Management Science*, 46(7), 893–911.

SKLAR, A. (1959): "Fonctions de répartition à n dimensions et leurs marges," *Publications de l'Institut Statistique de l'Université de Paris*, 8, 229–231.

STEFANOVA, D. (2009): "Dynamic hedging and extreme asset co-movements," Working paper, VU University Amsterdam.

TANG, K., AND W. XIONG (2012): "Index investment and financialization of commodities," *Financial Analysts Journal*, 68(6), 54–74.

THE ECONOMIST (2008): "The power and the glory," June 19th.

TRIGEORGIS, L. (1996): *Real options: Managerial flexibility and strategy in resource allocation*. MIT Press, Cambridge, MA.

TSENG, C. L., AND G. BARZ (2002): "Short-term generation asset valuation: A real options approach," *Operations Research*, 50(2), 297–310.

WERON, R. (2006): *Modeling and forecasting electricity loads and prices: A statistical approach*. John Wiley and Sons, Chichester.

WHITE, H. (2000): "A reality check for data snooping," *Econometrica*, 68(5), 1097–1126.